Cellular and Molecular Pathogenesis of Salmonid Alphavirus 1 in Atlantic Salmon *Salmo salar* L.

**THESIS SUBMITTED FOR THE DEGREE OF
DOCTOR OF PHILOSOPHY IN
AQUATIC VETERINARY STUDIES**

By

Tharangani Kaushallya Herath

BVSc

March 2010

INSTITUTE OF AQUACULTURE

UNIVERSITY OF STIRLING

To Nilantha, Vinethma

and

my mum Indu

Declaration

I, hereby declare that the work and the results presented in this thesis have been carried out by myself at the Institute of Aquaculture, University of Stirling, Scotland and have not been submitted for any other degree or qualification. All information from other sources has been acknowledged.

Tharangani K. Herath

Acknowledgements

Sophie Fridman for being an amazing friend to me and to my family, good luck for the thesis. Thank you very much Dr. and Mrs. Siriwardena you were always there for us, I will remember you all forever!

I cannot forget Professor Neil Horadagoda, who has shown me the essence of pathology and research; you will always be remembered and acknowledged! I also sincerely acknowledge my colleagues, especially Professor J.M.P.K Jayasinghe and Professor T.B Wanninayake at The Department of Aquaculture and Fisheries, Wayamba University of Sri Lanka for taking care of my duties during my period away for PhD studies.

Finally to my family, my loving husband Nilantha, I know you are there for me all the time, thanks for giving time and encouragement for me to be positive. Vinethma, you have been a blessing for us, you were the hope, you grew up with the thesis and thanks for giving pleasure and enthusiasm to our life. (Thanks for selecting pretty pink for some of the graphs!). Thanks for my parents and the family for always believing in me to achieve this goal!

List of abbreviations

+ssRN	positive sense single stranded RNA
µg	microgram
µl	microlitre
µm	micrometre
µM	micromolar
AEC	amino-ethyl carbazol reagent
ANOVA	analysis of variance
ApoREG	apoptosis regulatory factor
aRNA	amplified RNA
BcL-2	B cell aggressive lymphoma gene
BLAST	basic alignment search tool
bp	base pairs
BSA	bovine serum albumin
cDNA	complementary DNA
CHH-1	Chum salmon heart -1 cells
CHSE-214	Chinook salmon embryo 214 cells
CMC	cell mediated cytotoxicity
CMS	Cardiomyopathy syndrome
CPE	cytopathic effect
CPV	cytopathic vacuole
cRNA	*in vitro* copied RNA
Ct	threshold cycle
Cy	cyanine
d.p.i	days post infection
d.p.in	days post inoculation
DAP	death associated protein
DD	death domain
dH$_2$O	distilled water
DISC	death inducing signalling complex
DMSO	dimethyl sulphoxide
DNA	deoxyribonucleic acid
DPBS	Dulbecco's phosphate buffered saline without Ca and Mg
dsDNA	double stranded DNA
dsRNA	double stranded RNA
E	efficiency of qPCR
e.g.	example
EE	early endosomes
ELF-1α	translation elongation factor 1 α
eLF2α	translation elongation factor 2α
EM	electron microscopy
EMEM	Eagle's Minimal Essential Medium
EPC	Epithelioma papulosum cyprinid
ER	endoplasmic reticulum
EST	expressed sequence tags
et al.	et alia (and others)
EtBr	ethidium bromide
FAO	Food and Agriculture Organization
FCS	foetal calf serum
FHM	Fathead minnow
g	gram
GM	growth medium

h	hours
H&E	haematoxylin and eosin
H_2O_2	hydrogen peroxide
HBSS	Hank's buffered salt solution
HSMI	Heart and skeletal muscle inflammation
i.e.	id est (that is)
I.P.	Intraperitoneal
IFAT	immuno fluorescent antibody technique
Ig	immunoglobulin
IHC	immunohistochemistry
IHNV	infectious heamatopoietic necrosis virus
IL	interleukin
INF	interferon
IPNV	Infectious pancreatic necrosis virus
IPVN	immunoperoxidase based virus neutralisation
IRF	interferon regulatory factors
ISAV	Infectious salmon anaemia virus
ISG	interferon stimulated genes
ICVT	International Committee for Virus Taxonomy
IU	international units
JAK	Janus kinases
JAK/STAT	Janus Kinases and Signal Transducers and Activators of Transcription
JCVI	J. Craig Venter Institute
Kb	kilo base
L	litre
L-15	Leibovitz-15
LE	late endosomes
M	molar
MA	microarray
mAb	monoclonal antibody
MAPK	mitogen activated protein kinase
mg	milligram
MHC	major histocompatibility class
min	minute
ml	millilitre
MM	maintenance medium
mM	millimolar
MOI	multiplicity of infection
mRNA	messenger ribonucleic acid
NCBI	National Center for Biotechnology Information
NEAA	non essential amino acids
NF-κB	nuclear factor kappa-light-chain-enhancer
ng	nano gram
NK cell	natural killer cell
nm	nanometre
NOX	nitric oxide
nsP	non-structural protein
NSPD	Norwegian salmon pancreas disease
OIE	Office International des Epizooties
PAMP	pathogen associated molecular pattern
PBS	phosphate buffered saline
PD	pancreas disease
PKR	double-stranded RNA-activated protein kinase
qPCR	quantitative polymerase chain reaction
qRT-PCR	quantitative reverse transcription polymerase chain reaction

r^2	correlation co-efficiency
RAG	recombinant activator factor
RC	reference control
RER	rough endoplamic reticulum
RFP	finger proteins
-RNA	(-) strand RNA
RNA	ribonucleic acid
RT	reverse transcription
RTG-2	rainbow trout trout gonad cells
RT-PCR	reverse transcription polymerase chain reaction
SAV	salmonid alphavirus
SD	sleeping disease
SD	standard deviation
SE	standard error
sec	seconds
SEM	scanning electron microscopy
SG	SYBR green
SHK-1	salmon head kidney -1 cells
SPD	salmon pancreas disease
SPDV	salmon pancreas disease virus
SSC	saline-sodium citrate buffer
SSE	suppression subtractive hybridisation
STAT	signal transducers and activators of transcription
TAE	Tris acetate EDTA
TBS	Tris buffered saline
Tc	T-cytotoxic cells
$TCID_{50}$	50% tissues culture infective dose
TEM	Transmission electron microscopy
Th	T-helper cells
TLR	Toll like receptors
TNF-α	tumour necrosis factor alpha
Trypsin /EDTA	trypsin in 0.01 % ethylenediaminetetraacetic acid
TTBS	Tris buffered saline with Tween-20
TUNEL	Terminal deoxynucleotidyl transferase end labelling
TYK	tyrosine kinase
UK	United Kingdom
USA	United States of America
UV	ultraviolet
V	volt
v/v	volume/volume
VHSV	viral haemorrhagic septicaemia virus
VN	virus neutralisation
w/v	weight/volume
ZFPs	zinc finger proteins

Abstract

Salmonid alphaviruses (SAV) are a group of viruses that have recently emerged as a serious threat to the salmonid aquaculture industry in Europe. Over recent years, diseases caused by SAV have severely hampered the Scottish, Irish and Norwegian Atlantic salmon industry, and are considered to be among the major economically important viral diseases affecting the industry at present. Amongst the six subtypes characterised so far, Salmonid alphavirus 1 (SAV1) causes severe pathology in the heart, pancreas and the skeletal muscle of Atlantic salmon leading to death and growth retardation in the affected fish. The biochemical characteristics of the virus and the sequential pathology of the diseases caused by SAV have been described; however the mechanisms responsible for causing the disease and the host defence mechanisms against the virus are poorly defined. This thesis therefore examined the pathogenesis of SAV infection at the cellular and molecular level *in vivo* in salmon and *in vitro* in salmonid cells, with a special emphasis on host immune defence mechanisms against the virus.

SAV was first isolated from Chinook salmon embryo-214 (CHSE-214) cells in 1995 in Ireland. Several cell lines have since been used to grow the virus. In the present study, three established salmonid cell lines, Chum salmon heart -1 (CHH-1), CHSE-214 and Salmon head kidney -1 (SHK-1) were evaluated for their ability to support the isolation of SAV-1 from infected fish tissue, with CHH-1 cells giving the fastest cytopathic effect (CPE) during primary isolation. The CPE appeared as localised cell-rounding on CHH-1 and CHSE-214 cells, although in SHK-1 cells, the cells were seen to slough off the monolayer relatively later than with the other two cell lines during the infection.

The host response to SAV infection was evaluated by experimentally infecting Atlantic salmon parr using a cell culture-adapted virus isolate. A quantitative reverse transcription polymerase chain reaction (qRT-PCR) was developed to examine the virus load in the fish, from which it was found that the highest viral RNA copy number was detected at 5 day post infection (d.p.i), of the 90 day experimental infection period. Characteristic pathological lesions were only seen in the pancreas and the heart but not in the skeletal muscles of the infected fish. A gene expression study using qRT-PCR revealed the rapid induction of interferon (INF) and INF-associated genes in the head kidney of the infected fish compared to the control fish. The Mx protein was found to be highly expressed in the heart and the mucous membranes of infected fish by immunohistochemistry. Interestingly, the pathological changes that were seen occurred some time after the peak expression of genes associated with the INF-1-pathway. When the host-virus interaction of Atlantic salmon infected with SAV was examined using a microarray, a potent first line defence response was observed, together with the signatures of early activation of the adaptive immune response during the initial stages of the infection. Genes associated with transcription, translation and lipid metabolism were significantly differentially expressed in virus infected fish compared to control fish. A large array of antiviral genes was significantly expressed, amongst which were some of the genes also described in mammalian alphavirus infections. Genes associated with apoptosis and anti-apoptosis were also seen to be differentially regulated showing the complexity of the host-virus interaction. Collectively, all of these findings suggest that a non-specific antiviral immune response takes place providing rapid immune protection during the early stages of SAV infection in salmon.

In the study on morphogenesis of SAV in salmonid cells using electron microscopy (EM), a rapid internalization of virus into the cells and generation of replication

complexes using the secretory pathway of the cell, similar to mammalian alphavirus replication was observed. The mature viruses were released through surface projections, acquiring envelopes from the host cell membrane. From the ultrastructural studies of the salmonid cells infected with SAV, a progressive chromatin marginalisation and condensation could be seen, leading to cellular fragmentation, forming membrane bound apoptotic bodies, characteristic of progressive apoptosis. The activation of caspase-3 in the cytoplasm and genomic DNA damage were also seen in the infected fish cells, indicating that apoptosis is the main cause of cell death during SAV infection.

The results of this study have increased our knowledge and understanding of the cellular and molecular mechanisms involved in the pathogenesis of SAV infection, emphasising the importance of the first line defence mechanisms against SAV infection in salmon. This has given an interesting insight into the host mechanisms used to combat the virus during infection, and will undoubtedly be useful for designing new vaccines and management strategies for prevention and control of this important disease.

Publications and Presentations from the Thesis

Publications

T K. Herath, J. Z. Costa, K.D. Thompson, A. Adams and R. H. Richards (2009). Alternative Cell Lines for the Isolation of Salmon Alphavirus-1. Icelandic Agricultural Sciences (22)19-27.

Manuscript in preparation

T K. Herath, K.D. Thompson, J. E. Bron, J.B. Taggart .A. Adams and R. H. Richards Transcriptomic analysis of salmon alphavirus 1 infection (in preparation).

T K. Herath, K.D. Thompson, A. Adams and R. H. Richards. Interferon-mediated antiviral response in experimentally induced salmonid Alphavirus 1 infection in Atlantic salmon (in preparation).

T K. Herath, K.D. Thompson, A. Adams, R. H. Richards and H.W. Ferguson. The ultra structural morphogenesis of Salmonid Alphavirus (in preparation).

Scientific conferences and meetings

T.K. Herath, K.D. Thompson, J. E. Bron, J.B. Taggart, R. H. Richards and A. Adams. Transcriptomic analysis of Atlantic salmon host response to experimentally induced SAV-1 infection. 14th EAFP international conference, 14th -19th September 2009, Prague, Czech Republic (Oral presentation).

T.K. Herath, J. E. Bron, K.D. Thompson, A. Adams, R. H. Richards and J.B. Taggart. Host response to salmonid alphavirus infection. Fourth integrative physiology post-graduate students' conference 27-29th May 2009, University of Aberdeen, Aberdeen, UK (Invited oral presentation).

Tharangani Herath, Kim Thompson, Alexandra Adams, James Bron and Randolph Richards. Apoptosis in pathogenesis of salmon pancreas disease. International symposium on Scottish Aquaculture, A sustainable future. 21-22nd April 2009, The Edinburgh Conference Centre, Heriot-Watt University Edinburgh, UK (Poster presentation).

Tharangani Herath, Kim Thompson, Alexandra Adams and Randolph Richards, Pathogenesis and early defence mechanisms of Salmonid alphavirus 1 infection. PhD research conference, 28th October 2008, Institute of Aquaculture, University of Stirling (Oral presentation).

T. K Herath, K.D. Thompson, A. Adams and R.H Richards. Apoptosis-induced cell death in salmonid alphavirus infection. International conference on Fish Diseases and Fish Immunology. 6 – 9th September 2008, Reykjavik, Iceland (Poster presentation).

T.K. Herath, J. E. Bron, K.D. Thompson, A. Adams, R. H. Richards and J.B. Taggart. Gene expression profiling of Atlantic salmon experimentally infected with salmonid Alphavirus. Annual Scottish Fish immunology Research Centre meeting, 21st August 2008, University of Aberdeen, UK (Oral presentation).

Tharangani Herath, Kim Thompson, Alexandra Adams, Amer Diab, Matteo Minghetti and Randolph Richards. Early antiviral response in Atlantic salmon experimentally infected with Salmonid alphavirus 1. American Fisheries Society Fish Health Section,

14th annual meeting. 9-12th July 2008, Atlantic Veterinary College, University of Prince Edward Island, Canada (Oral presentation).

T. K Herath, K.D Thompson, A. Adams, R.H. Richards and H.W Ferguson. Utrastructural morphogenesis of Salmonid alphavirus 1. American Fisheries Society, Fish Health Section, 14th annual meeting. 9-12th July 2008, Atlantic Veterinary College, University of Prince Edward Island, Canada (Poster presentation).

Tharangani Herath, Kim Thompson, Alexandra Adams, Amer Diab, Matteo Minghetti and Randolph Richards. Antiviral gene expression in Atlantic salmon experimentally infected with salmonid alphavirus 1. EADGENE 4th annual meeting on Animal Genomics. 9-12th June 2008, Edinburgh, UK (Poster presentation).

Tharangani Herath, Kim Thompson, Alexandra Adams and Randolph Richards. PD work at Institute of Aquaculture; an up date. Trination PD meeting 5-9th November 2007, Bergen Norway (Oral presentation).

Tharangani Herath, Kim Thompson, Alexandra Adams and Randolph Richards. PD work at Institute of Aquaculture; an up date. Trination PD meeting 8-9th May 2008, Galway, Ireland (Oral presentation).

Tharangani Herath, Kim Thompson, Alexandra Adams Randolph Richards, PD work at Institute of Aquaculture; an up date. Trination PD meeting 5-8th March 2009 University of Stirling, UK (Oral presentation).

Table of Contents

List of Figures

transcribed into viral encoded (-) strand complementary RNA. Synthesis of RNA for poly-protein P1234 (shown above the genomic RNA) codes for 4 non-structural proteins nsP1-4 and RNA for poly-protein c-p62-6K-E1 codes for structural protein E1-E3, C capsid, protein 6K (shown below the Genomic RNA). 148

List of Tables

Chapter 1

General Introduction

1.1 Background

The overall expectation of this thesis was to explore the mechanisms of disease associated with salmonid alphavirus 1 (SAV1) infection in Atlantic salmon (*Salmo salar* L.) and in established salmonid cell lines, with a special emphasis on the immune response of infected fish. Salmonid alphaviruses have caused severe losses to the European salmon farming industry during recent years, although the actual loss to the industry still remains to be disclosed. Host–pathogen interactions and the defence mechanisms against SAV infections are still poorly understood. Understanding the mechanisms of the disease at a cellular and molecular level, in relation to the environment in which the host lives, will help in improving current management practices (Slauson & Cooper, 2002). This may also assist in the development of new strategies for controling and preventing SAV-associated disease, and ultimately eradicate the disease. Such strategies will hopefully ensure healthy stocks and the sustainability of the aquaculture industry while achieving production targets.

1.2 Fish health and fish viral diseases in global aquaculture

Global aquaculture production has increased tremendously during the last five decades (Liu & Sumalia, 2007) supplying half of the seafood demand globally for human consumption in 2008 (FAO, 2008). Aquaculture is also regarded as the fastest growing

food animal industry in the world at present. Atlantic salmon is the most popular cultured species in coldwater, marine aquaculture. Farmed salmon production has steadily increased over the last few decades, achieving live-weight production from 500 tons in 1970 to over 1.3 million tons in 2005, and accounting for 11 % of the overall harvest of aquaculture in 2008 (FAO, 2008). The leading salmon producers in the world, Norway, Chile, UK and Canada together provide over 85 % of the total world farmed salmon (Liu & Sumalia, 2007). This impressive level of growth is in part attributed to the decline in wild marine fisheries resources (Gozlan *et al*., 2006) and the emergence of welfare and conservation concerns of wild fish stocks, in addition to the increase in global fish and shellfish consumption because of the emphasis given to healthy eating habits.

Diseases are the cause of the most significant losses to the aquaculture industry, losses of the entire stock sometimes occurring over a few days. Viral diseases are a major threat to the industry and several new viral diseases have been described in salmon aquaculture following commercialisation of the species (Hogstad, 1993; Gozlan *et al.*, 2006; Liu & Sumalia, 2007). Therefore, effective fish health management plays a vital role in maintaining the sustainability of the industry, and has been given much more consideration in recent decades (Adams & Thompson, 2006). The viruses that cause enzootics in aquaculture may be present naturally in the environment, or may have been introduced in to the site (Gozlan *et al*., 2006). As an example, many of the newly emerged viral diseases such as Infectious Salmon Anaemia Virus (ISAV) and SAV in salmon were identified only after commercialisation of the industry a few decades ago, and were designated as diseases with 'unknown aetiology' initially. This suggests that

these viruses were already present in the environment without causing any disease, but optimisation of the conditions for fish farming may have also optimised the conditions for virus replication and transmission and in turn become epizootics. A recent report indicated that at least 94 pathogenic agents of known aetiology have been introduced to European waters via stock movements during recent aquaculture intensification (Gozlan *et al*., 2006). Therefore health and wellbeing of fish in aquaculture needs close monitoring with the introduction of effective disease control strategies.

The increased occurrence of viral disease in hatcheries and during the grow-out stages of salmon farming could result from increased stress and high stocking densities used in the intensified farming system. Poor hygiene measures, improper disease monitoring programmes and poor bio-security increases the risk of disease outbreaks (Murray & Peeler, 2004). Viral infections that originate in the farming environment not only threaten other farmed fish but also wild fish and fisheries, thus leading to increasing concerns by animal welfare groups (Gozlan *et al*., 2006).

The reports of viral diseases in fish date back to the middle ages. In the text relating fish diseases published in 1904 by Bruno Hofer of Germany, the person who was considered to be the father of fish pathology, noted that reports of carp pox were documented as early as in 1563 by a mediaeval zoologist K. Von Genser (Wolf, 1988). Although little was known about viral diseases of fish up until 30 years ago, our knowledge of fish viral diseases has increased impressively during the last two decades At present, the viruses known to be pathogenic to fish are divided into 11 families, including two families of DNA viruses (Family *Iridoviridae* and *Herpesviridae*) and nine families of RNA viruses (*Picornaviridae, Birnaviridae, Reoviridae, Rhabdoviridae,*

3

Orthomyxoviridae, Paramyxoviridae, Retroviridae, Coronaviridae and Togaviridae).
Emergence of diseases associated with RNA viruses in fish has increased the attention
of public and veterinary bodies. The fish disease commission of the Office International
des Epizooties (OIE), France has elaborated the fish diseases that have a socio-
economic and public health impact on aquatic animals transported internationally and
aquatic animal products. However, some of the newly emerged diseases that cause
severe damage to the industry such as SAV, are not listed as notifiable by OIE, possibly
due to the lack of information on the economic importance of the disease and the extent
of its global importance and geographic distribution. However, SAV is classified as a
notifiable disease by the Food Safety Authority in Norway, the major salmon producing
country in the world (Graham *et al.*, 2008; Viljugrein *et al.*, 2009; Aldrin *et al.*, 2010).

1.3 **Alphavirus (Family *Togaviridae*)**

The alphaviruses, of the family *Togaviridae,* are a group of RNA viruses with a world
wide distribution with the exception of Antarctica (Strauss & Strauss, 1994).
Alphaviruses have been isolated and identified from both vertebrates and invertebrates.
Typically, alphaviruses are transmitted by an arthropod vector (i.e. mosquitoes of *Aedes*
and *Culex* families and haematophagus arthropods such as mites, bugs and ticks), with
the exception of teleost alphaviruses. At least 27 serologically distinct alphavirus
species have been reported causing different diseases in vertebrates (Klimstra & Ryman,
2009). Alphaviruses can replicate in a broad range of vertebrate hosts, including
mammals, birds, reptiles and fish. Birds and small mammals serve as the natural
reservoirs for the virus, while humans act as a dead-end host in the life cycle of the virus
(Strauss & Strauss, 1994). The diseases caused by alphaviruses are associated with
either encephalitis (Eastern equine encephalitis EEE, Venezuelan equine encephalitis

VEE, Western equine encephalitis WEE) or poly-arthritis (Chikungunya, O'Nyong-Nyong, Ross river, Sindbis, Semliki forest) (Powers *et al.*, 2001). SAV is the only alphavirus so far reported to cause disease in fish (McLoughlin & Graham, 2007) and is considered to be atypical, with the ability of cross transmission between hosts, independently from vectors during the life cycle, compared to the classical arthropod borne alphavirus life cycle of other vertebrates (McLoughlin & Graham, 2007).

1.4 **Salmonid alphavirus**

1. 4. 1 **Diseases caused by salmonid alphaviruses**

Salmonid alphaviruses cause a severe, multi-systemic disease in farmed Atlantic salmon and rainbow trout (*Oncorhynchus mykiss* Walbaum) and are a newly emmerged group of viruses in Europe. They have been classified into six genotypically and geographically distinct subtypes; i.e. SAV1 (Weston *et al.*, 1999), SAV2 (Villoing *et al.*, 2000a), SAV3 (Hodneland *et al*., 2005) and SAV 4, 5, and 6 (Fringuelli *et al.*, 2008). Subtypes (SAV1, 3, 4, 5 and 6) are responsible for causing pancreas disease (PD) in Atlantic salmon, while SAV2 causes sleeping disease (SD) in fresh water reared rainbow trout and Atlantic salmon at seawater phase in Scotland, and SAV3 causes Norwegian salmon pancreas disease (NSPD) in Atlantic salmon and rainbow trout in Norway (Fringuelli *et al.*, 2008; Graham *et al.*, 2010). Subtypes SAV1, 2, 4 and 5 have been found in the UK, and SAV1, 4 and 6 are reported as causing outbreaks in Ireland. The third sub type, SAV3, has only been reported from Norway (Hodneland *et al.*, 2005; Hodneland & Endresen, 2006; Fringuelli *et al.*, 2008). Apart from Europe, PD had been reported once in the USA (Kent & Elston, 1987) and toga-like virus particles have been found associated with a disease outbreak reported as a dual infection with ISAV and alphavirus in salmon in New Brunswick, Canada (Kibenge *et al.*, 2000).

However, neither virus isolation nor sequence identity was attempted on samples taken during these outbreaks (McLoughlin & Graham, 2007; Graham *et al.*, 2010).

The conditions occurring in farmed Atlantic salmon referred to as exocrine pancreas disease (Munro *et al.*, 1984; McLoughlin & Graham, 2007; Graham *et al.*, 2010), polymyopathy syndrome and sudden death syndrome (Rodger, 1991) are all thought to be PD, named differently because of the variation seen in clinical and histopathology signs (McLoughlin & Graham, 2007). The different subtypes that have now been identified based on sequencing viral RNA shows sequence homogeneity to the other alphaviruses.

Pancreas disease or salmon pancreas disease (SPD) of farmed Atlantic salmon has been reported as occurring in Scotland since 1976 (Munro *et al.*, 1984; McVicar, 1987, Wheatley *et al.*, 1994). For some time the nature of the disease and the clinical signs associated with it led scientists to believe that the disease was of viral aetiology (McVicar, 1987; Raynard & Houghton, 1993), although the actual agent that was responsible for the disease, a Toga-like virus, was only isolated in Ireland by Nelson and others in 1995 by co-cultivating the head kidney of diseased fish in CHSE -214 cells (Nelson *et al.*, 1995). The virus that causes salmon pancreas disease (SPDV) was later identified as an alphavirus of the family *Togaviridae* (Weston *et al*, 1999). The biochemical characteristics of SPDV were similar to many other alphaviruses (Welsh *et al.*, 2000). Two of the major proteins of the virus with molecular weights of 55 kDa and 50 kDa were identified as E1 and E2 glycoproteins (Weston *et al.*, 1999; Welsh *et al.*, 2000) (Figure 1.1).

Sleeping disease in rainbow trout caused by SAV2 was considered to be a disease that only occurred in fresh water until recently when the virus was found in seawater farmed Atlantic salmon in Scotland (Fringuelli *et al*., 2008; Graham *et al*., 2009, 2010). It was named SD because the fish lie in a lateral posture on the bottom of the tank and only start moving once disturbed (Boucher, 1995). It presents similar histopathological changes to PD and was also suspected to have a viral etiology (Boucher & Laurencin, 1996). The virus that was responsible for causing the disease was first identified in France by Castric *et al.* in 1997, and was characterised as an atypical alphavirus based on its biochemical, physiological and morphological characteristics (Villoing *et al.*, 2000a). Sequence analysis studies later found that SD was closely related to PD and the common name 'salmonid alphavirus' for this group of viruses was then proposed (Weston *et al*., 2002) and it has un-officially been used by the scientific community, although the name has not yet been formally approved by the International Committee on Taxonomy of Viruses (ICTV). Apart from France, SD has also been reported from fresh water farmed rainbow trout in the UK (Branson, 2002; Graham *et al.*, 2003b), Ireland, Spain, Italy (Graham *et al.*, 2007b) and Germany (Bergmann *et al.*, 2008) (Table 1.1).

The third sub type of the group SAV3, is closely related to SAV1 and SAV2. The SAV sub- types 4, 5, and 6 have only been identified recently based on the sequence analysis of the E2 and nsP3 regions of the genome, and appear to be associated with a distinct geographical distribution. For example SAV4 has been found both in Scotland and Ireland, while SAV5 and SAV6 have been reported in marine farmed Atlantic salmon in Scotland and Ireland, respectively (Fringuelli *et al.*, 2008).
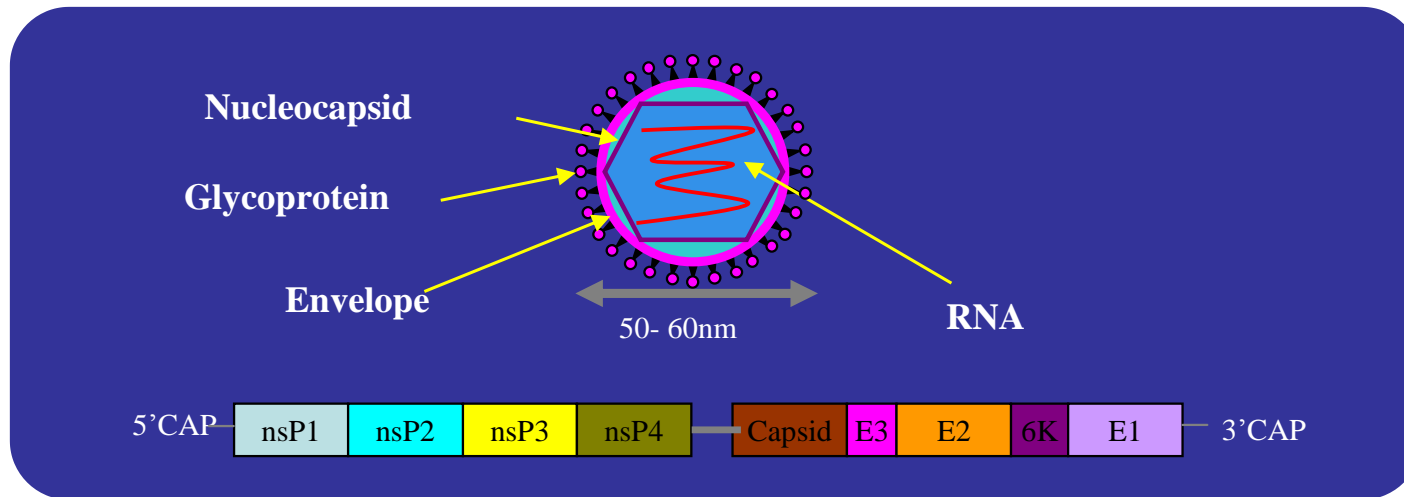
Figure 1. 1 Schematic diagram of SAV structure and the genome organization. The genomic RNA of the virus is surrounded by capsid proteins forming the nuclocapsid. The 5' end of the positive sense single strand RNA genome of the virus genome encodes 4 structural proteins while the 3' end encodes 5 structural proteins. The envelope of the virus is acquired while budding through the plasma membrane and it surrounds the nucleocapsid. The surface of the envelope is enriched with virus glycoprotein spikes.

These genetically and geographically distinct SAV sub-types cross-react serologically with each other, and it is therefore impossible to distinguish them from one another, unless sequencing or highly-sensitive molecular methods such as qRT-PCR are used.

Cross infection in Atlantic salmon, rainbow trout and brown trout with SAV1, SAV2 and SAV3 has also been demonstrated experimentally (Table 1.1). As PD and SD occurred in sea water and freshwater under natural condtions in salmon and rainbow trout respectively has allowed differential diagnosis of these two conditions from each other under natural conditions, but this has now changed with the recent identification of SAV2 from Atlantic salmon in sea water in Scotland (Fringuelli *et al.*, 2008).

1. 4. 2 **Salmonid alphavirus structure**

Sequencing of the 3' end of the SAV genome has demonstrated the presence of a conserved sequence typical of alphaviruses (Weston *et al.*, 1999, 2002; Villoing *et al.*, 2000a; Fringuelli *et al.*, 2008). Mature virions are approximately 65.5 ± 4.3 nm diameter (Nelson *et al.*, 1995) and are composed of a positive sense, single stranded RNA (+ssRNA) genome packed with capsid protein forming the nucleocapsid of the virus. The capsid proteins of classical alphaviruses are arranged in pentamers and hexamers to form T=4 icosahedral symmetry (Strauss and Strauss, 1994; Cann, 2005). The nucleocapsid of the virus is enveloped with a phospholipid bilayer, the composition of which resembles the host plasma membrane. The viral glycoproteins are anchored to the envelope and appear as spikes (Figure 1.1)

Table 1.1 Geographical distribution and natural and experimental hosts of different SAV subtypes (Fringuelli *et al.*, 2008).

Sub type	Disease	Location	Species affected	
			Natural infection	**Experimental infection**
SAV-1	PD	Scotland/Ireland	Atlantic salmon[a]	Atlantic salmon[a b] rainbow trout[a] brown trout[a]
SAV-2	SD/PD	France, Ireland, UK, Italy, Spain, Germany,	Rainbow trout[b] Atlantic salmon[a]	Atlantic salmon[b] rainbow trout[b] brown trout[b]
SAV-3	PD	Norway	Atlantic salmon[a] Rainbow trout[a]	Atlantic salmon[a b] Rainbow trout[a b]
SAV-4	PD	Scotland/Ireland	Atlantic salmon[a]	n/a
SAV-5	PD	Scotland	Atlantic salmon[a]	n/a
SAV-6	PD	Ireland	Atlantic salmon[a]	n/a

[a] Sea water, [b] Fresh water, [a b] Sea water and fresh water, SD sleeping disease, PD pancreas disease, n/a not known.

The 11.9 kb size genome of SAV is composed of two open reading frames, in which the 5' end of the genome encodes 4 non-structural proteins (nsP1-nsP4) essential for virus replication, and the 3' end of the genome encodes for 5 structural proteins (E1, 6K, E2, E3 and capsid protein) (Figure 1.1). Recently a further 8kDa protein (known as TF) has been shown to originate from the use of an alternative reading frame, and this protein is also incorporated into the mature virion (Firth *et al.,* 2008). Structural proteins E1 and E2 are considered as the major antigenic determinant sites and are arranged as heterodimers on the glycoprotein spikes. Three copies of the heterodimers intertwine together to form a glycoprotein spike and 80 spikes are organized into the T=4 icosahedral surface of the alphavirus (Mukhopadhyay *et al.*, 2010). The 3' end of the genome is also enriched with a non-coding poly-A tail.

The genomes of SAV1 and SAV2 are comprised of 11,919 and 11,900 nucleotides, respectively. As with other alphaviruses, SAV also appears to replicate in the cell cytoplasm and is then released to the external environment via budding from the plasma membrane, (McLoughlin & Graham, 2007), as shown below from salmonid cell cultures infected with SAV (Figure 1.2).
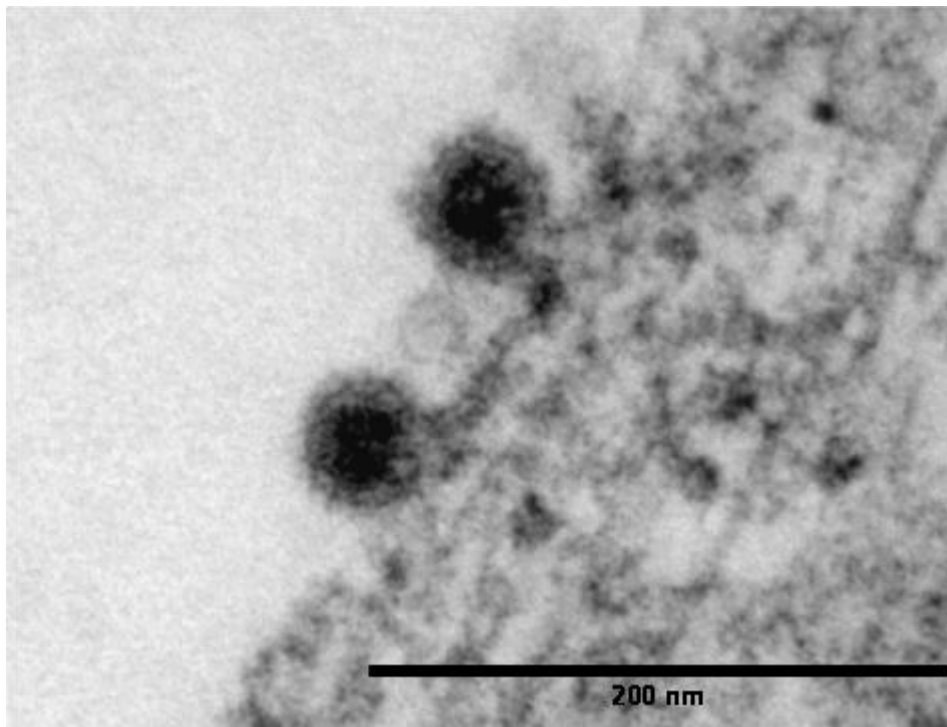
Figure 1. 2 Transverse electron micrograph of salmonid alphavirus 1, budding from CHSE-214 cell culture.

The nucleotide and amino acid sequences of SAV1 and SAV2 and SAV2 and SAV3 appear to be very similar. The nucleotide sequence identity and the amino acid identify of these three sub-types is above 90 % and 95 % respectively. The nucleotide identity

between SAV1 and SAV2 reference strains is 95% and 93.6%, respectively while showing a low level of homogenity (30-40%) with other alphaviruses (Weston *et al.*, 2002; McLoughlin & Graham, 2007). The SAVs differ structurally from mammalian alphaviruses by containing larger structural and non-structural proteins, on the unglycosylated E3 region, and the presence of short untranslated regions in the 5' and 3' ends of the genome.

1. 4. 3 **Pathology of SAV**

Clinical signs

The clinical presentation of PD can be per-acute, acute or chronic and fish can recover from the disease depending on the length and the severity of the signs presented in the fish (McLoughlin & Graham, 2007). The main clinical signs associated with PD in sea water reared Atlantic salmon (SAV1 and SAV3) are sudden inappetence, lethargy, crowding into corners, fish swimming close to the surface of the cages, increased amount of yellow faecal casts in the cages, illthrift, listlessness, inability to maintain posture and finally mortality (Munro *et al.*, 1984; Ferguson *et al.*, 1986b; McVicar, 1987; McLoughlin *et al.*, 2002). The clinical signs of chronic PD can also include slow growth and emaciation, resulting in 'runts' in the affected population (Desvignes *et al.*, 2002; McLoughlin *et al.*, 2002). Fin-erosion and ulceration commonly seen in diseased fish are considered to be secondary complications of the infection. In some instances, regurgitation of ingested food is seen, suggesting degeneration of the oesophageal striated muscles (Ferguson *et al.*, 1986a, 1986b). Severe heart and skeletal muscle failure can lead to sudden death in healthy looking fish in good condition (McLoughlin *et al.*, 2002). Spiral swimming, fish lying down in the bottom of the tank as if dead and then moving when handled is a clinical feature of fish with severe muscle damage

(McLoughlin & Graham, 2007). Impaired swimming can occur in SAV-affected fish as a result of the skeletal muscle lesions associated with SAV (Ferguson *et al.*, 1986b). The poor condition of the fish after recovery results from lack of feeding and/or digestive enzymes during the infection.

The sleeping nature of the rainbow trout infected with SD, as mentioned earlier, is presumed to be caused by extensive necrosis of the red skeletal muscle (McLoughlin & Graham, 2007). Significant bilateral exophthalmia, poor feeding performance, emaciation and low body fat levels have been observed in experimental infections 5-7 weeks post infection. All ages of rainbow trout are susceptible to SD but the severity of the clinical disease is greatest in fingerlings (10-15g). The clinical disease in older fish is milder, and infection can be present in fish even without showing apparent signs. The SD can extend up to 42 d.p.i along with lethargic swimming behavior in affected populations. Some of the immobile fish are hyper-excitable in response to disturbance (Boucher, 1995).

Gross pathology

The earliest gross signs of PD outbreaks are the absence of food in the gut of the fish and increased faecal casts in tanks. In some instances, petechiation in the fat around the pyloric caeca can be observed. During extended periods of infection, emaciated fish with long thin bodies with very little body fat can result and this results in downgrading of the stocks (McLoughlin *et al.*, 2002). Pale and mottled livers are sometimes observed in field outbreaks and although these have never been reported under experimental conditions, they could possibly be a complication secondary to the heart pathology and the pancreatic damage (Ferguson, *et al.*, 1986b; Taksdal *et al.*, 2007).

Histopathology

The characteristic histopathology of SAV essentially involves different combinations of lesions, of different severity in the exocrine pancreas, heart and skeletal muscle. In some instances, lesions associated with the oesophagus (Ferguson *et al.*, 1986a, 1986b) and the kidney (Taksdal *et al.*, 2007) were also reported. The presence of exocrine pancreatic lesions was the first sign to be seen in histology in SAV affected fish and this was was considered as the hallmark in diagnosing the disease (Munro *et al.*, 1984) until the association with myopathy was described by Ferguson and others (1986b). The classical lesions of SAV include severe acute exocrine necrosis of the pancreas followed by chronic fibroplasia in recovering animals (Ferguson *et al.*, 1986b; McVicar, 1987; McLoughlin *et al.*, 1995, 1996, 1997, 2002). Pancreatic lesions of NSPD were said to be more similar to Infectious Pancreatic Necrosis virus (IPNV) infection than to pancreatic lesions seen in PD reported in Scotland and Ireland (Poppe *et al.*, 1989), but SD gives similar lesions in the pancreas to that of PD.

Although the presence of heart and skeletal myopathies were not consistently seen in the study by McVicar (1987), they are frequently associated with the pathogenesis of SAV as seen by Ferguson *et al.*, (1986b), and Rodger *et al.,* (1994). The cardiac lesions seen in SAV-affected fish consist of different degrees of focal to diffuse myocardial degeneration and necrosis in both spongy and compact layers of the ventricle and the atrium, in addition to inflammation characterised by mononuclear cell infiltration (Ferguson *et al.*, 1986b; McLoughlin & Graham, 2007). The SD associated cardiac lesions seen during natural and experimental infections are also consistent with the heart lesions seen during PD, however heart lesions do not always occur with NSPD (Taksdal

et al., 2007). Skeletal lesions associated with SAV appear 2-3 weeks after the first signs of lesions in the pancreas, and are characterised by hyaline degeneration, a variable degree of inflammation and fibrosis in both red and white skeletal muscles (Ferguson *et al.*, 1986b; Murphy *et al.*, 1992; McLoughlin *et al.*, 2002). Skeletal lesions in rainbow trout during SD are considered to be more severe than the lesions seen with PD in Atlantic salmon (Ferguson, 2006).

The presence of interstitial cells filled with eosinophilic granular materials along the sinusoids of the kidney were also seen in NSPD induced by SAV3 (Taksdal *et al.*, 2007) and have occasionally been seen in some reported cases of PD occurring in the Shetland Islands, Scotland (McLoughlin & Graham, 2007). Focal gliosis in the brain of fish experimentally infected with SAV1 indicate the involvement of nervous tissue in the infection (McLoughlin & Graham, 2007). Degeneration of oesophageal muscles has also been reported in earlier descriptions of the diseases, but has not been reported recently (Ferguson *et al.*, 1986b; Ferguson, 2006).

1. 4. 4 **Pathogenesis of SAV**

The description of the pathogenesis of SAV has so far been based on the sequential pathology of fish naturally and experimentally infected with SAV. Initially, the presence of low levels of selenium and Vitamin E in the plasma of PD-affected fish led to the conclusion that PD was a result of some nutritional deficiency in salmon (Ferguson *et al.*, 1986a; Bell *et al.*, 1987; Raynard *et al.*, 1991; Pringle *et al.*, 1992; Grant *et al*., 1994; Rodger *et al.*, 1995), until it was discovered that the disease could be cross transmitted from diseased fish to healthy fish using kidney homogenates (McVicar, 1990; Raynard & Houghton, 1993; Wheatley *et al.*, 1994). The optimum

temperature for spread of the disease was found to be around 14°C and the infectious material was sensitive to chloroform suggesting the involvement of an enveloped virus (Nelson *et al.*, 1995). McLoughlin *et al.* (1996) have confirmed that virus grown in cell culture could reproduce the disease in Atlantic salmon post-smolts, the clinical signs of which were indistinguishable from field outbreaks, causing lesions in the pancreas, heart and skeletal muscles. Cross transmission studies carried out under experimental conditions revealed a different degree of susceptibility between Atlantic salmon, rainbow trout and brown trout (Boucher *et al.*, 1995) and variation in the strain susceptibility to the disease by Atlantic salmon (McLoughlin *et al.*, 2006). In two parallel experimental infections, conducted by injecting SAV1 derived from cell culture grown virus and SAV3 infected clinical material into fish, disease signs were observed to different degrees, suggesting variations in the degree of pathological outcome due to complex host, pathogen, and environment interaction. However, none of the experimental infections resulted in mortalities, as occur in field outbreaks (McLoughlin & Graham, 2007), until recently though this has apparently been shown by a Norwegian research group (unpublished data).

1. 4. 5 **Differential diagnosis**

Other conditions that are differentially diagnosed from SAV infections in Atlantic salmon include IPNV infection, Cardiomyopathy Syndrome (CMS) and Heart and Skeletal Muscle Inflammation (HSMI) (Ferguson, 2006; McLoughlin & Graham, 2007). IPNV is a widespread infectious disease of Atlantic salmon with known viral aetiology (*Aquabirnaviridae*) and also affects the exocrine pancreas, similar to SAV. It

can be easily differentiated from SAV infections by the presence of characteristic catarrhal enteritis and the absence of cardiac or skeletal pathology and by immunohistochemistry (McLoughlin *et al.*, 2002; McLoughlin & Graham, 2007). HSMI and CMS are newly described diseases in farmed Atlantic salmon in Scotland and Norway (Ferguson *et al.*, 1990; Rodger & Turnbull, 2000; Kongtorp *et al.*, 2004b). Both of these diseases appear similar to PD, and occur in the sea water phase of the Atlantic salmon life cycle. HSMI occurs in fish 5-9 months after they have been transferred to sea and CMS is said to occur in salmon in the second year at sea. Both diseases have been confirmed to be caused by an infectious agent recently and are suspected to be of viral aetiology (Kongtorp *et al.*, 2004a; Bruno & Noguera, 2009; Fritsvold *et al.*, 2009; Kongtorp & Taksdal, 2009). They both cause severe lesions in the heart of infected fish just like PD, but can still be differentially diagnosed from PD by the absence of pancreatic lesions (McLoughlin & Graham, 2007). However detection of SAV antibodies in the HSMI affected fish and concurrent occurrence of CMS and SAV have been seen in the field, making differential diagnosis difficult.

1. 4. 6 **Diagnostic tools for SAV**

Clinical signs and histopathology are used conventionally for diagnosis of SAV, how ever, the severity, and the distribution of lesions in the affected tissues and the clinical signs differ depending of the stage of the disease (per-acute, acute, sub-acute, chronic and recovery). Therefore, virus isolation, serology, RT-PCR and qRT-PCR techniques are all used in combination together with the clinical and histological findings to confirm the disease (Table 1.2).

Table 1.2 A diagnostic panel for PD, adapted from McLoughlin & Graham (2007).

Test	Per-acute	Acute	Sub-acute	Chronic	Recovered
Days post infection*	First week	First 10 days	7 -21 days	21-42 days	42 onwards
Signs		Appetite drops	Faecal casts	Mortality	Runts
Virus	Serum, Heart	Serum, heart	Serum, heart	-	-
Histology	n/a	Pancreas, heart	Pancreas, Heart	Heart, Muscle	Heart, Muscle
IHC	n/a	+	+	+	+/-
RT-PCR	+	+	+	+	+
Serology	-	-	-	+	+

* Depends on the temperature, and different pathological stages, + positive for the test, IHC Immunohistochemistry, RT-PCR Reverse transcription polymerase chain reaction, n/a not applicable.

The first isolation of SAV was performed by initially co-cultivating and subsequently serially passaging, PD affected Atlantic salmon kidney in CHSE-214 cells, the standard cell line used for routine laboratory isolation and growth of SAV (Nelson *et al.*, 1995; Graham *et al.*, 2008). The viral growth in CHSE-214 cells was confirmed by observing a CPE in the cells which occurred after several passages of the infected material and was characterised by initial cell rounding to form small discrete reflective groups of cells. The affected cells then become pyknotic, vacuolated and mis-shapen, this effect eventually spreading over the monolayer (Nelson *et al.*, 1995). The initial isolation of SAV using clinical material requires several passages to prove a CPE increasing the risk of obtaining false negative results during virus isolation from these cell cultures (McLoughlin & Graham, 2007). However, the speed and the extent to which the CPE

develops on the cell monolayers increases through serial passaging while adapting virus to the cell cultures. The delay of isolation of virus from the cell cultures is regarded as one of the main reasons for the delay in characterising the aetiology of the diseases as it took nearly seventeen years from the first report of the disease in 1978 (McVicar, 1987) to virus isolation in 1995 (Nelson *et al.*, 1995). Epithelioma papulosum cyprinid (EPC), Fathead minnow (FHM), bluegill fry-2 cells, rainbow trout fibroblast cell and rainbow trout gonad (RTG-2) cells have all been tested in addition to CHSE-214 cells in this initial virus isolation work, but CHSE-214 and RTG-2 were the only cell lines to produce a reliable CPE (Graham *et al*., 2008). However, in a recent study SAV was shown to be able to grow also in Atlantic salmon head kidney derived cells (TO), SHK-1 and Blue fin 2 (BF-2) cells (Graham *et al.,* 2008). Serum has been identified as the best clinical material to use for SAV isolation in cell cultures and the use of serum from an acute stage of an outbreak increases the possibility of obtaining a positive result. The ability to use comparatively fewer samples from live animals leads to serum becoming source of clinical material to use for SAV isolation (McLoughlin & Graham, 2007). A virus-specific monoclonal antibody (mAb) based on an immunostaining technique was developed (Todd *et al.*, 2001) to avoid obtaining the false negative results which occur from CPE-based virus isolation. Use of serum samples as the clinical material and the immunostaining as the detection method has greatly increased the sensitivity of the cell culture virus isolation technique and is presently the most common method employed for SAV diagnostics (Graham *et al.*, 2007a, 2008; McLoughlin & Graham, 2007). The same immunostaining method can also employed as virus neutralisation test to detect the presence or absence of virus specific neutralising antibodies in SAV affected fish. (Graham *et al.*, 2003a). This immunoperoxidase based virus neutralization (IPVN) test was adopted from a 24 well costar plate was based conventional virus neutralisation

(VN) test developed by McLoughlin *et al*, (1996), in which interpretation of results was based on end point titration by observing the development of CPE. In contrast to the IPVN method that is able to give results as fast as 3 days post inoculation (d.p.in), the VN test is only able to give results after 7 d.p.in. The ability to simultaneously detect the neutralising antibody titer and the presence of virus has increased the usefulness of this improved method and is widely being used for SAV diagnostics and research (Graham *et al.*, 2005, 2006a; McLoughlin *et al.*, 2006). Hence all subtypes of SAV fall within a single serotype (Christie et al., 1998; McLoughlin *et al.*, 1998; Graham *et al.*, 2003a, 2007a), IPVN can easily be employed for detecting virus or determining sero-prevalence of SAV infections (Graham *et al*., 2007a, 2010).

A two-step reverse transcription polymerase chain reaction RT-PCR assay developed by Villoing *et al.*, (2000b) was first used to detect SAV2 in natural outbreaks, but was found to be able to detect all SAV (Graham *et al.*, 2006b). Several conventional RT-PCR tests were subsequently developed in different laboratories (Hodneland *et al.*, 2005; Graham *et al.*, 2006b), although none of the tests was able to differentiate the sub-types without post PCR sequence analysis. The TaqMan based qRT-PCR developed by Hodneland & Endresen (2006) was able to differentiate SAV1, SAV2, and SAV3 differentially, increasing the usefulness of quantitative molecular techniques for SAV diagnostics. A SYBR green (SG) based qRT-PCR was also developed to quantify SAV in serum and tissues (Graham *et al.*, 2006b). Recently, 6 different sub-types of SAV have been characterised using cycle sequencing on a large number of virus isolates obtained from different geographical locations in Europe (Fringuelli *et al*., 2008; Graham *et al.*, 2009, 2010; Karlsen, *et al.*, 2009).

1. 4. 7 **Defence mechanisms**

A broad range immune response of PD-affected fish was observed under both natural (McVicar, 1987) and experimental (Houghton, 1994) conditions even before confirming the aetiology of the disease. Production of neutralizing antibodies in SAV-affected fish is known to play a significant role in clearing the virus and providing long lasting immunity. Passive immunisation of fish with convalescent sera from naturally infected fish or sera raised in salmon experimentally injected with kidney homogenate from diseased fish has been shown to give 100 % protection, without any pathology, highlighting the presence of neutralising antibodies in SAV infected fish (Murphy *et al.*, 1995; Houghton & Ellis, 1996). The appearance of neutralising antibody in the diseased fish was first detected around 10-16 days after initial infection, and fish become seroconverted by 21-28 days of infection (McLoughlin *et al.*, 1998; Desvignes *et al.*, 2002). Even though virus specific antibodies do not provide any information on the clinical status of the infection or the type of the virus involved, serology still plays a significant role in SAV diagnostics.

Increased phagocyte activity of the head kidney leukocytes and high lysozyme and complement levels in the infected fish at early stages of infection have been demonstrated by Desvignes *et al.*, (2002). The non-specific defence mechanisms associated with SAV are poorly characterised although it is known that mammalian alphavirus expresses a rapid INF mediated antiviral response.

1. 4. 8 **Disease transmission**

In general all the alphavirus infections are arthropod borne (arboviruses), which use haematophagous arthropods, probably mosquitoes or ticks as vectors in their life cycle with the virus able to replicate within these hosts (Weston *et al.*, 1999). However vector involvement has yet to be identified in SAV infections. Co-habitation infections between healthy and virus infected fish are seen under both natural and experimental infections indicating horizontal transmission of the virus (Raynard and Houghton, 1993; Houghton and Ellis, 1996; McLoughlin *et al.*, 1996) highlighting the SAV is biologically distinct from other alpha viruses. The phylogenetic studies (Fringuelli *et al.*, 2008) and epidemiology modelling studies (Viljugrein *et al.*, 2009; Aldrin *et al.*, 2010) also strongly support horizontal transmission of the disease.

Sea lice (*Lepeophtheirus salmonis*) and *Caligus elongatus* are suspected to be vectors in SAV transmission (Weston *et al.*, 1999). The resent isolation of alpha virus from elephant seal louse (*Lepidophthirus macrorhini*) (Linn *et al.*, 2001) gives a promising positive indication of the presence of vectors in the transmission cycle. In addition, SAV3 was found in *L salmonis* taken from diseased fish using real time PCR but it was not confirmed whether the virus was from the tissues of the parasite or poorly digested blood of salmon present in the gut of the parasite (Karlsen *et al.*, 2006). Information on the carrier status of SAV is not fully known. Graham *et al.*, (2006b) using qRT-PCR has observed the presence of viral RNA in the hearts of infected fish for extended period (90 days), suggesting a possible carrier stage of SAV, however studies are needed to confirm the significance of this with respect to the carrier status of the fish.

1. 4. 9 **Treatment and Control**

SAV appears to be confined to salmonids in Europe, although the possibility of global spread cannot be ignored with the extensive movement of stocks. Good management practices such as all in-all out stocking followed by an appropriate fallow period are recommended. In clinical outbreaks, many farms tend to withhold food for 5-10 days and this appears to decrease the number of mortalities. But, SAV infection can extend up to 2-3 months to infect the whole stock, and the above practice appeared to be not very feasible as a control measure, during the full length of the clinical phase of the infection. Instead, properly planned dietary management is always recommended in farms that are at risk and/or clinically ill. In addition new diets targetting SAV clinical outbreaks are now available in the field.

A commercially available SAV vaccine produced by Intervet Shering-plough is one of the few successful viral vaccines against viral diseases in fish. The first vaccination trial was carried out using a simple formalin-inactivated vaccine and was able to produce 100 % protection in vaccinated fish post-challenge. The success rate of this vaccination is considerably high, eliciting an effective immune protection in the vaccinated stocks, but the duration of the cross protection given against a novel viral attack appears variable. This highlights the need for a better vaccine and a vaccination regime against SAV for the prevention and control of the disease. A variation in disease susceptibility of Atlantic salmon has been observed between fish with different genetic origin, and fish of different smolting stages. This has led to establishing breeding programms by commercial groups to select SAV resistant strains for aquaculture.

1. 4. 10   **Epizootiology and economical importance**

The severity of an SAV outbreak, and associated mortalities, can vary greatly depending on the smolt strain, geographical location, water temperature and feeding regime. The disease was initially observed in salmon in the first year of sea transfer but now can be seen in salmon in their second year at sea (McLoughlin & Graham, 2007). The factors contributing to the massive economic losses of the salmon aquaculture industry by SAV include mortalities that range from 5-50 %, poor growth and runting in up to 10 % of the surviving fish after a disease outbreak, and the grading losses at the time of processing due to discoloured muscle resulting from damaged skeletal muscle (McLoughlin & Graham, 2007).

Pancreas disease was first reported in the mid-1980s in Ireland, and is now considered endemic to Irish waters. The occurrence of the disease has increased over time, and in 2007, more than 90 % of the marine sites have been diagnosed positive for SAV (Rodger & Mitchell, 2007). It is identified as the most significant infectious disease in the Irish salmon industry. The clinical disease can be seen at any time of the year and the mortality rate of the affected site can vary from 1 % - 48 %. A repeat occurrence of the infection at the same site in following years is common in Ireland, suggesting the existence of virus reservoirs at the site.

In Scotland, the number of SPD outbreaks and the distribution of the farms that are positive for PD virus have considerably increased in recent years. The SPD outbreaks in Scotland are reported throughout the year, with peak occurrence detected around August and September (Murray & Kilburn, 2009). The disease caused by SAV has accounted

for at least 11 % of total the annual biomass loss, to the Scottish salmon industry (Murray & Kilburn, 2009).

Pancreas disease was first reported in Norway in the 1980s (Poppe *et al.*, 1989), and now remains a problem for both sea reared Atlantic salmon and rainbow trout. The occurrence of NPDV outbreaks is reported throughout the year with the highest number of cases reported between May and October. Since 2007, Norwegian authorities have listed PD as a list-B notifieable disease within the country, setting up geographical zones, confining PD positive geographical areas, aiming to prevent the spread of the disease to the PD negative sites (Aldrin *et al.*, 2010).

1.5 Fish immune system and immune response to viral diseases

Teleosts form the link between vertebrates and invertebrates, and are considered as the most primitive vertebrate in an evolutionary sense to exhibit both innate and acquired immunity. As a result, the adaptive immune system of fish is comparatively primitive to that of the higher vertebrates, although the innate immune system is advanced in comparison to invertebrates (Plouffe *et al.*, 2005; Whyte, 2007). There is a complex interaction between the innate and the adaptive immune response. The fish immune system inherently elicits a potent immune response as it is continuously challenged by the pathogenic organism existing in the aquatic environment and it faces some extreme environmental conditions. Viral diseases have become one of the major challenges in aquaculture health management today and understanding the immune response towards viral diseases is essential for the future sustainability of the industry.

1. 5. 1 **Morphology of immune system of fish**

The major lymphoid organs present in teleosts are the head kidney, spleen, thymus, and mucosal-associated lymphoid tissue in skin, gill and gut. Macroscopic and microscopic morphology of fish immune organs are distinctly different from mammals. Unlike mammals, fish lack bone marrow and lymph nodes, and their head kidney is the main immune organ involved in lymphoid cell formation. In general their lymphoid tissue is composed of lymphatic cells, and a reticular frame work that maintains the structural integrity of the cellular components of the immune system. The cellular elements of the fish lymphoid tissue comprise lymphocytes, monocytes, macrophages, granulocytes (neutrophils, eosinophils, basophils) and thrombocytes (Press & Evensen, 1999; Roberts & Pearson, 2005). Non-specific cytotoxic cells, mast cells/eosinophilic granular cells, rodlet cells and dendritic cells are also reported from fish (Press & Evensen, 1999; Reite & Evensen, 2006). Melanomacrophages, a distinct type of cells enriched with melanin, haemosiderin, and lipofucsin are supposed to be involved in phagocytosis and are present in all the lymphoid organs in fish (Roberts & Pearson, 2005; Ferguson, 2006).

The kidney is located in the retroperitoneal region of the body cavity of fish and is composed predominantly of cells of the lympho-myeloid lineage. Fish head kidney tissue is involved in haematopoiesis as well as acting as a secondary lymphoid organ (Dalmo *et al.*, 1997). The tissue itself is mainly composed of sinusoids lined by endothelial cells, the adventitial cells which cover the endothelial cells adluminally and the reticular cells that are involved in phagocytosis. The sinusoidal macrophages and the endothelial cells of the head kidney are involved in trapping particles and substances from the circulation (Dalmo *et al.*, 1997). In addition, lymphoid cells of the head kidney

are also involved in antibody production and immune memory (Press & Evensen, 1999).

In teleosts, the spleen is composed mainly of a reticular cell network supporting blood-filled sinusoids that contain a diverse cell population and it is involved in haematopoiesis, clearance of macromolecules, antigen degradation, and processing (Watts *et al.*, 2001). The red pulp and the white pulp of the spleen can be easily differentiated in fish. Melanomacrophage centres are one of the distinct features seen in the spleen of fish and are involved in the destruction of erythrocytes (Press & Evensen, 1999).

The thymus is a paired organ that is situated in the dorsolateral region of the gill chambers, and consists of thymocytes separated from the external environment by a layer of epithelial cells. The cortex of the thymus is densely populated with thymocytes and some epithelial cells present in the medulla are believed to be involved in thymocyte maturation (Press & Evensen, 1999). The thymus appears to undergo involution during post-spawning and its size varies with seasonal changes (Press & Evensen, 1999).

Mucosal-associated lymphoid tissue can be seen in the gut, skin and gill of fish and acts as a local defence tissue in fish. Although gut associated lymphoid tissue is present in fish it is not organized as in mammals. The eosinophilic granular cells that are present between the stratum compactum and the circular muscle layer are believed to be involved in immune function such as inflammation and vasodilatation (Reite &

Evensen, 2006). Leukocytes and plasma cells are also present in skin and gill and act as localised defense cells.

1. 5. 2 **Innate immune system of fish**

The innate or non-specific immune system is present in most multi-cellular organisms. In fish the innate immune system plays an integral part in the defence against pathogens due to an underdeveloped, slowly responding adaptive immune system, compared to mammals (Watts *et al.*, 2001; Whyte, 2007). It is regarded as the 'first line of defence' and as a 'signal of danger' to the presence of foreign material, including pathogens. It also helps in activating the specific immune system during an infection to elicit specific immunity and long-lasting immune memory (Whyte, 2007). As an ectotherm, the innate immune system of fish is temperature independent, allowing them to respond at a variety of temperatures. (Magnadóttir, 2006).

The innate immune system comprises of physical, humoral and cellular factors (Magnadóttir, 2006; Whyte, 2007). The mucous layer and the epithelial cell lineage in the skin, gill and gut act as the main physical barriers that protect fish from pathogen entry. Mucus is rich in a variety of antimicrobial components such as antimicrobial peptides (defensins), lectins, pentraxins, and lysozymes, complement proteins and IgM (Yano, 1996). More recently IgT has also been identified and may have a role in mucosal immunity (Sunyer *et al.*, 2009). Many humoral factors are also involved in the innate immune function such as growth inhibitors (i.e transferins, INF and Mx protein), serum protease inhibitors (α2 macroglobulin, α1 anti-trypsin), various lytic factors (lysozymes, cathepsin, chitinase), complement, agglutinins, precipitins, natural

antibodies, cytokines including interleukin (IL)-1, IL-6, tumor necrosis factor- α (TNF-α), chemokines, acute phase proteins and antibacterial peptides. Acute phase proteins (C-reactive protein, serum amyloid) are also present in fish as humoral factors (Watts *et al.*, 2001).

The complement systems which can be activated through either classical, alternative or lectin-mediated pathways have all been characterised in fish. Different complement components have lytic, pro-inflammatory, opsonic, and chemotactic properties which can induce non-specific phagocytic activity (Boshra *et al.*, 2006). The complement pathway also bridges the innate and adaptive immune systems (Sunyer, *et al.*, 2003). In teleosts, complement factor C3, is present in a variety of different forms giving a greater efficiency to the alternative pathway, compared to mammals (Watts *et al.*, 2001). The complement system can be activated over a wider temperature range, and its activity varies depending on the season.

Non specific cytotoxic cells (NCC) and professional phagocytic cells (neutrophils and macrophages) are the main types of cell involved in non-specifically eliminating pathogens from fish (Moody *et al.,* 1985; Fischer *et al.*, 2006). Dendritic cells also participate in the innate defenses of fish (Graham and Secombes, 1988).

The innate immune system of fish can be modulated by different physical and biological factors including temperature, seasonal factors, pollution, handling and over-crowding, diet and food additives, such as immunostimulants and probiotics, drugs, vaccines, and importantly pathogens. Upon pathogen entry the innate immune system recognises the

stimuli as non-self by binding to Toll-like receptors (TLR), identifying molecules that are associated with the microbes such as polysaccharides, lipopolysaccharides, peptidoglycans, bacterial DNA and double stranded viral RNA (Magnadóttir, 2006). Molecules released as a result of tissue damage such as host DNA, RNA, heat shock proteins, chaperones and oligomannose of pre-secreted glycol proteins can also trigger the innate immune reaction. When the immune responses are induced by foreign molecules, opsonization and phagocytosis begins. Nitric oxide or reactive oxygen species based pathways are also involved in killing phagocytosed pathogens. Different cell signalling pathways, for example, the complement cascade and natural cytotoxic cells are activated as an acute phase response to eliminate pathogens.

1. 5. 3 Adaptive immune system

The adaptive immune system in fish is comparable to higher vertebrates, with the presence of all fundamental features including immunoglobulins (Ig), T-cells and T-cell receptors, the Major Histocompatibility complex (MHC) and Recognition Activator Genes 1 and 2 (RAG1 and RAG2) (Watts *et al.*, 2001). However, the adaptive immune system in fish, in comparson to mammals, has a low antibody repertoire, low immune memory, slow lymphocyte development and lacks in affinity maturation of B-cells (Magnadóttir, 2006), although it is still able to elicit a long lasting immune response during infections. These differences mean that the adaptive immune system in fish is less sophisticated than mammals. This appears to indicate that the adaptive immune system is less important to fish for their biological function, rather than of an inferiority compared to mammals (Kaattari, 1994; Watts *et al.*, 2001).

IgM was the only antibody known to be present in fish until IgD, IgT and IgZ were recently characterised (Randelli *et al*., 2008; Sunyer *et al.*, 2009) unlike mammals which have five classes of Ig, including IgA, IgD, IgG, IgE, and IgM. Fish IgM is present in serum, and mucous secretions of the skin and the gut. The molecular arrangement of teleost IgM is different from mammals as the light and heavy chains are held together by a non-covalent bond instead of disulphide bonds seen in mammalian IgM (Alvarez-Pellitero, 2008). The monomers of fish IgM are present as single monomers or in tetrameric form while IgM in mammals is in pentameric form (Watts *et al.*, 2001). The non covalent binding of IgM tetramers found in fish is believed to enhance the ability of the molecule to bind to different types of epitopes, adjusting their orientation (Solem & Stenvik, 2006). The antibody molecules (Ab) of fish possess relatively low intrinsic affinity and the antigen binding sites are limited in heterogenicity compared to mammals (Kaattari, 1994; Solem & Stenvik, 2006). The teleost IgM molecule is capable in opsonising pathogens to enhance phagocytosis by macrophages (Secombes & Fletcher, 1992; Solem & Stenvik, 2006). They are also able to activate the classical complement pathway, and act as effective agglutinators to foreign molecules. Due to the temperature dependent nature of the specific immune system, the antibody response of fish can be delayed for weeks (Watts *et al.*, 2001).

Information on specific cell-mediated immunity is not widely known in teleosts. Both T and B-lymphocytes are present in fish including salmonids, although the types and the function of different cell repertoires are still to be confirmed (Fischer *et al.*, 2006). The signatures for the presence for the T-cells were reported in fish a few decades ago and the cloning of T-cell receptors, MHC-I, MHC-II molecules and T-cell surface markers CD3, CD4 and CD8 represented a breakthrough in studies on T-cells, examining how

the associated adaptive immune mechanisms operate in fish (Secombes & Zou, 2005; Alvarez-Pellitero, 2008; Randelli *et al.*, 2008). There are two types of T-cells present, T-helper cells (Th) which are enriched with CD4 on the surface and cytotoxic T-cells (Tc) which express CD8 receptors. The antigen bound to the MHC class I and II are recognised by CD8 and CD4 present on the T cells respectively. Therefore MHC class molecules act as a bridge connecting the innate and adaptive immune response.

1.6 Functional genomics for studying immune system of salmon

Genomics is the development and application of genome-based technologies for studying the biological significance of genes under given conditions. It has become a key tool for comparative immunology research, and has now advanced to the next generation sequencing and whole genome sequencing. The measurements in changes in genes and gene function can be obtained by mapping the organism's DNA (genetic interaction mapping), or studying transcriptomics to evaluate changes in messenger ribonucleic acid (mRNA) expression using microarray (MA), serial analysis of gene expression (SEGE), suppression subtractive hybridisation (SSH) or at a protein level using proteomics (Ng *et al.*, 2005).

As one of the major aquaculture species, Atlantic salmon has been extensively used for genomic analysis in an attempt to explore the genome of Atlantic salmon to improve the growth, development, reproduction, disease resistance and response to infectious disease (von Schalburg *et al.*, 2005). Exploration of the salmonid genome is also used extensively to gain evolutionary information to help to solve the mysteries of how gene duplication took place, which is fundamental for describing the importance of gene

families, duplication and deletion of gene segments and mutations, to help in understanding various gene functions. Such information, such as physiological mechanisms of sex determination, is unarguably helpful in discovering important parameters for the expansion of Atlantic salmon aquaculture.

A large amount of genomic data from salmon has been discovered by cloning and generating of cDNA libraries. The expressed sequence tags (ESTs) enable the development of functional genomic tools such as microarray and SSH for salmon (Ng *et al.*, 2005; von Schalburg *et al.*, 2005; Rise *et al.*, 2006; Miller & Maclean, 2008; Taggart *et al.*, 2008). Cooperation between different research groups involved in developing arrays through the distribution of ESTs means that most of the data is now publicly available in the National Centre for Biotechnology Information (NCBI) and the J. Craig Venter Institute (JCVI) database (Miller & Maclean, 2008; Taggart *et al.*, 2008).

The emphasis on identifying the genes responsible for immune function in salmon and rainbow trout has been extensively explored during recent years (Martin *et al*., 2008). The discovery of shared homology between higher vertebrates and teleostean immune systems further strengthens the trend of exploring immune signatures using different species of fish, such as zebrafish (*Danio reiro*), medaka (*Oryzias latipes*) and more recently salmonids as model organisms to understand evolutionary immunology (Korth & Katze, 2002; Rise *et al.*, 2006; Martin *et al.*, 2008; Miller & Maclean, 2008). Apart from comparative and evolutionary immunology, functional genomics has been extensively used to study the health and disease control of fish and to assist in the

development of commercial vaccines against salmonid diseases (Cummings, 2002; Martin *et al*., 2006).

The ability to study global gene expression in the host during infection, using functional genomics, enables understanding of the whole disease mechanism rather than examining the different aspects separately. The information on host response to SAV is poorly known and a thorough understanding is required in order to design proper mitigating measures. The response of the host to SAV therefore is an ideal subject to study using functional genomics.

Aims and Objectives

The main aim of this thesis was to investigate the disease mechanisms involved in SAV1 infection in Atlantic salmon with respect to pathogenesis and host defence mechanisms at the tissue, cellular and molecular level. The objectives to achieve this were;

1. To isolate SAV from the head kidney of Atlantic salmon experimentally infected with SAV1 using different cell lines and to assess the virus load present in this host tissues (**Chapter 2**).

2. To assess the INF-mediated antiviral response observed in SAV1 infection and evaluate the pathology of the disease in relation to INF-mediated tissue response (**Chapter 3**).

3. To assess the host response to SAV1 infection using transcriptomics and qRT-PCR (**Chapter 4**)

4. To study the morphogenesis of SAV1 *in situ* in cell cultures to evaluate the replication pathway of the virus (**Chapter 5**)

5. To study the cell death mechanisms involved in SAV1 infection (**Chapter 6**)

Chapter 2

Isolation and Quantification of Salmonid Alphavirus 1 Following Experimental Infection in Atlantic Salmon

2.1 **Introduction**

Understanding how diseases progress during an infection, by elucidating pathogenesis and the transmission process is important for developing effective control strategies and therapeutics (Berger *et al.*, 2001). Changes in the interaction between the pathogen and its host facilitate the pathogen's success in establishing infection under favourable conditions (Cann, 2005). Such interaction also allows the pathogen to spread through its host and in turn disseminate the disease in the fish population. The success of the infection depends on factors relating to both the pathogen and the host. In viral diseases, the number of viral particles present and the virulence of the virus are factors relating to the pathogen, while the susceptibility of the host relies on a number of physical factors such as age, physiological status and immune status of the host. Being able to detect the virus and measure the kinetic status of the virus load in a population during infection are therefore useful for assessing the progression of the disease (Preiser *et al.*, 2000; Niesters, 2001).

Virus isolation from clinical samples is conventionally carried out using cell cultures and observing the development of a CPE caused by the virus on the cells. This method is considered the gold standard for the diagnosis of many different viral diseases of aquatic organisms, and is often used to certify that stocks of fish as disease-free (Anonymous, 2003). However, in recent years, the development of molecular methods

to detect viral nucleic acids has improved, allowing more sensitive detection and quantification of viruses compared to conventional methods, especially for slow growing viruses (Berger *et al.*, 2001). The introduction of quantitative molecular methods such as quantitative real-time PCR (qPCR) and qRT-PCR have led viral disease diagnosis and research into a new era. These methods have greatly improved diagnosis and thus control of viral diseases in clinical and veterinary medicine (Mackay *et al.*, 2002; Bustin *et al.*, 2005; Bustin & Mueller, 2005). Such technologies have been applied in many aspects of disease control for aquaculture, including disease diagnosis, epidemiology, pathogenesis, immunology, prophylaxis and disease management (Cunningham, 2002; Graham *et al.*, 2006b; Hodneland & Endresen, 2006; Workenhe *et al.*, 2008a, b).

The qPCR and qRT-PCR are both rapid and sensitive molecular tools, in which the former is used to quantify the DNA, while the latter is used to quantify RNA by generating a complementary DNA (cDNA) using reverse transcriptase (Valasek & Repa, 2005). Both methods are easily employed for the quantitative analysis of pathogens during infections. They are also considered more sensitive than conventional PCR. For quantification and detection of the virus during qPCR, measurements take place during the log phase of the amplification when the reaction conditions are optimal for PCR amplification (Bustin, 2000). The absence of post-PCR manipulation in qPCR also helps decrease the risk of contamination, which is often seen with conventional PCR (Mackay *et al.*, 2002). Furthermore, the products of conventional PCR are detected by agarose gel-electrophoresis in the presence of ethidium bromide (EtBr), visualising the band under ultra-violet light. The use of EtBr, a hazardous chemical, is not required in qPCR (Mackay *et al.*, 2002). Due to low cost and less laborious pre-optimization

required compared to qPCR, the conventional PCR is still widely in used in disease diagnosis.

The results of the qPCR\qRT-PCR can either be obtained as absolute or relative values. Absolute quantification of qPCR data requires the generation of a standard curve of a relevant standard, such as plasmid DNA or *in-vitro* transcribed RNA with a known copy number (Bustin, 2002, 2005). The results obtained from relative quantification of qRT-PCR data, on the other hand, are as a ratio of the test result normalized to a control sample relative to a reference house-keeping gene (Pfaffl, *et al.*, 2001, 2002, 2004; Pfaffl, 2006). Relative quantification is mainly used to measure levels of mRNA in gene expression studies (Pfaffl & Hageleit, 2001; Pfaffl, 2006). For virus infections, absolute quantification appears more relevant, to allow the amount of pathogen present to be determined (Bustin, 2000; Workenhe *et al.*, 2008a). However, in absolute quantification final quantity of the viral RNA is also, albeit to a less extent, interpreted relatively by comparison to a relavent unit e.g. copies per defined ng of total RNA, copies per genome, copies per cell, copies per gram of tissue, volume of plasma or serum (Niester, 2001). Thus, the accuracy of absolute quantificaton in real time PCR is always dependent on the reproduciblity of identical standard curves of target transcripts included in the same assays as test sample qPCR\qRT-PCR amplifications. In contrast, in relative quantification, as results are always measured comparatively to a house keeping gene, the unit of measurement is arbitrary and results of relative quantification are comparable across multiple qPCR assays. Data normalization is one of the essential steps to be carried out in qPCR (Bustin, 2002). Using matched sample size, ensuring good quality RNA and incorporating same quantities in RT step in qRT-PCR and

normalization using suitable and unregulated references or housekeeping genes is essential to obtain accurate and reliable qPCR\qRT-PCR result (Huggett, 2005).

Determining the increase in a fluorescent reporter during the PCR amplification in real-time is used to indicate the amount of target amplified during qPCR. Several different types of chemistry and instrumentations are available for this purpose. These are based on different types of fluorogenic reporters such as, SG, hydrolysis probes, molecular beacons, hybridisation probes, sunrise and scorpion primers and peptide nucleic acid light-up probes (Bustin, 2000; Valasek & Repa, 2005). The reaction using SG is considered the simplest and least expensive method to use and can easily be employed for both absolute and relative quantification of target transcripts (Niesters, 2001; Bustin *et al.*, 2005; Graham *et al.*, 2006b; Workenhe *et al.*, 2008a). SG is a DNA fluorescent dye, which binds to the minor grooves in double-stranded DNA and therefore the increase in production of double-stranded DNA (dsDNA) during the qPCR amplification. Increases in the amount of fluorescence present in the reaction can be monitored in real-time in qPCR to quantify the level of target transcripts present (Figure 2.1). Binding to all dsDNA without differentiating specific target from primer-dimer or non-specific products generated during the PCR cycle is a major draw-back with SG real-time chemistry. Pre-optimisation of the assay, however, can ensure the assay specificity (Niesters, 2001). A successful PCR reaction should give a single peak in melting curve analysis. Multiple melting points can be the result of primer-dimer formation, non-specific products in the cycle or amplification of reaction contaminants (Valasek & Repa, 2005). Therefore, careful interpretation of the results is needed to confirm that a single peak is present.

Different qRT-PCR assays have been developed to quantify a variety of RNA viruses in salmon (Munir & Kibenge, 2004; Starkey *et al.*, 2006; Workenhe *et al.*, 2008a) including SAV (Graham *et al.*, 2006b; Hodneland & Endresen, 2006). The assay developed based on SG real time chemistry by Graham *et al.*, (2006b) detected the presence of SAV in cell cultures, serum and tissues. Hodneland & Endresen (2006) described three different sequence-specific, highly sensitive Taqman probe qRT-PCR assays, one of which enabled the differential detection of SAV1, SAV2 and SAV3, while the other two assays detected SAV1 and SAV3 specifically. However, none of the assays attempted to measure the actual viral RNA copy number present in the samples, which is important in the sense of determining the level of infection present in the individual fish or groups of fish. For SAV diagnosis, cultivation and passage of the virus in cell culture can be extremely time consuming and requires experienced personnel to interpret the presence of a CPE, which is difficult to see during the initial stages of development (Nelson *et al*., 1995). Although different cell lines have been tested for SAV1 growth, little information is available on the use of these cell lines for primary virus isolation from clinically infected material. There is a need for optimised cell culture assays for rapid isolation of SAV1 for fast and effective diagnostics (McLoughlin & Graham 2007). Therefore, in the present study, three established salmonid cell lines, CHSE-214, CHH-1 (Fryer & Lannan, 1994) and SHK-1 cells (Dannevig *et al.*, 1997), were compared for their ability to isolate SAV1 from experimentally infected Atlantic salmon based on their growth characteristics and CPE development. Further, the establishment and propagation of the SAV infection was observed by an SG-based qRT-PCR assay, using the primers described by Graham *et al.,* (2006b), to determine the RNA copy numbers in SAV1 infected fish with the help of a standard curve prepared using *in-vitro* transcribed RNA.

1. SYBR Green fluorescence when bound to double stranded DNA

2. SYBR Green is released from DNA and fluorescence is dramatically reduced once DNA is denatured

3. Primer annealing and new PCR product generation during extension with the incorporation of SYBR green

4. At the end of polymerisation SYBR green binds to the double stranded DNA and emits fluorescence that can be detected and quantified.

Figure 2. 1 Schematic representation of the principles of SYBR Green real time PCR (Adapted from Bustin, 2001). The level of fluorescence increases when it binds to the double stranded DNA and dissociates upon DNA denaturation. The level of fluorescence increases in every PCR amplification during extension and is monitored for quantification in qPCR. (Double stranded DNA bound to SYBR green and single stranded DNA)

2.2 **Materials and Methods**

2. 2. 1 **Cell cultures**

The cell lines, CHSE-214, CHH-1 and SHK-1 were used for the study. All chemicals and media were purchased from Invitrogen, Paisley, UK and disposable plastics were obtained from Fisher Scientific, Leicestershire, UK unless otherwise stated. The former two cell lines were cultured in a growth medium (GM) containing Eagle's Minimal Essential Medium (EMEM), 2 mM L-glutamine, 1% non essential amino acids (NEAA) and 10 % (v/v) foetal calf serum (FCS) (Biosera, Ringmer, UK). For virus isolation, maintenance medium (MM) was prepared by adding antibiotics (penicillin 100 IU/ml, streptomycin 100 mg/ml and kanamycin 100 mg/ml) to the culture medium, while maintaining the serum concentration at 5 % (v/v). The GM and MM for SHK-1 cells, on the other hand, consisted of Leibovitz L-15 medium with GlutaMax, supplemented with 2 μM L-glutamine, 40 μM mercaptoethanol, 5 % (v/v) Australian foetal calf serum, penicillin (100 IU/ml) and streptomycin (100 mg/ml).

Propagation and maintenance of these cells were carried out following standard procedures. Briefly, 7-8 day old CHSE-214 and CHH-1 cells were washed x2 with Dulbecco's phosphate buffered saline (DPBS) and trypsinised for 4 min using x1 Trypsin /EDTA (x1 trypsin in 0.01 % of ethylenediaminetetraacetic acid). The flasks were then gently tapped to dislodge the cells from the bottom of the flask and mixed with aliquots of GM (i.e. 3 ml for cells in 25 ml flasks) to split cells into a 1:3 ratio and incubated in a 4 % CO_2 incubator at 22^oC for 18-24 h before infecting with the virus. The SHK-1 cells were split into 1:2 ratios, in the same manner as described above from 10 day old stock flasks and grown in L-15 medium in 22^oC for 48 h before being used for virus isolation.

2. 2. 2 **Culture of the virus**

An SAV1 isolate (F93-125) (Nelson *et al*, 1995; Weston *et al.*, 2002) that originated from an Irish outbreak of SPD, kindly provided by Dr. David Smail (Marine Scotland, Aberdeen, UK) was used in this study. Stock virus was taken from -70°C stocks and was passaged four times in CHSE-214 cells. At the initial passage, the neat virus from the stocks was absorbed onto the preformed CHSE-214 monolayers and harvested at 7 d.p.i by centrifuging the supernatant at 3500 x g for 10 min. In the subsequent passages, the virus supernatant was diluted 1:10 with Hank's buffered salt solution (HBSS) supplemented with 2% (v/v) foetal calf serum and was absorbed onto preformed CHSE-214 cells in 25 ml tissue culture flasks.

To prepare stock virus for the experimental infection, three replicates of 75 ml tissue culture flasks were seeded with CHSE-214 cells ($3x10^{7}$ cells/flask) and absorbed with 1:10 dilution of virus prepared from the third passage of stock virus for 4 h at 15°C in the presence of 1 % carbon dioxide. The GM was then carefully added to the flasks and they were incubated at 15°C in a 1 % CO_2 incubator while monitoring daily for cellular changes relative to uninfected control flasks (re-supplemented with the same GM). After the development of a CPE, cells were harvested 9 d.p.i. Then, a single cycle of freeze-thawing at -70°C was performed before the supernatant was clarified at 3500 x g for 10 min at 4°C in an Eppendorf 5804R centrifuge. The clarified supernatant was aliquoted and stored at -20°C. One aliquot was back-titrated onto CHSE-214 cells to determine the 50 % Tissue Culture Infective Dose ($TCID_{50}$).

2. 2. 3 **Virus titration by 50 % Tissue Culture Infective Dose (TCID$_{50}$).**

The concentration of virus present in a unit volume was estimated by TCID$_{50}$, which indicated the dose required to infect 50 % of inoculated cell cultures. This method relies on the presence and the detection of cytocidal virus particles in the sample (Burleson *et al.* 1992). The infectivity titrations were performed in flat bottom Nunc 96 well plates. To each well of the plate, except the first column of wells, was added 90 μl of HBSS diluent supplied with 2 % FCS. Virus (10 μl) or diluent as the negative control (10 μl) was pipetted into the first well of each row and then was titrated in ten-fold dilutions across the plate using a multi-channel pipette with new pipette tips to prevent virus carry-over in each individual dilution. One 25 ml flask of highly confluent CHSE-214 cells was harvested and diluted in 12 ml of GM for each 96 well plate. Each well of the titration plate was supplemented with 100 μl of above mentioned cell suspension. The plates were sealed with Nescofilm (Fisher Scientific) and incubated at 15°C with 1 % CO$_2$. Virus titres were calculated by the method of Spearman-Karber using the formula given below (Hierholzer *et al*., 1996), when the CPE became sufficiently advanced to assess visually, in general at 10-14 d.p.i.

$$\text{Spearman-Karber formula: } \textbf{Mean log TCID}_{50} = X + \frac{1}{2} \times d - d \times \Sigma\left(\frac{r}{n}\right)$$

Where, X = log of the highest reciprocal dilution.
d = log of the dilution interval.
r = number of test subjects not infected at any dilution.
n = number of test subjects inoculated at any dilution.

2. 2. 4 **Experimental infection of Atlantic salmon with SAV1**

Atlantic salmon parr (mean weight 48.5±9.2g, mean length 17.0±1.5 cm), obtained from Howietoun Hatchery, Scotland, UK, were experimentally infected with SAV1 following a one month quarantine period at the Aquaculture Research Facility, Institute of Aquaculture, University of Stirling, UK. The stock virus prepared above was injected I.P. into 50 fish (0.2 ml of 1 $\times 10^{7.33}$/ $TCID_{50}$ virus/fish), while control fish were injected with 0.2 ml of CHSE-214 cell culture supernatant. Challenged and control populations were held separately in 50 l fibreglass tanks supplied with flow-through water with a mean water temperature of $11\pm1^{o}C$ and monitored twice daily throughout the experimental period of 90 d.p.i. The head kidney of fish was aseptically sampled from 5, SAV1 injected and 5, control salmon at 0.5, 1, 3, 5, 7, 10, 14, 21, 42 and 90 d.p.i. The head kidney tissue was divided into two samples, one for virus isolation by cell culture and one for RNA extraction. Samples for virus isolation were collected into sterile Bijoux bottles and placed on ice until processed while the remainder was fixed in RNA*later*$^{®}$ (Applied Biosystems, Warrington, UK) in Nunc 1.5 ml Cryo-tubes.

2. 2. 5 **Isolation of SAV1 on CHSE-214 cells**

For virus isolation, the aseptically collected head kidneys from 1, 3, 5, 7, 10, 14, 21, 42, and 90 d.p.i were macerated on the same day after sampling with sterile sand to prepare a 1:50 (w/v) dilution of the kidney homogenate in HBSS supplemented with 2 % FCS, penicillin (100 IU/ml), streptomycin (100 mg/ml) and kanamycin (100 mg/ml). The kidney homogenate was clarified by centrifuging at 2000 x g for 15 min at $4^{o}C$ (Eppendorf 5804R). Supernatants were then filtered through a 45 µm filter into sterile universals. The clarified kidney homogenates (100 µl), and 1:100 and 1:1000 (v/v)

dilutions of these (100 µl), were absorbed onto 18-24 h old preformed CHSE-214 cell ($2x10^5$/well) monolayers in 24 well plates and incubated at 15^oC in a 1 % CO_2 incubator. After 4 h MM was carefully added on to the cell monolayers and plates were transferred back into the same incubator conditions. Plates were observed every other day for 28 days for the development of a CPE.

2. 2. 6 Comparison of CHH-1, CHSE-214 and SHK-1 cells for virus isolation

Frozen (-20^oC) kidney homogenates prepared from samples taken from fish on 3 d.p.i., and which were all CPE positive on CHSE-214 cells in the initial virus isolation, were thawed and absorbed onto the preformed monolayers of CHSE-214, CHH-1 and SHK-1 cells cultured in 24 well plates. Following absorption, MM was added to the CHSE-214 and CHH-1 cells, while L-15 with supplements was added to the SHK-1 cells. Cells were incubated at 15^oC and observed daily for the development of a CPE over the course of 25 days.

Aliquots of cell culture supernatants of the first passage from the infected CHSE-214 and CHH-1 monolayers were harvested after 10 days of incubation and stored at -20^oC until the $TCID_{50}$ was estimated for each sample. A ten-fold dilution series of each supernatant was made in 96 well plates using HBSS, and these were then absorbed for 1 h onto preformed CHSE-214 and CHH-1 monolayers prepared in 96 well plates, using three replicates for each sample. The $TCID_{50}$ was estimated according to the method described in Chapter 2.2.3 reading the plate after 15 d.p.i. The titres were compared

using a 2-sample t test, using Minitab v13 statistical software for Windows (Minitab Ltd, Coventry UK).

2. 2. 7 Detection and quantification of viral RNA

2.2.7.1 RNA extraction

After overnight infiltration at 4°C, the RNA*later*$^{®}$ was decanted from the head kidney tissues and these were then stored at -70°C until required for RNA extraction. This was carried out using TRI Reagent$^{®}$ (Applied Biosystems) as directed by the manufacturer. For this, 30-40 mg of the kidney sample was macerated individually with 0.8 ml of TRI Reagent$^{®}$ in nuclease free 1.5 ml eppendorf tubes (Fisher Scientific) with plastic pestles (Fisher Scientific). The homogenate was mixed with 0.16 ml of chilled chloroform (Sigma-Aldrich, Dorset, UK) and incubated at room temperature (RT) (22°C) for 15 min. Samples were then centrifuged at 12,000 x g for 15 min at 4°C. The supernatant was transferred to a fresh tube and 0.4 ml of chilled isopropanol was added (Sigma-Aldrich). The tubes were mixed several times by inverting, and then incubated for 10 min at RT before centrifuging at 4°C at 12,000 x g for 10 min. The supernatant was removed and pellets washed with 75 % chilled ethanol by centrifuging at 10,000 x g for 5 min. The RNA pellet was eluted in 30 µl of nuclease-free water and quantified on a Nano-drop 1000 spectrophotometer (Labtec Inc, Arizona, USA) before storing at -70°C. The quality of the RNA was examined by electrophoresis on a 1 % agarose gel (Sigma Aldrich), prepared in Tris-Acetate-EDTA (TAE) buffer and stained with 0.05 % ethidium bromide (Sigma Aldrich) and run at 80 V for 30 min.

2.2.7.2   Reverse transcription of RNA

Total RNA was reverse-transcribed to construct cDNA for the subsequent molecular applications using a *Reverse*-iT[TM] MAX 1st strand synthesis kit (Abgene, Epsom, UK) according to the manufacturer's instructions. Briefly, 1 µg of total RNA was mixed in a 1:3 ratio with anchored oligo-dT (500 ng/µl) and random hexamers (400 ng/µl), heated for 5 min at 70°C, then kept on ice for 2 min before adding 2 µl, 5mM dNTP, 4 µl 5x first strand synthesis buffer, 1 µl (50 IU/µl) *Reverse*-iT[TM] MAX RTase blend, 1 µl QRTase enhancer and then nuclease-free water to make the final reaction volume up to 20 µl. This mixture was incubated at 42°C for 1 h to allow cDNA synthesis to take place, followed by 10 min incubation at 75°C for enzyme inactivation and stored at -20°C prior to use.

2.2.7.3   RT-PCR

All primers necessary for molecular applications were purchased from MWG Biotech (London, UK). The RT-PCR to detect the presence of SAV in the head kidney tissue of experimentally infected and control fish was performed using a primer pair that produces a 539 base pair (bp) product (Hodneland & Endresen, 2006). For the PCR, 25 µl of reaction mixture containing 2 µl cDNA, 1.25 µl forward (5′-CGGGTGAAACATCTCTGCG-3′) and reverse (5′CTTGCCCTGGGTGATACTGG-3) primers (10 µM/ml), 8 µl nuclease free H$_2$O and 12.5 µl 2X ReddyMix[TM] PCR Master mix (composed of 0.625 U Thermoprime *Taq* DNA polymerase, 75mM Tris-HCL, 20mM (NH$_4$)$_2$SO$_4$, 1.5 mM MgCl$_2$, 0.01% (v/v) Tween® 20, 0.2 mM each of dNTP, dCTP, dGTP, and dTTP) (Abgene). The thermal cycle conditions consisted of 95°C initial denaturing for 5 min, followed by 40 cycles of 20s denaturing at 95°C, 30 s annealing at 55°C and 1 min extension at 72°C prior to final extension at 72°C for 5

min. The PCR products were visualized on a 1 % agarose gel stained with EtBr and viewed under a UV camera.

2.2.7.4 *In- vitro* transcription of RNA

Absolute quantification of virus loading in the kidneys of infected fish over time was performed using externally prepared RNA standards (Fronhoffs *et al.*, 2002; Workenhe *et al.*, 2008a). A linearised DNA template was obtained from a conventional RT-PCR by modifying a primer pair that gives a 227 bp product (Graham *et al.*, 2006b) designed on the E1 region of the SAV genome by tagging T7 RNA polymerase promoter to the 5' end (5'**TAATACGACTCACTATAGGG**GACTGGCCTCCTTACGGGG 3') and annealing with normal reverse primer sequence (5'TTACAACCGTGCGGTGCTGT3'). To obtain a large amount of *in-vitro* transcribed 'sense' RNA to be used in the downstream applications, the promoter tag has to be attached to the 5' end, (amino-terminal side of the sequence) as shown in Figure 2.2. The RT-PCR was performed as described before in Chapter 2.2.7.3 with modified primers (1.25 µl T7 promoter sequence tagged forward and

(a)   T7   **+1**
        TAATACGACTCACTATAGGGAGA

(b)
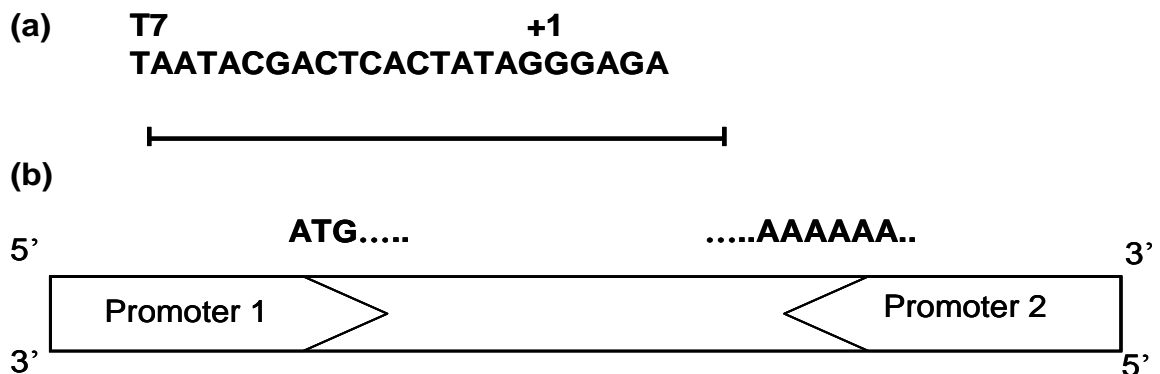
Figure 2. 2 (a) T7 Promoter sequence (b) Attaching RNA polymerase corresponding to promoter 1 will make the same sequence as the original RNA, also called sense RNA. If using promoter 2, anti-sense RNA will be transcribed (*in-situ* hybridization)

normal reverse primers at 10 µM ml^{-1} concentration) at an annealing temperature of 58°C. The PCR product was then purified using QIAquick PCR purification kit (Qiagen, Crawley, UK.) and the purity and the uniqueness of the size of the product was assessed on 1 % agarose gels. The DNA content of the purified PCR product was measured on a Nanodrop 1000 before being used as the template for the *in-vitro* transcription process to obtain a large amount of sense primer using a MEGAscript® high yield transcription kit (Ambion, UK).

The *in-vitro* transcription reaction was assembled at room temperature (21-25°C) by mixing 0.2 µg of DNA obtained from PCR, 2 µl of 10x reaction buffer, 2 µl of each nucleotide solution (UTP, ATP, CTP,GTP), 2 µl of enzyme mix and the final volume was scaled up to 20 µl with nuclease free water. The reaction mix was incubated for 14 h at 37°C. The reaction was terminated by adding 1 µl of TURBO DNAse to the mixture and incubated for 15 min at 37°C. The RNA transcripts obtained from *in-vitro* transcription (cRNA) were then purified with phenol:chloroform extraction and isopropanol precipitation. This method was chosen, based on the manufacturer's recommendations for transcripts that encoded products less than 500 bp in size. For this, 115 µl of nuclease free water and 15 µl of ammonium acetate were mixed into the *in-vitro* transcribed RNA solution. This was thoroughly mixed, then was extracted first with an equal volume of phenol:chloroform and again with an equal volume of chloroform. To precipitate the cRNA, an equal volume of isopropanol was added to the aqueous phase, placed in a new tube, and chilled at -20°C for 20 min before centrifuging at 13,000 x g for 15 min at 4°C. The cRNA pellet was finally washed with cold ethanol and resuspended in nuclease free water.

2.2.7.5   Construction of *in-vitro* transcribed RNA standards

Concentrations of cRNA transcripts were measured spectrophotometrically in triplicate on a Nanodrop 1000 after incubating for 3 min at 70°C. The initial number of RNA molecules per µl was estimated using the following formula in which molecules in one micro litre (N) were extrapolated by concentration of the cRNA (C), fragment size (K) and a factor derived from molecular mass and Avogadro constant (182.5×10^{13}).

$$N \text{ (molecules per µl)} = \frac{C(\text{cRNA µg/ul})}{K(\text{fragment size/bp})} \times 182.5 \times 10^{13}$$

A ten fold serial dilution of cRNA transcripts was made immediately after measuring the RNA ranging from 10^{12} - 10^{4} copies and 10 µl aliquots of these were stored at -70°C. To synthesise the standard curve using SG qRT-PCR, cDNA synthesis was carried out using 2 µl of each dilution, as described in Chapter 2.2.7.2.

2.2.7.6   Standard curve preparation and quantification of SAV load in kidney tissue

The virus load in the head kidney of Atlantic salmon experimentally infected with SAV1 was determined using SG qRT-PCR with a 227 bp size primer on a Techne Quantica® Thermal cycler (Thistle Scientific, Glasgow, UK). The test samples and the standards were assayed in duplicate. Individual qPCR reactions of 20 µl were prepared in the wells of Thermofast 96 well clear plates (Abgene), consisting of 1 µl of 10 µM forward (5'GACTGGCCTCCTTACGGGG3') and reverse (5'TTACAACCGTGCGGTGCTGT 3') primers, 10 µl of SG PCR master mix

(Abgene) and 3 µl of nuclease free water. The test sample consisted either of 5 µl of dilution (10^{-1}) of total RNA derived cDNA or 5 µl of different dilutions of the cRNA derived cDNA (R-cDNA) for the standard curve. The cycling conditions used for the assays are given in Table 2.1. Primer efficiency (E) and the relative co-efficiency of the standard curve were optimised before use in the actual test.

Table 2. 1 Thermal cycling conditions used in the Techne Quantica® Thermal cycler for the qRT-PCR assay to quantify SAV.

Enzyme activation	15 min	at	$95^{o}C$	
Denaturation	20s	at	$95^{o}C$	
Annealing	20 s	at	$58^{o}C$	45 cycles
Extension	30s	at	$72^{o}C$	
Dissociation peak 70-90°C measure at every 0.5^{o}C				

To generate the standard curve, ten-fold serial dilutions of R-cDNA were amplified in a Quantica® thermal cycler. The Ct values of the standards (Y-axis) were plotted against the log concentration of the cDNA dilutions (X-axis). The slope and correlation coefficient (r) of the standard curve was used to estimate the quality of the standard curve. The value of the slope was employed in the formula $\{E=(10^{-1/slope})-1\}$ to determine the efficiency (E) of the target amplification. To assess the repeatability and the reproducibility of the assay the test was repeated three times using the same conditions with two replicates of each R-cDNA dilution. The specificity of the assay was performed by dissociation peak (melting point) analysis using 'Quansoft' software of the Quantica® thermal cycler that analyses the baseline and threshold values automatically at the end of each run.

In order to measure the absolute SAV RNA copy number, 10^{-1} dilutions of the cDNA obtained from reverse transcription of total RNA (1 µg) of the head kidney of both infected and control fish sampled at 0.5 1, 3, 5, 7, 10, 14, 21, 42 and 90 d.p.i were analyzed by qRT-PCR with a standard curve employed in each plate. The viral copy number in 1 µg of total RNA from the head kidney of virus infected fish was estimated by multiplying the viral genome copies equivalent in 20 µl of the qRT-PCR reaction mix (n) that was estimated by the 'Consoft' software by a factor (200/10x20/5) based on the use of 5 µl of cDNA from 200 µl of 10^{-1} dilution. Statistical analysis was performed with Minitab v13 statistical software for Windows. The actual copy number resulting from the qRT-PCR was tested for normality (Anderson-Darling test) and compared for the significance between time points using one-way ANOVA ($\leq$ 0.05) and Fisher's individual error rate in Minitab v13 statistical software for Windows. Results of 42 d.p.i were not included in the significance test.

2.3 **Results**

2. 3. 1 **Isolation of SAV-1 on CHSE-214 cells**

Initially CHSE-214 cells were used to detect the presence of virus from the infected kidney samples to establish the best sampling point for the subsequent studies (i.e. d.p.i.). All CHSE-214 cells absorbed with kidney homogenate sampled from fish at 1 d.p.i. developed a CPE in the cells (Figure 2.3) from 21 d.p.i. In contrast, kidney sampled at 3 d.p.i. produced a CPE on CHSE-214 cells from 10 d.p.i. Three out of the five infected kidney samples taken at 5 and 7 d.p.i. developed a CPE on cells. However, no CPE was obtained with samples taken from fish at 21 d.p.i. or thereafter, or with any of the control fish.
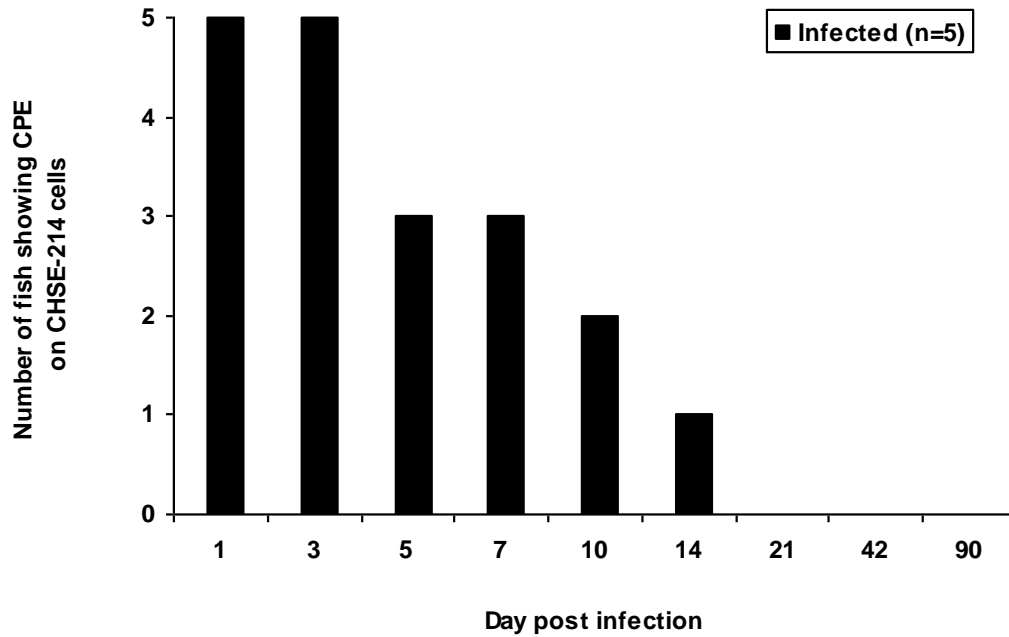
Figure 2. 3 The development of a cytopathic effect (CPE) on CHSE-214 cells with SAV1 infected kidney sampled at different times (1-90 Day post infection). None of the fish were positive for CPE from 21 Day post infection.

2. 3. 2 **Comparison of different cell lines for virus isolation, morphology and titration**

Since the samples taken at 3 d.p.i. resulted in the most rapid development of a CPE in CHSE-214 cells, these samples (i.e. 3 d.p.i) were used to compare the suitability of the three cell lines (i.e. CHSE-214, CHH-1 and SHK-1 cells) (see Chapter 2.3.1) for virus isolation. Of the three cell lines absorbed with infected kidney homogenate, CHH-1 cells gave the earliest CPE. This started to appear in 3 of the replicate samples from 6 d.p.i, and all replicates become CPE-positive by 15 d.p.i. (Table 2.2).

The CHSE-214 cells, the cell line conventionally used for SAV1 isolation, showed a CPE with 2 of the replicate samples at 10 d.p.i, and all the replicate wells were positive by 20 d.p.i. For both these cell lines, a CPE developed faster in subsequent passages of

the virus (Table 2.2). In contrast, the CPE which developed in SHK-1 cells started to appear at 20 d.p.i. and only 4 fish were positive for virus with this cell line by 25 d.p.i. However, all samples were CPE-positive in subsequent passages on SHK-1 cells (Table 2.2). The mean $TCID_{50}$ obtained on CHSE-214 ($1x10^{3.64\pm1.76}$) and CHH-1 ($1x10^{3.36\pm1.4}$) cells were not significantly different ($p \leq 0.05$) from each other on the first passage of the virus. The virus titre on SHK-1 cells was not measured due to the slow development of the CPE in this cell line.

The morphological appearance of the CPE was similar in both CHSE-214 and CHH-1 cells, starting as a localized rounding of cells on the surface of the cell monolayer, which then spread over the cell line with cells sloughing off the edges of the affected areas. In contrast, SHK-1 cells started to loosen from the monolayer when it started to produce a CPE from 20 d.p.i. (Figure 2.4).

Table 2. 2 Development of a cytopathic effect in Chinook salmon embryo cells (CHSE-214), Chum salmon heart -1 (CHH-1) and Salmon head kidney -1 (SHK-1) cells during primary virus isolation, absorbing kidney homogenate of fish and the subsequent two passages of the virus (n=5). CHSE-214 and CHH-1 cell cultures were harvested at 10 day post-inoculation on passage 1 and 2, and therefore no data are available after this time point. Samples derived from SHK-1 cells were not used for viral titre estimation and the experiment was stopped after passage 1. P0- Primary inoculation, P1-Passage 1, P2-Passage 2.

Days post inoculation	CHSE-214			CHH-I			SHK-1		
	P0	P1	P2	P0	P1	P2	P0	P1	P2
1	0	0	0	0	0	0	0	0	-
3	0	1	3	0	3	5	0	0	-
6	0	4	5	3	5	5	0	0	-
10	2	5	5	4	5	5	0	1	-
15	4	-	-	5	-	-	0	3	-
20	5	-	-	5	-	-	3	5	-
25	5	-	-	5	-	-	4	5	-
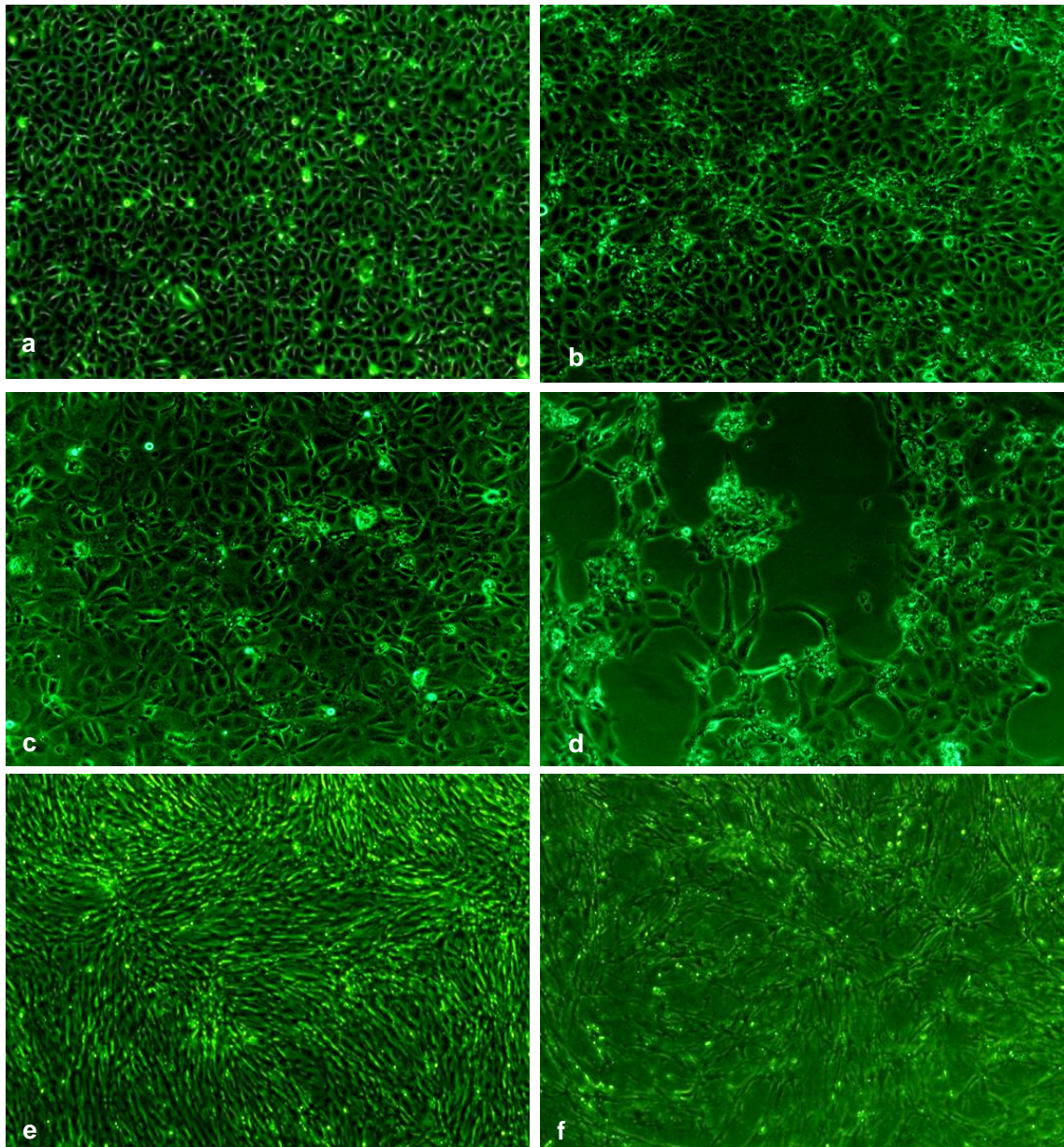
Figure 2. 4 Cytopathic effect (CPE) in three different cell lines inoculated with kidney homogenate sampled at 3 d.p.i. from SAV1 infected salmon. (a) Non-infected Chinook salmon embryo-214 (CHSE-214) cells. (b) Infected CHSE-214 cells on 6 day post-inoculation (d.p.in). (c) Non-infected Chum salmon heart -1 (CHH-1) cells. (d) infected CHH-1 cells on 6 d.p.in. (e) Non-infected Salmon head kidney-1 (SHK-1) cells. (f) Infected SHK-1 cells on 20 d.p.in.

2. 3. 3 Detection and quantification of viral RNA

2.3.3.1 Generation of cRNA standards and standard curve

The PCR with a modified primer pair at 227 bp produced a single product (Figure 2.5). The product size of the primer tagged with the T7 promoter was slightly larger than the original 227 bp PCR product as expected (Figure 2.5). The concentration of the stock cRNA was 1.7605 µg/µl. Therefore the extrapolated molecular number in the stock cRNA was (N) 1.415×10^{13} molecules/µl and the copy numbers of the ten-fold dilutions (10^{-1}- 10^{-10}) series made was ranged from 1.4153×10^{12}-1.4153×10^{3} molecules/µl. These cRNA dilution series were then reverse-transcribed into cDNA before being employed in qRT- PCR.
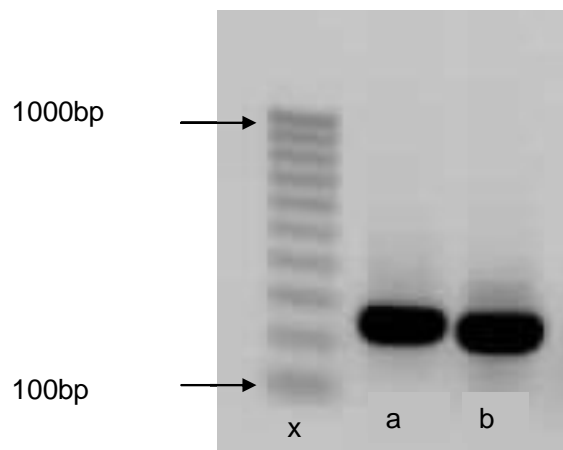
Figure 2. 5 Production of a 227 bp PCR product by the primer pair on a 1 % agarose gel electrophoresis (a) tagged with T7 promotor and (b) un-tagged normal primer and (x) the 100 bp PCR ladder.

Thermal cycling of the ten-fold serial dilutions of R-cDNA produced an acceptable standard curve (Figure 2.6.a). The dynamic range of the dilution series that was used to produce the standard curve ranged from dilution 10^{-1}-10^{-8} (Figure 2.6.a.b), and therefore the detectable number of copies ranged from 2.8306×10^{12}- 2.8306×10^{5}. A strong

linear relationship with a correlation co-efficient of (r^2) 0.99 between the fractional number and the log of the starting copy number was noted (Figure 2.6.a). The slope of the line was (m) –3.281 and the efficiency of the assay was (E) 2.02 (Figure 2.6.a), both suggestive of optimal PCR efficiency. Furthermore, it resulted in a single melting point at 85°C without any delectable primer-dimer or non-specific fragments (Figure 2.6.c,d).
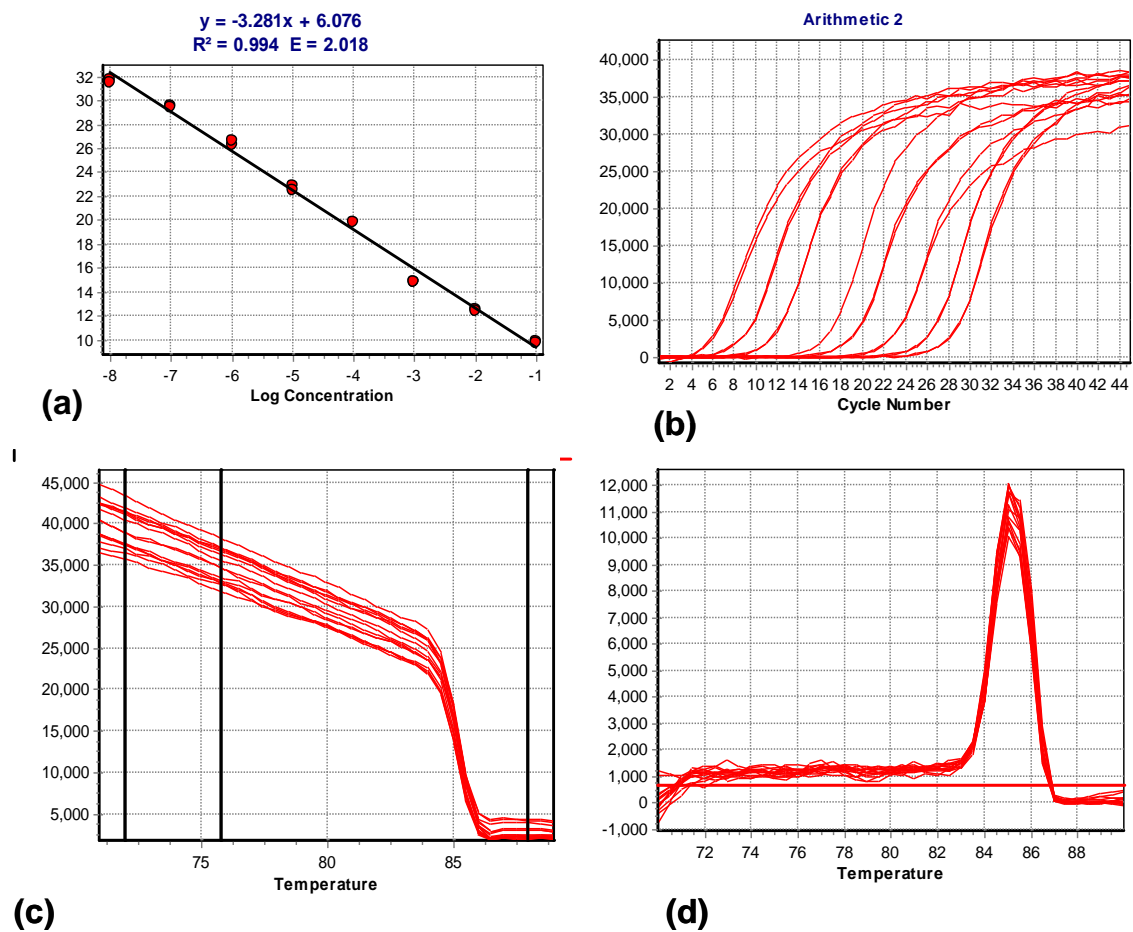
Figure 2. 6 Results of quantitative reverse-transcription polymerase reaction (qRT-PCR) for in-vitro transcribed RNA (cRNA) optimization (a) standard curve generated from ct values (y-axis) versus 10-fold dilution of cDNA derived from cRNA (x-axis), (b) qRT-PCR amplification curves for ten-fold dilutions of the standards (c,d) dissociation curve analysis of qRT-PCR of the standard samples.

2.3.3.2 Assessment of the assay sensitivity and reproducibility

The reproducibility of the assay was confirmed by repeating the assay three times using same cDNA stocks (Table 2.3). The variation of the efficiency was 2.031 ± 0.031 and the variation of correlation co-efficiency was 0.992 ± 0.003. The specificity of the assay was determined from the melting peak analysis (Table 2.4) which was found to be $85.17 \pm 0.09^{\circ}C$. Agarose-gel electrophoresis of the standard curve provided a single band of expected size (data not shown). Reliable melting curve results were only obtained from the infected group of fish, not the control fish, confirming the specificity of the assay.

Table 2. 3 Reproducibility of qRT-PCR for SAV with primer 227 using cDNA derived from *in-vitro* transcribed cRNA for three different runs. (Ct-cycle – threshold, R^2 - correlation coefficiency, E - efficiency, S.D.- standard deviation, CV% - coefficincy of variation).

Dilution	Run (Ct value)			Mean	S.D.	CV%
	Run 1	**Run 2**	**Run 3**	**Mean**	**S.D.**	**CV%**
10^{-1}	9.31	9.79	9.8	9.63	0.28	2.9
10^{-2}	12.37	12.45	12.9	12.57	0.28	2.27
10^{-3}	15.86	14.83	16.48	15.72	0.83	5.309
10^{-4}	19.52	19.81	19.88	19.73	0.19	0.96
10^{-5}	23.04	22.65	23.45	23.04	0.4	1.73
10^{-6}	26.18	26.45	26.32	26.31	0.13	0.51
10^{-7}	28.52	29.44	28.84	28.93	0.46	1.6
10^{-8}	31.68	31.59	32.86	32.04	0.7	2.21
R^2	**0.996**	**0.994**	**0.998**			
E	**2.016**	**2.018**	**2.059**			

Table 2. 4 Dissociation curve (Tm value) analysis for the dilutions used to prepare the standard curve for three runs. (SD – standard deviation)

Dilution	Run (Tm value)		
	Run 1	Run 2	Run 3
10^{-1}	85.06	85.15	85.27
10^{-2}	85.07	85.17	85.22
10^{-3}	85.13	85.25	85.25
10^{-4}	85.2	85.28	85.31
10^{-5}	85.24	85.04	85.31
10^{-6}	85.13	84.88	85.28
10^{-7}	85.08	85.07	85.29
10^{-8}	85.13	85.08	85.28
Mean± SD	**85.13±0.062**	**85.11±0.126**	**85.28±0.031**

2.3.3.2 Detection and quantification of SAV-1 in kidney tissues by RT-PCR and qRT-PCR

The results of the RT-PCR and qRT-PCR analysis of the head kidney of Atlantic salmon injected with SAV1 are shown in Figure 2.7. All fish injected with SAV1 were positive in both assays at 1 and 3 d.p.i. Four fish were positive by RT-PCR at 5 d.p.i., and three fish at 7 d.p.i. However, all infected fish sampled at day 5 and 7 were positive for virus by qRT-PCR analysis. Four out of five fish were positive in both tests at 10 d.p.i. Two fish gave positive bands in 1 % agarose gel at 21 d.p.i. while three were positive by qRT-PCR at this time point. Although one fish was positive for virus in the dissociation curve analysis in qRT-PCR at 42 d.p.i, none of the fish was positive by RT-PCR. All control fish were negative for SAV1 by both RT-PCR and qRT-PCR.
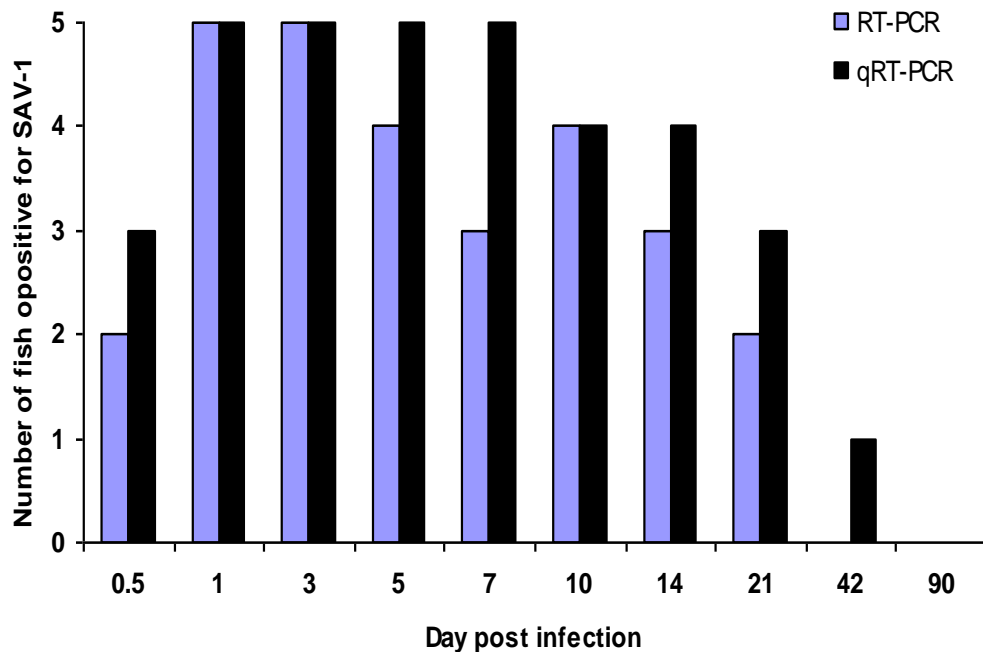
Figure 2. 7 Number of fish positive for SAV by reverse transcription polymerase chain reaction (RT-PCR) and quantitative real-time reverse transcription polymerase chain reaction (qRT-PCR) following analysis of kidneys sampled at different times (1-90 day post infection) of experimentally induced SAV1 infection. Note no fish were positive for any of the test by 90 d.p.i

The highest viral RNA copy number $4.11 \times 10^9 \pm 1.72 \times 10^9$ (Mean±SD) was observed at 5 d.p.i. (Figure 2.8). The lowest mean viral copy number ($8.77 \times 10^7 \pm 3.1 \times 10^7$) was detected at 0.5 d.p.i. and was significantly different from 1, 3, 5, and 7 d.p.i. The mean viral RNA copy number of infected fish at 14 and 21 d.p.i was also significantly different from the mean viral RNA copy number of 1, 3, 5, and 7 d.p.i. Interestingly, one out of five fish was positive for qRT-PCR on 42 d.p.i with a higher level of viral RNA copy number (1.35×10^9). A large individual variation of viral RNA copy number was detected especially at 1, 3, 5 and 7 d.p.i (Figure 2.8).
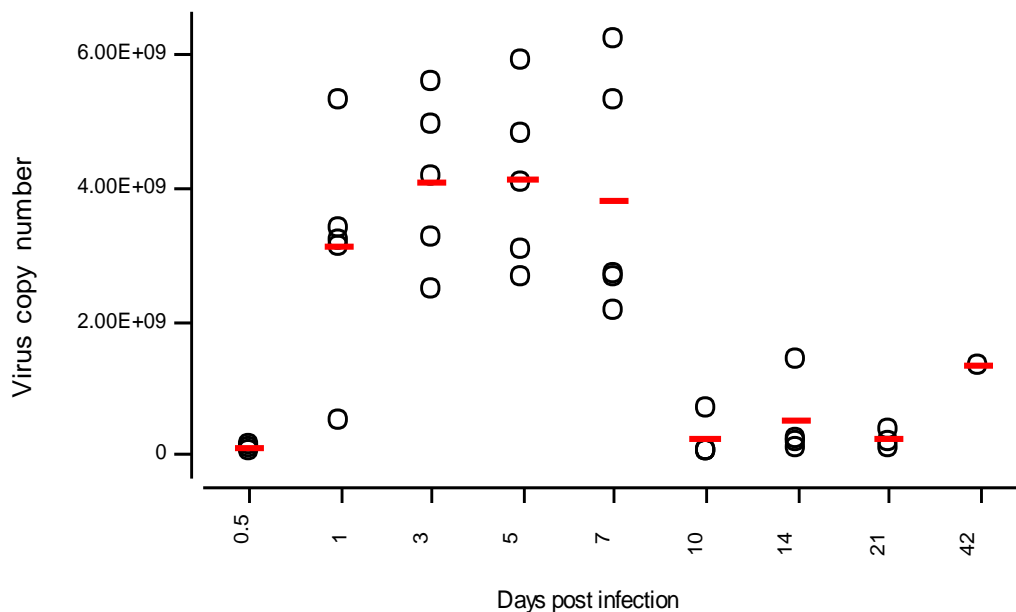
Figure 2. 8 Copy number of the virus detected by SYBR Green qRT-PCR in fish infected with SAV positive fish at 1-90 day post infection (d.p.i). Red solid line indicates the sample mean and the open circles represent positive individual fish. Note one fish became positive for virus at 42 d.p.i .

2.4 **Discussion**

A variety of different methods are currently used to identify SAV including pathology, virus isolation, RT-PCR, an immunoperoxidase based improved virus neutralisation test and immunofluorescent antibody techniques (IFAT) (Christie *et al.*, 1998, 2007; McLoughlin & Graham, 2007; Graham *et al.*, 2008, 2010). In virology diagnostics, the faster the cell line develops a CPE the quicker a diagnosis can be made, and the more rapidly a clinical or regulatory response can take place. SAV are considered to be slow growing fish viruses, especially during primary virus isolation from clinical samples (Nelson *et al.*, 1995; Christie *et al.*, 2007). The CHSE-214 cell line is commonly used in SAV1 research and diagnostics (Christie *et al*., 2007; McLoughlin & Graham, 2007)

however, a number of drawbacks have been reported with use of this cell line in primary virus isolation, such as a delayed CPE on primary inoculation and the requirement for several passages to develop a visible CPE. In some instances, this leads to increased false negative results (Nicola *et al.*, 1999; Jewhurst *et al.*, 2004). The suitability of different cell lines for effective diagnosis of SAV1 was therefore examined using CHH-1 and SHK-1 along with CHSE-214 cells, with the aim evaluating them as a possible alternative for SAV1 isolation instead of CHSE-214. In addition, the amount of virus present in the head kidney of experimentally infected Atlantic salmon was also measured using a qRT-PCR to study the virus kinetics during establishment and propagation of experimentally induced SAV1 infection.

From initial virus isolation using CHSE-214 cells, high numbers of fish were found to be infected with SAV during the 1st week post infection. A CPE started to develop with the kidney samples taken at 1 d.p.i only after 20 d.p.in compared to the kidney samples taken at 3 d.p.i which gave a CPE from day 10 after primary inoculation. The late development of CPE from samples taken at 1 d.p.i could possibly be due to the low level of infectious particles in the sample or could also be from contamination by remnants of the original I.P. injection.

From the results of the cell culture, the kidney homogenates prepared from 3 d.p.i. samples were used for the subsequent comparative studies because it was assumed that these samples had a higher virus load compared to the other sampling points. With regard to virus isolation, the appearance of a CPE was faster in CHH-1 cells compared with the other two cell lines, although the virus titre was not significantly different to that obtained with CHSE-214 cells after the first passage of the virus. On the other hand

SHK-1 cells produced a CPE much later than the other two cell lines, with CPE starting to appear around 20 d.p.in.

The CHH-1 cells are fibroblast cells that originated from Chum salmon (*Oncorhynchus keta* Walbaum) heart (Lannan *et al*., 1984; Fryer & Lannan, 1994) and were found to perform better for primary SAV1 isolation and propagation in this experiment compared to conventional CHSE-214 cells, which are epithelial cells that originate from Chinook salmon (*Oncorhynchus tshawytscha* Walbaum) embryo. As the CHH-1 cell line is of cardiac origin, it may be useful for studying the host response to the virus *in-vitro,* since the heart is one of the major target organs of this virus.

The SHK-1 cells are macrophage-like, derived from Atlantic salmon head kidney leukocytes (Dannevig *et al.*, 1997), and have been used in immunological, antiviral and host pathogen interaction studies *in-vitro* for different viral diseases affecting salmonids (Jensen & Robertsen, 2002; Martin *et al*., 2007) including SAV (Gahlawat *et al.*, 2009). The CPE development in SHK-1 was delayed compared to the other two cell lines used in this study supporting the observation of Graham *et al.*, (2008) who also found that not all SAV isolates grew in this cell line and always gave a lower titre than CHSE-214. In a recent study by Gahlawat *et al.*, (2009), that was conducted to observe antiviral gene expression, they also found SHK cells to be relatively resistant to SAV infection. No CPE was reported even at 14 d.p.in, the day the last sample was taken. However, the ability of SHK-1 cells to support SAV1 isolation and propagation as seen in this study suggests that this cell line is still a useful tool for studying the immunological and anti-viral mechanisms of the host against this group of viruses. On the other hand, CHSE-214 cells do not have an inherent ability to produce an antiviral effect against the virus

(Jensen et al., 2002) which limits their usefulness for host-pathogen interaction studies *in-vitro*.

Detecting ongoing viral infection rapidly and quantitatively in fish is important for effective disease diagnosis and for studies examining virus-host interactions. It is known that SAV isolation from clinical samples is difficult; therefore an RT-PCR assay was performed to confirm the presence of virus in the tissue samples using a pre-optimized primer pair that produced a 536 bp PCR product (Hodneland & Endresen, 2006). Similar to cell culture results, RT-PCR also detected high numbers of SAV1 positive fish at the early stage of infection but with increased sensitivity. Overall, 60 % of fish were positive for the virus by RT-PCR over the 90 day experimental period compared with the cell culture where only 42 % of the fish were positive.

Actual quantification of copy number of the viral RNA present in kidney tissue of infected fish was performed using a 227 bp primer designed from the E1 region of the SAV genome (Graham *et al.*, 2006b). In contrast to the original assay described by Graham *et al.*, (2006b), which used cloned synthetic transcripts, the present qRT-PCR assay was developed using RNA transcribed *in-vitro.* Absolute quantification of the target gene using a synthetic transcript was used here to measure the actual number of molecules present in the test sample with the help of the standard curve (Fronhoffs *et al.*, 2002). In this, the forward primer sequence of the target transcript was modified by tagging a T7 promoter, which acts as a polymerase to generate large amounts of synthetic RNA transcripts *in-vitro.* The PCR product obtained was used as the template and the T7 promoter initiates the transcription reaction. The target copy number of the purified RNA was then estimated as described by Fronhoffs *et al.,* (2002) to obtain a

standard curve for absolute quantification of the viral RNA copy number. T7 promoter-based transcription is the most commonly used method for RNA synthesis *in-vitro* in molecular biology applications including real-time PCR (Fronhoffs *et al.*, 2002). In this method, the same primer was used both to prepare the synthetic RNA and for the qRT-PCR. Hence the same transcript was amplified in both test and the standard samples in the same plate, the actual number of target molecules present in the test sample were determined in relation to the amount of RNA transcripts present in the standards (Fronhoffs *et al.*, 2002; Workenhe *et al.*, 2008a). Viral RNA quantification using synthetic RNA, as described here, was recently performed for quantifying ISAV (Workenhe *et al.*, 2008a). Use of *in-vitro* transcribed RNA for the absolute quantification has simplified the absolute qRT-PCR assay avoiding the need for cloning to generate synthetic transcripts to obtain the standard curve.

The SG real time chemistry used in this study was chosen due to its low cost and simplicity. The ability to simultaneously detect the virus load and the presence or absence of the virus in the test samples enhances the usefulness of the assay compared to conventional RT-PCR. To improve the sensitivity of the assay fluorogenic probes (Hodneland & Endresen, 2006) or molecular beacon methods could have been used, but SG proved suitable enough for the present study and allowed the main objectives to be accomplished (i.e. quantifying the target transcripts to evaluate the virus load over time and to examine the kinetics of viral infection). High repeatability was demonstrated during pre-optimization of the assay and the results were similar to these of the initial assay performed by Graham *et al.,* (2006b) using the same primer pair. The melting peak analysis showed a single product that peaked around $85^{o}C$ suggesting high specificity. A wider dynamic range was observed for the assay with detection of viral

copies between 10^{12} and 10^5. This was a ten-fold increase of target transcript detection compared to the original assay described by Graham *et al*., (2006b).

In general qRT-PCR assays are considered to be 10-100 times more sensitive than conventional RT-PCR. In this study, out of the total fish injected with the virus, 58 % and 68 % fish were positive for SAV by RT-PCR and qRT-PCR respectively, indicating high sensitivity of the qRT-PCR assay. In general, theose fish that were positive by qRT-PCR but not by RT-PCR had high Ct values suggesting that only fish that had high viral content were reported positive by RT-PCR. The highest mean of target transcripts was observed in the sample taken at 5 d.p.i.. The sample of 3 d.p.i, which has given the fastest CPE on CHSE-214 at the initial virus isolation also had a high level of transcripts, but had 1×10^6 copies less than samples taken at 5 d.p.i. This difference could possibly be due to the variation in the level of virus present in individual fish. The low amount of target molecules present in samples taken at 0.5 d.p.i and 1 d.p.i was significantly different and suggest that active replication of virus had possibly commenced around 1 d.p.i in the infected fish. Although the level of viral RNA does not directly indicate the virulence or infectivity of the virus (Niesters, 2001), it still provides useful supportive information to confirm the results of cell culture. Further more, the high viral copy numbers at the early stages and the mean copy number were not significantly different between time points of 1, 3, 5 and 7 d.p.i. in this experiment and could possibly be an indirect reflection of viraemia in infected fish. The dramatic reduction in virus loading at 10 d.p.i, and thereafter could be reflective of antibody associated viral clearance, as seen around 10-14 d.p.i. in a similar experiment carried out by Christie *et al*., (2007). The detection of virus in fish that was positive at 42 d.p.i,

and the infection in this could be possibly be result from initial I.P. injection of SAV1 in which establishment of infection may have delyaed.

In summary, the qRT-PCR assay developed here enabled quantification of viral-load of SAV in the head kidney over time, giving an indication of how the virus establishes infection in experimentally infected fish, and this information will be used in host-virus interaction studies in future chapters to describe the pathogenesis and immune mechanisms associated with SAV1 infection. The qRT-PCR assay appeared to be more sensitive than conventional cell culture and RT-PCR, and therefore will be useful for assessing the virus-load in field samples. It has also been shown that CHH-1 cells give a faster CPE than the conventionally used CHSE-214 cells, which is interesting as these cells are derived from heart, one of the target organs of the disease

Chapter 3

Interferon-mediated Antiviral Response in Experimentally Induced Salmonid Alphavirus 1 Infection in Atlantic Salmon

3.1 Introduction

Understanding the host immune response to disease can help in the improvement of vaccines and therapeutics to combat disease outbreaks. It is known that innate immune mechanisms play a vital role in protecting fish against viral diseases (Whyte, 2007), and this has been an active area of discussion in recent years in order to manage diseases in aquaculture (Martin *et al.*, 2008). Interferons are cytokines that induce an antiviral state in cells as a first line of defence against pathogens in vertebrates, particularly against viruses (Abbas *et al.*, 2000). These molecules have also been reported in teleosts including salmon (Robertsen *et al.*, 2003; Robertsen 2006, 2008). The classical IFNs or IFN-I consist of two types of molecule INF α and INF β (INF α/β), and are induced in all nucleated vertebrate cells by the presence of double stranded RNA (dsRNA), such viruses or poly I:C (Abbas *et al.*, 2000; Sen, 2001). Interferon II (IFN-II), on the other hand, is represented solely by INF-γ and is produced by natural killer cell (NK cell) and Th1 cells after stimulation with Interleukin-12 (IL-12), IL-18, mitogen, or antigens (Schroder *et al.*, 2004; Zou *et al.*, 2005). This protective cytokine can act on many different cell types, including macrophages, T-cells, and NK cells (Zou *et al.*, 2005; Castro *et al.*, 2008). Both IFN-I and IFN-II signal to the nucleus of the cell via the Janus kinases and Signal Transducers and Activators of Transcription (Jak/STAT) pathway using different receptors and mediators. Formation of complexes of IFN-I and heterodymaric IFN-I receptors (IFNAR1 and IFNAR2) activate Jak1, and tyrosine

kinase 2 (Tyk2), and together are involved in the phosphorylation and heterodimerisation of STAT (STAT1 and STAT2) transcription factors (Figure 3.1). Translocation of heterodymeric STAT1/2 occurs in association with interferon regulatory factor 3 (IRF3) in the presence of interferon stimulated gene 3 (ISGF3), into the nucleus of the cell where it binds to IFN-stimulated response elements. These initiate the transcription of large numbers of genes, including some that possess antiviral properties such as Mx proteins (Robertsen *et al.*, 2003; Robertsen, 2006; Zhang *et al.*, 2007).

In contrast, formation of active INF-γ and INF-γ receptor (IFNGR1 and IFNGR2) complex stimulate the phosphorylation of STAT1. The subsequent nuclear translocation of this complex binds to the specific sites on the promoters of INF-γ, and stimulates the INF-γ recognition or response elements that induce transcription of genes involved in immune defence function (Schroder *et al.*, 2004) (Figure 3.2). Information on functional studies relating to the role of the INF system in the defence against viral infections in teleosts is lacking (Robertsen, 2006), however the INF-I associated antiviral mechanism has been observed *in vivo* in fish infected with IPNV (Robertsen *et al*., 2003) ISAV in Atlantic salmon (Kileng *et al*., 2007; McBeath *et al.*, 2007). There are also a number of reports relating to *in-vitro* work in both primary and continuous cell cultures for a number of different viruses (Workenhe *et al.*, 2008b). For example, SAV induced INF-I responses have recently been demonstrated in different salmon cell lines (Gahlawat *et al*., 2009) although studies *in-vivo* of the functional significance of INF-1 in SAV infection have not yet been described. The antiviral activity of salmon Mx protein against ISAV and IPNV virus has also been demonstrated *in-vivo* and *in-vitro* in salmon in detail (Jensen & Robertsen, 2000; Jensen *et al.*, 2002).
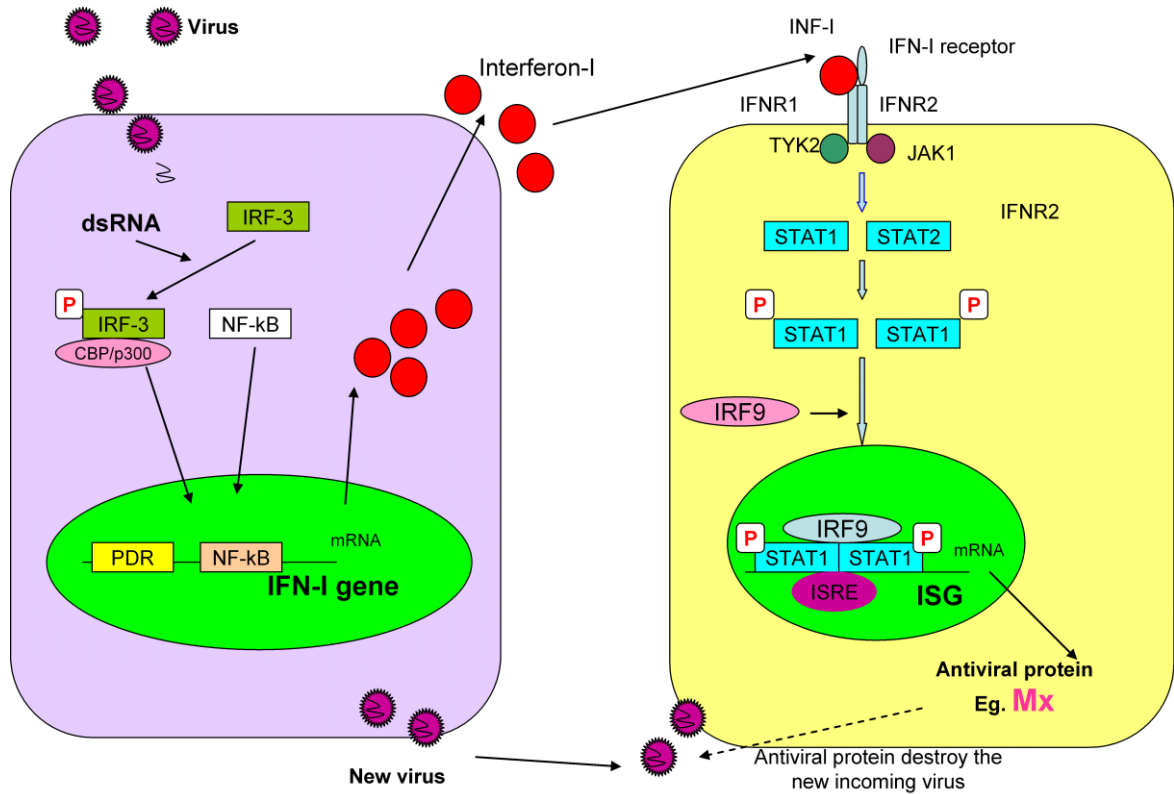
Figure 3. 1 Schematic representation of virus induced interferon –I (IFN-I) pathway of vertebrates adapted from Robertsen, (2006). Recognition of virus encoded double stranded RNA (dsRNA) by the cell activates the transcription factors nuclear factor kappa B (NF-kB) and interferon regulatory factor – 3 (IRF-3). Nuclear translocation of phosphorylated IRF-3 and transcriptional co-activator CBP/p300 complex and the NF-kB initiate the transcription of INF-I associated genes. IFN-I receptors are present in most vertebrate cells. Binding of secreted INF-I to the Interferon-I receptors (INFRI, INFR2) on the cell membrane stimulates the Janus kinase (JAK) and thyrosine kinase (Tyk2) and signals phosphorylation of STAT. The activated STAT coupled with interferon regulatory factor 9 (IRF9) enters the nucleus. Binding of STAT complex with interferon-stimulated responsive elements in the promoter regions of interferon-stimulated genes leads to transcription of antiviral protein (i.e Mx protein).
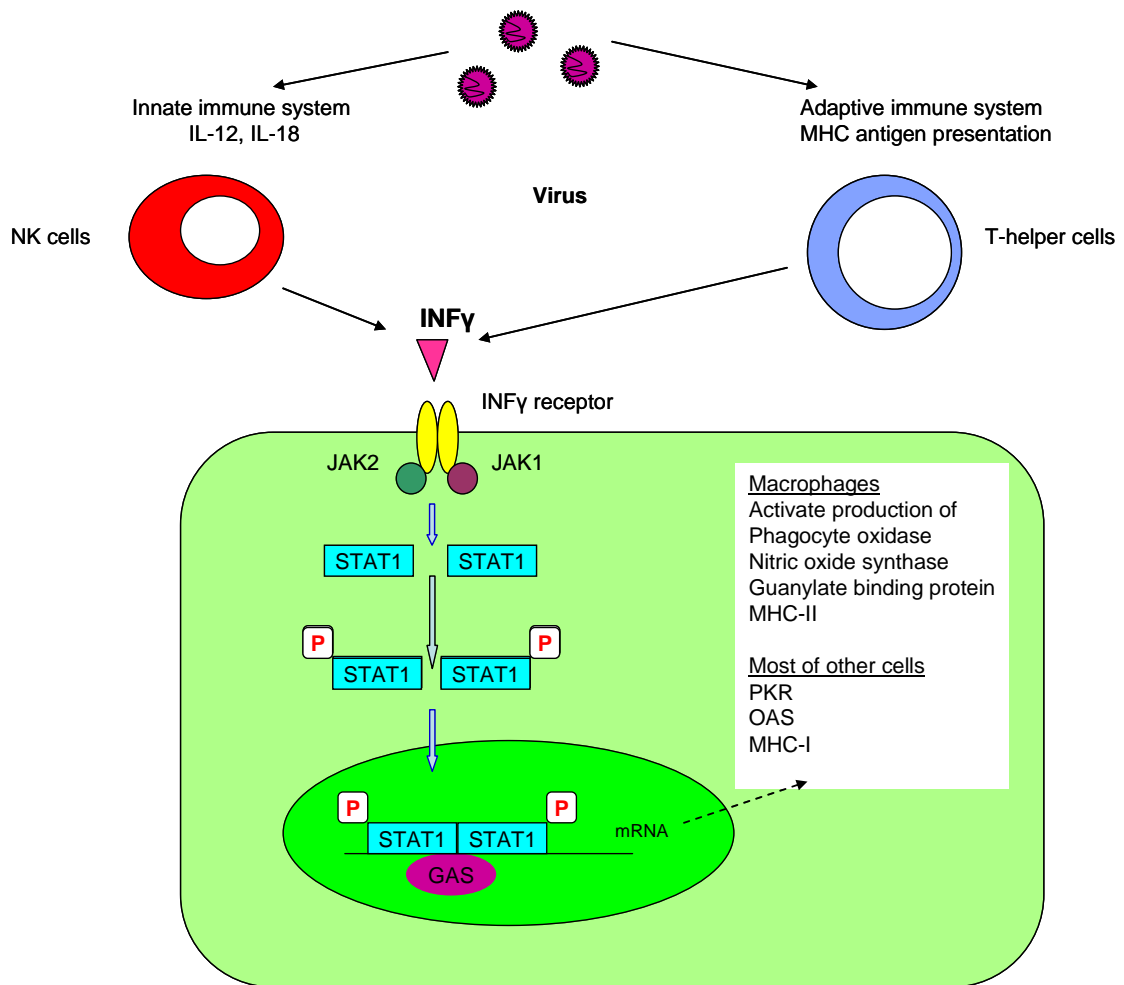
Figure 3. 2 Schematic representation of pathogen (i.e. virus) induced interferon-γ (INF-γ) pathway adapted from Robertsen, (2006). Both innate and adaptive immune responses stimulate INF- γ production in vertebrate cells. Natural Killer cells (NK cells) that are stimulated by interleukin-12 and -18 initiate production of INF- γ as a non-specific immune response during the innate immune response. In the adaptive-immune response T-helper cells initiate the production of INF-γ. Coupling of INF-γ to the INF- γ receptors stimulates the JAK-STAT pathway and results in nuclear translocation of STAT 1 and STAT 2. Binding of STAT with the specific site of the INF- γ responsive genes (GAS) in the nucleus initiates the transcription of a wide range of INF- γ responsive genes resulting in up-regulation of macrophage mediated virus destruction and antiviral protein (i.e. PKR, OAS) synthesis.

The gene encoding INF-γ has recently been sequenced in salmonids (Zou *et al.*, 2005; Robertsen, 2006; Purcell *et al.*, 2009), although the evidence for functional activities of these molecules was described some time before (Graham & Secombes, 1988). In general, INF-γ is involved in both the innate and the cell-mediated adaptive immune responses and is involved in combating both intra-cellular and extra-cellular pathogens (Schroder *et al.*, 2004; Castro *et al.*, 2008).

Administration of INF-I *in-vivo* reduces viraemia and pathogenesis suggesting it could possibly be used as an antiviral treatment. It has also been reported that the virus becomes more virulent in mammals in natural viral infections in the absence of an INF system (Sen, 2001). Further, Mx protein-associated immune protection has been observed in DNA vaccinated fish against viral haemorrhagic septicaemia virus (VHSV) during the early stages of the virus challenge used to assess the protection provided by the DNA vaccine (McLauchlan *et al.*, 2003; Acosta *et al.*, 2005). In an evolutionary sense there is a dynamic equilibrium between the virus and the host's INF system. The INF system is able to manipulate the virus replication cycle either via the INF pathway or the immune system and most probably affects a single or a number of steps in the virus replication cycle such as virus penetration and un-coating, mRNA transcription, viral protein synthesis, viral genome replication, assembly, or release depending on the group of viruses involved and the target tissues specific for the particular virus being examined (Robertsen *et al.*, 2003; Zhang *et al.*, 2007). However it has become evident that viruses also possess unique mechanisms in protecting themselves from the INF system (Cann, 2005).

The sequential pathology during SAV infection has been extensively studied under both natural and experimental conditions, although the actual pathogenesis of the virus has not yet been fully described (McVicar, 1987; McLoughlin *et al.*, 1995; 1996; McLoughlin & Graham, 2007). Apart from the role of antibody mediated virus neutralization, the information relating to immune and antiviral mechanisms against the disease is also lacking (McLoughlin & Graham, 2007; Gahlawat *et al.*, 2009). Therefore, the present study was carried out to examine the antiviral mechanisms involved in an experimental SAV1 infection in salmon with particular interest in the interferon system and its involvement in pathogenesis of the virus.

3.2 **Materials and methods**

3. 2. 1 **Experimental infection and sample collection**

Disease-free Atlantic salmon were artificially infected with SAV1 as described in Chapter 2.2.4. Samples were collected from 5, SAV1 injected and 5, control salmon at 1, 3, 5, 7, 10, 14, 21, 42 and 90 d.p.i. Heart, pancreas with pyloric caeca, skeletal muscles, skin, gill, kidney, liver, spleen and brain of both infected and control fish were fixed in 10 % neutral buffered formalin for 48 h. The head kidneys of 0.5, 1, 3, 5, 7 and 10 d.p.i were collected as described in Chapter 2.2.4 for gene expression studies.

3. 2. 2 **Histopathology**

Formalin fixed tissues collected as described in Chapter 3.2.1 were processed in an automatic tissue processor for 21 h before embedding them in paraffin wax using a Leica[®] Jung histo-embedder. The blocks were trimmed to expose the tissues and 5 µm thick sections were cut using disposable metal knives and Shandon Finess[®] microtome

before placed on glass microscope slides. The slides were placed in an oven for at least 1 h at 60°C to allow the tissue to adhere to the slide. The tissues were stained with Haematoxylin and Eosin (H&E) and examined under an Olympus light microscope. The degree of severity and extent of the lesions present in the tissue was scored arbitrarily using a scale developed by Christie *et al* (2007) with modifications (see Table 3.1)

3. 2. 3 **Real time PCR for INF-I, INF –II and Mx protein expression**

The expression of an Interferon-mediated antiviral response during an experimentally induced SAV1 infection was examined using the cDNA obtained from infected and control fish described in Chapter 2.2.7.2 using a SG qRT-PCR measured on a Techne Quantica$^{\circledR}$ Thermal cycler (Thistle Scientific, Glasgow, UK). INF-I, INF-II and Mx protein gene expression were measured in the head kidneys collected at 0.5, 1, 3, 5, 7, 10 and 14 d.p.i. relative to translation elongation factor-1α (ELF-1α), used as the house keeping gene. All primers were purchased from MWG Biotech (London, UK). The information of primer sequences used is provided in Table 3.2 of this study. All the samples tested in the qRT-PCR assays were performed in duplicate. Individual qPCR reactions of 20 μl were prepared in the wells of Thermofast 96 well clear plates (Abgene), consisting of 5 μl of 10^{-1} dilution of the total RNA derived cDNA, 1 μl of 10 μM forward and reverse primer and 10 μl of SG PCR master mix (Abgene) and 3 μl of nuclease free water. The cycling conditions used for the assays are given in Table 3.3 together with the optimized annealing temperatures. Primer efficiency (E) and relative co-efficiency of the standard curve were optimised before use in the actual test. The mean of Ct values of duplicates used in the assay were exported into Excel and expression level of the INF-1 INF-II and Mx protein were calculated using REST$^{\circledR}$ software relative to the ELF-1α (Pfaffl, *et al.,* 2002).

Table 3. 1 The scale that developed by Christie *et al.*, (2007) was used (with modifications) to score the lesions in the heart and the pancreas of Atlantic salmon infected with SAV1.

Heart		Pancreas	
SCORE	**DESCRIPTION**	**SCORE**	**DESCRIPTION**
Myocardial degeneration and necrosis		**Pancreatic degeneration**	
0	Normal	0	Normal pancreas
1	Focal myocardial degeneration	1	Focal pancreatic acinar cell necrosis
2	Multifocal myocardial degeneration	2	Multifocal necrosis/atrophy of pancreatic acinar cells
3	Severe diffuse myocardial degeneration	3	Total absence of pancreatic acinar tissue
4	Repair	4	Recovery of the pancreas
Myocardial Inflammation		**Pancreatic Inflammation**	
0	No inflammatory infiltration	0	No inflammatory infiltration
1	Mild infiltration	1	Mild infiltration
2	Moderate	2	Moderate
3	Severe	3	Severe
Myocardial Fibrosis		**Pancreatic Fibrosis**	
0	No fibrous tissue formation	0	No fibrous tissue formation
1	Mild	1	Mild
2	Moderate	2	Moderate
3	Severe	3	Severe
Epicarditis			
0	No epicarditis		
1	Mild epicarditis		
2	Moderate epicarditis		
3	Severe epicarditis		

3. 2. 4 **Immunohistochemistry for Mx protein**

The Mx protein distribution in tissues was assessed with immunostaining using a polyclonal rabbit anti-Mx antibody, kindly provided by Dr. B. Collet, Marine Scotland, Aberdeen, UK and Vector Elite ABC kit (Vector Laboratories, Peterborough, UK). The antibody was raised against a synthetic peptide (LNQHYEEKVRPC) located in the N terminal region of the Atlantic salmon Mx protein (Das *et al.*, 2007; 2008) by Sigma peptide antisera service. The immunohistochemistry staining protocol was adapted from Das *et al.,* (2007) with minor modifications.Briefly, 5 μm thick tissue sections were placed onto poly-L-Lycine coated glass slides.

Table 3. 2 Thermal cycling conditions used in the Techne Quantica® Thermal cycler for the qRT-PCR assay to quantify INF-I associated genes.

Enzyme activation	15 min	at	$95^{o}C$	
Denaturation	20s	at	$95^{o}C$	
Annealing	20 s	at optimal temperature		45 cycles
Extension	30s	at $72^{o}C$		
Dissociation peak 70-90°C measure at very 0.5^{o}C				

These were cleared in xylene (2 x 10min) and subsequently hydrated in an ethanol series (Sigma aldrich) 100 % (2 x 5 min), 90 %, 70 %, and 50 %, (1 x 2 min) then immersed in running tap water. Tissue sections were encircled with a wax pen (Vector Laboratories) and endogenous peroxidases blocked with 3 % hydrogen peroxide (Sigma Aldrich) in dH$_2$O for 5 min. Slides were washed in Tris-buffered saline (TBS) (Appendix 1) for 3 min followed by 3 min in TBS containing 0.05 % Tween-20 (Sigma

Table 3. 3 Primer sequences for different genes, product size (amplicon bp), temperature and optimized efficiency of the qRT-PCR assay used to demonstrate INF pathway associated gene expression during SAV1 infection in Atlantic salmon. Translation elongation factorv 1α was used as the house keeping gene to quantify relative expression of INF-I, Mx protein and INF II. The primer name denotes the forward (F) and reverse (R) sequence.

Gene	Primer name	Primer sequence (5'-3')	Amplicon size (bp)	Product Tm (C°)	Efficiency
Interferon-I (α/β)	INF-1 (F)	TGCAGTATGCAGAGCGTGTG	100	56	1.91
	INF-I (R)	TCTCCTCCCATCTGGTCCAG			
Mx Protein	Mx-pro (F)	ACGTCCCAGACCTCACACTC	200	58	1.91
	Mx-pro (R)	GTCCACCTCTTGTGCCATCT			
Interferon -II(γ)	INF-II (γ) (F)	GGCTCTGTCCGAGTTCATTACC	98	59	1.90
	INF-II (γ) (R)	GGGCTTGCCGTCTCTTCC			
Translation elongation factor 1α	ELF-1α (F)	CTGCCCCTCCAGGACGTTTACAA	147	58	1.87
	ELF-1α (R)	CACCGGGCATAGCCGATTCC			

Aldrich) (TTBS) (Appendix 1). All the sections were incubated with 10 % horse serum provided with the Vector ABC kit in a humid box for 30 min at room temperature to saturate the non-specific protein binding sites. Excess serum was removed by tapping the slides before incubating with 100 µl of Mx polyclonal antibody diluted in PBS (1:400) in a humid box overnight at 4°C. The next day slides were washed with TTBS before incubating with horse anti-rabbit Ig for 30 min in RT (22°C) according to the manufacturer's instructions. Slides were rinsed in TTBS for 5 min followed by a 5 min wash in TBS prior to incubating with 150 µl of amino-ethyl carbazol (AEC) reagent (Sigma Aldrich) for 10 min and washed with dH_2O. Sections were counter stained with Mayer's haematoxylin for 2 min and the reaction was stopped by immersing in running tap water. Slides were then mounted with Citifluor (Citifluor Ltd, Leicester, UK), an aqueous based mounting media mixed with PBS in a 1:1 ratio and observed under an Olympus light microscope for the presence of Mx protein. The amount of Mx protein present was scored on three randomly selected fields (x 400) on different organs, mucous membranes (gill, skin and gut) and target organs of the virus (heart, pancreas, skeletal muscles, kidney) using a scale developed to quantify the signal strength (no signal= 0, very few cells stained = 1 (<5 %), a few cells stained =2 (<20%), more cells stained = 3 (<70 %), cells diffusely stained = 4 (90%). The significance of the signal strength between time points was compared using Kruskal-Wallis test. The significance of the signal strength at each time point relative to the previous time point and between infected and control tissues were evaluated using a Mann-Whitney U-test.

3.3 **Results**

3. 3. 1 **Histopathology**

Pathological changes were evident in the heart and pancreas of the experimentally infected fish, while the histology of the control fish appeared normal. The heart lesions were observed in the infected fish from 10 d.p.i. (Figure 3.3). Four of the experimentally infected fish showed signs of cardiac lesions by 10 d.p.i while all 5 fish sampled on both 14 and 21 d.p.i had lesions in the heart. Three out of the five fish sampled had lesions in the heart on 42 d.p.i. Only one fish showed heart lesions on 90 d.p.i (Figure 3.3). The lesions in the affected hearts were noted on the pericardium and compact and spongy myocardium of the ventricle consisted of mild to moderate cardiomyocyte degeneration and cellular infiltration in the ventricle. A moderate to severe, localised to diffuse mononuclear cell infiltration was noted both in the spongy and the compact myocardium (Figure 3.4 b, c). The epicardium of the infected fish was infiltrated with mononuclear cells (Figure 3.4.d). The degenerated cardiomyocytes become strongly eosinophilic, shrunken and granular with pyknotic nuclei, further to loss of striation (Figure 3.5 a, b, c). and formation of mural thrombi on the endocardial surface was also noticed in infected fish (Figure 3.5.d).

The inflammation characterised by mononuclear infiltration was in the epicardium (epicarditis) and the ventricular myocardium and started to appear 7 d.p.i. and it steadily increased in the epicardium until 14 d.p.i and until 42 d.pi in the ventricle (Figure 3.6). The myocardial degeneration also started to appear from 7 d.p.i with the highest score of fish showing degenerative lesions in the heart at 21 d.p.i. (Figure 3.6). Only one fish showed mild degenerative lesions in the heart at 90 d.p.i, but no signs of fibrosis or

healing were noted in any of the virus-injected fish hearts throughout the experimental period.
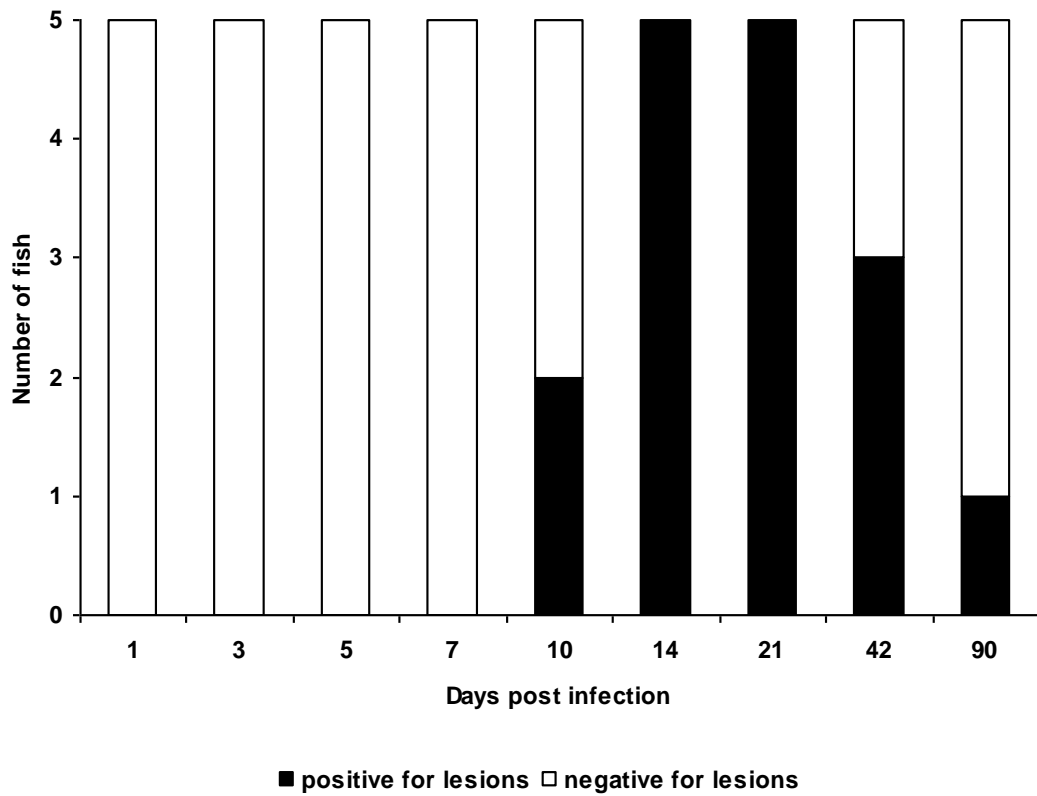
Figure 3. 3 Number of fish that had histopathological changes in the heart at different times (1- 90 Day post-infection).
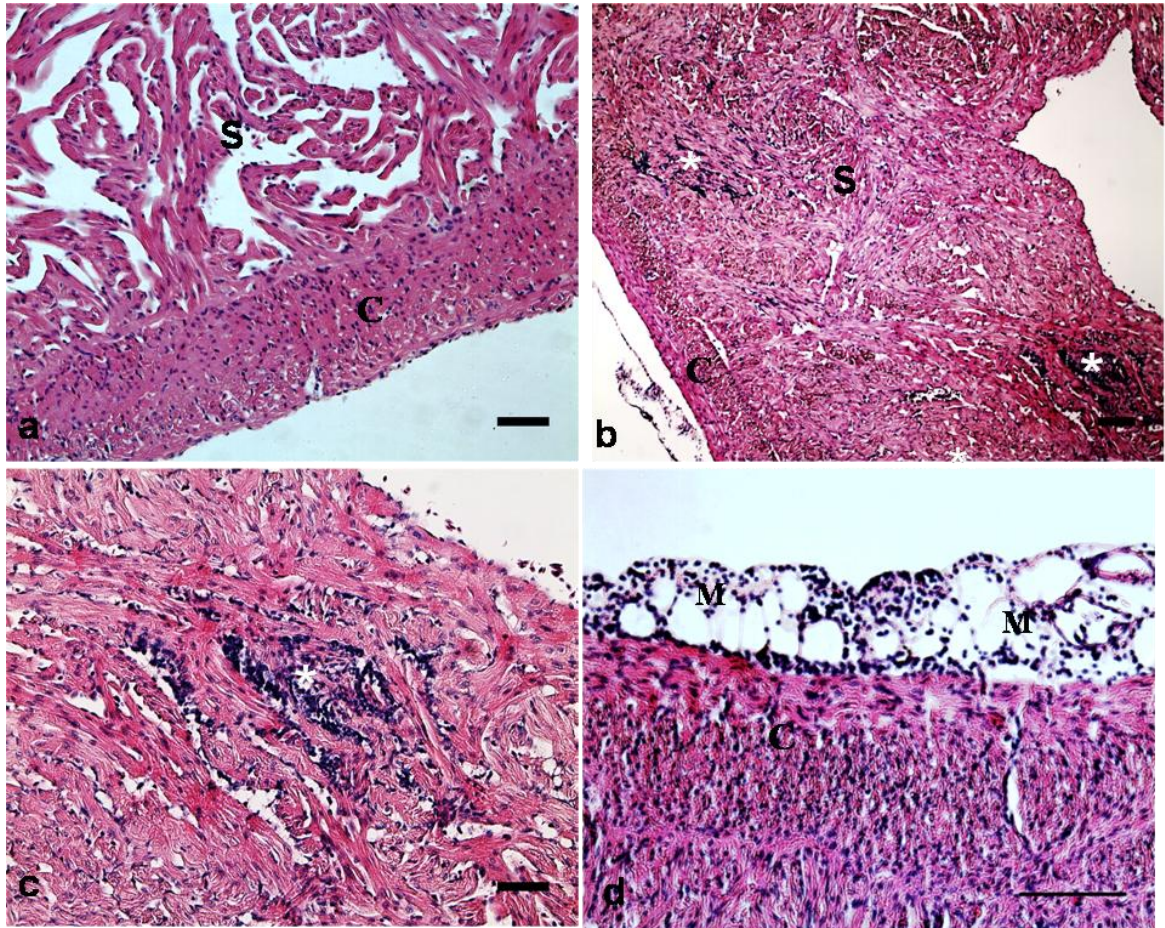
Figure 3. 4 Light microscopy of H&E stained sections of heart (a) spongy (S) and compact (C) layers of a healthy heart from a control fish and (b) lower magnification of multifocal cell infiltration (*),(c) extensive mononuclear cell infiltration (*) in spongy layer of the ventricle on 14 d.p.i, (d) extensive mononuclear infiltration (M) in epicardium on 10 d.p.i. of fish experimentally infected with SAV1 (Scale bar a,c =60 µm b = 100 µm, d = 60 µm).
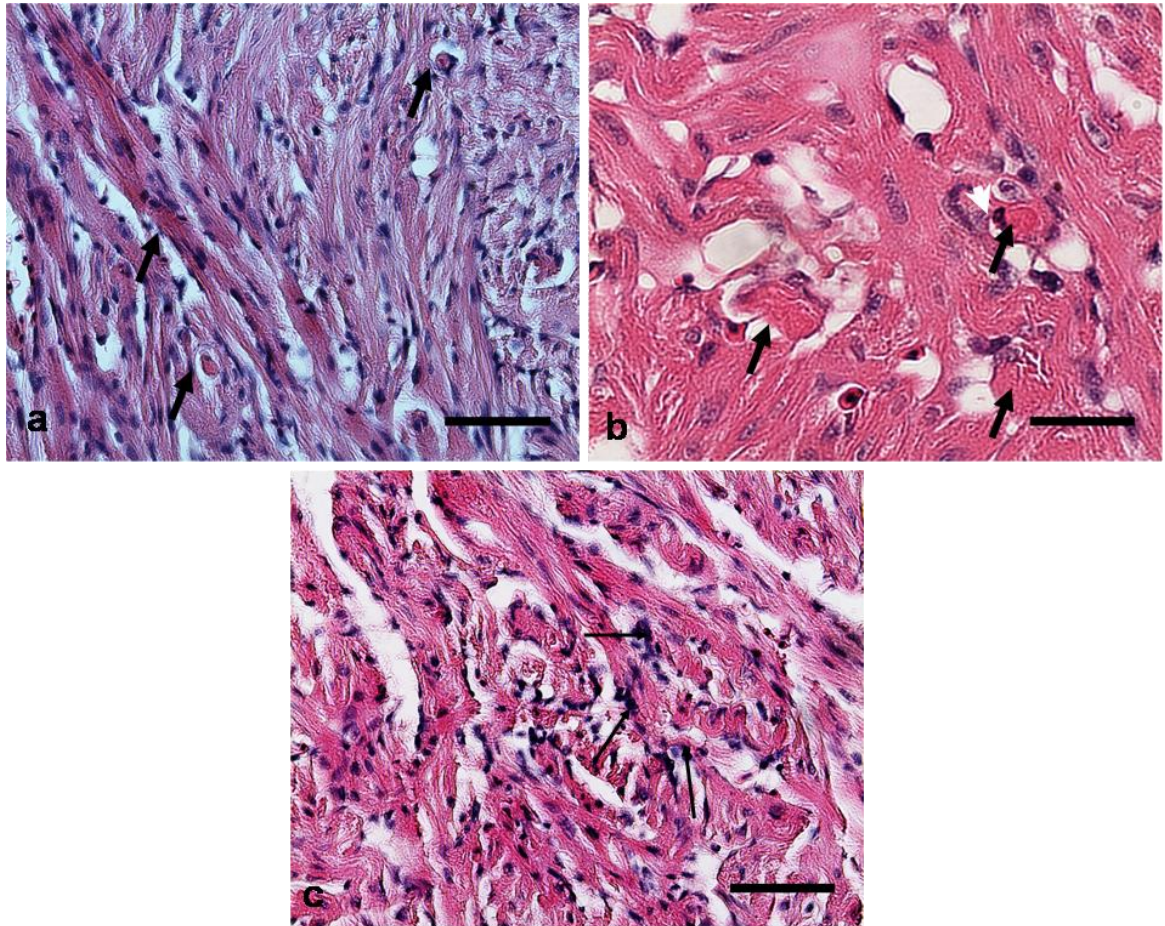
Figure 3. 5 Light microscopy of H&E stained sections of heart (a) lower magnification of myocardial degeneration (arrow) of spongy layer on 14 d.p.i (b) higher magnification of myocardial degeneration (thick arrow) and nuclear pyknosis, and (c) mural thrombi formation on the endocardial surface (thin arrow) of the ventricle on 14 d.p.i. of fish experimentally infected with (Scale bar a, c = 60 μm, b = 30)
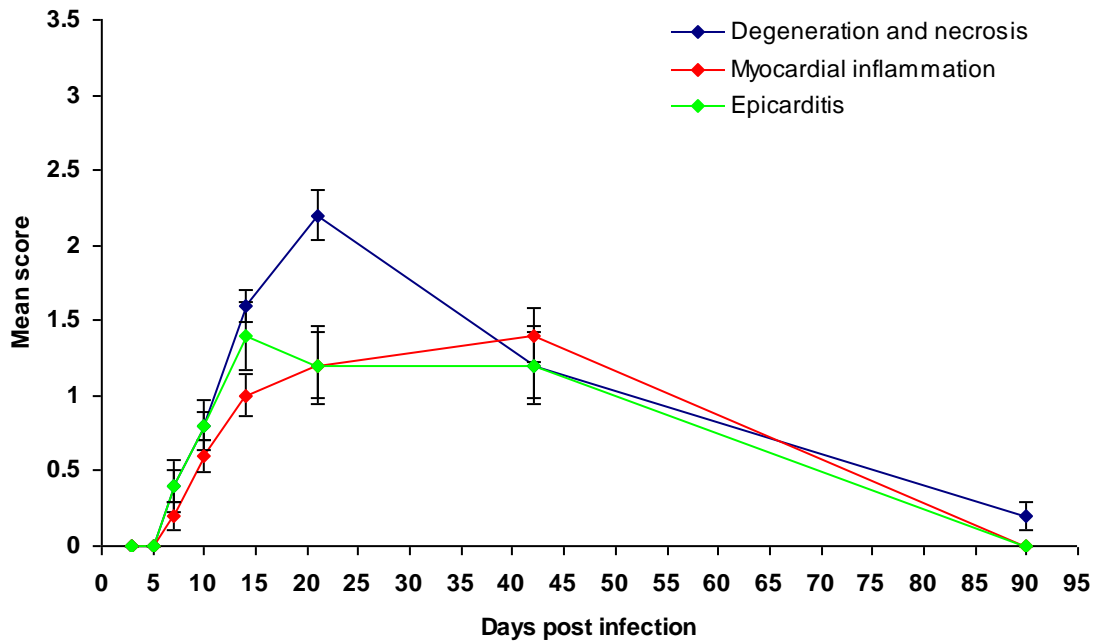
Figure 3. 6 Mean score for pathological changes in the heart of SAV1 infected fish over time (1- 90 Day post-infection).

Moderate to severe pancreatic lesions were observed in SAV1 infected fish from 5 d.p.i until 90 d.p.i. There were four fish that had lesions in the pancreas by 5 d.p.i and all infected fish had lesions in the pancreas on 7, 10, 14 and 21 d.p.i. (Figure 3.7). The pancreas of control fish consisted of healthy exocrine (Figure 3.8.a) and endocrine tissue seen adjacent to the healthy adipose tissue around the pyloric caecae. Initially, lesions appeared as mild basophilic exocrine pancreatic cell rounding and pyknosis around 5 d.p.i and this then developed to severe degeneration and necrosis from around 7 -14 d.p.i (Figure 3.8.b-d) with on-going apoptosis in exocrine pancreas on 7 and 10 d.p.i. (Figure 3.8.b). Mild to moderate, and in a few instances severe inflammation, characterised by mononuclear cell infiltration was detected around the damaged exocrine pancreas from 7 d.p.i (Fig 3.8.c-d). The complete absence, loss or very scanty exocrine cells were detected from 21 d.p.i. (Figure 3.9.a-c) with some inflammatory

cells in some instances. Very few fish had signs of fibroplasia in the pancreas, although recovering acinar cells become apparent around 21 d.p.i (Figure 3.9.d).
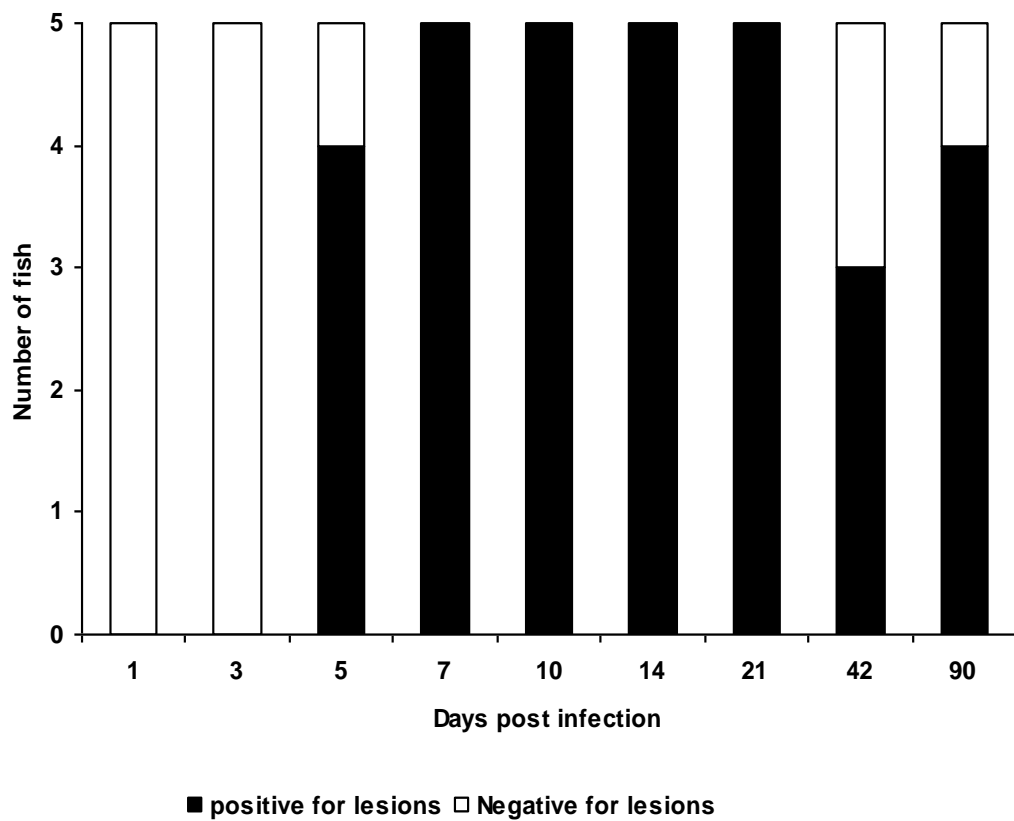
Figure 3. 7 Number of fish that had histopathological changes in the pancreas over time (1- 90 Day post-infection)
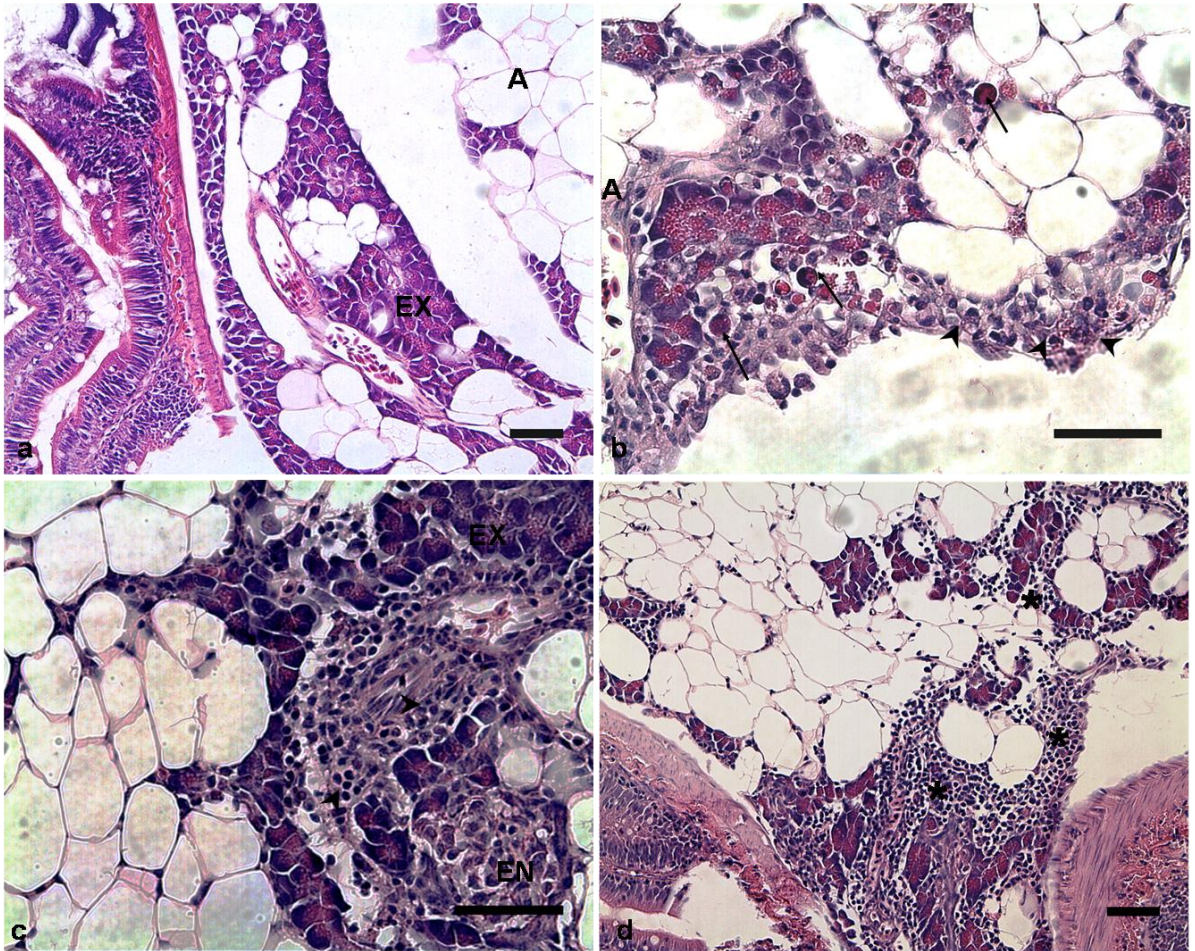
Figure 3. 8 Light microscopy of H&E stained sections of the pancreas of Atlantic salmon. (a) healthy exocrine pancreas (EX) and adjacent adipose tissue (A) of control fish (b) severe cell rounding and necrosis of exocrine pancreas (arrow head) and apoptosis (arrow) at 7 d.p.i (c) lower magnification of severe exocrine degeneration (arrow head) and unaffected endocrine pancreas (EN) with (d) extensive mononuclear infiltration (*) in the damaged exocrine pancreas 14 d.p.i of fish experimentally infected with SAV1 (Scale bar a - d = 60 µm)
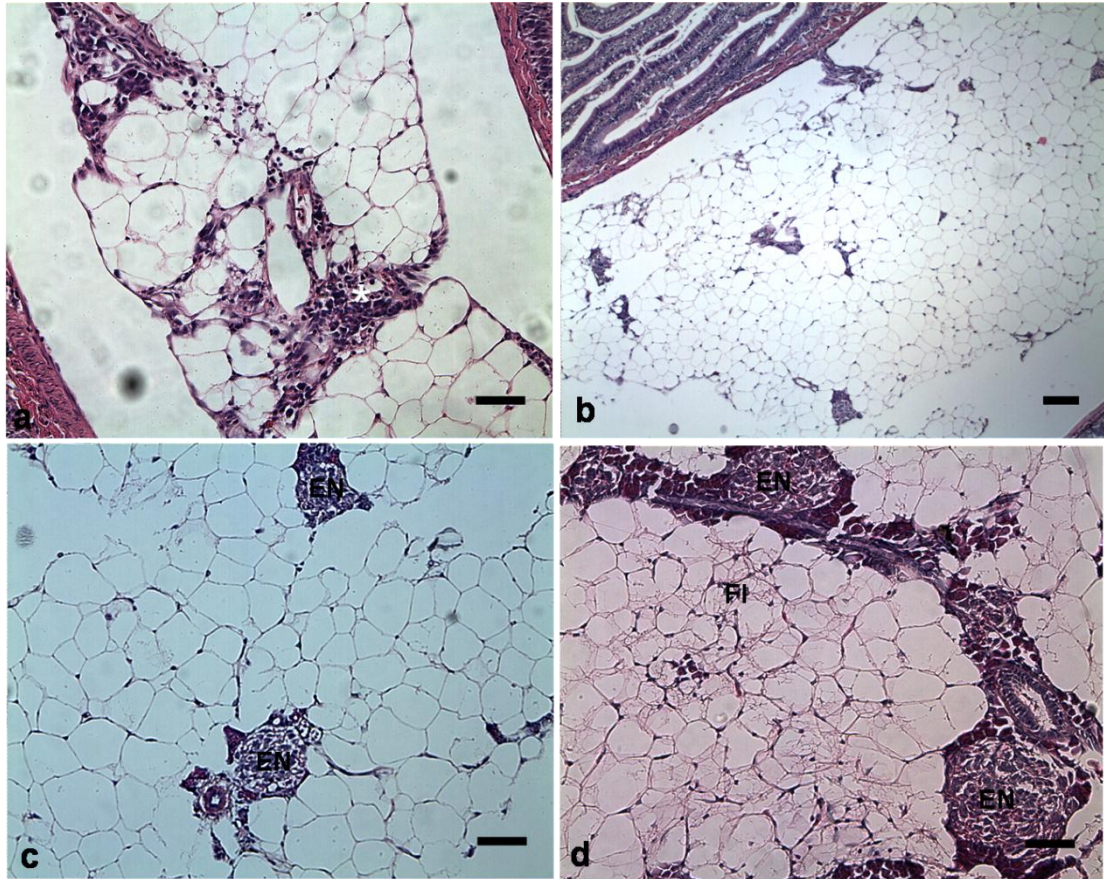
Figure 3. 9 Light microscopy of H&E stained sections of the pancreas of Atlantic salmon (a) severe loss of exocrine pancreas with mild mononuclear cell infiltration at 21 d.p.i, (b) complete absence of exocrine pancreas on 21 (c) undamaged endocrine pancreas (EN) with complete absence of exocrine pancreas at 21 d.p.i and (d) exocrine pancreas recovery with mild fibroplasia (FI) in adipose tissue in fish experimentally infected SAV1 (Scale bar a, c = 60 μm, b = 30)

The highest proportion of fish with acinar cell degeneration and necrosis was detected at 14 d.p.i. (Figure 3.10). The degree of tissue inflammation was highest at 10 d.p.i. and signs of the exocrine pancreatic recovery were apparent from 21 d.p.i with advanced regeneration occurring later at around 90 d.p.i. (Figure 3.10). A mild fibroplasia was simultaneously noted in recovering pancreas from 21 d.p.i. (Figure 3.10).

3. 3. 2 Real time PCR for INF-I, INFII and Mx protein expression

The expression of INF-1, Mx protein and INF-II relative to the ELF-1α house-keeping gene in the head kidney of infected fish compared to the control fish at 12h and 1, 3, 5, 7,10, 14 d.p.i. is shown in Figure 3.11. All three target genes were found to be down-regulated at 12 h p.i. and then started to be up-regulated from 1 d.p.i. The INF-1 expression in infected fish was significantly different from that of control fish at all sampling points except 12 h.p.i and 5 d.p.i. with maximum INF-1 expression occurring 3 d.p.i with a 250 fold increase. The highest fold change of Mx protein was also detected on 3 d.p.i in the infected fish compared to controls and the levels of expression were significantly different between infected and control fish at all the sampling points except 12 h.p.i. and 10 d.p.i (Figure 3.11.b). The peak expression of INF-II was detected at 7 d.p.i. and the expression in infected fish were significantly different from control fish at all the sampling points except 12 h.p.i (Figure 3.11.c).
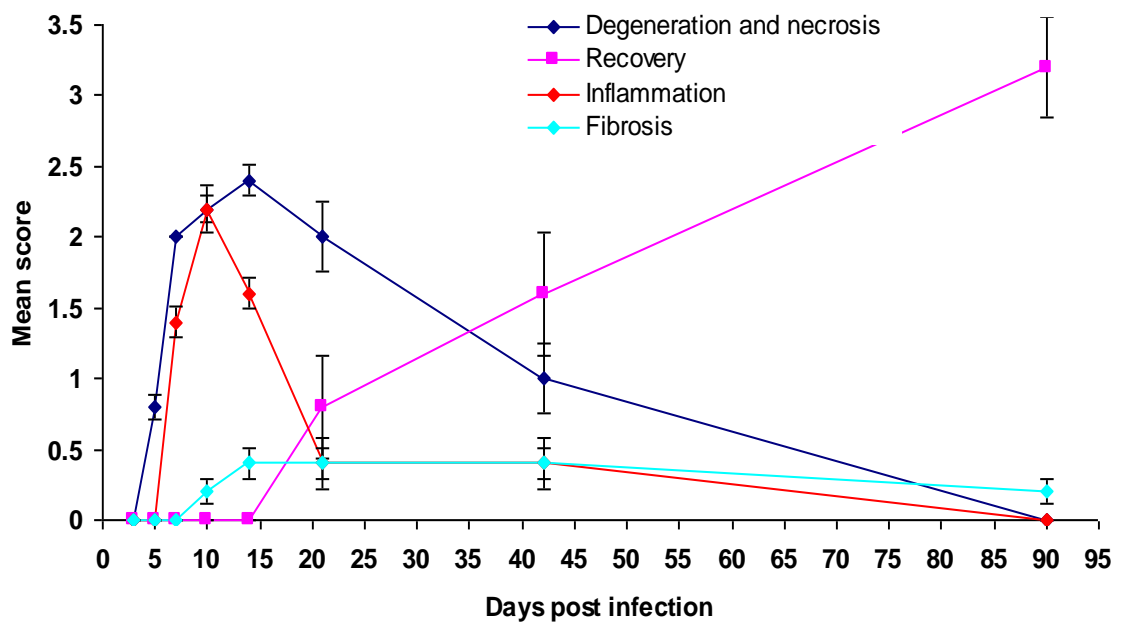
Figure 3. 10 Mean score for pathological changes in the pancreas of SAV1 infected fish over time (1- 90 Day post-infection).

(a)

(b)

(c)
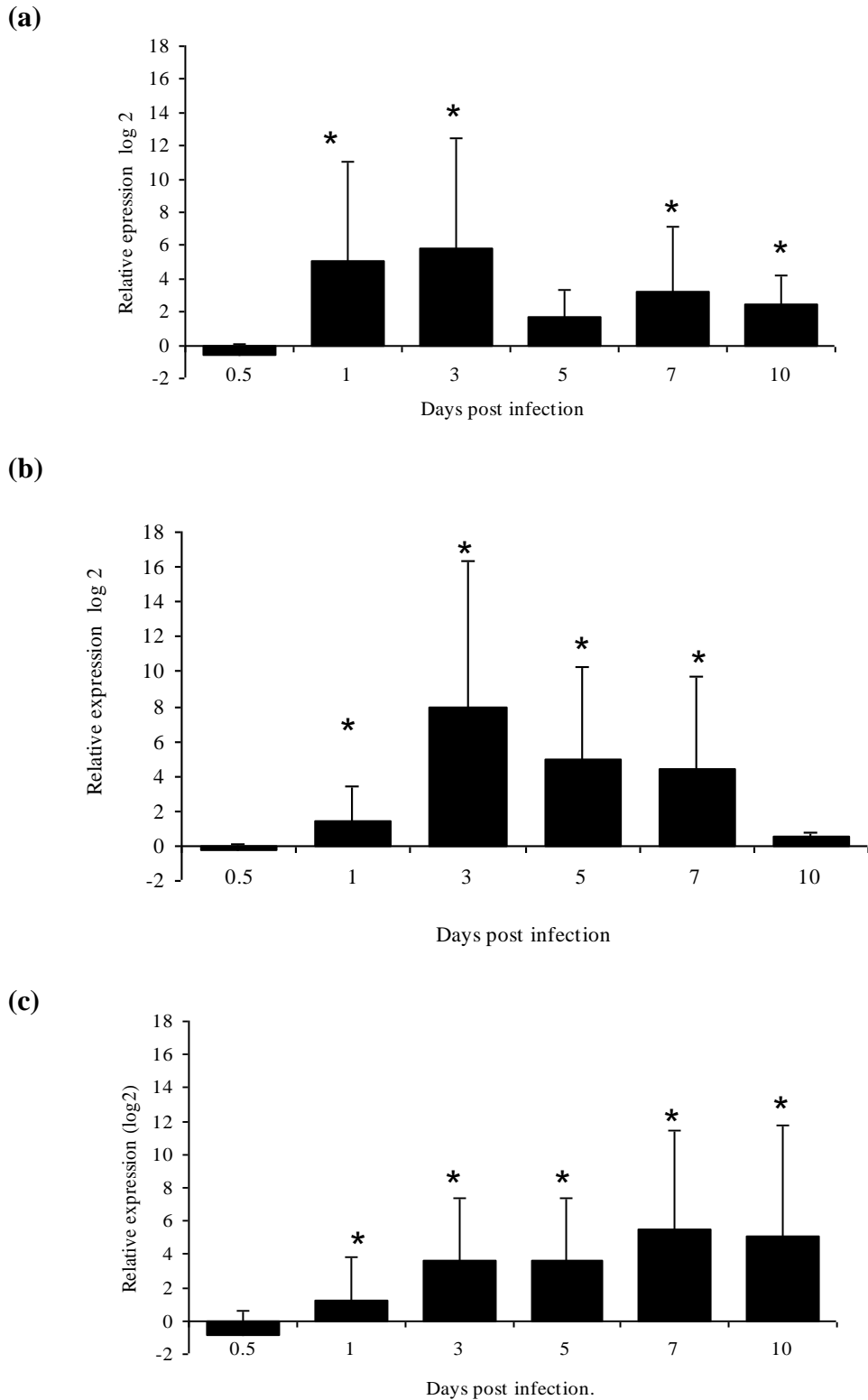
Figure 3. 11 Kinetics of real time RT-PCR expression of (a) interferon-I, (b) Mx protein and (c) INF-II in kidney of fish injected intra-peritoneally with salmonid alphavirus 1 compared to the control injected with cell culture supernatant. The data represent the average expression level $\pm$ SE relative to translation elongation factor 1α (n=5). Statistical significance levels have been indicated (*) (P $\leq$ 0.05).

3. 3. 3 **Immunohistochemistry for Mx protein expression**

The Mx protein expression in the gill, heart, kidney, pancreas, liver, skeletal muscle and liver of infected and control fish was examined on 3, 5, 7, and 10 d.p.i. The most notable amount of Mx protein expression was observed in the both compact and spongy layers of the ventricle of the heart of infected fish (Figure 3.12. c-d). Positive Mx signals were initially localised around the peri-nuclear area (Figure 3.12.e) and then became more diffuse throughout the cardiac muscles (Figure 3.12.f). The proportion of infected fish which had positive staining for Mx protein in the heart was significantly different from control fish at 5, 7, 10 d.p.i (Figure 3.13) and the Mx protein staining of the infected fish at 5 d.p.i was significantly different from the infected fish sampled on 3 d.p.i. (Figure 3.13).

The main area of staining in the kidney was associated with the tubular system (Figure 3.14.a-f) and the highest intensity of staining was noted on 3 d.p.i. (Figure 3.14.d). Interestingly, Mx expression in the kidney was significantly different between infected and control fish at both 3 and 5 d.p.i (Figure 3.15.d).

Staining for Mx was also detected on mucous membranes, especially around the mucous cells of the gills and the skin and the gut (data not shown) of both control and infected fish. The expression was intense in the infected fish gill (Figure 3.16 b,d), which was significantly different from control fish at 3 and 5 d.p.i (Figure 3.17). The positive staining observed in the skin was mainly distributed in the epidermis and was significantly different in infected fish compared to control fish only at 10 d.p.i. (Figure 3.19).
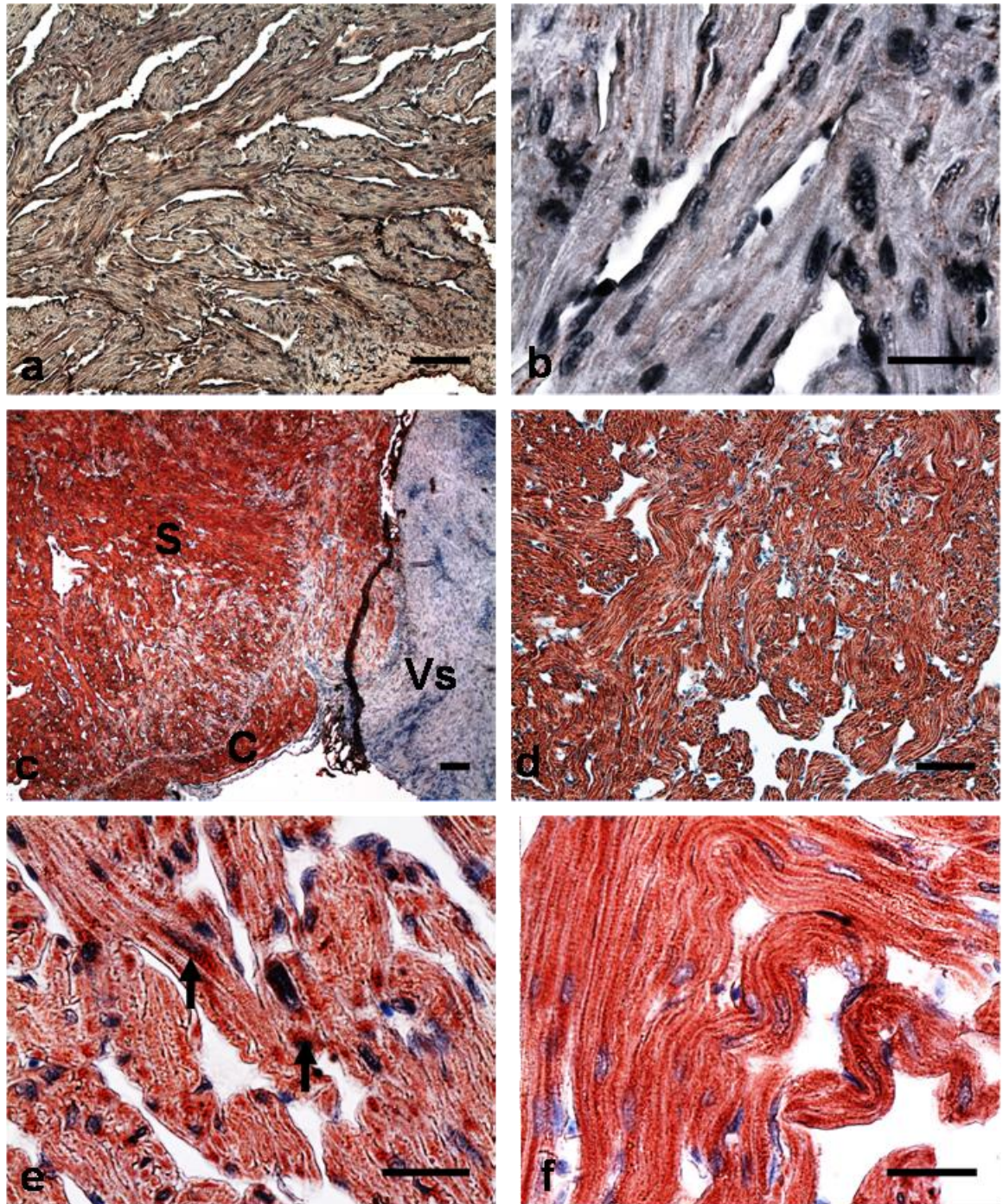
Figure 3. 12 Immunohistochemistry study of Mx protein expression in the heart of Atlantic salmon. (a) Lower magnification and (b) higher magnification of the ventricle in the control fish with no Mx staining. (c) Diffuse immunostaining in the spongy (S) and compact layer (C). Note the venus arteriosus (Vs) with no staining (VS) (d) diffuse staining in the spongy myocardium of the ventricle at 10 d.p.i. (e) accumulation of staining around the nuclei of cardiomyocytes and (f) Higher magnification of the spongy myocardium with diffuse immunostaining at 10 d.p.i. in fish experimentally infected with SAV1 (Scale bar a, d = 60 μm, b,e & f =30 μm and c= 4 μm)
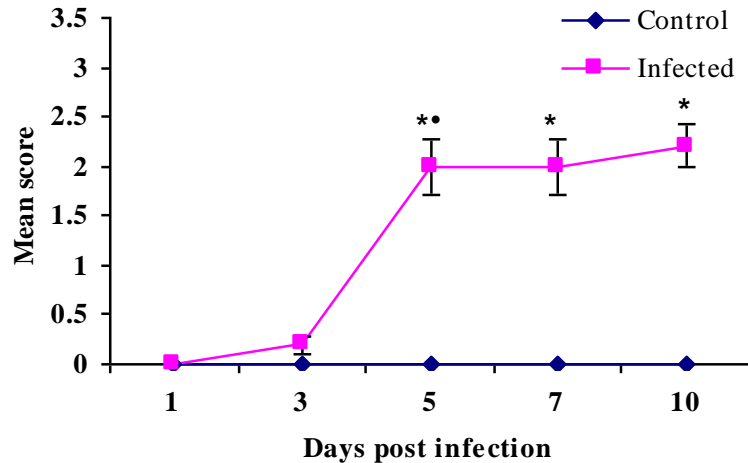
Figure 3. 13 Mean score ±SE of immunohistochemistry staining for Mx protein in the heart over the time. The significant difference between SAV 1 infected and control fish (p ≤0.05) at each time point and between previous time point of sampling are denoted by * and • respectively.

None of the intensities of the gut of infected fish were significantly different from control fish at any of the sampling points and this staining was mostly concentrated around the mucous cells.

3.4 **Discussion**

From the results of pathology, qRT-PCR and immunohistochemistry performed in this study, a rapid induction of INF-I, INF-II and Mx protein gene expression was seen in the head kidney of Atlantic salmon, along with tissue damage associated with the SAV infection. While no mortalities occurred during the 90 day experimental period, lethargy, reduced swimming and listlessness were observed in some of the virus injected fish from 5 d.p.i until 21 d.p.i.

The absence of mortalities in SAV infected fish under experimental conditions was not unexpected since this has been the case with most other experimental infections carried out with SAV (Boucher *et al.*, 1995; McLoughlin *et al.*, 1996; Boucher & Laurencin,
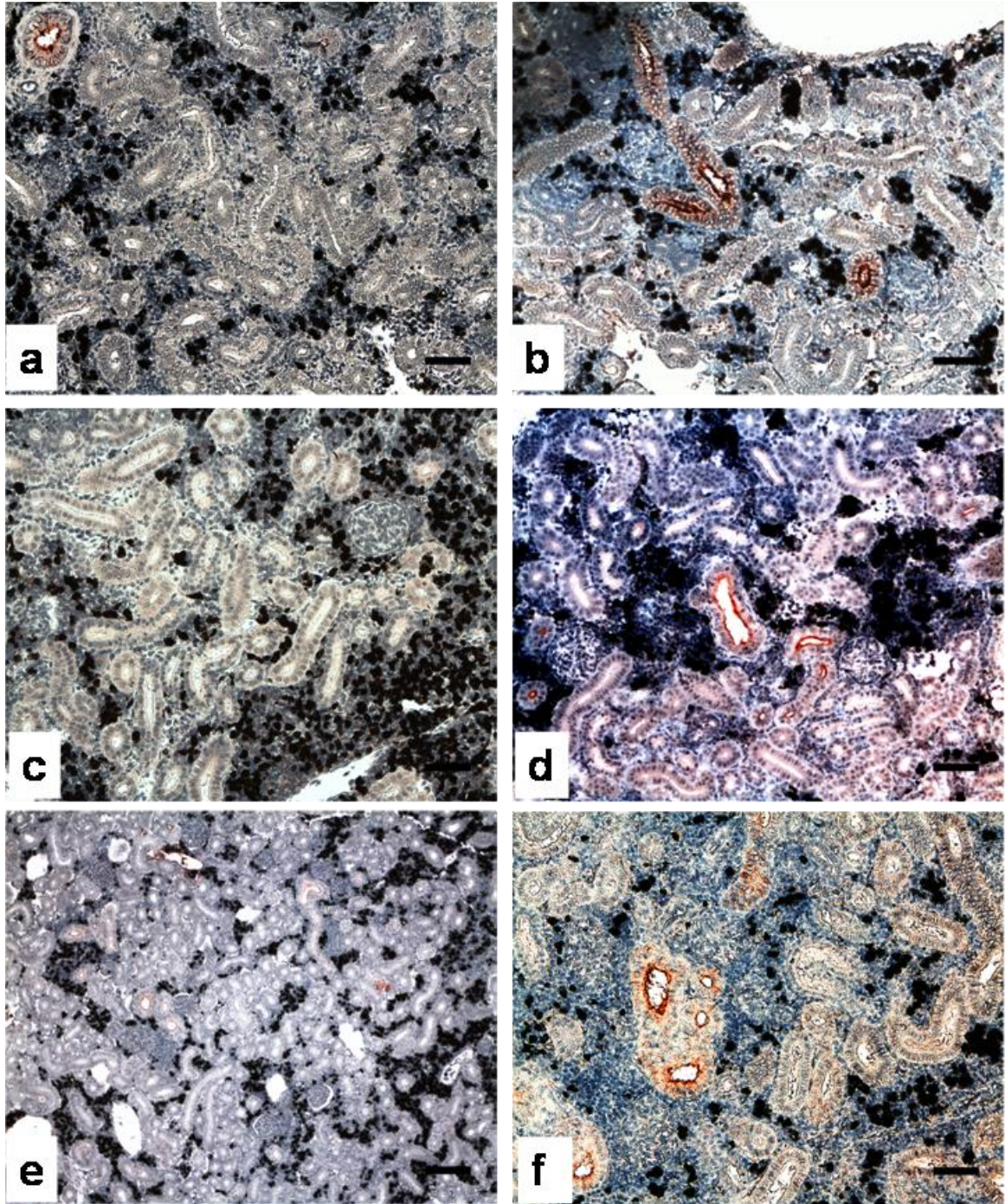
Figure 3. 14 Immunohistochemistry study of Mx protein in the kidney of Atlantic salmon (a) Control and (b) infected with SAV1 at 1d.p.i (c) control and (d) infected at 3 d.p.i (e) control and (f) infected at 7 d.p.i. Note higher degree of staining in the infected fish compared to control and the accumulation of stain in the tubular system at all three time points of sampling. (Scale bar 60 μm)
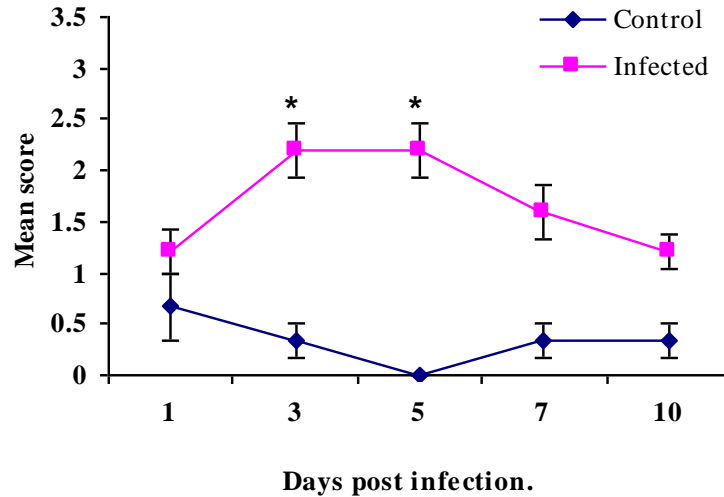
Figure 3. 15 Mean score ± SE of Mx protein expression in the kidney over the time (n=5). The significant difference between infected with SAV1and control fish (p≤0.05) at each time point is denoted by *.

1996; Desvignes *et al*., 2002; Weston *et al*., 2002; Christie *et al*., 2007). However, there are reports of mortalities occurring in SAV infections under experimental conditions, resulting from increased levels of stress during the trial, such as injecting fish with cortisol, but this type of treatment is not allowed under the regulations for animal experimentation in the UK. In a natural challenge, SAV1 has been reported to cause between 5 and 50 % mortalities in infected fish, with 100 % morbidity in the population (Rodger & Mitchell, 2007). Farmed fish are obviously subjected to a greater level of stress induced by pathogen load, water current and predators in the natural environment compared to experimentally induced infections. The complexity of the host-pathogen interactions complicated by different natural environmental factors has made SAV1 infections difficult to reproduce experimentally. Further, the virus isolate used in this experiment may have been attenuated during passage in cell culture as described by Andersen *et al*, (2007) leading to a less virulent infection in fish.
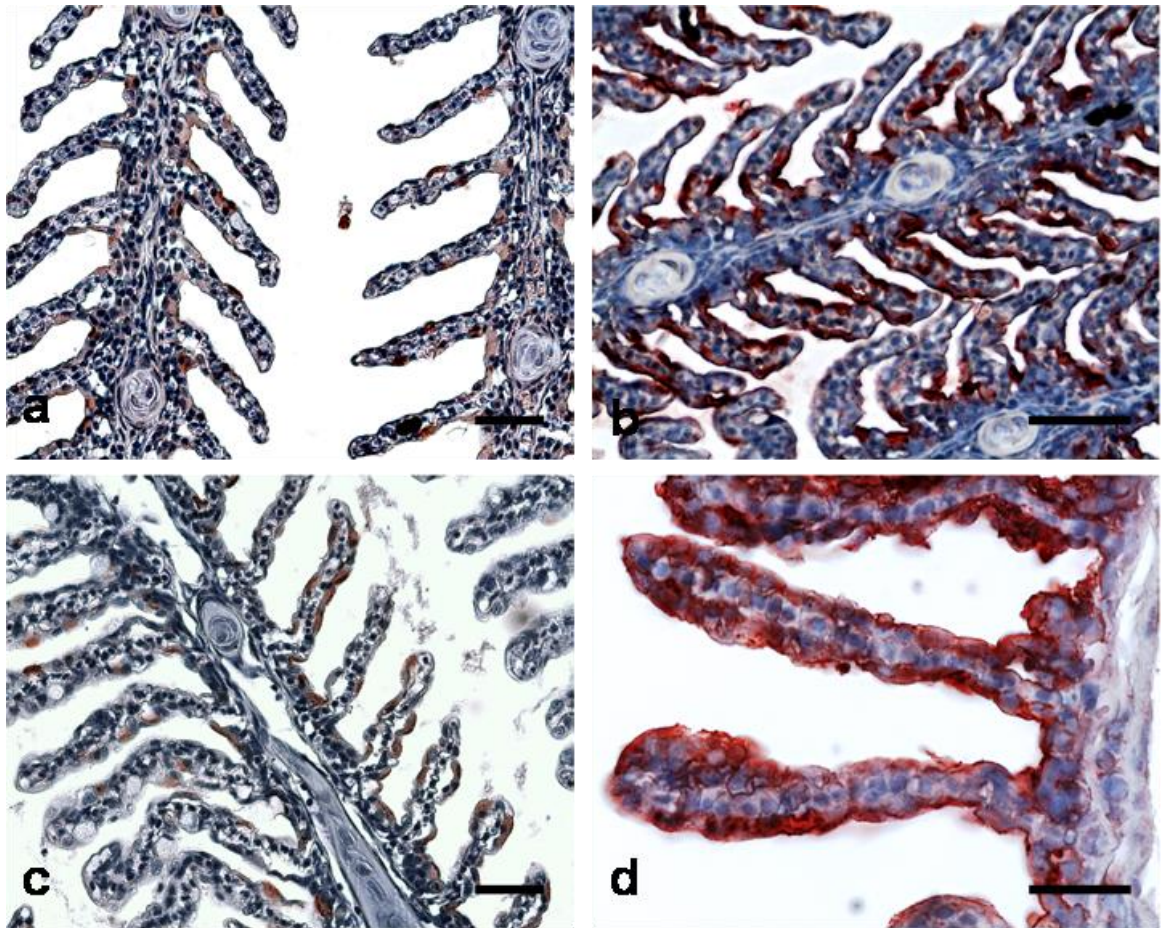
Figure 3. 16 Immunohistochemistry staining of Mx protein expression of control and exprimentallty infected with SAV1 of Atlantic salmon gill. Gill filaments at 5 d.p.i (a) control with mild (b) SAV1 infected fish moderate staining and 10 d.p.i (c) control with mild (d) SAV1 infected with diffuse staining. Note goblet cells with high intensity of staining. (Scale bar a, b & c,= 60 μm, d = 30 μm)
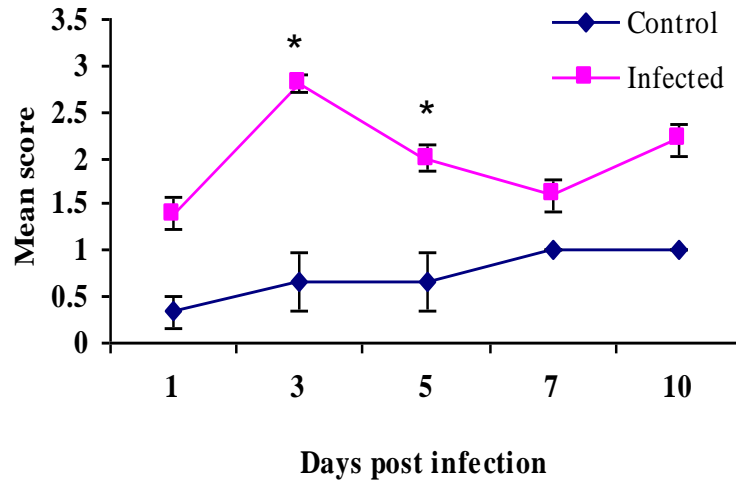
Figure 3. 17 Mean score ± SE of Mx protein expression in the gill over time (n=5). The significant difference between infected with SAV1 and control fish (p≤0.05) at each time point is denoted by *.

The lesions associated with the SAV infection were detected in the epicardium, myocardium and endocardium of infected fish. The appearance of epicarditis, characterised by infiltration of mononuclear cells in the epicardium was one of the earliest changes seen in the heart of infected fish. This has not been frequently seen with SAV infections however Christie *et al.,* (2007) also observed mononuclear cell infiltration into the epicardium in an experimental infection of SAV3. But epicarditis is consistently seen in HSMI in Atlantic salmon, which is a recently described infectious disease in salmon with possible viral aetiology (Kongtorp *et al.*, 2004a, b). The reason for the epicarditis which only recently seen in association with experimentally induced SAV is not clear however, may have results from the changes in the virus itself or changes induced cell culture derived viruses used in the experimental infections.
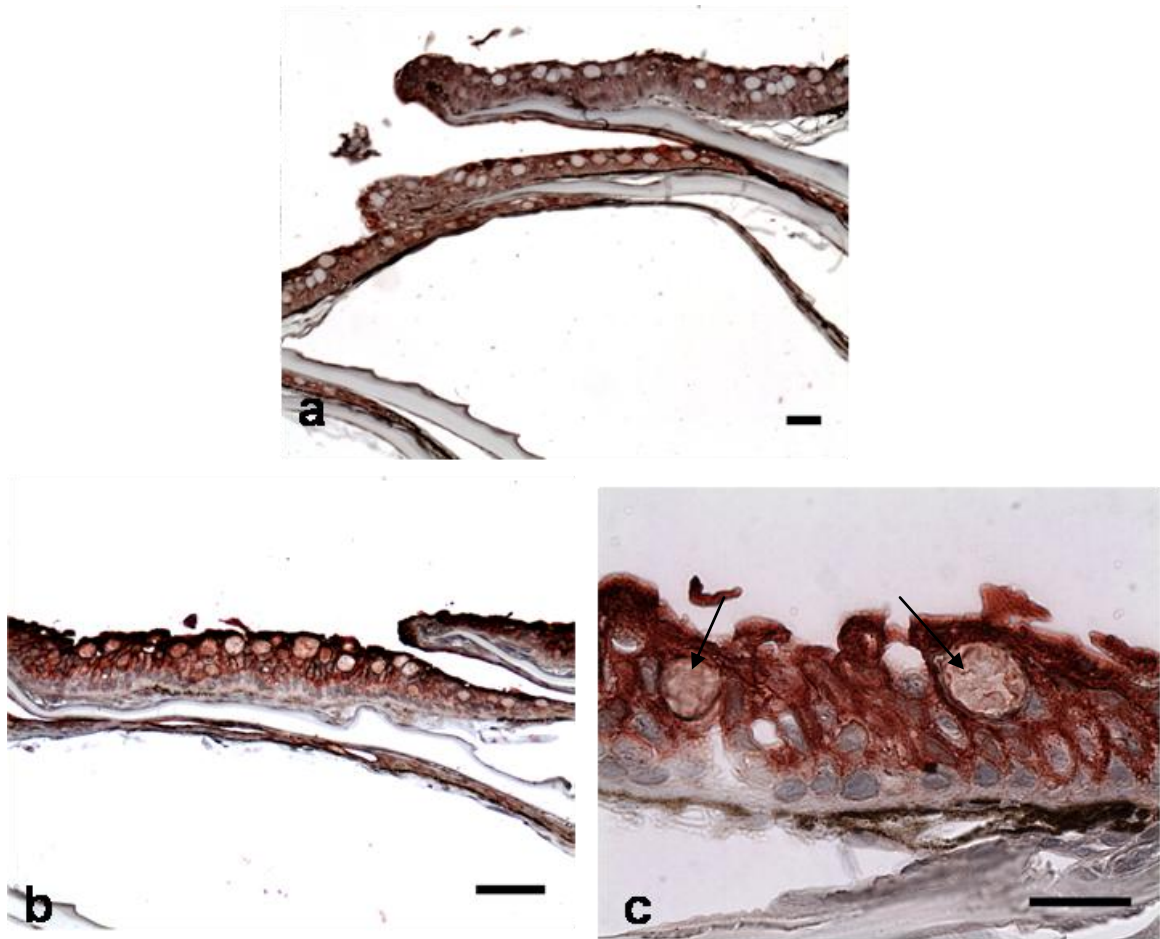
Figure 3. 18 Immunohistochemistry (IHC) staining of Mx protein in the skin of Atlantic salmon at 3 d.p.i. (a) Mild staining in control fish and intense staining in the skin of SAV1 infected fish (b) lower magnification and (c) higher magnification at 3 d.p.i. Note IHC staining is mainly accumulated around the goblet cells.
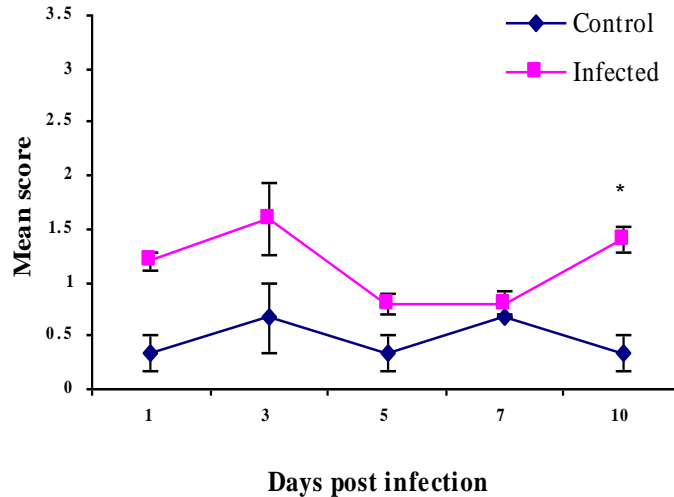
Figure 3. 19 Mean score ± SE of Mx protein expression in the skin over time (n=5). The significant difference between SAV1 infected and control fish (p≤0.05) at each time point is denoted by *.

The myocarditis and cellular infiltration observed in this experiment was characteristic of SAV infection although the severity was moderate in the present study compared to that seen in field outbreaks. The formation of mural thrombi on the endocardial surface, as seen in the present study has been reported previously with SPD infections (Ferguson *et al.*, 1986b). An increase in the severity of mural thrombosis can give rise to detrimental effects such as congestive heart failure which has been identified as the cause of death in chronic SAV infection.

The development of lesions in the pancreas is consistent with previous experimental studies and field observations for SAV infections (McVicar, 1987; McLoughlin *et al.*, 1995; 1996; 1997). The lesions started to appear relatively early in the time course of the infection and were observed up until 21 d.p.i before recovery from the lesions observed in the samples taken at 42 d.p.i. Classical signs, such as cell rounding, apoptosis and necrosis in the pancreas were noted in this study. The degree of

fibroplasia was relatively mild in affected pancreas and associated fat tissues. Similar levels of low grade fibroplasia were also seen in SAV3 field infections (Taksdal *et al.*, 2007), and it could possibly be the result of an early recovery with less inflammation present in affected tissues (Buckley *et al.*, 2001). The presence of few fish in the study showing mild to moderate mononuclear cell infiltration indicates possible inflammation and subsequent recovery of the pancreas. Interestingly, these findings indicate that acute SAV infection can recover without showing any signs of fibroplasia in the pancreas.

Salmonids are known to produce a rapid INF-1 and Mx response during a variety of different virus infections (Robertsen, 2008). Similarly, i.p injection of SAV1 was also found to induce a rapid INF-I, INF-II and Mx protein response in the head kidney tissues of Atlantic salmon. Peak INF-I and Mx protein expression were seen at 3 d.p.i. This was faster than the expression of these genes seen in similar studies conducted focusing on IPNV and ISAV infections in salmon (McBeath *et al.*, 2007) and may indicate a difference in host response against different viral infections.

Mammalian alphaviruses are known to be potent inducers of INF-I and a large number of interferon stimulated genes (ISG) including Mx protein (Landis *et al.,* 1998*;* Johnston *et al.*, 2001; Zhang *et al.*, 2007; Ryman & Klimstra, 2008). In this experiment activation of INF-1 and Mx protein was detected in the very early stages of the infection peaking at 3. d.p.i. A significant increase in INF-1 and Mx protein gene expression from day 3 d.p.i was indicative of active virus replication and establishment of infection in the head kidney of the challenged fish. However a dramatic drop in INF-1 expression was observed by 5 d.p.i although this apparently increased again on 7 d.p.i. In contrast, Mx protein expression steadily dropped after peaking at 3 d.p.i. The drop in INF-I

expression at 5 d.p.i could possibly be the result of individual variation in fish sampled at this time point (since fish were being sacrificed for sampling) rather than an actual drop of gene expression in respect to virus infection. The rate and degree of the infection is the factor that determines the degree of an INF-1 response and therefore it is not uncommon to see this type of transient regulation of cytokines and associated genes in cellular milieu, as well as a different degree of host response towards the virus infection (Robertsen, 2006; Haller *et al.*, 2007b). Similar results were noted in some of the other studies carried out in salmon using ISAV and IPNV infections (McBeath *et al.*, 2007). However with regards to the high Mx transcription observed in this experiment, the functional significance of INF-1 should be irrespective of the low level of INF-transcription detected.

The exact molecular mechanism by which Mx protein can destroy the virus is unknown (Leong *et al.*, 1998; Lee & Vidal, 2002; Haller *et al*., 2007a, b). In general, Mx protein molecules stack with each other to form a co-polymer near to the membranous structures in the cytoplasm such as endoplamic reticulum (ER) and Golgi boundaries. These co-polymers are believed to be involved in wrapping the viral nucleoproteins, preventing formation of replication complexes in RNA viruses or re-directing them to alternative sites in which genome replication cannot take place (Haller *et al.*, 2007a). Further, the formation of Mx protein and virus nucleocapsid complexes was mostly localised near to the nuclear membranes (MacKenzie *et al.* 2006). As a positive stranded RNA virus that extensively uses plasma membranes in replication (Helenius, 1995), SAV1 nucleocapsid could possibly be interacting with Mx protein on the cellular membranes and subjected to destruction. The strong immunohistochemistry (IHC) staining co-localised around the peri-nuclear region of the cardiomyocytes at 5 d.p.i

could have resulted from the formation of such Mx complexes. The diffuse staining observed at late sampling points (i.e. 10 d.p.i) was indicative of extensive Mx protein recruitment to the site with the advancement of the infection as described by Haller *et al.* (2007a). However, this has provided interesting information on Mx protein expression indicating that innate immune mechanisms operate in salmonid heart during viral infections, supporting the evidence that Mx protein is a reliable marker in monitoring INF-1 production in salmonid heart diseases.

Expression of INF-γ was also up-regulated in the early stages of the infection peaking at 7 d.p.i. In mammals, INF-γ stimulates the production of reactive oxygen and nitrogen species to kill intra-cellular pathogens and induces the production of antiviral proteins such as 2'5'-oligoadenylate synthetase, dsRNA-dependent protein kinase, guanylate binding protein and adenosine deaminase (Schroder et al., 2004). Furthermore, it also regulates the leukocyte trafficking to the injured site, enhances T-cell proliferation and antigen presentation (Abbas *et al.*, 2000). However, very little is known about the INF-γ activity in viral diseases and its involvement in the immune response in salmon (Robertsen, 2008). In this study, parallel expression of both INF-I and II suggests its possible involvement in exerting an innate immune response to the infection. The expression was only monitored in the head kidney tissue, which is a tissue rich in immune cells and it showed the possibility of using this organ as an indicator for monitoring INF-γ response. The exact cells involved in producing these molecules are still not clearly defined in fish although it has been demonstrated that lineages of NK cells and cytotoxic CD8+ cells are involved in mammalian INF-γ production (Fischer *et al.*, 2006). Gene expression alone does not provide clarification for this and therefore,

further morphological evidence would be beneficial in predicting the exact function and involvement of salmon INF-γ in immune response to viral disease.

The IHC signalling of Mx protein expression in kidney was mostly restricted to the tubules and a significant difference in signal strength was noted in infected fish at all time points supporting the expression of Mx protein in SAV1 infections in kidney tubules. However it would be interesting to evaluate this further to assess the involvement of kidney tubules in SAV pathogenesis.

The mucous membranes of salmon should play a significant role in the pathogenesis of SAV. In contrast to a vector involved lifecycle in mammalian alphavirus, atypical SAV (Villoing *et al.,* 2000a*)* should use mucous membranes as the portal of entry to the host. There is no information available on the virus shedding mechanism so far in SAV however co-habitation infection was demonstrated. The intense Mx signals seen in the mucous membranes of infected fish with IHC staining seen in the present study suggested a high pathogen load associated with these tissues and its possible involvement in virus destruction. Interestingly, the IHC signal for Mx protein was seen on the outside of the cells in the mucous membranes in addition to mucous cells, suggesting the wide distribution and possible reticular cell involvement in Mx production. The intra-peritoneal route used to induce the infection in this experiment is not a natural means of establishing SAV infection. However the involvement of mucous membrane (i.e. gills gut and skin) seen with the Mx protein IHC provides a suspicion of active involvement of cells in these tissues for virus infection and would therefore be useful in further assessment in understanding the pathogenesis of the disease.

The histological lesions observed in the fish were confined to the heart and the pancreas of the infected fish although skeletal muscles are also reported to be involved in the infection (Boucher *et al.*, 1995; McLoughlin *et al.*, 1995; 1997; McLoughlin & Graham, 2007). Skeletal lesions are the last pathology to be observed in sequential pathology for SAV infections, and the absence of these during the experimental infection could possibly be a result of rapid virus clearance via potent INF-mediated innate immune response or different tissue tropisms of the particular virus used in this study. The inverse relation of Mx expression and the severity of pathology in the heart also support this hypothesis in which Mx production could possibly clear the virus preventing progression of the infection in the heart. Furthermore, in the pancreas, the severe pathology would have resulted from low level of antiviral protein expression indicated by the low IHC staining for Mx protein. However the loss of virulence resulting from passaging the virus several times in cell cultures over time (Karlsen *et al.*, 2006), as occurs in mammalian Alphaviruses (Weaver *et al.*, 1999; Powers *et al.*, 2001) could be another reason for the low level of pathology seen in this study

In conclusion, SAV1 infection induces a rapid INF respond in salmon. Pathological changes were evident in tissues with low INF response or subsequent to the INF response. This highlights an INF-associated innate immune response which provides the first line defence in SAV infection, and possible manipulation of this may be useful in controlling SAV-1 in salmon.

Chapter 4

Transcriptomic Analysis of the Host Response in Early Stage Salmonid Alphavirus Infection in Atlantic Salmon

4.1 Introduction

The effect of a virus on its host can produce a variety of physiological outcomes, ranging from mild asymptomatic disease to the death of the host, or by transforming the host into a life long carrier of the virus. Host response to viral disease involves a complex interplay of cellular mechanisms, especially involving immune and antiviral mechanisms (Cummings & Relman, 2000; Miller & Maclean, 2008). Understanding how this physiological orchestration of the host response alters during a particular disease helps in the development of effective control measures for the disease (Schena *et al.*, 1995). The use of functional genomics has improved the understanding of the molecular and functional mechanisms which are altered during a pathogenic insult at the genomic level (Goetz & MacKenzie, 2008). Transcriptomics, the analysis of expression mRNA in the cell, tissue or at the organism level is a commonly used tool for evaluating the co-opted cellular process in response to a pathogen. Development of a microarray, which is a composite representation of genomic material of an organism, spotted onto a solid membrane, provides a versatile platform to study transcriptomics simultaneously for a large number of genes, even for the whole genome in some instances. This multiplex, quantitative, biotechnology tool, in its simplicity, offers a comprehensive high throughput of samples, and is an attractive approach for studying the interaction between the infectious agent and the associated host (Cummings & Relman, 2000).

The format of the microarrays differs depending on the material (probes) and the platform being used (Cummings & Relman, 2000). Affymetrix gene chip, glass slide arrays and membrane-based arrays are the main platforms but glass slide microarrays are considered the most versatile. The cDNA microarrays are designed from probes derived from PCR products generated from cDNA libraries or clone collections of genomic DNA (Schena *et al.*, 1995). The spots on cDNA miroarrays range from 100-300 µm and are printed robotically on pre-determined positions of glass or nylon membranes, and more than 30000 known cDNA probes can be incorporated onto a normal microscopic slide (Schulze & Downward, 2001; Gracey & Cossins, 2003). Oligonucleotide arrays, in contrast, use synthetic single stranded oligonuceotides of 20-25 mers in size, and are printed on either glass surfaces or on silicone surfaces by a photolithographic technique (Schena *et al.*, 1995; Goetz & MacKenzie, 2008; Martin *et al.*, 2008). Oligonucleotide arrays are far more advanced than cDNA arrays and are commercially available for different species (Schulze & Downward, 2001; Gracey & Cossins, 2003). The oligonucleotides arrays are designed to represent the most unique parts of the gene, to allow the discrimination of the most related transcripts, or splice-variants thus enabling the elimination of non-specific cross-hybridization (Schena *et al.*, 1995). However, low cost, flexibility and the fact that there is no need for primary sequence information for the printing of the DNA element, favours the use of cDNA arrays compared to oligonucleotide arrays (Cummings & Relman, 2000). Developments in sequencing technology have enabled easier procurement of EST, short sequences that act as a proxy identification tag for much longer pieces of un-sequenced cDNA, these are fundamental for the development of cDNA and oligonucleotide microarrays used in large scale expression analysis (Alne *et al.*, 2004).

Good target preparation and experimental design are vital in successful microarray experiments. In target preparation for microarray, cellular mRNA or amplified RNA (aRNA) from the particular experiment is specifically labelled with cyanine dyes (Cy3 and Cy5) by affinity purification and reverse transcribed by priming with oligo-dt or random primers. This is then hybridized against gene-specific probes spotted on the array slide under high-stringency conditions, which facilitate specific hybridizations. The average florescence of each replicate hybridized spot (the fluorescence being a proxy for the amount of probe target bound) is measured providing an estimate of the level of expression for a given gene or target transcript. Based on the identities of the probes on the microarray, the level of expression of their respective target genes can be quantified. New programs interpreting the microarray data into biological information in relation to the conditions tested requires extensive data analysis and presentation to obtain meaningful results. Even though microarrays are considered to be sensitive molecular tools, there is a greater likelihood of the generation of false positive results. Independent validation tests for post-analysis such as qRT-PCR, protein expression or northern-blotting are therefore necessary to confirm the results obtained. In addition, data generated from the microarray itself only provide a picture of the mRNA expression at a given time under given conditions. The biological function of the gene ultimately occurs through post-transcriptional modification, protein expression and associated post-translational modifications, and this is considered as another pitfall of microarray analysis. However, considering the labour-intensiveness, time and the cost involved in proteomics, analysis of global gene expression stands as a very useful method to give relatively rapid information on signalling pathways and disease status (Schena *et al.*, 1995).

Use of DNA microarray technology, first described in 1995 (Schena *et al.*, 1995; Cummings & Relman, 2000) has provided a platform for investigating the disease status and the understanding of the mechanisms of disease in humans and other animals (Cummings & Relman, 2000; Cummings, 2002; Korth & Katze, 2002; Jung & Chae, 2006; Taylor *et al.*, 2008), including fish (Goetz & MacKenzie, 2008; Martin *et al.*, 2008). Microarrays are not only available for the host itself, but are also available for the pathogen, enabling exploration of physiology, virulence/resistant factors, pharmacogenomics and genotyping of the pathogen (Cummings & Relman, 2000). In a wider sense, microarray technology can contribute to the rational design and evaluation of vaccines and other therapeutics, and in selection of health management traits, which could be useful for improving resistance to diseases of commercially farmed animals (Goetz & MacKenzie, 2008).

In the recent past high density cDNA or oligoarrays have been developed for a number of different fish species including zebrafish *Danio rerio* (Christoper *et al.*, 2002), Atlantic salmon *Salmo salar* L (Adzhubei *et al.,* 2007*)*, catfish *Ictalurus spp.* (Liu *et al.*, 2008), sea bream *Sparus aurata* and Atlantic halibut *Hippoglossus hippoglossus* (Douglas *et al.*, 2007) rainbow trout *Oncorhynchus mykiss* Walbaum (Govoroun *et al.*, 2006) and fathead minnow *Pimephales promelas* Rafinesque (Douglas, 2006; Goetz & MacKenzie, 2008; Miller & Maclean, 2008). Microarrays have been validated and used in a range of different aspects of aquaculture research such as ecological, evolutionary and environmental studies including the variability of gene expression of natural populations, speciation, ecotype diversity, environmental remediation and host pathogen interaction (Goetz & MacKenzie, 2008). In addition arrays for salmon and zebrafish have been successfully employed for cross-hybridisation studies, involving other

species which were not targeted in the design of the initial probe set (Goetz & MacKenzie, 2008).

Due to commercial interest, several microarrays have been developed for salmonid species and used to examine different aspects for improving production. In relation to host-pathogen interactions in salmonids, microarrays are being used to examine the response to stress (MacKenzie, *et al.*, 2004; Krasnov *et al.*, 2005), viral infections such as infectious salmon anaemia virus (ISAV) (Jorgensen *et al.*, 2008), infectious haematopoietic necrosis virus (IHNV) (MacKenzie *et al.*, 2006; Miller *et al.*, 2007), and viral haemorrhagic septicaemia virus (VHSV) (Byon *et al.*, 2005), bacterial diseases such as furunculosis (Martin *et al.*, 2006) and piscine rickettsial disease (Rise *et al.*, 2004), and parasitic diseases such as amoebic gill disease (Young *et al.*, 2008) and sea lice infection (Olsvik *et al.*, 2008) as well as to examine the effects of therapeutic interventions (Martin *et al.*, 2008).

Disease development and the sequential pathology of salmonid alphavirus infections have been studied extensively in both naturally infected farmed Atlantic salmon and in Atlantic salmon, rainbow trout and brown trout (*Salmo trutta*) subjected to experimentally induced SAV infections (McLoughlin *et al.*, 1995, 1996, 1998; McLoughlin & Graham, 2007). In infected Atlantic salmon the disease is characterised by initial viraemia followed by severe pathology in the pancreas, heart and skeletal muscle (McLoughlin *et al.*, 1995, 1997; McLoughlin & Graham, 2007; Taksdal *et al.*, 2007) and in some cases the kidney (Taksdal *et al.*, 2007). In response to infection with SAV1, the host produces a neutralising antibody response and displays long-lasting acquired immunity (Graham *et al.*, 2003b; McLoughlin *et al.*, 2006). Desvignes *et al.*,

(2002) studied the pathogenesis and immune mechanisms of SAV in Atlantic salmon and noted haematogenous spread of the virus, increased phagocytic activity in the head kidney of infected fish, and increased lysozyme and complement activity in the plasma of SPDV-infected Atlantic salmon parr. However the molecular mechanisms involved in SAV pathogenesis and the host antiviral response are still poorly understood.

As stated before, viruses are able to modulate host cellular processes to assist their own propagation, thus allowing the infection to become established and a disease state to develop (Korth & Katze, 2002). The altered or co-opted systems can provide key targets for the development of management strategies or therapeutic interventions for improving disease control (Miller *et al.*, 2007). With the ability to simultaneously measure cellular changes and alterations in associated pathways using microarrays, this technology was employed in the present study to examine early transcriptional events in the host response to an experimentally-induced SAV1 infection in Atlantic salmon parr. Emphasis was placed on the identification of genes associated with immune regulation, antiviral response and mechanisms of cell death during the early stages of infection, as these have particular relevance in understanding SAV1 pathogenesis. This information will, in turn, help to improve the management of SAV infection in salmon by identifying potential targets for control measures and vaccine development.

4.2 **Materials and Methods**

4. 2. 1 **4.2.1 RNA Amplification**

Total RNA was extracted from the head kidney of Atlantic salmon parr artificially infected with SAV1 (n=5) and control fish injected with CHSE-214 cells culture supernatant (n=5) sampled at 1, 3 and 5 d.p.i as described in Chapter 2.3.1. An Ambion

'Amino-Allyl MessageAMP™ II aRNA Amplification kit' (Applied Biosystems) was used to amplify the extracted RNA (aRNA) in order to obtain sufficient quantities for downstream applications, nominally resulting in 100-fold amplification of RNA. A single round of amplification was carried out using 700 ng of total RNA extracted from head kidney of infected and control fish sampled on 1, 3, and 5 d.p.i according to the manufacturer's instructions. In brief, T_7Oligo (dT) primed RNA was reverse transcribed at 42^oC for 2 h to obtain first-strand cDNA. Single-strand cDNA with T7 promoters at the 5' end was then converted into dsDNA at 16^oC for 2 h, using DNA polymerase. This was then filter-purified with the filter supplied with the kit to remove excess reagents. In addition, extraneous RNA was degraded with RNase present in the second strand synthesis mix. Amino allyl-modified aRNA was then prepared by transcribing dsDNA templates *in-vitro* at 37^oC for 14 h. After filter purification to remove unincorporated dNTPs, salt, enzymes and inorganic phosphates, the aRNA was quantified using a NanoDrop 1000 spectrophotometer and its quality was assessed by electrophoresis on 1 % agarose gel. An equal volume of aRNA (20 µl) from each sample was pooled to make a reference control (RC) and all RNA samples were stored at -70^oC until further use.

4. 2. 2 Dye coupling and purification

Infected and control aRNA samples were labelled with Cy3™dye, and the pooled RC sample was labelled with Cy5™dye (GE Healthcare, Product Nos. PA23001 and PA25001 respectively), according to the manufacturer's instructions. Briefly, dye samples were prepared by suspending them in ultra-pure dimethyl sulphoxide (DMSO) (Sigma-Aldrich). Nuclease-free water was mixed with aRNA (1.2 µg) to give a final volume of 4 µL to which, 1 µl of 0.5 M $NaHCO_3$ and 5 µL of dye solution (either Cy3

or Cy5) was added. This was incubated at 25°C on a heat-block in the dark for 1 h. Illustra^{TM}AutoSeq G-50 (GE Healthcare) dye-terminator spin columns were used to remove the uncoupled dye. After removing the bottom closure from the columns, they were centrifuged at 2000 x g for 1 min and subsequently loaded with dye-labelled aRNA before centrifuging for 1 min at 2000 x g. The success of the dye coupling was assessed by electrophoresis of 0.5 ml of labelled sample on a 1 % agarose gel stained with EtBr and visualization using a Typhoon scanner (GE Healthcare). The concentration of labelled aRNA was determined using a NanoDrop 1000 spectrophotometer. Samples were stored at -70°C prior to use.

4. 2. 3 Microarray hybridization and scanning

The TRAITS Version 2.0 Atlantic salmon cDNA microarray, comprising 16,950 features and developed by the Salmotrip consortium (Taggart *et al.*, 2008) was used for the study. Altogether, 30 arrays were used for this experiment comprising replicate 5 fish samples collected at three different time points (1, 3 and 5 .d.p.i.) from two states (infected and control). For each array a Cy3-coupled test sample was hybridized versus the Cy5-coupled pooled reference control.

Array slides were pre-hybridised to prevent non-specific hybridisation by washing them with nuclease-free water in an EasyDip^{TM} slide staining system (Canemco, Canada) (3 rinses, 30 sec each) followed by pre-hybridization in 5 x saline-sodium citrate buffer (SSC), 0.2 % SDS and 1.5 % bovine serum albumin (BSA) (Sigma-Aldrich) for 2 h at 50°C. Slides were then rinsed as before, dried by centrifugation at 500 x g for 5 min and loaded into a Lucidia semi-automated hybridization system (GE Healthcare). The hybridisation master mix consisted of 170 µl of 0.5 x Ultrahyb (1:1 ratio of Ultrahyb

and 4x SSC pH 7.0 Ambion), 20 µl Poly A (10 mg ml^{-1}, Sigma-Aldrich), and 10 µl of herring sperm DNA (10 mg ml^{-1}, Sigma-Aldrich) per sample. After dispensing 200 µl into labelled 1.5 ml tubes, the tubes were warmed to 60°C. Cy3 and Cy5 labelled samples were placed in 0.2 ml PCR tubes and denatured at 95°C for 3 min before adding to the warmed master mix. Samples were kept in the dark at 60°C until they were loaded into hybridisation chambers containing the array slides. Hybridisation solution (180 µL) was injected into each chamber using a Hamilton syringe which was thoroughly rinsed with heated MilliQ water (60ºC) after each use. The hybridisation programme comprised of chamber heating to 70°C for 10 min, hybridisation at 42°C for 17 h with pulse-mixing every 15 min, then washing: Wash-1, 1.0 x SSC, 0.1 % SDS, 800 µl flush at a rate of 8 µl sec^{-1}; Wash-2, 0.3 x SSC, 0.2 % SDS, flushing 800 µl at a flow rate of 8 µl sec^{-1}; and finally reducing the temperature to 40°C before removing the slides for high stringency washes. Manual high stringency washings were carried out at 45ºC on a Stuart Orbital incubator, with two 3 min washes of 0.2 × SSC, and three 2 washes of 0.1× SSC, followed by a 20 sec dip in 0.1× SSC. Slides were dried by centrifuging at 500 x g for 5 min in an EasyDip container with a sheet of paper towel at the bottom to absorb moisture. The hybridised slides were kept in the dark prior to scanning. Individual slides were scanned using a Perkin Elmer ScanArray Express HT scanner at 10 µm resolution. Both laser power (80-90 %) and photomultiplier tube gain (80-90 %) were adjusted to keep spot intensities within the linear portion of the response.

4. 2. 4 **Data processing**

The raw scanned intensities were imported into BlueFuse software (BlueGnome, Cambridge, UK), which employs an advanced statistical algorithm that allows optimal

separation of signal and noise, to deliver accurate and reproducible results, enhancing the quality of weakly expressed genes and the dynamic range of the experiment. All features were checked for quality, and abnormal or bad spots were identified. The linear-intensities of the replicate features were fused using a proprietary Bluefuse algorithm before transferring into Genespring GX version 10.0 (Agilent Technologies, UK) for analysis of expression. Data imported into Genespring was normalized using a Lowess correction. Quality parameters generated by Bluefuse (Blue fuse quality ≥ 0.05 in 3 out of 6 and Bluefuse confidence > 0.2 in 3 out of 6) were used to filter data for high quality. Final quality filtering in Genespring left 10,578 targets appropriate for statistical analysis. These data were examined using volcano plots to observe the gene behaviour over time. Differences between infected and control samples were compared with a Welch's t-test (unpaired samples with unequal variance)($p \leq 0.05$) for each time-point and the effects of infection and the interaction of infection and time point on gene expression was estimated using a 2-way ANOVA ($p \leq 0.05$). False discovery rate correction was not employed for analysis as this has been found to be over conservative in former studies carried out in the lab (personal communication Drs. J. Taggart and J.E. Bron) often removing 'fine' differential expression of key genes as confirmed by qRT-PCR. The gene up-down regulations of these interactions (fold change cut off value ± 1.3) were taken into account in interpreting the final outcome, and identified using GeneSpring GX software. The functional associations of the differentially expressed genes were studied with prepared gene lists. For this the top 1000 significantly, differentially expressed genes of the ANOVA lists of infection and infection and time point interaction were filtered by discarding un-known, un-named, no-hit, or with no identity to obtain a known identity. The lists results were then subjected for functional classification. The fold changes obtained from t-tests of those genes at different time

points were also combined to the final list. The functional analysis has grouped the top selected genes and was used to generate the heat maps for visualising up-down regulation of the genes. Significantly differentially expressed genes, identified for given states, were used for KEGG pathway analysis in order to assess the impact of infection on key metabolic and other physiological pathways.

4. 2. 5 **Validation of differential expression by RT-PCR**

The qRT-PCR was performed on a selected subset of key genes found to be significantly differentially expressed by microarray analysis. These genes were first compared to Atlantic salmon ESTs deposited in Genbank. Primer3 software v.0.4.0 was used to design primers based on the EST sequences for clones included in the TRAITS v.2 array, and these were selected and optimised prior to use in the experiment. Information on primers and efficiencies is listed in Table 4.1.

The qRT-PCR was performed by first constructing complementary DNA (cDNA) for 1 µg aRNA using the method described in Chapter 2.2.7.4. Each sample was tested in duplicate for in the qRT-PCR for each gene in a Quantica® real time PCR machine. The PCR reaction comprised 5 µL cDNA dilution, 1 µL of each primer (10 µM ml^{-1}) and 10 µL of Absolute QPCR SYBR Green Mix x2 (ABgene). All reactions were assembled with minimal light exposure and were subjected to thermal cycling immediately after assembly. The cycling conditions were: incubation at 95°C for 15 min in order to activate the Thermo-Start® DNA polymerase present in the mix followed by 45 PCR cycles consisting of heating for 15 sec at 95°C for denaturing, 30 sec at the desired temperature (Table 4.1) for annealing and further a 30 sec at 72°C for extension. The Ct value, which corresponds to the number of cycles at which the fluorescence emission

was monitored in real time was analyzed using REST-348 software. The target genes were normalized against 3 housekeeping genes (Table 4.1). PCR efficiency (E) was estimated in each run using a serial dilution of cDNA and efficiencies of 1.8-2.09 were considered acceptable.

4.3 **Results**

The host response induced by the SAV-1 infection in experimentally infected Atlantic salmon was studied by microarray analysis. An unpaired t-test ($p \leq 0.05$) comparing uninfected and infected populations at 1 day post infection (d.p.i) revealed a total of 464 significantly, differentially expressed genes of which 240 were up-regulated and 224 down-regulated, whilst a total of 976 and 892 genes were significantly, differentially up-regulated at 3 and 5 d.p.i., respectively. The numbers of genes found to be down-regulated on 3 and 5 d.p.i. were 921 and 691, respectively. The gene behaviour of exposed versus unexposed fish, analysed by volcano plots, was found to be considerably different at 1 d.p.i. compared to 3 and 5 d.p.i. (Figure 4.1.a-1.c). The statistical analysis of the interaction of infection with time, using 2-way ANOVA ($p \leq$ 0.05), showed 2564 genes which were significantly, differentially regulated over time in terms of the interaction of infection and time, while 3478 genes were differentially expressed with respect to the infection alone. The top 1000 significantly differentially expressed genes from ANOVA lists of infection and infection and time point interaction were checked for identity by discarding un-named, unknown, no-hits and no identity hits and resulted in 504 and 437 genes respectively from the lists. Gene lists of infection and infection time-point were then analysed for identity and the possible gene function.

Table 4. 1 Primers used for quantitative reverse transcription PCR (qRT-PCR).

Gene	Primer Name	Primer Sequence (5'-3')	Amplicon (bp)	Product Tm (C°)	Efficiency
Viperin	TC_ViP_F TC_ViP_R	GTGGAAGAGGCCATTCAGTTCAGT AGTGCAGTTAAACAGGCGGAAAGT	193	58	2.00
Chemokine CC like protein	CHE-CC_F CHE-CC_R	TGGACCGCCTCATCAAGAAGTGC ATGGGGGTGGAGGTGGTGGTGTT	131	58	2.02
Interferon induced protein 15	ISG-15- F ISG-15R	CTGAAAAACGAAAAGGGCCA GCAGGGACTCCCTCCTTGTT	100	58	2.03
Zinc finger protein	ZFP313_F ZFP313_R	TCCCTCATGGAGAACTGAGG GTTGCCACCCACCCTTACTA	143	58	1.83
Interferon regulatory factor 2	INFR2_F INFR2_R	AATCGATGCCCAAACTGAAC CATCCCCATCAGTGTTTTCC	176	58	2.09
Apoptosis regulatory	Apop-reg_F Apop-reg_R	ATGAAGAAAAGCCCCGAGAT ACCAAAGAGGAGCCAATTCC	117	58	2.05
MHC class I	MHC-1_F MHC-1_R	GGCACGAGGGATCCATTTA TAAGAACATTATGACAGAAGGCATGA	90	58	2.04
B cell lymphoma	BcL-2_F BcL-2_R	CAGAGGCACCTCCAGACTTC CTGGACCCTCTCCTCCTTCT	144	58	2.07
Serum amyloid A-1	SAA-1_F SAA-1_R	GTTCCAGTGGTCGAGGACAT ATTTGGTCTGTAGCGGTTGG	95	58	2.04
Coffilin	FlatL_B_2F FlatL_B_2R	AGCCTATGACCAACCCACTG TGTTCACAGCTCGTTTACCG	224	60	2.04
Beta-actin	B_ACT-F B_ACT-R	ACTGGGACGACATGGAGAAG GGGGTGTTGAAGGTCTCAAA	157	58	2.01
Translation elongation factor 1α	ELF1α-F ELF1α-R	CTGCCCCTCCAGGACGTTTACAA CACCGGGCATAGCCGATTCC	147	58	1.87

From the two lists, the selected 269 (ANOVA infection p≤ 0.005 and ANOVA infection time-point p≤ 0.03) genes were used for the final functional classification. The functional classes of genes found to be differentially expressed during the SAV infection consisted of genes related to establishing infection, immune-related, virus-induced and apoptosis-associated genes.

4. 3. 1 **Establishing infection and alteration of host metabolism**

A large group of genes associated with cellular stress were significantly, differentially expressed, and the majority of these were up-regulated in the infected fish over time. The up-regulated genes included heat shock proteins, proteasome-associated genes, and members of the ATPase family genes (Figure 4.2). Gene expression relating to cellular transport and vesicular trafficking (collagen a3(I), fibronectin variant 3, ABC transporter, ABC transporter precursor, metalloproteinase 2) were significantly, differentially regulated and these were probably involved in virus entry and subsequent replication (Figure 4.3). Actin-associated genes (adducine 3γ, fibronectin variant 3, ATP-binding cassette sub-family D member 2), as well as numerous membrane transport-related genes (solute carrier family protein 10, 20, 25, 31, tetraspanin 1, and protocadherin-9), were differentially regulated. Early and late endosome-associated genes (adaptor-related protein complex 3β2, adaptor-related protein complex 3σ1) were significantly, differentially expressed highlighting possible membrane-dependent virus replication (Figure 4.4). Translation elongation factors (factor 2α and 1β2) were down regulated at 3 and 5 d.p.i which could be indicative of virus-mediated protein synthesis shut down (Figure 4.4). Ubiqutine and ubiqutine associated genes were also significantly diferentially regulated in infected fish compared to control fish (Figure 4.4). In addition genes associated with cholesterol metabolism (3-hydroxyacyl- CoA

dehydrogenase type 2, acetyl-Coenzyme A acetyltransferase 1, low density lipoprotein receptor-related protein) were up-regulated on both days 3 and 5 (Figure 4.4).

4. 3. 2 **Host response**

4.3.2.1 **Innate immune response**

A large proportion of significantly, differentially expressed genes were associated with the innate and adaptive immune response. Up-regulation of interferon regulatory factors I and II (IRF I and II), interferon type-Iα2 (INF-Iα2) and INF-1α2 associated gene was seen from 1 d.p.i. in infected fish, as was the up-regulation of interferon induced proteins (ISG-15 like protein, INF-inducible Gig-2, INF inducible protein-58 and Mx3 protein) (Figure 4.5). The gene encoding the key responder to external stimuli, nuclear factor kappa-light-chain-enhancer of activated B-cells (NF-κB), was found to be up-regulated in infected fish, while down-regulation of NF-κB inhibitor, alpha-like protein B (INF-κBα), was seen at all three time points (Figure 4.5). Atlantic salmon double stranded RNA (dsRNA) activated Z-DNA binding protein kinase was also up-regulated. Further innate immune responsive transcripts, including the cytokines IL-15 and IL-18, TNFα and acute phase proteins (serum amyloid A, fibrinogen beta chain) were also seen to be significantly differentially regulated (Figure 4.5).
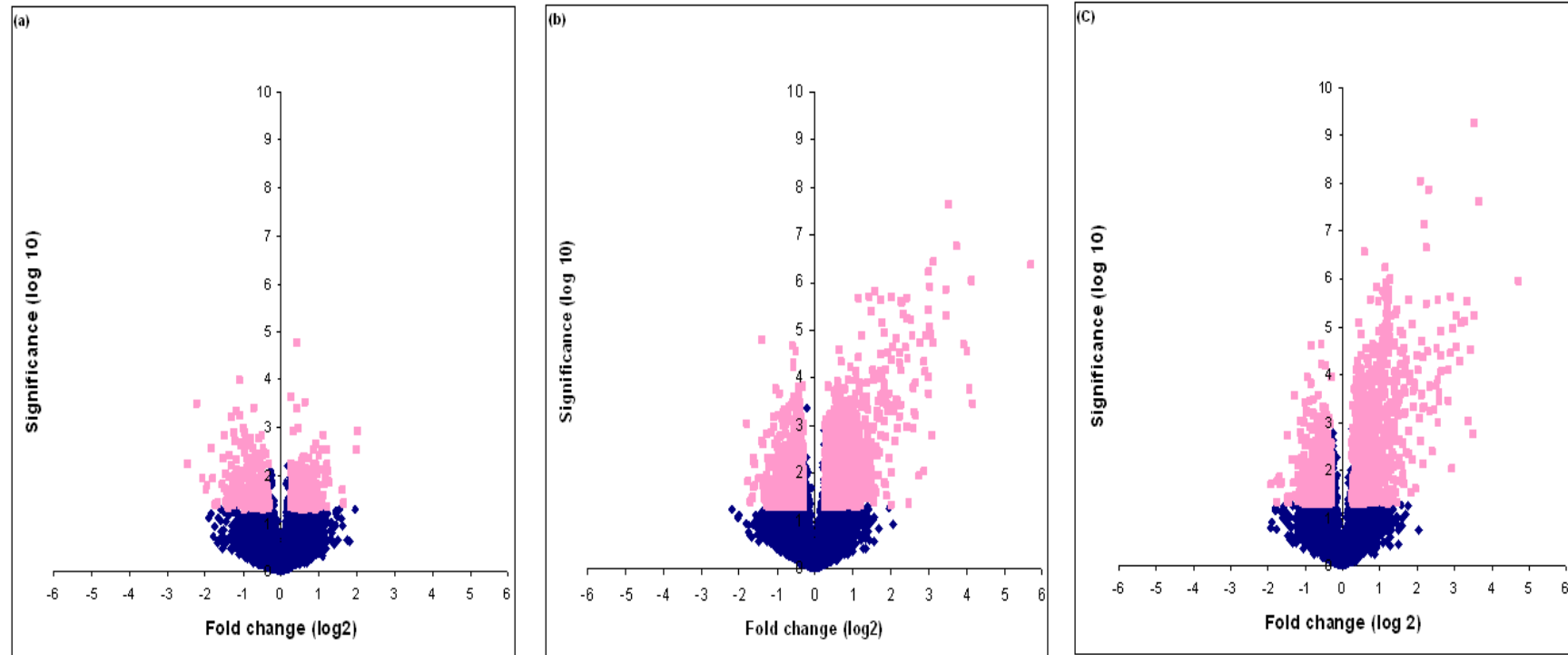
Figure 4. 1 The gene expression of SAV1 exposed verses un-exposed fish. Normalized, differentially expressed genes (significant ☐ and non-significant ■) identified by volcano plots. Genes with *p*-values < 0.05 and $\log_2$ expression ratios were plotted against $\log_{10}$ expression ratio for the three different time points (a) 1 d.p.i, (b) 3 d.p.i and (c) 5 d.p.i.

4.3.2.2 Complement system

A number of signatures of complement pathway activation were observed during the course of infection. Complement component C1q-like adipose specific protein, and factor B genes, associated with classical pathway and lectin pathway-associated mannose binding protein (lectin mannose-binding 1) were significantly up regulated at 3 d.p.i. while complement C4-q1, a gene common to both the classical and lectin pathways was also up-regulated (Figure 4.5). Alternative complement pathway members adipisin and complement factor D, were also up-regulated in addition to some complement factor genes such as CD97 (Figure 4.5).

Day 1 p.i	Day 3 p.i	Day 5 p.i	Gene name
-1.03	1.30	1.36	ATPase AAA domain containing 1a
-5.50	-1.17	1.05	ATPase AAA domain containing 1b
1.01	1.34	1.50	ATPase H+ transporting V1D
1.15	-1.48	-1.30	ATPase H+ transporting V1G1
1.07	-1.32	-1.36	Hyperosmotic protein 21
-1.51	-1.26	-1.41	Proteasome 26S
1.23	1.32	1.41	Proteasome β1
1.37	2.16	2.00	Proteasome activator
1.06	1.84	1.82	Proteasome α20S 4S
1.43	2.16	1.35	Proteasome delta
1.41	1.25	1.46	Proteasome α1
1.12	-1.46	-1.20	Glyoxalase 1
-1.13	1.52	1.40	Peroxiredoxin 6
-1.16	2.13	2.12	Heat shock 70kDa
-1.08	1.40	1.17	Heat shock cognate 70 kDa
-1.04	-1.39	-1.26	Heat shock factor 2
1.05	2.26	2.79	Heat shock factor binding 1
-1.15	1.20	1.55	Heat shock protein 9
1.03	1.38	1.26	Heat shock protein 9B
-1.13	-2.13	-1.48	t-comlx-assod-testis-expressed 1
1.08	1.85	1.40	Heat shock 90kDa-ATPase activator

Figure 4. 2 Heat map of significantly, differentially expressed, cellular stress associated genes of Atlantic salmon head kidney during an experimentally induced salmonid alphavirus infection. Columns represent time points with significantly, differentially expressed genes of challenged fish compared to un-challenged fish at 1, 3, and 5 d.p.i. Shades of red denotes gene up-regulation and green denotes down-regulation. Note, the numeric in each box indicate the fold change of the particular gene at the given time point.

Day 1 p.i	Day 3 p.i	Day 5 p.i	Gene name
0.5	1.0	-0.1	Adducin 3γ
-0.3	0.5	0.5	ABC transporter
-0.1	0.9	1.2	ABC transporter precursor
2.1	0.0	0.1	ATP-binding cas-sub-family D-mem- 2
0.1	1.3	2.1	Calcium-transporting ATPase 3
-0.1	0.7	0.8	Collagen a3(I)
0.1	-0.7	-0.4	DNA binding & differentiation
-0.1	0.2	0.6	DNA for growth hormone
-0.1	0.4	0.3	DNA J subfamily A member 2
0.0	0.1	0.2	Fibronectin variant 3 mRNA
-0.1	0.3	0.4	High mobility group protein 5
-0.1	1.8	1.6	Lipoate protein homolog
-0.1	0.7	1.3	Metalloproteinase 2
0.6	0.0	0.0	Peroxisome proli-activat beta 2A
0.2	-0.1	0.6	PHD finger protein 19 iso-a
0.1	1.1	1.7	Protocadherin-9
0.0	1.7	0.3	RAE1 RNA export 1 homolog
-0.5	1.5	1.3	RAN binding protein 2
0.0	-0.3	-1.8	Rev protein
0.1	-0.4	-0.3	Solute carrier family 10
0.3	-1.3	-0.5	Solute carrier family 20 (PO$_4$)
1.4	-0.2	0.8	Solute carrier family 25 member 5
-0.1	-0.5	-0.8	Solute carrier family 31 member 2
-0.1	0.5	0.5	Tetraspanin 1
-0.3	0.9	0.9	Valosin containing protein (Seq 1)
0.0	0.3	0.3	Valosin containing protein (Seq 2)

Figure 4. 3 Heat map of significantly, differentially expressed, cellular transport and vesicular trafficking associated genes of Atlantic salmon head kidney during an experimentally induced salmonid alphavirus infection. Columns represent time points with significantly, differentially expressed genes of challenged fish compared to un-challenged fish at 1, 3, and 5 d.p.i. Shades of red denotes gene up-regulation and green denotes down-regulation. Note, the numeric in each box indicate the fold change of the particular gene at the given time point.

Day 1 p.i	Day 3 p.i	Day 5 p.i	Gene name
1.17	1.38	1.41	**3-hydroxyacyl-CoA dehydrogenase type-2**
1.37	1.53	1.65	**Acetyl-Coenzyme A acetyltransferase 1**
-1.01	2.19	2.23	**Adaptor-related protein 3β2**
-1.13	-2.30	1.10	**Adaptor-related protein 3σ1**
-1.06	1.35	1.18	**Apolipoprotein E**
1.04	6.07	5.56	**Ataxin 2-binding protein 1**
1.12	1.09	1.44	**Carboxylesterase**
-1.10	3.24	2.96	**CCAAT/enhancer binding protein alpha**
1.14	1.99	1.61	**CCAAT/enhancer binding protein beta**
1.02	1.42	1.83	**DEAH (Asp-Glu-Ala-His) box polypeptide 15**
1.10	-1.31	-1.91	**Elongation factor 2α (seq 1)**
1.24	-1.31	-2.10	**Elongation factor 2α (seq 2)**
1.05	3.49	2.91	**Estrogen responsive finger protein**
1.07	1.56	1.43	**Glucosamine-6-phosphate deaminase 2 isoform 1**
1.07	2.08	2.60	**Glucose phosphate isomerase a**
-1.17	1.47	1.27	**Glutamine synthetase**
1.18	-1.21	-1.38	**Glycerol-3-phosphate dehydrogenase**
1.49	2.27	3.42	**Glycosyl transferase family 2**
-1.18	1.51	2.32	**Low density lipoprotein receptor-related protein 1 (seq 1)**
-1.03	2.36	2.63	**Low density lipoprotein receptor-related protein 1 (seq 2)**
-1.04	-1.41	-1.90	**Polyadenylate-binding protein-interacting protein 2**
1.12	-1.90	-1.94	**Polyadenylate-binding protein-interacting protein 3**
-1.20	1.23	1.83	**Polymerase (RNA) II (DNA directed) polypeptide D**
-2.27	-1.52	1.12	**Ribosomal 18S RNA gene and internal transcribed spacer 1**
1.06	-1.24	-1.36	**Ribosomal protein 40S S5**
-1.07	1.48	1.11	**Ribosomal protein 40S S8**
1.11	-1.35	-1.18	**Ribosomal protein 60S**
-1.01	4.07	5.96	**Ribosomal protein HL23**
1.15	-1.41	-1.41	**Ribosomal protein L10a**
-1.03	1.99	2.30	**Ribosomal protein L13a isoform**
-1.06	1.65	1.37	**Ribosomal protein L21**
1.02	8.33	8.88	**Ribosomal protein L22 60S**
1.02	1.44	1.56	**Ribosomal protein L32**
1.06	-1.34	-1.18	**Ribosomal protein L36a large subunit**
-1.19	1.66	2.18	**Ribosomal protein L37**
1.19	-1.19	-1.37	**Ribosomal protein L6 60S**
1.16	-1.13	-1.38	**Ribosomal protein L7**
-1.05	1.25	1.30	**Ribosomal protein L7 protein**
1.21	-1.32	-1.39	**Ribosomal protein L7a**
-1.04	1.18	1.22	**Ribosomal protein S26**
-2.81	-1.03	1.02	**rRNA promoter binding protein**
-1.04	1.82	1.27	**Translation elongation factor 1β2**
-1.05	-1.82	-2.20	**Translation elongation factor 2 like**
-1.18	1.95	1.88	**Translation initiation factor 4γ1 isoform 4**
-1.03	1.31	1.28	**Ubiquitin**
-1.08	1.53	1.43	**Ubiquitin protein ligase variant**
1.18	-1.49	-1.52	**Ubiquitin-conjugating enzyme E2E 3**
1.06	2.54	2.07	**Ubiquitin-conjugating enzyme E2G 2**

Figure 4. 4 Heat map of significantly, differentially expressed, cellular transcription, translation and metabolism associated genes of Atlantic salmon head kidney during an experimentally induced salmonid alphavirus infection. Columns represent time points with significantly, differentially expressed genes of challenged fish compared to un-challenged fish at 1, 3, and 5 d.p.i. Shades of red denotes gene up-regulation and green denotes down-regulation. Note, the numeric in each box indicate the fold change of the particular gene at the given time poin

4.3.2.3 Adaptive immune response

Both T- and B-cell pathway-associated genes were significantly, differentially expressed in the infected population compared to control fish. MHC I and associated genes (MHC-I, MHC-I a and b, MHC-I antigen, beta microglobulin and tapsin) were up-regulated from 3 d.p.i., while two probes for MHC class II- associated genes showed up-regulation and two showed down-regulation in infected fish (Figure 4.6). Chemokines responsible for activation and maturation of adaptive immune responses were also significantly, differentially expressed with CC-like and CXC-like chemokines being up-regulated from 3 d.p.i. Conversely, CXC chemokine-receptors were-down regulated at all three time points.

Genes involved in T-cell activation (T-cell antigen receptor beta, pre-B cell enhancing factor) and in T-cell mediated adhesion and inflammation (L-selectin) (Figure 4.6) also appeared to be activated in infected fish. In addition the gene for defender against death (DAD-1), a protein involved in T cell proliferation, was up- regulated at 3 and 5 d.p.i. in infected fish, highlighting an early onset of T-cell activation during SAV-1 infection (Figure 4.6).

Activation of tumour necrosis factor ligand super-family member 13B (TNF-13B), also known as B cell proliferation factor (BAPF) was observed in infected fish from 3 d.p.i. onwards. Immunoglobulin light chain precursor (IgL) and immunoglobulin heavy chain (two of IgH.A locus and IgH.M heavy chain) were moderately up- regulated from 3 d.p.i. (Figure 4.6).

Day 1 p.i	Day 3 p.i	Day 5 p.i	Gene name
-1.04	-1.01	-2.08	Amyloid βA4 precursor binding family B-2
1.93	2.23	1.02	C1q-like adipose specific protein (Seq 1)
1.24	3.95	3.31	C1q-like adipose specific protein (Seq 1)
1.05	2.87	1.59	CD9 protein (Seq 1)
1.99	1.75	1.58	CD9 protein (Seq 2)
1.03	2.02	2.14	CD9 protein (Seq 3)
1.02	2.26	2.65	CD9 protein (Seq 4)
-1.09	1.57	1.53	CD97 antigen isoform 2
-1.03	1.52	1.38	CD97 antigen isoform 2 precursor
-1.15	-1.36	-1.32	Coagulation factor VIII precursor
-1.07	1.98	2.31	Complement C4-q1
-1.15	-1.42	-1.63	Cytokine receptor gamma
1.14	8.83	7.84	Fibrinogen beta chain
-1.09	1.69	2.20	G-protein signaling 5
1.09	-1.10	-1.73	G-protein signaling 6
1.23	3.15	1.45	INF regulatory factor I (Seq 1)
1.09	2.84	1.59	INF regulatory factor I (Seq 2)
1.08	1.98	1.99	INF regulatory factor I (Seq 3)
1.09	1.63	1.76	INF regulatory factor I (Seq 4)
-1.32	2.84	2.51	INF regulatory-factor II
1.04	2.36	2.37	INF-induced 35 kDa
-1.10	2.81	2.61	INF-inducible protein 58
-1.22	8.04	4.21	INF-inducible protein Gig2 (Seq 1)
1.21	3.76	2.23	INF-inducible protein Gig2 (Seq 2)
-1.24	11.15	9.66	INF-inducible protein Gig2 (Seq 3)
-1.13	6.77	11.36	INF-inducible protein Gig2 (Seq 4)
1.16	2.74	1.57	INFα2
-1.10	1.56	1.16	INFα2 associated
-1.00	2.17	1.62	Interferon inducible protein 1
-1.08	1.59	1.88	Interferon regulatory
-1.02	-1.42	1.05	Interleukin 15
-1.44	-1.33	-1.96	Interleukin 15
-1.18	2.15	2.87	Interleukin 18
1.14	52.65	26.18	ISG-15 like protein
-1.09	-1.16	-1.18	Lectin mannose-binding 1
-1.06	1.16	1.13	Leucine-rich repeat kinase 1
1.29	8.81	7.45	Mx3 protein
1.06	-1.12	-1.31	Myosin heavy chain
1.04	-1.31	-1.62	Myosin heavy polypeptide 11
-2.09	-1.26	-1.18	NF-kB
-1.10	1.90	2.26	NF-kB inhibitor alphalike protein B
-1.20	1.80	1.46	Nitric oxide synthase interacting
1.15	1.89	1.74	NOD₃ protein
-1.37	2.61	1.39	Peroxisome proliferator-activated R_beta2A
1.14	-1.52	-1.51	Properdin P factor complement 1
1.33	-1.41	-1.98	Selenoprotein X 1
1.15	-1.47	-2.02	Serine protease-L protein (Seq 1)
1.14	2.97	2.77	Serine protease-L protein (Seq 2)
-1.03	1.94	1.97	Serum amyloid A
1.08	2.25	2.17	Similar to Interferon-induced 35 kDa
1.20	2.12	1.89	STAT1 (Seq 1)
-1.05	2.62	2.93	STAT4 (Seq 1)
-1.03	5.06	4.50	STAT4 (Seq 2)
1.42	2.37	2.10	Vertebrate INF-induced protein 44
-1.21	3.32	2.49	Z-DNA binding protein kinase

Figure 4.5 Heat map of significantly, differentially expressed, innate immune recognition associated genes of Atlantic salmon head kidney during an experimentally induced salmonid alphavirus infection. Columns represent time points with significantly, differentially expressed genes of challenged fish compared to un-challenged fish at 1, 3, and 5 d.p.i. Shades of red denotes gene up-regulation and green denotes down-regulation. Note, the numeric in each box indicate the fold change of the particular gene at the given time point.

Day 1 p.i	Day 3 p.i	Day 5 p.i	Gene name
1.38	1.29	1.73	**Beta-2 microglobulin (Seq 1)**
-1.06	1.92	2.38	**Beta-2 microglobulin (Seq 2)**
-1.03	1.90	2.67	**Beta-2 microglobulin (Seq 3)**
-1.01	1.64	1.32	**Bone marrow macrophage**
1.20	-1.75	-1.36	**Cathepsin D (Seq 1)**
1.12	-1.49	-1.76	**Cathepsin D (Seq 2)**
-1.17	-1.82	-1.47	**Cathepsin F precursor**
-1.10	1.67	1.32	**CD40**
-1.06	6.28	8.44	**Chemo CC-like protein (Seq 2)**
1.15	5.63	1.69	**Chemo CXCL10-like**
-1.96	-1.13	1.05	**Chemo receptor-like 1**
-1.67	-1.74	-1.69	**CXC chemo receptor (Seq 1)**
-1.53	-1.60	-1.49	**CXC chemo receptor (Seq 2)**
1.05	1.63	1.70	**DAD-1**
1.10	1.45	1.91	**Ig light chain precursor (Seq 1)**
-1.08	1.46	1.42	**Ig light chain precursor (Seq 2)**
1.96	1.26	1.25	**Ig mu binding protein 2 isoform 1**
1.23	2.44	1.61	**Ig tau heavy chain secretory**
-1.08	1.78	1.26	**IgH.A locus (Seq 1)**
-1.07	1.66	2.06	**IgH.A locus (Seq 2)**
-1.06	1.78	2.03	**IgM heavy chain**
-1.16	7.47	4.36	**Limitrin**
-1.18	2.29	2.14	**MHC class I**
1.00	1.98	2.50	**MHC class I a (Seq 1)**
1.00	1.42	1.44	**MHC class I a (Seq 2)**
-1.11	1.95	2.37	**MHC class I antigen**
1.08	2.01	1.54	**MHC class I b (Seq 1)**
1.06	1.39	1.31	**MHC class I b (Seq 2)**
-1.29	1.52	1.57	**MHCII-alpha (Seq 1)**
-1.63	-3.45	-1.06	**MHCII-alpha (Seq 2)**
1.18	4.22	3.25	**MHCII-alpha (Seq 3)**
-1.17	-1.53	-1.73	**MHCII-α and Raftlin-like PSG**
1.51	2.38	2.36	**Pre-B cell enhancing factor**
1.29	2.30	1.06	**Selectin L**
1.01	3.61	1.91	**Tapasin-B (TAPBP) (Seq 1)**
-1.23	1.29	1.60	**Tapasin-B (TAPBP) (Seq 2)**
1.07	1.36	1.66	**T-cell antigen receptor**
-1.04	1.88	2.28	**TNF-13b**

Figure 4. 6 Heat map of significantly, differentially expressed, adaptive immune recognition associated genes of Atlantic salmon head kidney during an experimentally induced salmonid alphavirus infection. Columns represent time points with significantly, differentially expressed genes of challenged fish compared to un-challenged fish at 1, 3, and 5 d.p.i. Shades of red denotes gene up-regulation and green denotes down-regulation. Note, the numeric in each box indicate the fold change of the particular gene at the given time point.

Additionally, a number of immunoglobulin associated genes (limitrin, Ig mu binding protein 2 isoform 1 and Ig tau heavy chain secretary) were up-regulated from 1 d.p.i.

4.3.2.4   Virus induced and antiviral response

Large numbers of virus-induced proteins were expressed in response to SAV-1 infection, including some of the key genes associated with Alphavirus infections such as zinc finger proteins (ZFPs) (Figure 4.7). Viral haemorrhagic septicaemia virus induced (VHSV induced) proteins were notably up-regulated with high-fold changes (Figure 4.7). For example, VHSV-5 was 15 fold up-regulated at 3 d.p.i. In addition ring finger proteins (RFPs), were also up-regulated at 3 and 5 d.p.i. Genes that encode proteins involved in antiviral-replication were also significantly differentially expressed (ferritin heavy SU, ferritin heavy polypeptide-like, barrier to autointegration factor 1 and cyclin T2) (Figure 4.7).

4.3.2.5   Cell death associated genes

Differential expression of a considerable number of genes associated with cell death was observed at all sampling points in infected fish. These included apoptosis inducers (cytochrome p450, cytochrome C oxidase subunit, death associated protein, TNF-alpha induced protein 2), pro-apoptotic (proteosome activator subunits and associated genes) apoptotic (annexine max4, caspase 7) as well as anti-apoptotic genes (B aggressive lymphoma gene BcL-2, insulin-L_growth factor precursor) (Figure 4.8). These were indicative of mechanisms for maintaining tissue homeostasis despite the virus insult.

Day 1 p.i	Day 3 p.i	Day 5 p.i	Gene name
-1.00	1.68	1.29	**Atrial natriuretic peptide**
1.33	4.92	4.49	**Barrier to autointegration fac 1(Seq 1)**
1.22	4.86	4.58	**Barrier to autointegration fac 1(Seq 2)**
1.05	1.40	1.67	**Beta-1 tubulin (Seq 1)**
-1.08	1.57	1.06	**Beta-1 tubulin (Seq 2)**
1.21	1.41	1.29	**Beta-1 tubulin (Seq 3)**
-1.71	-1.34	-1.97	**Cyclin T2**
1.02	1.42	1.83	**DEAH (Asp-Glu-Ala-His) 15**
-1.09	-1.52	-1.76	**EBV-induced G-protein receptor 2**
-1.27	2.52	2.45	**Envelope polyprotein**
-1.10	3.03	2.44	**Envelope protein**
-1.07	1.41	1.82	**Ferritin heavy polypeptide-like**
-1.03	1.58	1.71	**Ferritin heavy SU (Seq 1)**
1.00	1.73	1.79	**Ferritin heavy SU (Seq 2)**
1.01	1.54	1.67	**FLV subgroup C receptor-related 2**
1.80	-1.12	1.23	**Pentraxin**
-1.17	1.91	1.40	**RING finger protein 4 (Seq 1)**
1.94	1.90	1.43	**RING finger protein 4 (Seq 2)**
-2.33	-1.33	-1.35	**RING finger protein 153**
1.09	8.17	7.17	**VHSV- induced protein 5 (Seq 1)**
1.07	15.29	10.73	**VHSV- induced protein 5 (Seq 2)**
1.12	3.35	1.85	**VHSV- induced protein (Seq 1)**
-1.06	1.33	1.31	**VHSV- induced protein (Seq 2)**
1.05	4.11	3.87	**VHSV- induced protein (Seq 3)**
1.50	13.53	10.42	**VHSV- induced protein (Seq 4)**
-1.03	11.72	11.67	**VHSV- induced protein (Seq 5)**
-1.24	8.05	5.02	**VHSV- induced protein (Seq 6)**
-1.88	2.75	1.96	**VHSV- induced protein (Seq 7)**
-1.47	2.85	3.11	**VHSV- induced protein (Seq 8)**
-1.24	2.71	2.69	**VHSV- induced protein (Seq 9)**
-1.19	5.57	4.52	**VHSV- induced protein (Seq 10)**
-1.09	8.21	5.12	**VHSV- induced protein (Seq 11)**
1.05	4.73	4.37	**VHSV- induced protein (Seq 12)**
-1.00	4.20	4.79	**VHSV- induced protein (Seq 13)**
-1.31	2.25	2.72	**VHSV- induced protein-10 (Seq 1)**
1.02	3.09	2.72	**VHSV- induced protein-10 (Seq 2)**
1.56	18.24	12.63	**VHSV- induced protein-4 (Seq 1)**
1.07	17.16	11.68	**VHSV- induced protein-4 (Seq 2)**
-1.19	2.81	2.58	**Vig-2**
-1.06	16.21	10.09	**Viperin (Vig1) (Seq 1)**
-1.05	3.40	2.65	**Viperin (Vig1) (Seq 1)**
-3.53	-1.07	-2.20	**Viral A-type inclusion protein**
2.05	2.58	2.42	**Zinc finger CCCH domain 1**
-1.01	1.50	1.21	**Zinc finger protein 180 isoform 1**
-1.27	1.36	1.70	**Zinc finger protein 207 isoform 3**
-1.05	2.17	2.07	**Zinc Finger Protein 313 protein**
-1.12	1.42	1.47	**Zinc finger protein 406**

Figure 4. 7 Heat map of significantly, differentially expressed, virus induced genes of Atlantic salmon head kidney during an experimentally induced salmonid alphavirus infection. Columns represent time points with significantly, differentially expressed genes of challenged fish compared to un-challenged fish at 1, 3, and 5 d.p.i. Shades of red denotes gene up-regulation and green denotes down-regulation. Note, the numeric in each box indicate the fold change of the particular gene at the given time point.

Day 1 p.i	Day 3 p.i	Day 5 p.i	Gene name
1.05	3.34	2.92	ADP-ribosylation factor 3b
1.02	-1.44	-1.73	Annexin max4
-1.17	1.88	2.31	Apoptosis regulating basic protein
1.26	1.42	1.29	Apoptosis response zinc finger
1.02	1.55	1.88	B aggressive lymphoma gene
-1.04	1.26	1.32	B insulin-L_GF-1 I tupe B (IGF-I.1)
-1.15	1.58	1.24	Caspase 7
1.16	-1.75	-1.22	Cyp19b-I gene for P450
1.06	-1.35	-1.23	Cytochrome C oxidase SU-Vic
1.05	-1.17	-1.19	Cytochrome C-1 isoform
-1.05	-2.18	-1.41	Cytochrome P450 (Seq 1)
-1.04	-1.70	-2.42	Cytochrome P450 (Seq 2)
-1.05	1.52	1.20	Death-associated protein 1
-1.29	-1.37	-1.20	H3 histone family 3B (Seq 1)
1.30	2.29	1.30	H3 histone family 3B (Seq 2)
-2.05	-1.01	-1.25	Id1 protein (Seq 1)
1.15	-1.32	-1.33	Id2 protein (Seq 2)
1.12	-1.27	-1.43	Insulin-L_ GF-I precursor (Seq 1)
1.05	1.46	1.90	Insulin-L_GF-I precursor (Seq 1)
-1.04	1.63	1.90	Novel Ras family member
1.15	-1.28	-1.47	p35 transplantation AG homologue
-1.15	1.76	2.21	TNF- alpha induced protein 2
1.33	2.29	1.38	Translationally-controlled tumor protein

Figure 4. 8 Heat map of significantly, differentially expressed, apoptosis associated genes of Atlantic salmon head kidney during an experimentally induced salmonid alphavirus infection. Columns represent time points with significantly, differentially expressed genes of challenged fish compared to un-challenged fish at 1, 3, and 5 d.p.i. Shades of red denotes gene up-regulation and green denotes down-regulation. Note, the numeric in each box indicate the fold change of the particular gene at the given time point.

4.3.2.6 qRT-PCR

Nine transcripts were selected from the significantly, differentially regulated genes for qRT-PCR analysis. The selected genes were taken from the different functional categories, based on their usefulness as potential biomarkers of viral infection. Preference was given to significantly, differentially regulated transcripts with high fold change between infected and control samples and with known identity from ASG14 and BLASTN searches. The candidate genes chosen comprised pro-inflammatory cytokines (CHC-chemokines), interferon associated genes (INFRII and ISG15) and acute phase protein (serum amyloid A-1) representative of the innate immune response, MHC-1 from the adaptive immune response related genes, viperin (TC_VIP) and zinc finger protein as antiviral proteins (ZFP) and apoptosis regulatory factor (ApoREG) to represent apoptosis associated genes. All selected genes examined in qRT-PCR, gave similar results to those obtained from the microarray analysis, with high fold changes (Figure 4.9). A comparison of fold change obtained with the microarray and in the qRT-PCR is presented in Table 4.2.

4.4 Discussion

In Atlantic salmon, SAV-1 infection appears to have a profound effect on gene expression profiles in infected fish as measured by microarray. The time points selected for this study were chosen from experimental Atlantic salmon SAV1 challenges in which the highest number of virus-positive fish occurred 3 d.p.i., as assessed by cell culture and RT-PCR (Herath *et al.*, 2009). Time points were selected to represent stages
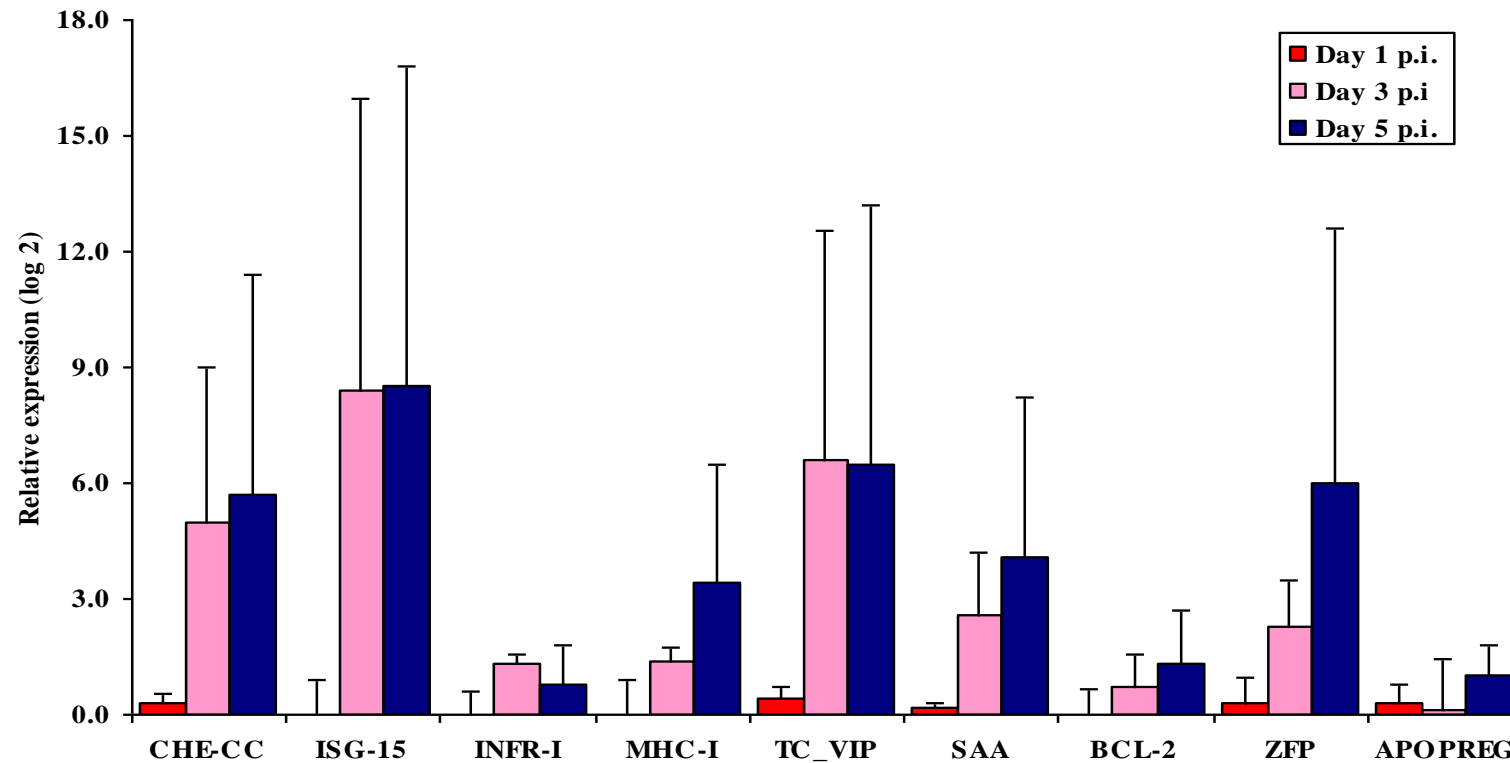
Figure 4. 9 Quantitative RT-PCR (qRT-PCR) of selected genes. The results of 9 significantly differentially regulated genes from microarray analysis were validated by qRT-PCR. The relative expression ratios (Log 2) of infected fish were calculated compared to control fish by the ΔΔct method. Both control and infected fish expression values were normalised using three housekeeping genes; translation elongation factor 1, Beta actin (actin) and flat liner Coffilin. (Chemokine CC like protein, CHC-CC, Interferon stimulated gene-15 (ISG-15), Interferon regulatory factor 2 (INFR2), Major histocompatability class_I (MHC_I), Virus induced protein TC (TC-VIP), Serum amyloid (SAA), B-cell lymphoma associated - 2 (BCL-2), Zinc-finger protein (ZFP), Apoptosis regulatory factor (APOPREG)

Table 4. 2 Microarray and qRT-PCR fold changes (FC) of the transcripts used for qRT-PCR assay

Gene	Microarray FC			qRT-PCR FC		
	Day 1	Day 3	Day 5	Day 1	Day 3	Day 5
Chemokine CC like protein	-1.1	6.3	8.4	1.2	32.2	52.1
Interferon induced protein 15 (ISG-15)	2.1	52.7	26.2	-1.1	353.9	339.5
Interferon regulatory factor 2	1.1	2.0	2.0	-1.076	2.5	1.8
MHC class I	1.0	2.0	2.4	1	2.7	10.5
Serum amyloid A-1	1.1	3	2.8	1.1	17.1	6.1
Viperin	-1.1	16.2	10.1	1.2	97	93.9
B cell lymphoma	1.0.	2.7	2.9	-1.1	10.6	2.4
Zinc finger protein	1.9	2.2	2.1	1.3	4.8	6.1
Apoptosis-regulating basic protein	1.3	2.3	1.3	1.2	1.1	2

in the infection process preceding the appearance of visible pathological changes. The microarray analysis was performed on total RNA extracted from individual fish head kidney samples. It is appreciated that the decision to use head kidney as a source of RNA has provided a kidney-centric view of the wider infection process, however this tissue was considered likely to provide the best single tissue overview of expressional changes in terms of immune response, cell death and antiviral mechanisms. The kidney is recognised as a central immune organ in teleosts (Ellis, 2001; Roberts, 2003; Ferguson, 2006), as well as being involved in excretion, osmotic balance and neuroimmuno-endocrine regulation, similar to terrestrial animals (Tort *et al.*, 1998). Head kidney of Atlantic salmon has commonly been used as the source of RNA for transcriptomic studies for other viral diseases (Miller et al., 2007; Jorgensen et al., 2008) and in addition, has been shown to experience pathological changes in response

to subtype SAV3, the Norwegian form of the SAV infection in Atlantic salmon (Taksdal *et al*., 2007).

The use of individual samples, as opposed to pooled samples, has allowed not only generic variability to be examined but also individual variability. Some authors believe that using pooled RNA samples should be avoided as it can mask sources of variability (Pavlidis, 2003), especially when studying infectious diseases. High variability between individuals in response to infection was clearly observed in this experiment (data not shown), but this may have been indicative of either different levels of virus loading during the infection or differences in intrinsic genetic history between individuals. In terms of genetic difference, cultured Atlantic salmon stocks are considered to be relatively heterogeneous because of the limited number of generations so far used in culture.

Establishment of infection

The mechanisms of host response to an infectious disease and the host's innate resistance to a given pathogen are determined by a complex interaction between components of the innate and adaptive immune pathways (Douglas, 2006). Viral infection induces a range of complex defence mechanisms co-ordinated by orchestration of diverse physiological pathways to eliminate the virus without detrimental costs to the host (Johnston *et al.*, 2001). To establish an infection, the virus must breach the physical barriers of the fish (*i.e.* the skin and mucosa of gut and gills) whereupon the host's innate immune mechanisms are triggered. These involve activation of different immune cells (granulocytes, natural killer cells and dendritic cells) or secretion of extra-cellular factors (*e.g.* lysozyme, complement) in an attempt to halt the invading pathogen.

Alphaviruses are generally vector-borne pathogens, and mosquitoes, for example ,are involved in breaching this barrier and introducing virus into the mammalian host (Strauss & Strauss, 1994; Raymen & Klimstra, 2008). Aquatic alphaviruses, however, appear to be able to cross the physical barrier without the interaction of a vector and are therefore classified as atypical alphaviruses (Villoing *et al.*, 2000a), and for this reason it has been suggested that they be listed in a separate taxonomic group (Fringuelli *et al*., 2008). Whilst no vector has yet been identified, increased sea lice (*Lepeophtheirus salmonis* Krøyer) numbers have been described as a risk factor for spread and outbreaks of SAV infections (Rodger & Mitchell, 2007; Petterson et al., 2009) but their role as vectors has not yet been demonstrated (Petterson *et al.*, 2009).

Enveloped viruses, such as alphaviruses, generally enter the cell using receptor-mediated endocytosis (Helenius *et al.*, 1988). Although the exact receptor used by the alphavirus to enter the cell has not been identified (Linn *et al*., 2005) involvement of cholesterol and lipid rafts, membrane fusion with endosomes, and formation of replication complexes in association with intracellular membranes such as endoplasmic reticulum and golgi complexes have been noted during viral entry (Strauss & Strauss, 1994; Wengler *et al.*, 2003; Susuki & Susuki, 2006; Medigeshi *et al.*, 2008; Ng *et al.*, 2008). Significant, differential expression of genes involved in cholesterol metabolism was observed in the present study, and could possibly be involved in establishing viral infection as seen in mammalian Alphavirus infection by facilitating virus entry (Ng *et al.*, 2008). The altered lipid metabolism could also be a result of virus infection itself, as the virus shows tropism to the tissues with high levels of lipid metabolism such as the pancreas and skeletal muscles (Ferguson, 2006).

Innate immune mechanism

Teleostean immune systems share similar functional mechanisms in eliminating pathogens to those of higher vertebrates. (Plouffe *et al.*, 2005). Many of the genes that encode defence molecules in the genome of fish are closely similar to the particular genes in mammals allowing fish to represent a principle evolutionary precursor of innate and acquired immunity (Plouffe *et al.*, 2005). The emphasis on identifying the genes that are responsible for eliciting immune mechanisms in viral diseases in salmonids has increased greatly during the last decade together with the application of microarray technology to explore global gene expression during viral infections.

Innate immunity plays a crucial role in the early phase of defence against viral infection and also triggers specific immune mechanisms to protect the host from the pathogen (Barber, 2001). For viruses in general, host-cell contact is recognised by immune as well as non-immune cells, through motifs that signal 'danger' of the presence of a virus i.e. pathogen-associated molecular patterns (PAMPs) (Raymen & Klimstra, 2008). Primarily, PAMPs activate toll-like receptors (TLR) allowing the immune system to recognise a specific pathogen or insult, and to raise a relevant response (Abbas *et al.*, 2000; Purcell *et al*., 2006). The KEGG pathway analysis used in this study highlighted substantial, differential expression of genes related to activation of TLR 2 and 9, which function to subsequently promote the activation of pro-inflammatory cytokines and interferons (Purcell *et al.*, 2006). Subsequent activation of TLR-related pathways such as JAK/STAT, or mitogen activated protein kinase (MAPK) was also observed. TLR 9 is normally expressed on the endosomal membranes, and receptor-mediated endocytosis and membrane fusion of SAV would probably have activated this receptor and hence caused activation of the INF-I system also seen in this study. Up-regulation of

interferon-regulatory, interferon-induced and INF-α2 and INF-α2 associated genes was observed. It is not surprising to see weak signals for INF-I, because only a few cells would be stimulated to produce INF-I in the first instance by direct contact with the virus, before paracrine signalling to other cells leads to the production of effector molecules. Phosphorylation of tyrosine kinase 2 (TYK2) and JAK1, by activation of the JAK/STAT pathway as observed here, transduces signals in the nucleus causing expression of interferon-inducible genes and subsequently the production of proteins that possess direct antiviral activity (Zhang *et al.*, 2007).

Interferon can activate double-stranded RNA-activated protein kinase (PKR), which has potent anti-viral and anti-proliferative activities. Up-regulation of Atlantic salmon double-stranded RNA (dsRNA) activating Z-DNA binding protein was observed in the present study, this being a recently characterised gene in salmon considered to be orthologous to mammalian PKR (Bergan *et al*., 2008). Mammalian PKR is involved in the initiation of several signalling pathways such as NF-kB, MAPK, STAT-1, p53, INFRF-1 and apoptosis, however, the best characterised function of PKR is phosphorylation of translation elongation factor 2α (eLF2α) (Bergan *et al.*, 2008; Raymen & Klimstra, 2008), which leads to inhibition in initiation of the host and viral RNA translation and resulting shutdown of cellular protein synthesis (Raymen & Klimstra, 2008). Down-regulation of eIF2α was observed at all sampling points, possibly indicative of cellular protein synthesis shut-down occurring in conjunction with up-regulation of Z-DNA binding protein. Activation of the NF-kB pathway was indirectly related to the down-regulation of INF-kB alpha-inhibitor like protein, which could possibly be a result of post-translational or post-transcriptional modification by the virus and associated protein shut-off mechanisms (Barry *et al.*, 2009; Frolov &

Schlesinger, 1999). However, this would have enhanced the translocation of NF-kB complexes into the nucleus which in turn bind to specific DNA sequences called DNA response elements (DNA-RE), forming DNA-RE\NF-kB complexes that can be responsible for inducing downstream host defence mechanisms. NF-kB is involved in switching on a diverse array of cellular mechanisms including acute phase response, inflammation, and immune response and cell cycle changes involving disease pathogenesis, and it has therefore been suggested that its activity could be used therapeutically to minimize adverse effects caused by activation of a number of different pathways (Lee & Burckart, 1998).

A considerable number of interferon-induced genes showed high-fold up-regulation in infected fish such as ISG-15, Mx protein, viperin and ZFP. ISG-15, an ubiquitine ligase-like protein that showed the highest fold change in this microarray and the qRT-PCR study, may have been involved in proteasome triggering and protein degradation (Rokenes *et al.*, 2007) during the infection. Viperin is an interferon-induced cytoplasmic protein, involved in destroying enveloped viruses by disrupting lipid raft formation involved in virus budding (Waheed & Freed, 2007). ZFP is also involved in virus destruction, particularly in alphavirus infections, and Mx protein is the most commonly studied antiviral molecule in different salmonid viral disease conditions (Das *et al.*, 2009). Strong induction of INF-I has been observed *in vitro* in salmon head kidney cells (SHK-1) and Atlantic salmon head kidney leukocytes (TO) cells infected with SAV-1 (Gahlawat *et al.*, 2009). Collectively, these results suggest that INF-I is a key protein employed by Atlantic salmon to combat SAV-1 infections, similar to the case for mammalian alphavirus infections (Zhang et al., 2007; Raymen & Klimstra, 2008; Barry *et al.*, 2009). The induction of these pro-inflammatory cytokines produces a

state in the cellular system where cytokine mechanisms become destructive to the host instead of protective. Such a situation can give rise to a systemic inflammatory response (SIRS) in infected fish, a clinical phenomenon commonly encountered in the pathogenesis of mammalian alphavirus infections, often responsible for causing mortality (Raymen & Klimstra, 2008).

Adaptive immune response

The adaptive immune system is involved in antigen recognition and immune memory. An active shift in adaptive immune-related signatures was demonstrated in infected fish compared to control fish in this study.

In acquiring T-cell mediated immunity, antigen presentation is the prime pre-requisite for T-cell activation followed by subsequent cell migration under the control of various chemokines (Fischer *et al.*, 2006). Up-regulation of genes associated with T-cell activation like DAD and T-cell antigen receptors was detected as early as 3 d.p.i. in infected fish, suggesting an early onset of specific immune responses to the viral infection. Specific T-cell migration is enhanced by chemokines in virus infections, and in this study CC-like chemokine, which is thought to be involved in the activation of mononuclear cells i.e. lymphocytes and monocytes, was seen to be up regulated both by microarray and qRT-PCR. The CXC ligand-10 (CXCL-10), also termed 10 kDa γ-interferon (INF-γ)-induced protein, was up-regulated and was presumably involved in chemo-attraction of monocytes, NK cells and dendritic cells as well as T-cell activation (Schroder *et al.*, 2004). Although the INF-γ gene was not seen amongst the significantly expressed genes, this experiment has provided indirect evidence of its involvement in the immune response in SAV1 infection, which has not been described before. The

chemokine CXC receptor, thought to be a chemotactic factor for neutrophils (Abbas *et al.*, 2000), appeared to be down-regulated in this experiment, possibly suggesting that SAV1 could hamper the cellular inflammatory response during an infection.

Polymorphic MHC I and II are important factors in antigen processing and presenting T-cells in terms of eliciting appropriate immune responses to infection (Jorgensen *et al.*, 2006). MHC class I-associated antigen presentation to CD8$^+$ T-cells is involved in destroying cells infected with intracellular pathogens such as viruses, while MHC class-II associated antigen presentation to CD4$^+$ cells is involved in activating macrophages to destroy phagocytosed microbes e.g. bacteria (Abbas *et al.*, 2000). Only one type of classical MHC-I locus (*Sasa UBE*) has been identified in Atlantic salmon (Grimholt *et al.*, 2002; Kjoglum *et al.*, 2006) and is involved in response to a range of different viral diseases as well as in mediating disease resistance (Jorgenesen *et al.*, 2007). Destruction of virus-infected cells via MHC-I restricted, cell mediated cytotoxicity (CMC) occurs through receptors and molecules on both effectors and target cells (Fischer *et al.*, 2006), and is potent in clearing virus from the host system. Up- regulation of T-cell receptors and MHC-I molecules was noted in infected fish, suggesting active CMC, although the elements of CD8$^+$ response were not amongst the significantly differentiated genes.

B-cell responses are believed to be a key feature of the adaptive immune response for clearing extracellular virus (Levin *et al.*, 1991), and are reported to be activated around 14 d.p.i in fish. Seven immunoglobulin-associated genes and B-cell enhancing factors were observed to be significantly expressed in infected fish, with up-regulation of B-cell activity noted 3 d.p.i in virus-infected fish. Although little is known about the transcriptional regulation of the humoral immune response in fish (Philstrom &

Bengten, 1996), SAV1 is associated with a strong neutralising antibody response, detected in both experimental and natural infections around 10 -16 d.p.i. (Graham *et al.*, 2006a, 2007a). In this study, transcriptomic changes were observed in Ig-associated genes comparatively early in the infection, although the functional significance of this observation is not clear. The up-regulation of immunoglobulin and secreted antibody seen could represent a dual function of immunoglobulin i.e. receptor function in blood and body fluids (Philstrom & Bengten, 1996) and a systemic defence against a viraemia. Although antibody responses are generally considered to occur later in the infection process in cold-water fish, transcriptomic analysis of a range of different viral diseases indicates apparent early activation of Ig signatures in infected fish (Cann, 2005; Jorgensen *et al.*, 2008). Such observations require further research in order to provide a better understanding of the functional significance of the early activation of these pathologies. The fold-changes of expression were not particularly high during this time window of infection and it would therefore be interesting to evaluate the same transcripts later in the infection process in order to help interpret the significance of this early activation.

Virus induced proteins and viral clearance

During viral attack, a distinct transcriptional programme is activated in the host via PAMP recognition systems, leading to activation of appropriate antiviral responses in order to eliminate the pathogen from the system (Cann, 2005). A large number of genes considered by other authors to act as antiviral proteins (Miller *et al.*, 2007), but whose identity and functional significance are largely unknown, were seen to be differentially regulated in this study. Interestingly, 20 different VHSV-induced proteins were up-regulated with high fold changes observed. The functional involvement is known for

few of these proteins such as Vig-1, which is involved in the synthesis of enzymatic co-factors of the nitric oxide (NOX) pathway (Boudinot *et al.*, 1999, 2001). Genes associated with the NOX pathway (nitric oxide synthase interacting protein, NOD_3 protein) were significantly up-regulated at 3 and 5 d.p.i. The induction of a large array of virus-induced proteins indicates a key role for non-specific immune mechanisms in clearing virus, suggesting such mechanisms could provide a key element for planning mitigation strategies against the infection.

The ZFP and RFP proteins exhibit broad spectrum anti-viral activity against mammalian alphavirus infection by blocking the translation of alphavirus nsP, thereby preventing accumulation of genomic RNA in the cytoplasm (Bick *et al*., 2003). The apparent up-regulation of ZFP in both microarray and qRT-PCR in infected fish compared to control fish provides some evidence for similar antiviral mechanisms to those seen in mammals. Up-regulation of BAF was also observed. An increase in this factor has been noted in other salmon RNA virus transcriptomic studies such as those involving IHNV (Miller *et al.*, 2007) and ISAV (Jorgensen *et al.*, 2008). One suggestion is that it is involved in facilitating antiviral protein transcription against viruses within host DNA *e.g.* retroviruses (Segura-Totten & Wilson, 2004). Down-regulation of cyclin-T protein, a negative regulator of human immunodeficiency virus type 1 (HIV-1), was also observed and is another indicator of the fact that a range of non-specific antiviral proteins is involved in destroying RNA viruses in salmon. Thus, proteins with the ability to bind diverse motifs can work as co-factors and restrict virus propagation, and were widely in evidence in this study, although their exact anti-viral activity has yet to be established.

Cell death mechanisms

Apoptosis has been identified as the hallmark of cell death in mammalian alphavirus infections, and is reported to be a major contributor to pathogenesis (Griffin & Hardwick, 1998; Segura-Totten & Wilson, 2004). Disturbance in the balance between pro-apoptotic and anti-apoptotic states through a persistent shift towards cell death induced by apoptosis (Segura-Totten & Wilson, 2004; Taylor *et al.*, 2008) can either act as a defensive mechanism preventing viral spread to unaffected cells, or can be co-opted by the virus to disseminate the infection. Apoptosis can be extrinsically activated in virus-infected cells through the death receptor (CD95/FaS and TNFR1) complexed to TNF (Barber, 2001), thereby activating caspase, the serine protease involved in down-stream protein degradation. In the current study, an up-regulation of TNF-α1 and caspase 7 was observed in infected fish throughout the experimental period, suggesting active programmed cell death occurring in infected kidney tissue. In addition, a novel Ras family member gene, annexine max4, was also up-regulated in infected fish, and this gene is also believed to be involved in apoptosis. Genes responsible for DNA damage were also up-regulated in infected fish, this being indicative of endonucleosomal cleavage and DNA fragmentation in cells infected with virus. Histopathological studies of both natural and experimentally induced SAV infections have described evidence of apoptosis in pancreas and heart (Barber, 2001; Taksdal *et al.*, 2007), and this was also observed in the current study in H & E stained sections of pancreas (see Figure 3.8.b). DNA fragmentation and loss of plasma membrane symmetry in peripheral blood and head kidney cells were also observed after 5 d.p.i. in SAV1 infected fish in another study carried out in IoA supporting the results of the microarray study.

Expression of the anti-apoptotic B-cell lymphoma-associated gene 2 (BcL-2) was up-regulated in both the microarray and qRT-PCR, suggesting the presence of host-mechanisms to protect cells from apoptosis. It is not unusual to see simultaneous expression of apoptotic inducers and inhibitors in multi-cellular organisms (Miller *et al.*, 2007; Taylor *et al.*, 2008), since the host needs to closely control apoptosis to prevent run-away tissue damage over-riding the benefits accruing from anti-viral activities.

In conclusion, this study has revealed significant, differential gene expression in Atlantic salmon subjected to the earliest stages of SAV1 infection, involving a broad range of immune pathways. Alphavirus-induced viral clearance by the host is believed to be principally mediated via α and β –interferon, and specifically by virus neutralising antibodies. A strong induction of a large repertoire of INF-I pathway associated genes and early activation of MHC-I molecules were observed in this study, leading to the conclusion that all three immune mechanisms; INF-I mediated non-specific clearance, MHC-I associated viral clearance, possibly mediated via cell killing, and antibody-mediated virus clearance, collectively play a role in viral clearance in SAV1 infection at different stages in the progression of the disease.

Chapter 5

Ultrastructural Morphogenesis of Salmonid Alphavirus 1

5.1 **Introduction**

Viruses are obligate, intracellular parasites that are able to alter the structural components and the functional mechanisms of their host cells during infection and propagation. RNA viruses, in particular, are able to undergo spontaneous mutations to avoid the antiviral mechanisms of their hosts in order to maintain their viability. A complex interaction exists between the virus and host, and the virus is able to recruit various cellular organelles from its host to produce virus progeny (Cann, 2005; Novoa *et al.*, 2005). Generally, the morphology of the virus is important for classification and actual identification of the viruses and ultrastructural examination of viral propagation in host cells is often used to help in identifying the virus. This includes describing how the virus particles are assembled and how cellular damage results from the infection process (Faquet *et al.*, 2005). Viruses undergo a series of events during the biogenesis process in host cells. For enveloped viruses, this includes attachment and entry of the virus into the host cell, un-coating, genome replication, maturation, and virion release. Any of these steps can potentially be the target of antiviral drugs, and therefore knowledge of the life cycle of a virus is fundamental for providing effective control strategies (Pohjala *et al.*, 2008; Qi *et al.*, 2008), and this has become an important area of modern medical research (Perera *et al.*, 2008).

Alphavirus replication and morphogenesis has been studied intensively over the past 40

years using Sindbis virus and Semliki forest virus as virus models (Acheson & Tamm, 1967; Söderlund, 1973; Garoff *et al*., 1978; Helenius *et al.*, 1980, 1988; Kim *et al.*, 2004) and more recently using Ross river virus and Chikengunya virus (Garoff *et al.*, 2004; de Lamballerie *et al.*, 2009). Due to the simplicity of the genome structure, alphaviruses have become a model for cell and molecular biology research. In addition, they are widely used in 'reverse genetics' as vectors for vaccine delivery, large scale protein production, gene therapy, and protein expression for mammalian molecular medicine (Schelesinger & Dubenskey, 1999; Lundstrom, 2009).

As +ssRNA viruses, with icosohedral symmetry, alphaviruses replicate in the cytoplasm of their host cells (Strauss & Strauss, 1994; Kujala *et al.*, 2001) by using various cellular membranes for viral RNA synthesis. For the initiation of viral infection, alphaviruses enter their host cell via receptor-mediated endocytosis, and subsequent conformational changes occur as a result of the low pH in the endocytic vesicles facilitating the release of the RNA genome into the cytosol (Waarts *et al.*, 2002; Vonderheit & Helenius, 2005). Morphologically, the formation of replication complexes in alphavirus infection is characterised by the formation of membrane-bound structures, and the virus is able to alter the cellular secretory pathways for the assembly of the replication complexes (Grimley *et al.*, 1968). During the formation of the replication complexes, genomic RNA is dissociated from the nucleocapsid of the virus and incorporated into ribosomes to initiate the translation of 5' encoded non-structural poly-proteins (Singh & Helenius, 1992). This is regarded as the initial trigger for alphavirus replication.

A schematic overview of alphavirus RNA replication is shown in Figure 5.1. The

positive-sense genomic RNA of the alphavirus acts directly as the messenger for generation of viral encoded minus (-) strand RNA (-RNA) and structural and non-structural proteins of the virus. The nsP are initially translated into a poly-protein (P1234) and then cleaved into four nsP (nsP1-nsP4) (Figure 5.1) (Strauss & Strauss, 1994; Kujala *et al.*, 2001) which in turn act as the catalysts for subsequent genomic and sub-genomic RNA production (Figure 5.1). Of the four nsP proteins, nsP1 is believed to be the initiation factor for -RNA synthesis, and coding of a methyltransferase, while nsP2 is involved in generating a 26S subgenomic RNA (Peranen & Kaariainen, 1991). The phosphoprotein nsP3, is also thought to be involved in RNA synthesis although the exact function of the protein has not yet been characterised, and the nsP4 is considered to be the elongation factor in the RNA polymerase complex. The full length -RNA synthesized from the positive strand alphavirus RNA genome, is subsequently involved in the transcription of new genomic RNA and sub-genomic RNA that encodes for the structural protein (Strauss & Strauss, 1994).

The structural proteins of alphavirus are synthesised from the 26S sub-genomic RNA derived from transcribing the 3' end of the genome that encodes structural protein as a poly protein (C-p62-6K-E1). The serine protease activity of the C-protein cleaves itself from the structural polyprotein and this is incorporated into the 42S subgenomic RNA to form the nucleocapsid (Strauss & Strauss, 1994; Forsell *et al.*, 2000; Kujala *et al.*, 2001). The remaining polyprotein p62-6K-E1 is then cleaved into membrane proteins p62, 6K and E1 during the translocation through the endoplasmic reticulum of the cell (Figure 5.1). The structural proteins of the virus are then processed and transported via the secretory pathways of the host cell (Garoff *et al.*, 1978, 1994). The 6K protein facilitates the transportation of the spike complex consisting of polyprotein p62 and E1

via endoplasmic reticulum of the host cell (ER) for virus assembly. The P62 and E1 from a heterodimeric complex during their transport via ER and Golgi apparatus. The spike complex is cleaved by furine-type proteases into E2 and E3 in the trans-Golgi network before reaching the cytoplasmic membrane, however, the E1 and E2 heterodimeric complex is preserved (Figure 5.1) which is later involved in determining the antigenicity of the virus. The nucleocapsids bind with the E2 during virus budding, helping to tighten the envelope around the virus.
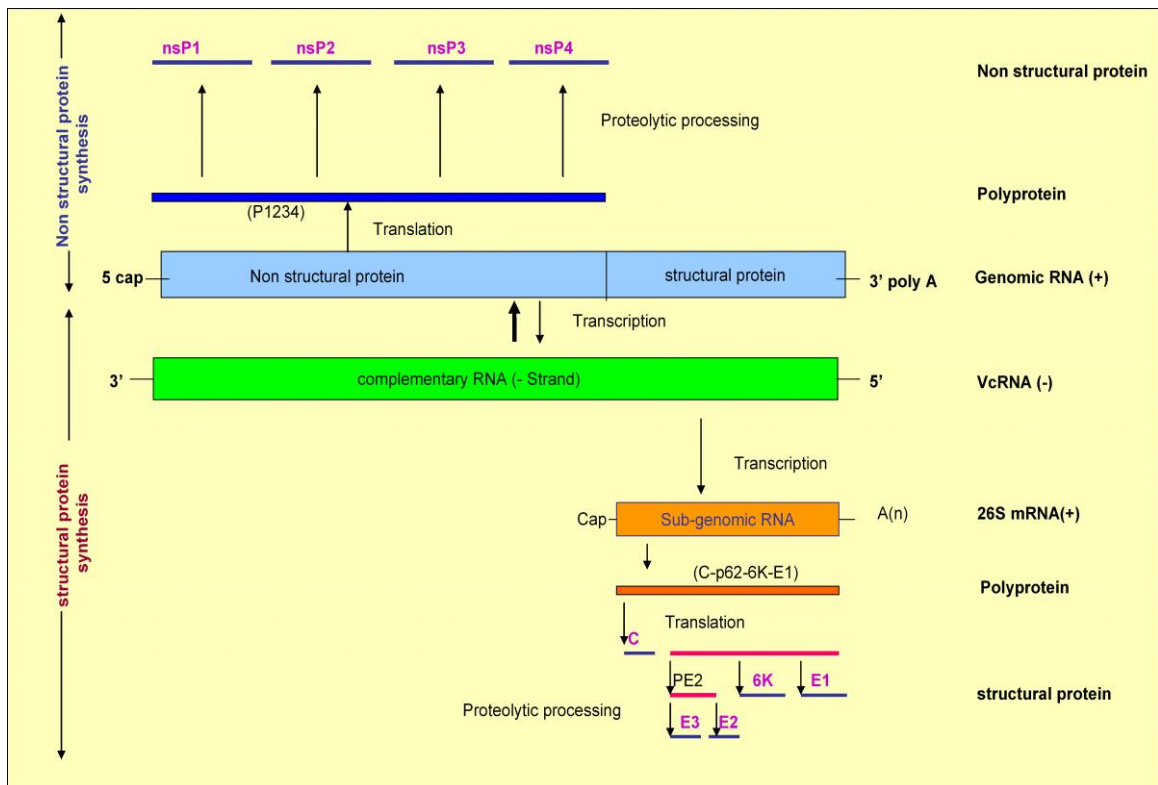
Figure 5. 1 Schematic diagram of genome replication and protein synthesis of alphaviruses (adapted from Strauss & Strauss, 1994). Genomic RNA (+) consisting of two open reading frames. RNA for non-structural proteins and structural proteins are transcribed into viral encoded (-) strand complementary RNA. Synthesis of RNA for poly-protein P1234 (shown above the genomic RNA) codes for 4 non-structural proteins nsP1-4 and RNA for poly-protein c-p62-6K-E1 codes for structural protein E1-E3, C capsid, protein 6K (shown below the Genomic RNA).

Salmonid alphaviruses are distinctly different from mammalian alphaviruses and cluster into a separate group in genotyping, due to the low homogeneity of their genetic makeup compared to mammalian alphaviruses (Powers *et al.*, 2001; Weston *et al.*, 2002; Hodneland & Endresen, 2006). The other main biochemical differences of SAV compared to higher vertebrate alphaviruses is the presence of larger structural and non-structural proteins, un-glycosylated E3 protein and a shorter non-transcribing 5'-3' region in the genetic codon of the genome. Six closely related SAV subtypes have been sequenced from salmonids (Fringuelli *et al.*, 2008; Karlsen *et al.*, 2009). These differences, together with their vector-independent transmission, have led to the suggestion that SAV should be classified in a separate taxonomic group (McLoughlin & Graham, 2007; Andersen *et al.*, 2007; Petterson *et al.*, 2009). To date, there has been little information available on the mode of entry of the virus into their host cell, receptor type used or information on the actual biogenesis process of SAV, which would assist in classifying and understanding the molecular mechanisms in the viral pathogenesis process. As with mammalian alphaviruses, SAVs are also thought to replicate in the cytoplasm of their host cells (McLoughlin & Graham, 2007) although no sub-cellular location or the organelles involved in the process have been characterised. Budding of SAV from the plasma membrane has been seen *in-vitro* from established cell cultures (McLoughlin & Graham, 2007) and viral particles with morphology similar to alphavirus have been seen in transmission electron microscopy (TEM) in negatively stained cell pellets (Nelson *et al.*, 1995). Furthermore, an increase in the density of the rough ER and extremely enlarged structures resembling mitochondria had been seen in exocrine pancreatic cells of PD-infected farmed salmon (McVicar, 1987). In contrast to mammalian alphavirus, morphogenesis of SAV *in-situ* has not yet been studied in detail. Therefore, the present study was conducted to elucidate the replication pathway

of SAV in CHSE-214 cells, and to provide information on SAV biogenesis to aid in the understanding of the cellular pathogenesis which occurs during SAV infections.

5.2 **Materials and methods**

5. 2. 1 **Culture of the virus**

The virus was cultured in CHSE-214 cells for this study. Cell culture and propagation was carried out as described in Chapter 2.2.1 using SAV-1, isolate F93-125. Virus was taken from -70°C stocks and passaged 4 times on CHSE-214 cells for 7 days in each passage. A 1:10 dilution of the supernatant was absorbed onto cell monolayers which had been prepared the day before and cultured overnight at 20°C in 1% CO_2. A 5ml aliquot of the virus supernatant from the final passage was frozen at -20°C for back titration on CHSE-214 cells to estimate the $TCID_{50}$ as described in Chapter 2.2.3. All the passages were carried out in 25 ml Nunc tissue culture flasks except the last passage (P11) which was performed in 5 x 75ml Nunc tissue culture flasks.

5. 2. 2 **Growth curve**

A growth curve was performed to determine viral growth and release from the CHSE-214 cells. For this, 25 ml Nunc tissue culture flasks (n=32) were prepared as above by adding 1.2 x 10^{6}cells/flask. The cell number was determined using Trypan blue exclusion. In brief, 7 day old CHSE-214 cells grown in 75 ml flasks (n=3) were washed x2 with DPBS and trypsinised with 1% Trypsin+EDTA. The excess trypsin was decanted after 5-7 min and cells were detached from the bottom of the flask by tapping the flask and 9 ml of GM was added into each flask to make a homogenous cell suspension. The cell suspension was gently but thoroughly mixed before transferring

0.3 ml into a Bijoux bottle and mixing with 0.3 ml of 0.5% Trypan blue (Sigma Aldrich). The number of cells in the suspension was determined using a Neubauer haemocytometer.

Cells were cultured overnight before absorbing them with stock SAV-1 virus isolate F93-125. To obtain at a multiplicity of infection (MOI) of virus, a one flask of overnight grown cells were trypsinised and the cell number was estimated by trypan blue exclusion method. Then the amount of virus determined by estimating $TCDI_{50}$ was adjusted to obtain MOI=1, which represent the ratio of cell to infectious virus particles. At the same time control cells were absorbed with HBSS supplemented with 2 % FCS, and both sets of cells were incubated at 4^oC for 1 h at 15^oC in1 % CO_2. Flasks were then supplemented with 5 ml GM. Three virus-infected flasks and one control flask were harvested at 1, 3, 5, 7, 9, 12, 14 and 21 days post-inoculation (d.p.in). Cell culture supernatant (3 ml) was carefully removed from each flask into sterile centrifuge tubes. A cell scraper was used to remove the cells that remained attached to the bottom of the flasks and this was freeze-thawed once at -70^oC for 20 min. All supernatants were then centrifuged at 1000 x g for 10 min and the cell-free supernatants were back-titrated individually on 96 Nunc tissue culture plates to obtain the extra-cellular and total virus titre respectively (see Chapter 2.2.3). The cell associated virus titre was extrapolated by subtracting the virus titre of the supernatant alone from the virus titre of the freeze-thawed cell suspension.

5. 2. 3 **Transmission electron microscopy**

Stock SAV1 isolate F93-125, was absorbed onto preformed CHSE-214 cell monolayers at a MOI of 1, as described above (see Chapter 5.2.2). Samples were collected at 1, 4, 8,

24 and 48 hours post-inoculation (h.p.in.).Two virus-infected and one control flask were harvested into 2.5 ml of 2.5 % (v/v) gluteraldehyde in 100 mM sodium cacodylate buffer (pH 7.2) using a cell scraper. The cell suspension was centrifuged at 1000 x g for 10 min and the cell pellet was then fixed in 2.5 ml of fresh 2.5 % gluteraldehyde for 4 h in 4°C before rinsing overnight with 1 M sucrose buffer. For post fixation, the cell pellet was placed in 1 % buffered Osmium and then dehydrated in an acetone series at 22°C before embedding it in low viscosity resin. Ultra-thin sections of the pellet were prepared and placed on 200 mesh Formvar-coated copper grids, which were first stained with uranyl acetate followed by Reynold's lead citrate. The sections were observed under an FEI Tecnai Spirit G2 Bio Twin Transverse electron microscope.

5. 2. 4 Negative staining of SAV-1 for electron microscopy

Four 75 ml flasks of CHSE-214 cells were cultured overnight before absorbing them with a 1:10 dilution of SAV-1 isolate F93-125, for 1 h then incubating them at 15°C in CO_2 after supplementing with GM. In parallel, control cells were absorbed with HBSS containing 2 % FCS. Virus was cultured until it produced a full CPE in the cells for 9 d.p.in. Virus supernatant was harvested from the flasks and centrifuged at 1000 x g for 10 min. The supernatant was further clarified at 12,000 x g for 13 min in a SW 28 Rotor Beckman L-80 ultra-centrifuge. The final clarification was carried out at 100,000 x g for 1 h and 35 min. For the ultra-centrifugation 13.5 ml Ultra-Clear™ tubes (Beckman, High Wycombe, UK) were used. The supernatant from the ultra-centrifuge was decanted and the excess fluid removed by inverting the tubes for 2 min. The pellet was re-suspended in 100 µl of sterile PBS and incubated for 30 min to allow the pellet to disperse.A drop of virus suspension was then loaded onto a 3 mm Formvar Carbon film 200 mesh copper grids and allowed to absorb for 2 min. The excess fluid was removed

from the grid, before staining the grids with methylamine tungstate for 2 min. The grids were dried for 5 min after blotting off the excess stain. The specimen was observed under a FEI Tecnai Spirit G2 Bio Twin TEM for the presence of virus particles.

5.3 **Results**

5. 3. 1 **Growth curve**

The highest total viral titre (ie. Extra-cellular virus and cell associated virus) was obtained from the sample harvested at 7 d.p.in (TCID$_{50}$ $1x10^{6.9}$/ml), and it then started to decline from 7 d.p.in until the last sampling point at 21 d.p.in. The titre of cell-associated virus was higher than virus in the supernatant at 1, 3 and 5 d.p.in. The maximum cell-associated titre was noted at 3 d.p.in and then declined from 5 d.p.in onwards (Figure 5.2). The viral content of the supernatant steadily increased until 7 d.p.in and then decreased by 10 fold at 9 d.p.i at which point a full CPE was noted. The titre of the virus then remained relatively constant over the remainder of the experimental period (Figure 5.2).

5. 3. 2 **Transmission electron microscopy**

 The early endosomes (EE) were randomly dispersed in the cytoplasm and varied greatly in size from small to large vesicles (Figure 5.3.a & b). The vesicles became enlarged and hollow around 8 h.p.in. appearing more amorphous and multiple vesicular inclusions with a few intact-looking virus particles (Figure 5.3.c).They resembled late endosomes (LE) and these also varied in size. Both EE and LE were simultaneously encountered around 8 h.p.in (Figure 5.3.c) and the EE were more electron dense and amorphous compared to LE (Figure 5.4.a,b).
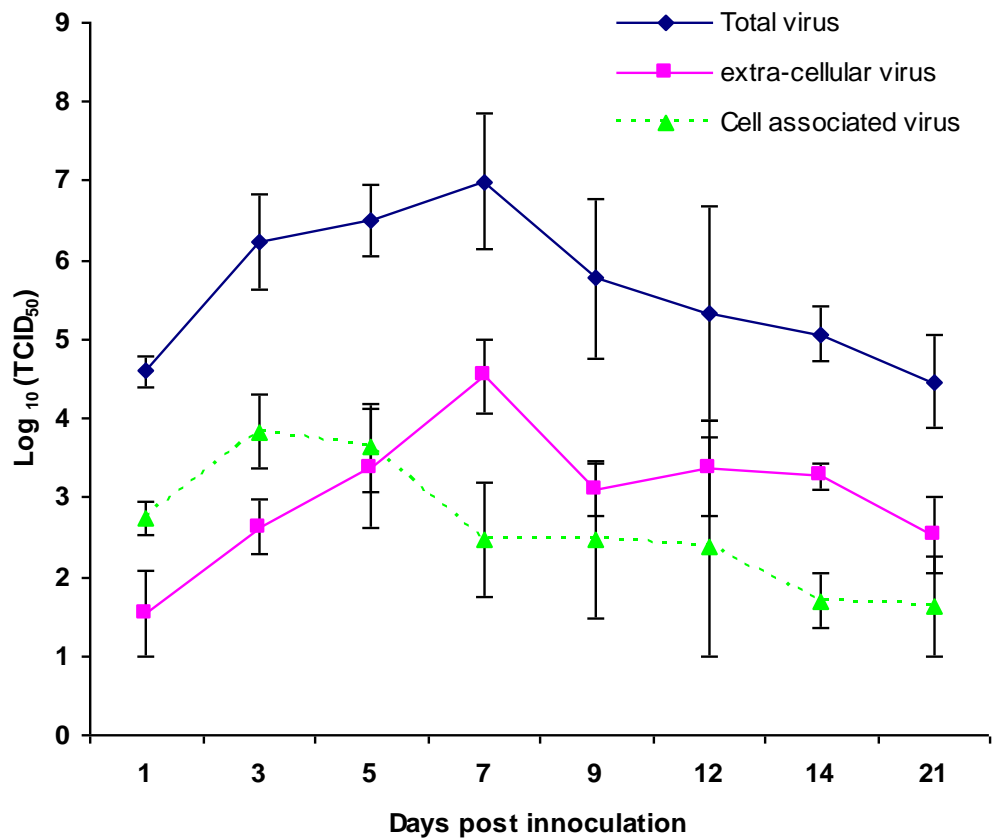
Figure 5. 2 Growth curve of SAV-1 isolate F93-125 in CHSE-214 cells. Virus supernatant without cells and with cells after a single freeze-thawing cycle were harvested at 1-21 Day post infection and back titrated on CHSE-214 cells in order to determine the $TCID_{50}$ of the extra-cellular and total virus respectively. The amount of cell-associated virus was extrapolated by subtracting extra-cellular virus from the total virus yield.

Vesicular structures that appeared to be alphavirus RNA replication complexes (i.e. cytopathic vacuoles (CPV) were first noted around 24 h.p.in. (Figure 5.5). These CPVs were mostly seen in association with rough endoplasmic reticulum (RER) (Figure 5.5. and 5.6.a). They appeared as multiple intra-vacuolar invaginations developing from the vesicles to form multiple spherical-bodies, referred to as spherules (Figure 5.6.a). An electron dense centre was frequently seen in association with RER (Figure 5.6.a). They appeared as multiple intra-vacuolar invaginations developing from the vesicles to form multiple spherules (Figure 5.6.a).

154

An electron dense centre was frequently seen in association with the spherules, and thread-like structures appeared to be projecting through the neck of the spherules (Figure 5.6.a). In some instances, structures that resembled the spherules were seen in association with fuzzy-coated vesicles near to the ER (Figure 5.6.b). Some type II CPV, (CPV-II), not associated with RER were also observed at 24 h.p.in (Figure 5.6.c).

Increased numbers of Golgi apparatus were found scattered throughout the cytoplasm of infected cells at 24 h.p.in. (Figure 5.7.a). The ends of the Golgi cistern were enlarged and lined with fuzzy membranes (Figure 5.7.b), that presumably were the origin of the vesicles with fuzzy membranes (90-110 nm) found scattered in the cytoplasm (Figure 5.7.b) and near to the plasma membrane (Figure 5.7.c).

Mature virions were seen budding from the cytoplasmic membranes as shown in Figure 5.8.a. These were first noticed at around 24 h.p.in and appeared as projections through the limiting cell membrane (Figure 5.8.a) and were then transformed into dark centred spheres (50-60 nm). Virus uptake through the coated pit and virus budding through the membrane projections were often seen in the same cell at a later stage in the infection (Figure 5.8.b).The periphery of the particle was light and appeared fuzzy. Numerous viral buds were seen lining the plasma membrane of some of the infected cells by 48 h.p.in. (Figure 5.9.a,b). The virus-infected cells appeared to be more vesicular compared to control cells at 24 h.p.in. A large number of electron dense structures that appear to be damaged cellular debris were also seen around cells that had infected with the virus. There were no apparent chnges were noticed in contol cells compared to the infected cells in any of the time points.
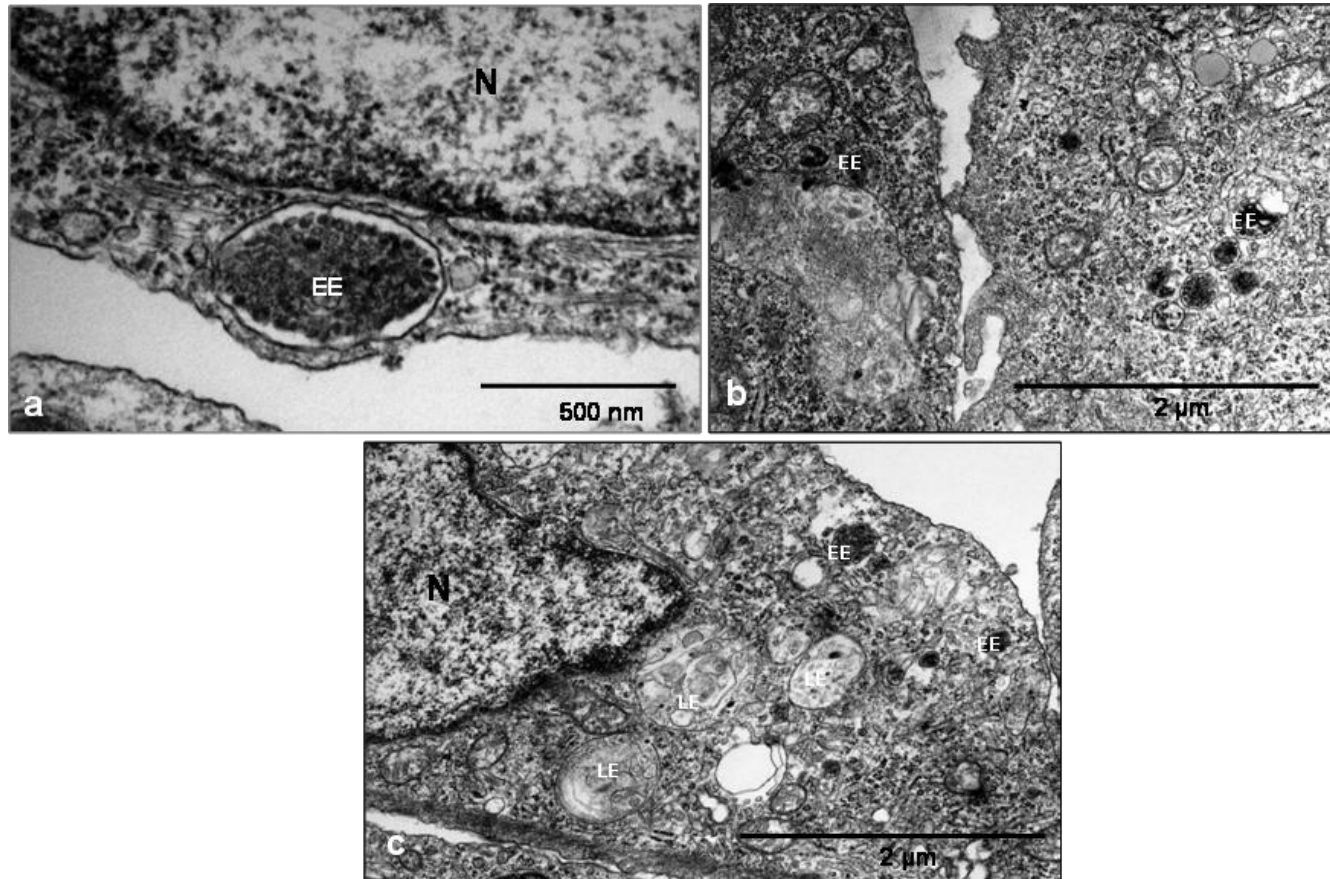
Figure 5. 3 Transmission electron micrograph of CHSE-214 cells inoculated with SAV1. (a) An early endosome (EE) near to the plasma membrane and the nucleus (N) at 4 h.p.in, (b) multiple EE in the cytoplasm, enriched with electron dense particles, presumably internalised virus particles at 4 h.p.in. and (c) large vacuoles enriched with amorphous material suggestive of late endosomes (LE) at 8 h.p.in.
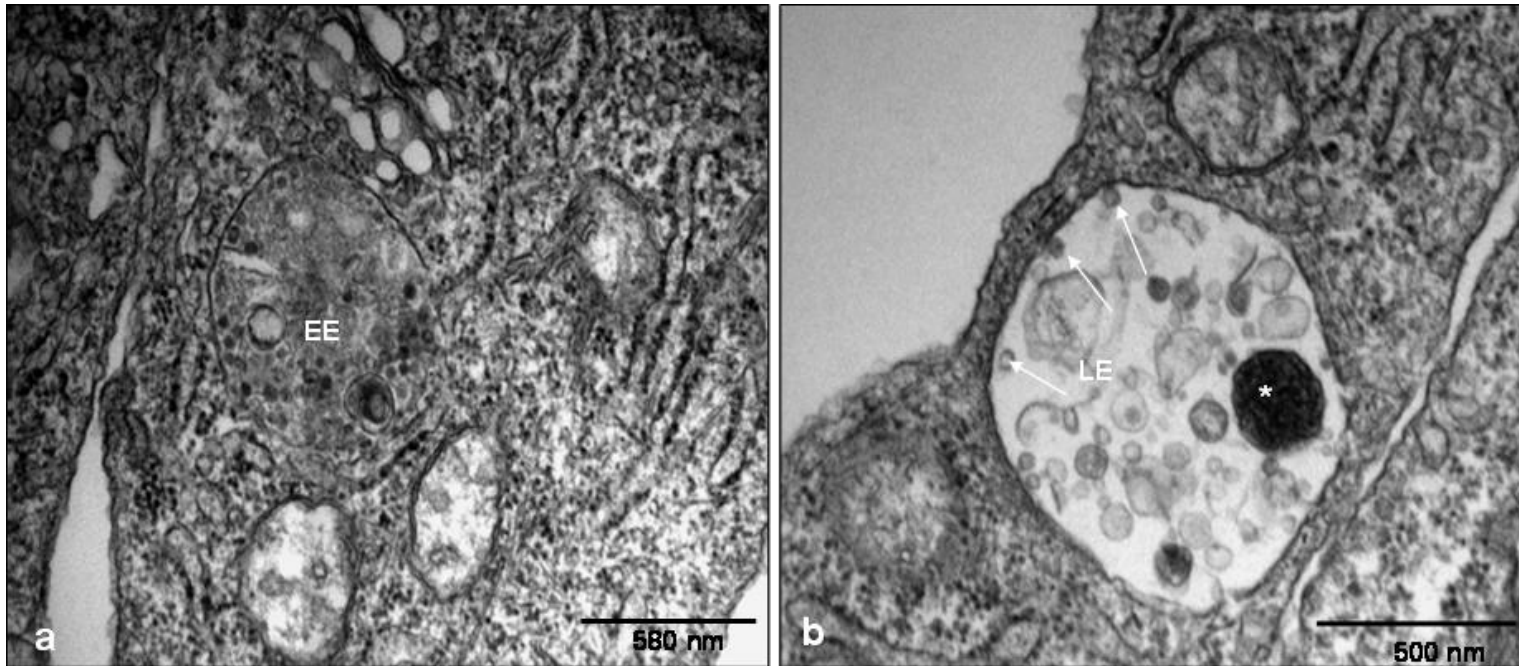
Figure 5. 4 Transmission electron micrograph of CHSE-214 cells inoculated with SAV1 at 8 h.p.in (a) Early endosomes (EE) with few intact looking viruses, and (b) Late endosomes (LE) enriched with degenerating material called a residual body (*) with vesicles at the periphery (white arrows).
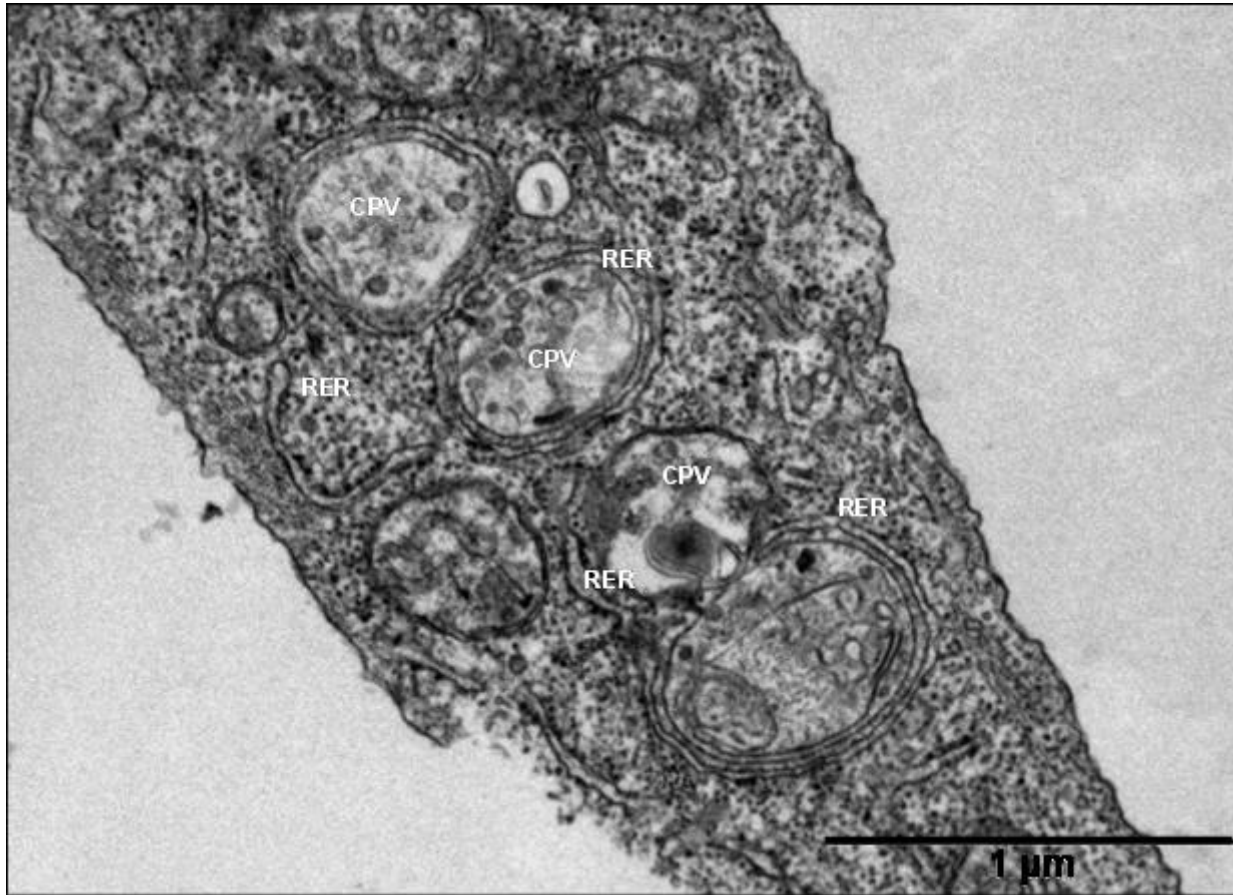
Figure 5. 5 Ultra-structure of membrane associated replication complexes of SAV1 in CHSE-214 cells at 24 h.p.in (a) a typical alphavirus replication complex with cytopathic vacuoles (CPV) in association with rough endoplasmic reticulum (RER).
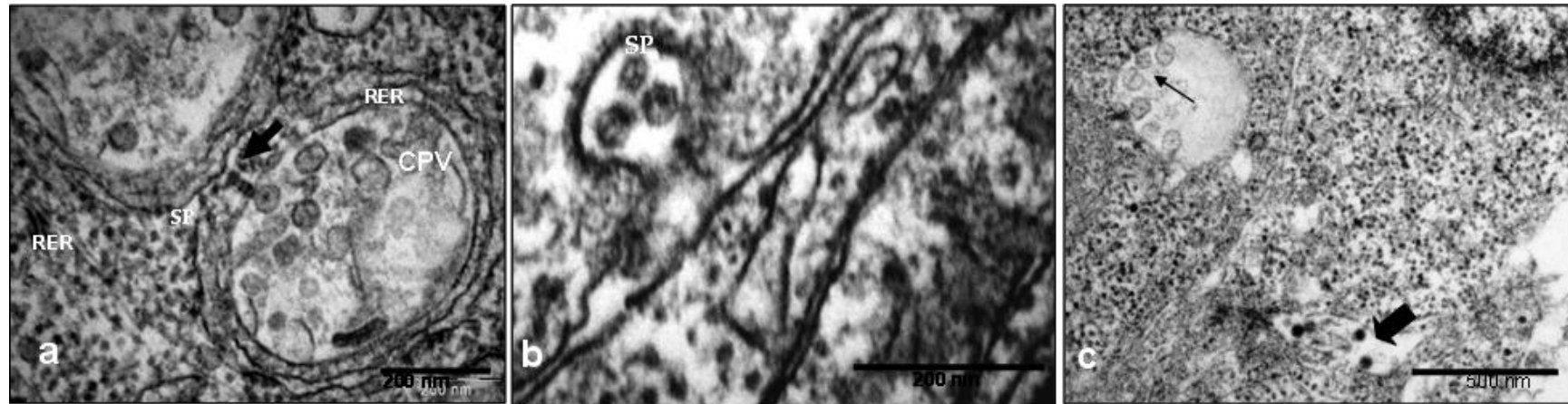
Figure 5. 6 Ultra-structure of membrane associated replication complexes of SAV-1 in CHSE-214 cells at 24 h.p.in (a) Spherules (SP) with electron dense centre and neck continuing to cytoplasm (arrow). Note rough endoplasmic reticulum (RER) around the CPV, (b) Spherules (SP) associated with fuzzy coated vesicles forming a CPV and the adjacent RER and (c) CPV II with spherules (thin arrow) note that there was no CPV-RER association and also the virus budding from plasma membrane (thick arrow).
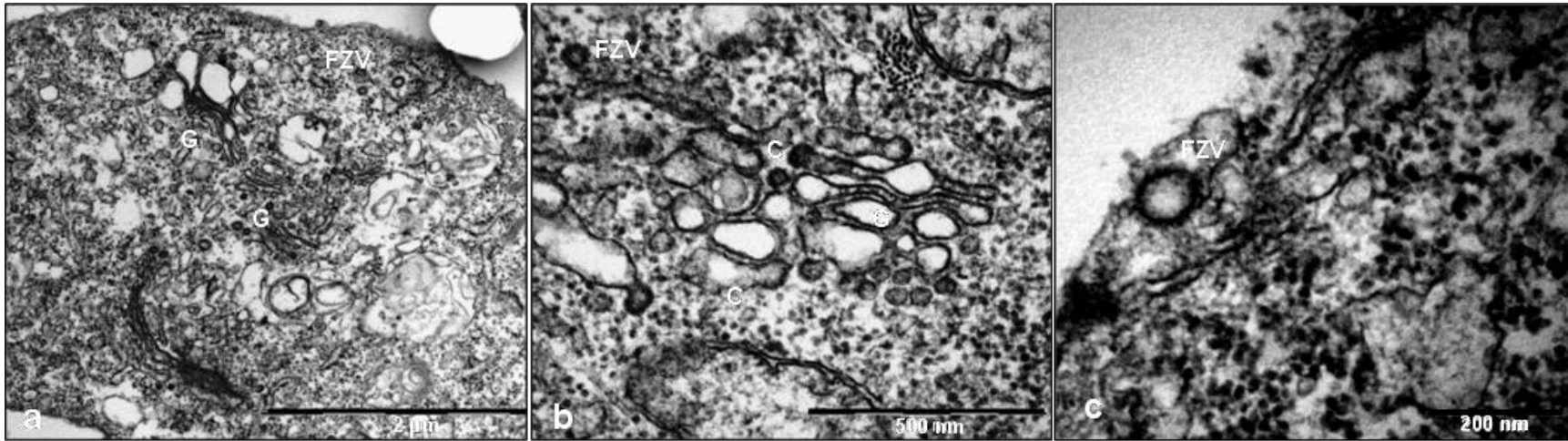
Figure 5. 7 Transmission electron micrograph of SAV1 infected CHSE-214 cells at 24 h.p.in. (a) lower magnification of the cytoplasm with multiple prominent Golgi-apparatus (G) and fuzzy-coated vesicle (FZV) (b) Formation of fuzzy coated vesicles from the Golgi cistern (C) and fuzzy coated vesicles (FZV) (c) A vesicles with fuzzy coat (FZV) near to the plasma membrane.
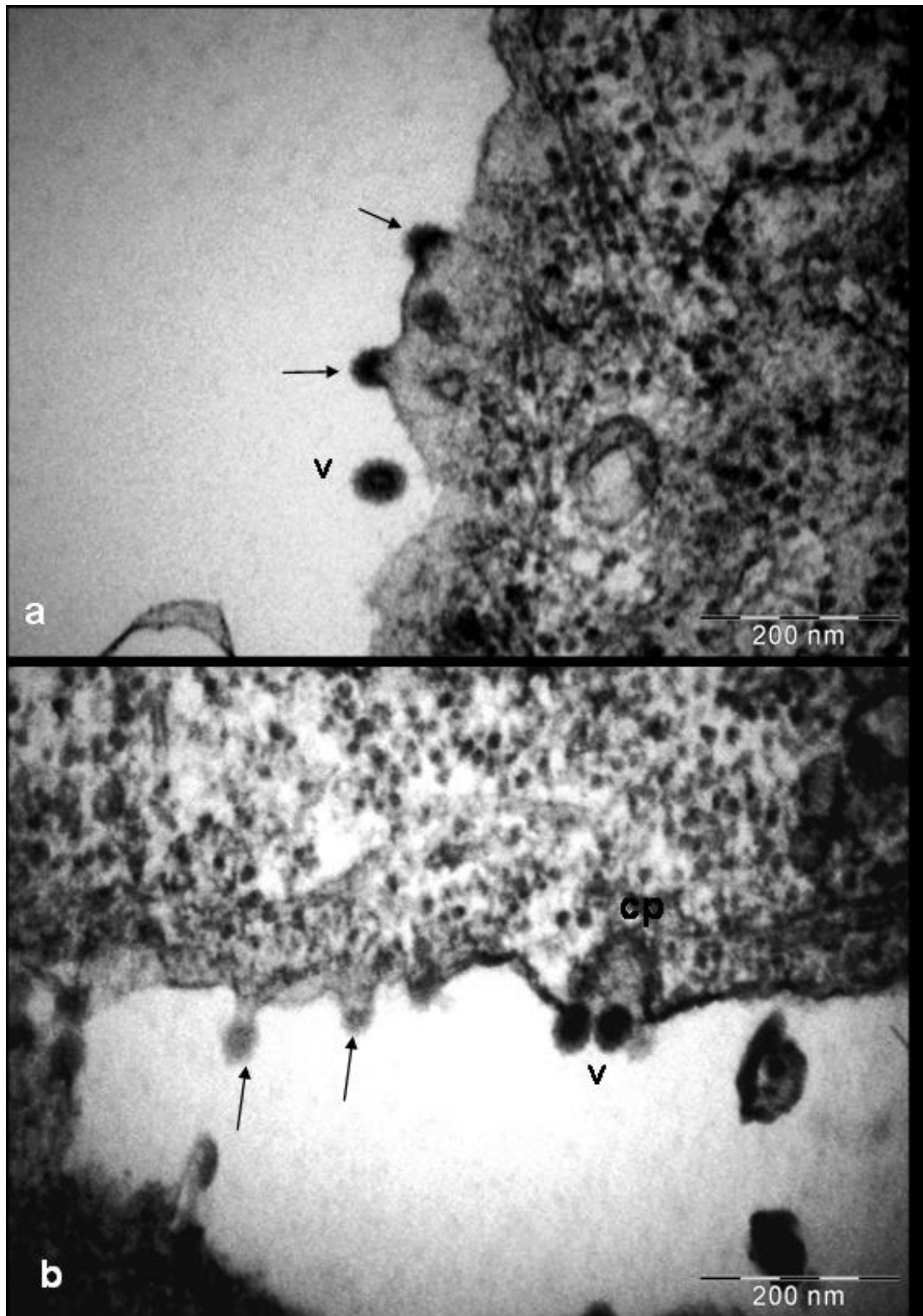
Figure 5. 8 Transmission electron micrographs of CHSE-214 cells inoculated SAV1 (a) Virus budding (arrow) through a membrane projection and a complete virion (V) at 24 h.p.in, (b) budding virus (arrow) and mature virions (V) near to a coated pit (CP)
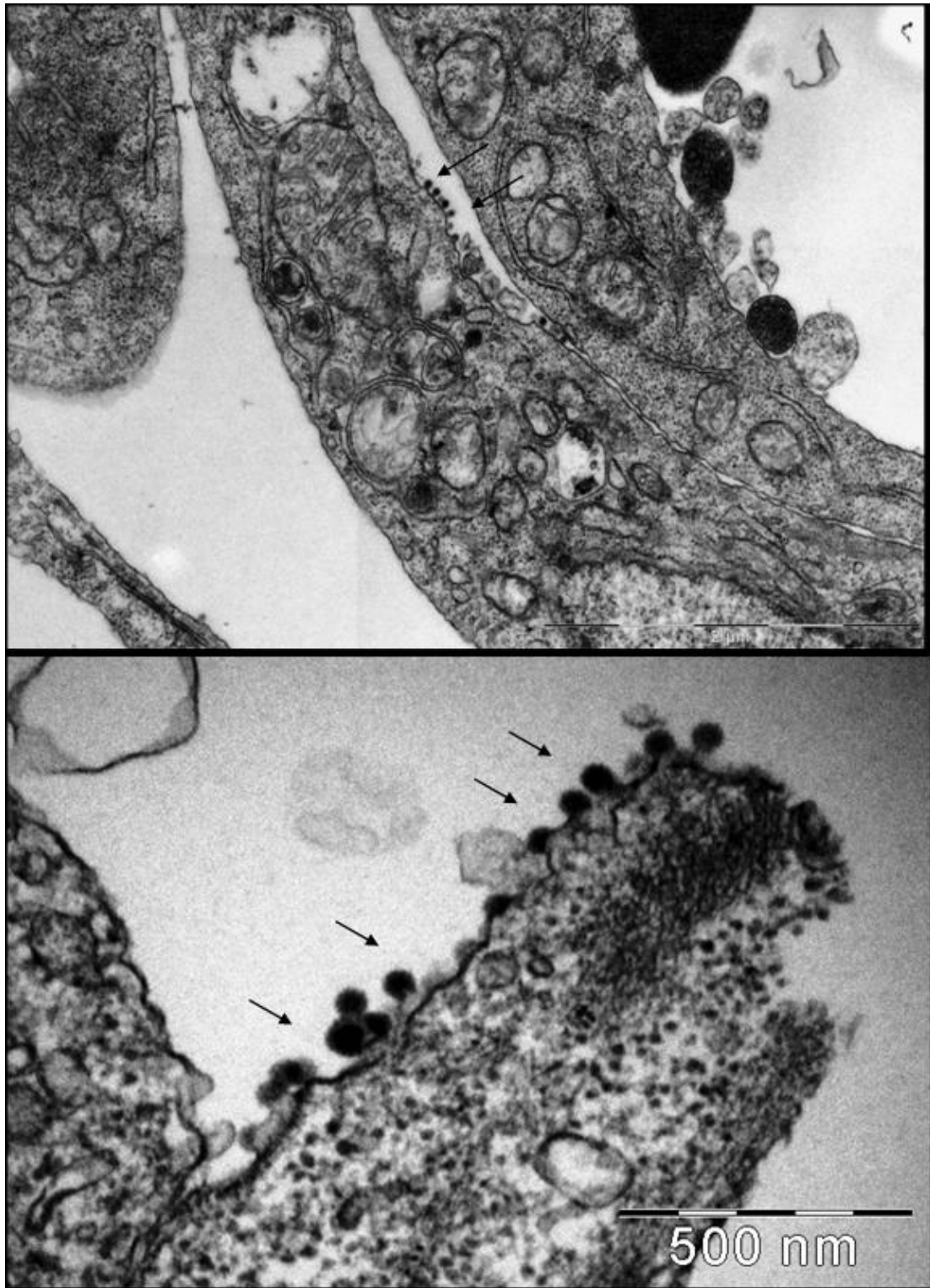
Figure 5. 9 Transmission electron micrographs of CHSE-214 cells inoculated with SAV1 at 48 h.p.in. (a) Lower magnification and (b) higher magnification of multiple virus buds (arrow) along the plasma membrane.

5. 3. 3 **Negative staining of virus**

From the negatively stained preparations, complete viral particles were observed to be roughly spherical in shape. The diameter of the viral particles ranged 56.74 ± 7.9 nm in size this was surrounded by radial projections (Figure 5.10). The diameter of the inner circular structure of the particle or the core measured 36.32 ± 3.6 nm in size. Some disrupted virions were also detected in the vicinity of the intact particles.
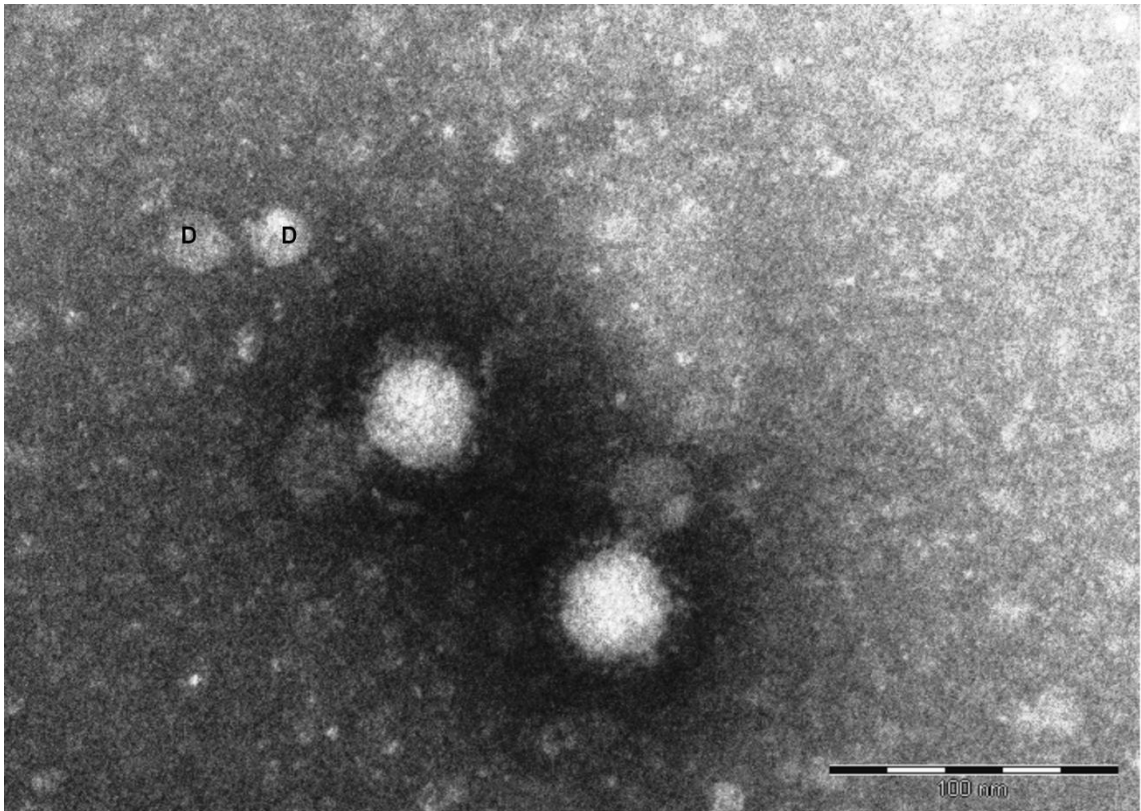
Figure 5. 10 Transmission electron micrograph of negatively stained SAV1. Supernatant from CHSE-214 infected with the virus for 7 days was clarified and pelleted. The cell pellet was stained with 2 % phosphotungstic acid. Note the globular nature of the virus particles which were surrounded by surface projections. Some disrupted virus particles were also noted (D)

5.4 **Discussion**

Studying the assembly of the virion morphologically is useful for the understanding of host-virus interactions in detail and is particularly useful in establishing possible therapeutic targets (Perera *et al.*, 2008). The process of SAV1 biogenesis in cell-cultures *in-vitro* was examined in this study. A growth curve was performed to examine the SAV1 propagation in CHSE-214 cells to establish the best time points to sample in the morphogenesis study. The highest cell associated virus level was detected at 3 d.p.in and therefore sampling was carryout before 3 d.p.in. (1- 48 h.p.in) to obtain all stages of SAV replication cycle. A low MOI was used in the study with the expectation of infection propagation over an extended period of time. This also has restricted the number of virus particles present to prevent over-infection of the cells and the build up of defective infective particles. From the growth curve, the titre of the cell-associated virus was seen to be decreased from 3 d.p.in, although the titre of total virus measured increased indicating efficient release of virus into the cell supernatant. A full CPE in the cell cultures was only observed from 9 d.p.in. onwards. Thereafter, virus production would have been reduced or prevented due to the low number of viable cells that were left in the cell culture. However, virus in the supernatant remained infectious even up to 21 d.p.in.

In order for the virus to establish an infection in the cells and for virus propagation, the incoming infectious virus particles should be present in the cytosol. In general, enveloped viruses are internalised using receptor-mediated endocytosis (Froshauer *et al*., 1988a; Novoa *et al.*, 2005) and this has also been demonstrated for alphaviruses (Helenius *et al.*, 1980, 1985, 1988; Ng *et al*., 2008). In this study, a few virus particles were found outside or on the plasma membrane at 1 h.p.in. However, a large number of

internalised, intact-looking virus particles were observed within the membrane-bound vacuoles, resembling EE at 1 h.p.in suggesting a rapid internalization of SAV which is similar to the infections seen in the mammalian alphaviruses (Strauss & Strauss, 1994). However, it was not possible to observe the initial processes used by the virus in the present study. Internalization of alphavirus is described as a rapid receptor-mediated endocytosis in mammalian alphavirus infections at high MOI levels (Morgan *et al*., 1960; Acheson & Tamm, 1967; Helenius *et al*., 1980). The receptors used for alphavirus cellular entry appeared to be host-specific rather than virus-specific due to the diversity of the hosts, ranging from invertebrates to vertebrates (Strauss & Strauss, 1994; Ng *et al.*, 2008). The use of cholesterol rich membranes in virus entry has been specifically described for alphavirus infections (Kujala *et al.*, 2001; Ng *et al*., 2008), and the target tissues of SAV are also comprised of high lipid metabolizing tissues in salmon (Ferguson, 2006), although, there is no information available on how SAV virus enters the cell at the molecular level. Identification of an SAV-entry receptor would be a landmark in SAV research as it would assist in the development of therapeutic and control strategies, and further work in this area is required.

It is known that endosomes and lysosomes play a significant role in entry and un-coating of many enveloped viruses (Helenius *et al.*, 1985, 1988), including alphaviruses (Magliano *et al.*, 1998). At the initial endocytic event of virus entry, EE are generated, and these are characterised by membrane bound intra-cytoplasmic structures enriched with foreign material, such as the endocytosed viruses seen in this study. In general, formation of the LE in alphavirus infection is a rapid process triggered by a lowering of the pH in the EE (Helenius *et al.*, 1988). Structures resembling LE appeared as early as 8 h.p.in in this study enriched with amorphous material characteristic of LE. Electron

dense amorphous residual bodies were seen inside the LE which could have possibly resulted from the destruction of some of the engulfed viruses and extra-cellular material due to lowering of the pH inside the EE (Magliano *et al.*, 1998).

The altered cellular sites involved in viral biogenesis, often referred to as 'virus factories' can easily be seen in virus infected cells as they are enriched with viral structural components or virus associated proteins during the virus replication process (Novoa *et al.*, 2005). Most of the +ssRNA virus genome replication takes place on intra-cytoplasmic membranes of the host cell, and the virus is able to modify this membrane in a manner unique to the particular group of viruses (Schwartz *et al.*, 2004). The replication process of alphavirus is mediated by virus and host endocyte membrane fusion, and is facilitated by low pH and the presence of cholesterol and sphingolipid in the host cell membrane (Waarts *et al.*, 2002; Ng *et al.*, 2008). The fusion of the virus-host membrane is mediated by viral spike protein E1, which is re-arranged into a homodimeric form from the heterodimeric E1-E2 complex (Waarts *et al.*, 2002) within the acidic compartment (Marsh *et al.*, 1986). The structures that result from the modification of the endosomal membrane in this process are called cytopathic vacuoles (CPV), and are considered to be the alphavirus replication factories (Schwartz *et al.*, 2004; Novoa *et al.*, 2005), as they are involved in virus-specific RNA replication (Kujala *et al.*, 2001). Two types of CPV have been described in association with mammalian alphavirus infection (Grimley *et al.*, 1968; Peranen & Kaariainen, 1991). Type I CPV (CPV-I) appears early in the replication process (Grimley *et al.*, 1968), while type II CPV (CPV II) generally appears late in the virus biogenesis process. The CPV-I is characterised by multiple membranous intra-vacuolar spherules that line the periphery of the vacuoles connecting to the cytoplasm with a narrow membranous neck

(Grimley *et al.*, 1968) which form in association with endoplasmic reticulum. The spherules that line the limiting membrane of the CPV have been described as the hallmark of the CPV, and presumably are derived from the fusion of virus components during the process of delivering genomic material to host cytoplasm for replication (Froshauer *et al.*, 1988a; Kujala *et al.*, 2001). The electron dense plug that radiates to the outside from the spherules is often comprised of granules, and is considered as nascent RNA utilised for translation and nucleocapsid assembly (Kujala *et al.*, 2001). The network formed between the interaction of the CPV-I and the endoplasmic reticulum forms the specific factory for alphavirus RNA synthesis (Grimley *et al.*, 1968; Froshauer *et al.*, 1988a, 1988b, 1988c; Novoa *et al.*, 2005; Ng *et al.*, 2008) The vacuolar structures seen in this study from 8 h.p.in, equipped with small dark membrane invaginations arising from the limiting membrane, appeared to be CPV-1 of SAV. These were always seen to be associated with RER, and these complexes could possibly be the sites involved in genome replication of SAV.

An increased number of Golgi apparatus were observed in the infected cells compared to the control cells and consisted of fuzzy-coated membranes at the end of the cisterni which possibly gave rise to the fuzzy-coated vesicles seen in the cytoplasm. These vesicles appeared to be involved in forming coated pits in virus endocytosis, in some instances even generating CPV-like structures. In general, some of the vesicles formed from Golgi are involved in receptor-mediated endocytosis in association with the coating protein clathrin, giving it a "fuzzy" appearance (Morgan *et al.*, 1960; Peranen & Kaariainen, 1991). The coated pits associated with virus uptake were frequently observed in the study 24 and 48 h.p.in, as a single virus particle-coated pit complex. These virus particles were believed to be newly synthesised virus particles and the

clathrin coated vesicles were derived from Golgi apparatus (DeTulleo and Kirchhausen, 1998). This observation suggested that SAV endocytosis was extremely rapid and associated with coated pits. Some of the mammalian alphaviruses such as Semliki forest virus have been described as using coated pits for virus entry (Morgan *et al.*, 1960; Helenius *et al.*, 1980; Peranen & Kaariainen, 1991; De Tulleo & Kirchhausen, 1998), although the possible involvement of Golgi in forming coated pits has not been reported previously. Therefore, the modification in Golgi apparatus could possibly be a unique virus synchronized process that facilitates the endocytosis of SAV1, but further analysis in different types of fish cells and salmon itself would be useful to verify this mechanism.

The alphavirus nucleocapsid assembles on the ER, by incorporating virus genome and the capsid protein together, which is then transferred toward the peripheral cytoplasm for budding. The present work was unable to demonstrate capsid formation under EM. However, the direct incorporation of a host cell membrane into the virus particle was noted during the budding process, as is seen to occur with other types of alphavirus infections (Acheson & Tamm, 1967). Complete virion assembly was easily recognised under EM in this study. Virus buds protruded through a cytoplasmic projection on the cell membrane. The alphavirus envelope is formed from a host plasma membrane incoperated with viral spike proteins i.e. E2E1 heterodymeric complexes (Groff *et al.*, 1998). The nucleocapsid formed in the cytoplasm is only incorporated by membranes that express virus glycoprotein (Suomalainen *et al.*, 1992; Kujala *et al.*, 2001). The nucleocapsid binds with the C-terminus of the E2 glycoprotein spike and pulls the envelope tightly around the virus, (Kujala *et al.*, 2001). However, the exact driving force for this process has not yet been elucidated (Groff *et al.*, 1998). Two models have

been suggested for this; the original model described by Söderlund, (1973), suggested the force for envelope formation comes from the binding of icosahedral nucleocapsid with glycoproteins in the membrane (Söderlund, 1973; Suomalainen *et al.*, 1992; Strauss & Strauss, 1994; Groff *et al*., 1998), and the alternative model suggested that binding of disordered nucleocapsid (icosahedral symmetry not achieved yet) with membrane glycoprotein induces virus shell formation and subsequent budding while completing the nucleocapsid formation (Forsell *et al.*, 2000; Hong *et al*., 2006). The absence of visible nucleocapsid in the cytoplasm of the cells in this study possibly suggests that the second mechanism has been used where the complete virion only becomes visible after budding.

The CPE of CHSE-214 cells observed under light microscopy was only detected at 3 d.p.in, although extensive virus budding was detected 24 h before that in this study. This highlights the fact that ongoing virus infection can easily be detected under EM early in an infection, before CPE appeared on the cell cultures. In addition, this also indicates that CPE only appeared after extensive damage to the host cells by the virus. Virus emerging through the plasma membrane and associated membrane pinching must contributed greatly to this damage leading to ultimate death of the host cells, as has been proven for mammalian alphavirus (Glasgow *et al.*, 1998; Kujala *et al.*, 2001).

Virus particles structurally similar to that of other mammalian alphaviruses (Acheson & Tamm, 1967; Strauss & Strauss, 1994) and other salmonid alphaviruses (Nelson *et al.*, 1995) were detected in negatively stained electron micrographs although the size of the particles was comparatively smaller to the descriptions of salmon alphavirus of previous studies (Nelson *et al., 1995)*.

In conclusion, this study confirmed that SAV1 replication occurs in the cytoplasm of host cells. Most of the important developmental stages of the SAV1 were demonstrated within the time frame of this study. According to the morphological evidence SAV1 replication in CHSE-214 cells was similar to that proposed for mammalian alphavirus infections, but with some interesting differences. The cytoplasmic changes seen following infection of CHSE-214 cells were associated with cellular secretory pathways as occurs with mammalian alphavirus infections. The main changes reside in alterations in cytoplamic vacuoles and the Golgi apparatus. The excess production of Golgi complexes and associated fuzzy membrane structures resembles the clathrin-coated vesicles presumably involved in receptor-mediated virus endocytosis. However, the involvement of mitochondria in SAV replication was not recognised in this study, as observed by McVicar in 1987, in the exocrine pancreas. As there appears to be no mitochondrial involvement in mammalian alphavirus infection, those enlarged vacuolated structures in the pancreas could possibly be either the presence of endosomes or the CPV instead of enlarged mitochondria. However for final confirmation of this, a detailed study will be necessary using salmon infected with SAV

Chapter 6

Apoptosis Induced Cell Death Caused by Salmonid Alphavirus 1

6.1 Introduction

The outcome of host-virus interactions is determined by a variety of different virus and host associated factors. In extreme cases, this interaction leads to the death of the cells, which in turn benefits the host by preventing further spread of the infection in their hosts. On the other hand some viruses induce cell death as a lytic mechanism of the cell for further propagation and in some instances as a mechanism of persistence of the virus in the host (Griffin & Hardwick, 1997). Cell death is mediated by two main mechanisms in multicellular organisms, i.e. necrosis or apoptosis. Necrosis is a passive degenerative event characterised by cell swelling, degeneration, disruption and loss of plasma membrane integrity followed by cyoplasmic vacuolation and death (Slauson & Cooper, 2002; Joseph *et al.*, 2004). In contrast, apoptosis is an energy driven physiological process, initiated either by external stimuli such as infectious agents (e.g. virus and toxins), or is driven by the organism itself as a physiological event during development or as a defence mechanism (White, 1996; Hay & Kannourakis, 2002; Takle & Andersen, 2007).

Cysteine-aspartic proteases (caspases) mediate a variety of cellular events in multicellular organisms including apoptosis, necrosis and inflammation. They are however, responsible for the key regulatory elements in apoptosis. Caspases are synthesized in an inactive form, consisting of pro and catalytic domains in the precursor molecule. The proteolytic cleavage of the catalytic domain transfers the inactive

proenzyme into an enzymatically-active heterotetrameric complex (Takle & Andersen, 2007). The members of the caspase family are subdivided into two groups; initiators and effectors. The initiator caspases include caspase-2, -5, -8, -9, -11 and -12 and these have long pro-catalytic domains, which are activated by autocatalytic cleavage in response to apoptotic signals. The effector caspases, (caspase-3, -6 and -7) have shorter pro-domains and need to be activated by an initiator caspase (Takle & Andersen, 2007). Caspases-3, -6, -7 and -14 have been identified in Atlantic salmon and caspase-3 (-3a and-3b) and caspase-6 (-6a and -6b) genes appear to be duplicated encoding two paralogous genes (Takle *et al.*, 2006; Takle & Andersen, 2007).

Apoptosis is mediated by either intrinsic or extrinsic pathways. In the extrinsic pathway, it is initiated by binding of specific cytokine ligands such as Fas or TNF-related apoptosis inducing ligands (TRAL) to a transmembrane death domain (DD). Binding of death receptor and ligand recruit adaptor proteins (FADD) form the death inducing signalling complex (DISC), which is responsible for activating caspase-8. In contrast, the intrinsic pathway is activated by factors that cause DNA damage such as UV irradiation, growth factor withdrawal, heat shock and chemotherapeutic drugs (Barber, 2001; Takle & Andersen, 2007). It causes depolarisation and release of cytochrome c into the cytoplasm which can activate caspase-9 by binding to apoptotic protease activating factor 1 (Apaf-1) (Figure 6.1). Caspase 3 is the central effector in programmed death of the cell and can be activated by both extrinsic and intrinsic pathways (Figure 6.1). The activation of initiator caspase (caspase- 8 or-9) involves the cleaving of inactive pro-caspase 3 motifs from its inactive p17 and p12 domains to its active form, caspase -3 through autocatalytic cleaving (Figure 6.1). The active caspase -
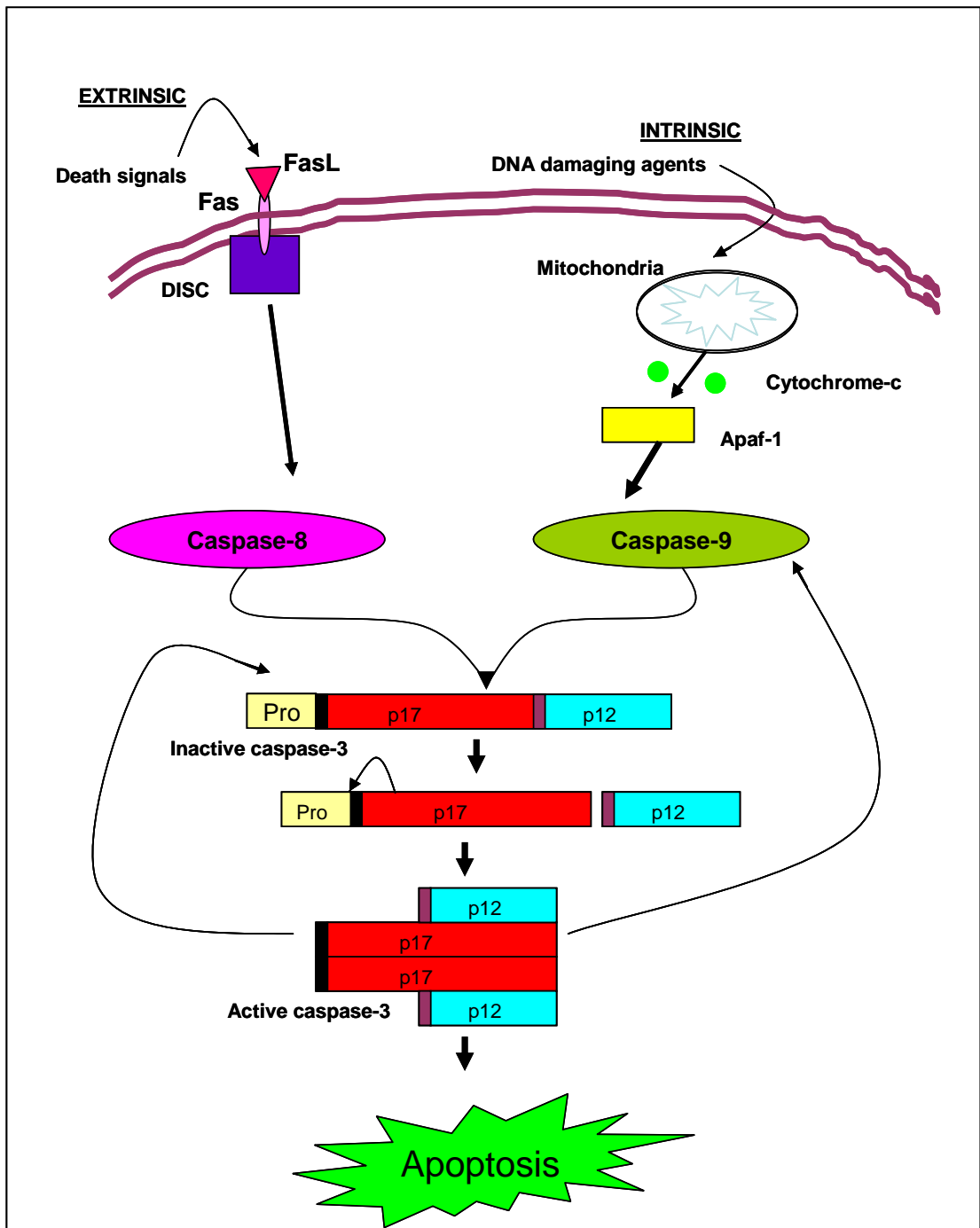
Figure 6. 1 A simplified schematic illustration of the caspase mediated apoptotic pathway. Please see the text for description. DISC (death inducing signaling complex), FasL (fas-ligand) and Apaf-1 (apoptotic protease activating factor-1) are involved in the process

3 is responsible for proteolysing a variety of different proteins and mediating the subsequent events which occur during apoptosis. Cleavage of caspase-3 substrates causes morphological changes in the affected cell including chromatin condensation, nuclear fragmentation and membrane blebbings, which ultimately result in the fragmentation of the cell into membrane bound particles referred to as apoptotic bodies. The apoptotic bodies have the ability to confine the damaged cellular matter thus preventing harmful effects to the neighbouring healthy cells, until they have been cleared by phagocytosis. This also prevents provoking any inflammatory response in damaged tissues in contrast to necrosis which induces a cellular inflammatory response (Hay & Kannourakis, 2002).

Apoptosis can be identified by observing cellular morphological, biochemical and molecular changes which occur in the cell. In routine histology, under light microscopy, apoptotic cells can be observed as highly eosinophilic cytoplasmic masses with dense nuclear fragments (Walker & Quirke, 2001).The main morphological changes of apoptosis at an ultrastructural level include cell shrinkage, nuclear condensation, plasma membrane blebbing and subsequent formation of membrane bound apoptotic bodies (Griffin & Hardwick, 1997; Walker & Quirke, 2001; Slauson & Cooper, 2002). Fluorescent antibody-based immunoassaying is also widely used to evaluate biochemical changes during apoptosis. In addition, evaluation of DNA damage by Terminal deoxynucleotidyl transferase end labelling (TUNEL) and agarose gel electrophoresis is also used to confirm apoptosis related to cell death in response to a pathogenic insult.

During viral infections, apoptosis sometimes acts as an antiviral mechanism driven by the host to prevent viral spread by limiting the time and the cellular machinery available for virus replication, (O'Brien, 1998; Barber, 2001). It is also regarded as an integral part of the cellular innate immune response (Everette & McFadden, 1999). Nevertheless viruses can also induce apoptosis as a lytic mechanism to disseminate from, or maintain, persistent infection of the virus in the host cells (Hardwick, 2001). Understanding the morphological, biochemical and molecular events of cell death during an infection helps to identify the factors that initiate apoptosis. This in turn could help in developing methods to combat viral infections. At present, little is known about the molecular mechanisms that lead to cell death during SAV1 infection. However, in mammals, alphavirus induced cell death is characterised by apoptosis and is believed to be the means by which the virus is able to establish persistent infections in some of the vertebrate hosts (Griffin & Hardwick, 1997, 1998; Griffin, 2005). With respect to SAV in salmon, several sequential pathology studies have shown apoptosis in the pancreas and the heart of SAV infected fish (Desvignes *et al.*, 2002; McLoughlin & Graham, 2007; Taksdal e*t al.*, 2007). Apoptotic cells were also seen in the pancreas of experimentally infected salmon with the H&E stain, under light microscopy, performed earlier in chapter 3. However these observations do not confirm that apoptosis is the sole means by which cell death occurs during an SAV infection. Studies *in-vivo* in Atlantic salmon have demonstrated ongoing apoptosis during the early stages of experimental infection of SAV1, however, characterization of apoptosis at a tissue level is difficult (Costa *et al.*, 2007). Therefore, in the present study mechanisms of SAV1-associated cell death were confirmed by studying morphological changes under EM and confocal microscopy and quantified by image analysis in two established salmonid cell lines, CHH-1 and CHSE-214, infected with SAV1 *in- vitro.*

6.2 **Materials and Methods**

6. 2. 1 **Preparation of stock virus**

The SAV1 isolate F02-143 passage 5 (P5) and isolate p42P (P14) were kindly provided by Dr. David Graham, Veterinary Sciences Division, Agri-food and Biosciences Institute, Stormont, Belfast, UK and Dr. David Smail, Marine Scotland, Aberdeen respectively. Virus stocks for the study were prepared by growing the two isolates in CHH-1 cells seeded into $75cm^2$ Nunc tissue culture flasks for 7 days at 15^oC with 1.4 % CO_2, as described in Chapter 2.2.2. After freeze-thawing once and scraping the cells from the flasks, cell supernatants were centrifuged at 3500 x g for 10 min in a chilled 5804R Beckman coulter centrifuge. Aliquots of the stock virus supernatants were frozen at -20^oC for further use and ten fold dilutions of the frozen tissue culture extracts were back-titrated on CHH-1 cells prepared in 96 well plates to determine the $TCID_{50}$ as described in Chapter 2.2.4.

6. 2. 2 **Infection of cells with virus**

The CHH-1 and CHSE-214 cells were prepared either in $25cm^2$ Nunc flasks or on 13 mm glass cover slips (Fisher Scientific) placed in 24-well tissue culture plates. Cell numbers were determined by using the Trypan blue$^{\circledR}$ exclusion method as described in Chapter 5.2.2, before culturing the cells overnight to obtain a 70 % confluent monolayer. The seeding densities used were similar for both cell lines, in which, $25cm^2$ tissue culture flasks were seeded with 1 x 10^5 flask^{-1} or 13 mm cover-slips in 24-well plates were seeded with $1x10^4$cells well^{-1}. Stock virus diluted in HBSS supplemented with 2 % FCS just before absorbing the virus for 1 h onto the overnight grown

monolayers (MOI<1). Control cells were absorbed with diluents for 1 h and both groups of cells were re-supplemented with MM and maintained in 1.4 % carbon dioxide at $15^{o}C$.

6. 2. 3 Transmission electron microscopy

Two replicate cultures of virus infected cells and one of non-infected control CHH-1 and CHSE-214 cells, which had been grown in 25 cm^2 flasks, were harvested at 1, 2 and 5 d.p.in. Cells were processed for TEM following the method described in Chapter 5.2.3. The sections were observed under an FEI Tecnai Spirit G2 Bio Twin Transverse electron microscope for cytoplasmic and nuclear changes.

6. 2. 4 Scanning electron microscopy

Two replicates of infected and one of control CHSE-214 cells on cover slips, at 1 and 3 d.p.in, were fixed 2.5 % (v/v) gluteraldehyde in 100 mM sodium cacodylate buffer and fixed overnight at $4^{o}C$. Specimens were rinsed in 100 mM sodium cacodylate buffer for 4 h, post fixed in 1 % (w/v) osmium tetroxide in 100 mM of sodium cacodylate buffer for 2 h and dehydrated in an ethanol series before critical point drying in a Bal-Tec 030 critical point dryer. Specimens were observed using a Jeol JSM6460LV scanning electron microscope (SEM) for cell surface changes.

6. 2. 5 DNA extraction and gel electrophoresis

The CHSE-214 and CHH-1 cells were grown in 25 cm^2 tissue culture flasks and infected with virus isolate F02-143. Monolayers of virus infected and control cells were

harvested at 4 h, 8 h, 24 h and 1 day, 3 day, and 5 d.p.in. Cells were first washed x 2 with DPBS, and then scraped into fresh DPBS (2.5 ml) and centrifuged at 1000 x g for 10 min to obtain a cell pellet. Genomic DNA was extracted from the cells using a NucleoSpin®Tissue kit (MACHEREY-NAGEL, Abgene) following the manufacturer's instructions. One microgram of extracted DNA in 10 µl of elution buffer supplied with the extraction kit was mixed 1:l (v/v) with loading dye (Abgene, UK) and the samples were electrophoresed on 1.2 % (w/v) agarose gel stained with 0.5 µgml^{-1} EtBr for 2 h at 40 V. Gels were observed under UV trans-illumination.

6. 2. 6 Determining apoptosis using immunofluorescent confocal microscopy

A confocal laser scanning microscope was used to evaluate the nuclear and cytoplasmic changes caused by the SAV 1 infection. The changes caused by different virus isolates over time were tested in CHH-1 using samples collected at 1, 3, 5, and 7 d.p.in. Cells were grown on cover slips placed in 24-well plates. Two rows of 24-well plates were infected with virus either F02-143 or p42P at an MOI<1 as described before. The remaining two rows in each 24 well plates were used as the test controls. Virus-infected and control cells were fixed by adding equal volumes of freshly prepared Carnoy's fixative (v/v methanol: glacial acetic acid 3:1) to the existing medum already in the 24-well plates. After 2 min of initial fixation, medium and fixative were carefully removed from the wells using a micropipette and further fixations (2 x 5 min) were carried out with 0.5 ml of fresh fixative.

6.2.6.1 Caspase-3 staining

An anti-human/mouse active caspase-3 affinity purified polyclonal antibody (R&D Systems, Oxfordshire, UK) was used to examine the activation of caspase in the virus infected cells. Cells grown on cover slips and infected with virus were fixed as described above and were then permeablised with 0.5% Titron-X in PBS for 30min before commencing double fluorescent staining for confocal microscopy. The cells were incubated with caspase-3 affinity purified polyclonal antibody diluted 1:500 (v/v) with primary antibody diluent (1 % BSA, 0.5 % Titron X-100, in 0.01 M PBS pH=7.2) for 1 h. The cover slips were washed with PBS for 3 x 5 min and incubated with Texas red-conjugated rabbit-antimouse IgG 1:250 (v/v) (Vector) for 1 h at 22°C. Cover slips were then washed 3 x 5 min with PBS before performing the nuclear staining described in section 6.2.6.2.

6.2.6.2 Hoechst 33258 staining

Hoechst 33258 stain (Sigma Aldrich) was used for the nuclear staining. Hoechst 33258 staining solution was freshly made by diluting 50 mg/ml stock solution to 1 µg/ml (v/v) with PBS containing 1 mg/ml polyvinylpyrrolidone. Cover slips stained with anti-caspase-3 polyclonal were immersed in Hoechst 33258 working solution for 30 min and rinsed 1 x 3 min in de-ionised water before mounting on glass microscopic-slides using Citiflor. The whole staining procedure was performed with minimal exposure to the light and kept in the dark where ever possible.

6.2.6.3 Confocal imaging

The cover slips mounted on glass microscopic slides were observed using a Leica TCS SP2 AOBS confocal scanning laser microscope coupled to a DM TRE2 inverted microscope (Leica) employing a x 63 oil-/glycerol immersion objective. Images were captured from a randomly selected field of the cover slip, using grey, red, blue and green channels using recommended excitation and emission wavelengths for the different fluorescent dyes used (Table 6.1). Thirty serial depth images (z-stack) were taken from each sample. All the images were taken by scanning a frame area 1024 × 1024 pixels (X x Y um) in the x, y plane, and for each image stack (30 images) the maximum intensity was projected onto a single 2D image (Leica Maximum Projection).

Table 6. 1 Properties of the fluorescent dyes used to measure different apoptotic targets.

Label Target	Probe	Channel	Excitation maximum (nm)	Emission maximum (nm)	Laser line
Caspase-3	Texas red	Red	587	602	543
Nuclei	Hoechst 33258	Blue	365	480	405

6.2.6.4 Image analysis

For the image analysis, the Carl Zeiss KS300 image analysis platform was used. Analysis employed a custom mode macro script developed by James Bron, Institute of Aquacultre, University of Stirling, allowing quantification of a number of morphometric and densitometric features of target fields (whole image) or individual objects (e.g.

nuclei). These features included area, mean signal intensity and counts. The script provides as an output of measurement data for each image and processed images for subsequent quality control and visual interpretation. The script encoded a fixed series of operations with no user-interaction in order to ensure consistency between measurements and remove user bias. Use of digital analysis in this context is much faster than manual analysis, more accurate and allows improved inter-user repeatability. For quantification of nuclear changes, nuclei were segmented from the background using a colour segmentation function. Adjoining segmented nuclei were then separated from one another using a grain separation function. The nuclei and nuclear fragments captured were subjected to a size threshold to exclude noise and the final segmented area was used as a mask for densitometric and morphometric measurements for each nucleus or nuclear fragment. Measurements used for the present analysis consisted of individual nuclear areas and mean intensity of signal per nucleus (functioning as a proxy for DNA damage).

In detection of caspase, the threshold of the caspase was pulled-out from the background. To obtain the cellular area cells were demarcated by marking the background or low level of caspase. The mean caspase intensity for the area of a field covered by cells was then measured.

6.2.5.4 Statistical analysis

Data were assessed for normality (Anderson-Darling Test) and homogeneity of variance (Levene's Test or F-Test). Where data failed assumptions an attempt was made to transform them using appropriate transformations including Box-Cox. Where

assumptions still could not be met, data were subjected to non-parametric analysis. Where assumptions were met, parametric analyses were employed. Statistical significance of mean area of the nuclei of infected (F93-124 and F02-143) and control cells was compared using the Kruskal-Wallis test. The Mann-Whitney U test ($\leq$0.05) was used as the post-hoc comparison to compare the significance between control and infection and two different virus infections.

6.3 **Results**

6. 3. 1 **Transmission electron microscopy**

The morphological changes seen in the cytoplasm of both CHH-1 and CHSE-214 cells appeared similar. At the early stages of infection, i.e. 24 h.p.in the cytoplasm of the infected cells became hollow and vacuolar compared to control cells (Figure 6.2.b). Chromatin margination, characterised by an accumulation of chromatin in the inner periphery of the nuclear envelope, was seen in a few cells (10 %) at 24 h.p.in and in a large number of cells (> 40 %) by 48 h.p.in (Figure 6.2 b, c & d). Chromatin condensation, characterised by clumping of nuclear chromatin in the centre of the nuclei, was evident in some cells, from 48 h.p.in (Figure 6. 2 c & d). Cell fragmentation and formation of apoptotic bodies started to appear in the virus-infected cells (< 10 %) by 24 h.p.in, and became progressive at 48 h.p.in (40 % of the infected cells) (Figure 6.3). Electron dense micronuclei were noted within most of the fragmented cells (Figure 6.3).
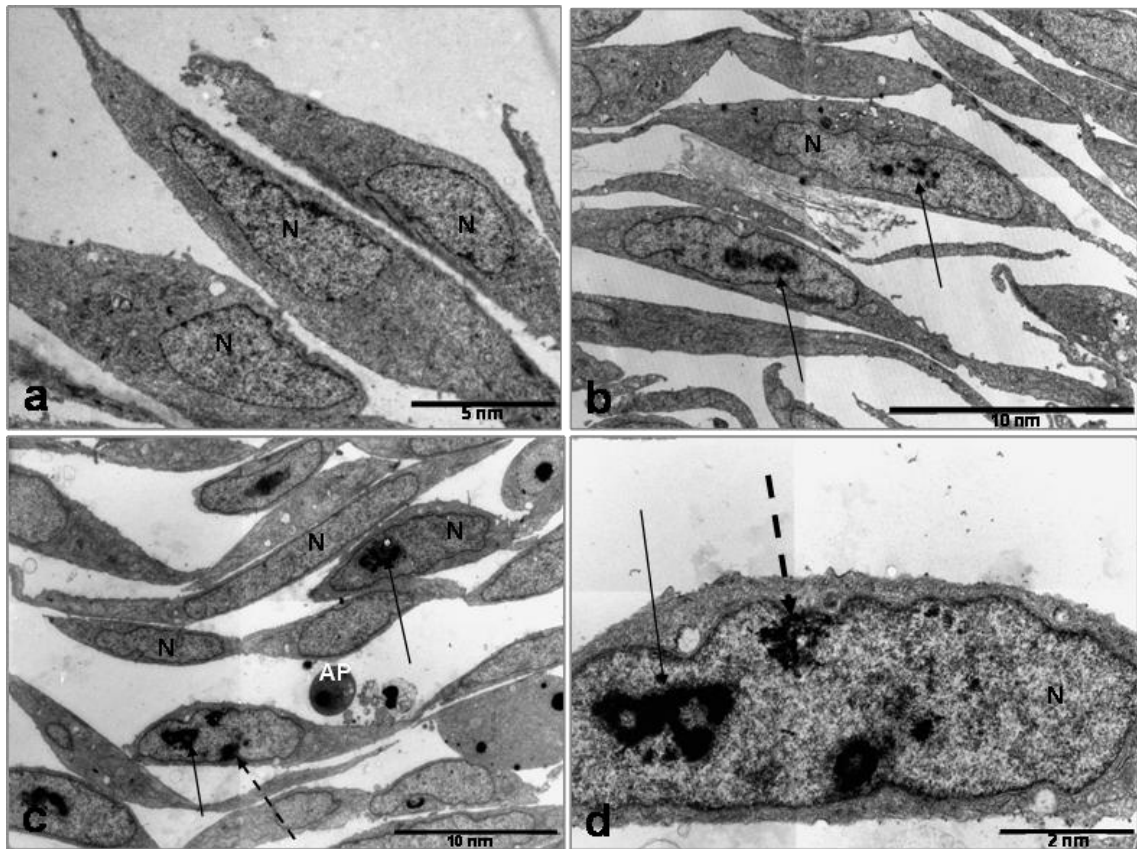
Figure 6. 2 Transmission electron micrographs of CHH-1 cells (a) negative control at 24 h p.in. and infected with SAV1 (b) 24 (c) & (d) 48 h p.in. (b, c & d) Progressive chromatin condensation (arrow) and chromatin margination (dashed arrow) were noticed in the nucleus (N) of the virus infected cells characteristic of cells undergoing death. (c) Apoptosis (AP) was seen at 48 h.p.in with electron dense micronuclei.
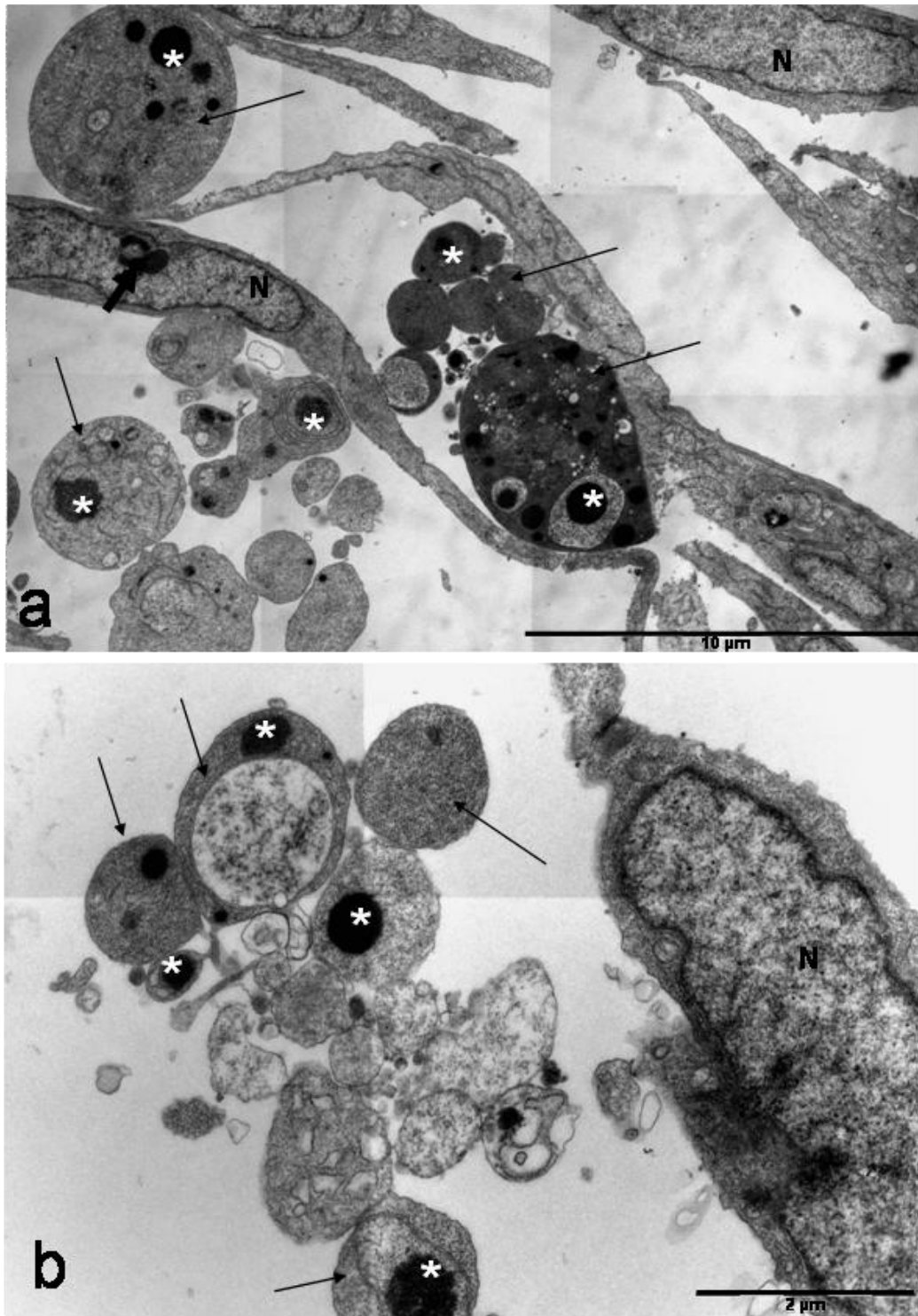
Figure 6. 3 Transmission electron micrograph of (a) CHSE-214 and (b) CHH-1 cells infected with SAV-1 at 48 h p.in. with severe progressive apoptosis characterised by formation of apoptotic bodies (arrow) and electron dense micronuclei (*). Nuclear chromatin condensation (thick arrow) was noticed in some of the cells that still maintained the cellular architecture. Nucleus (N).

6. 3. 2 Scanning electron microscopy

SEM of virus control cells showed that cells were uniformly attached to the cover slips, although cells on the cover slips of infected cells started to detach from 48 h.p.in (Figure 6.4.a & b). Some of the cells show characteristic membrane blebbing (Figure 6.4.c).
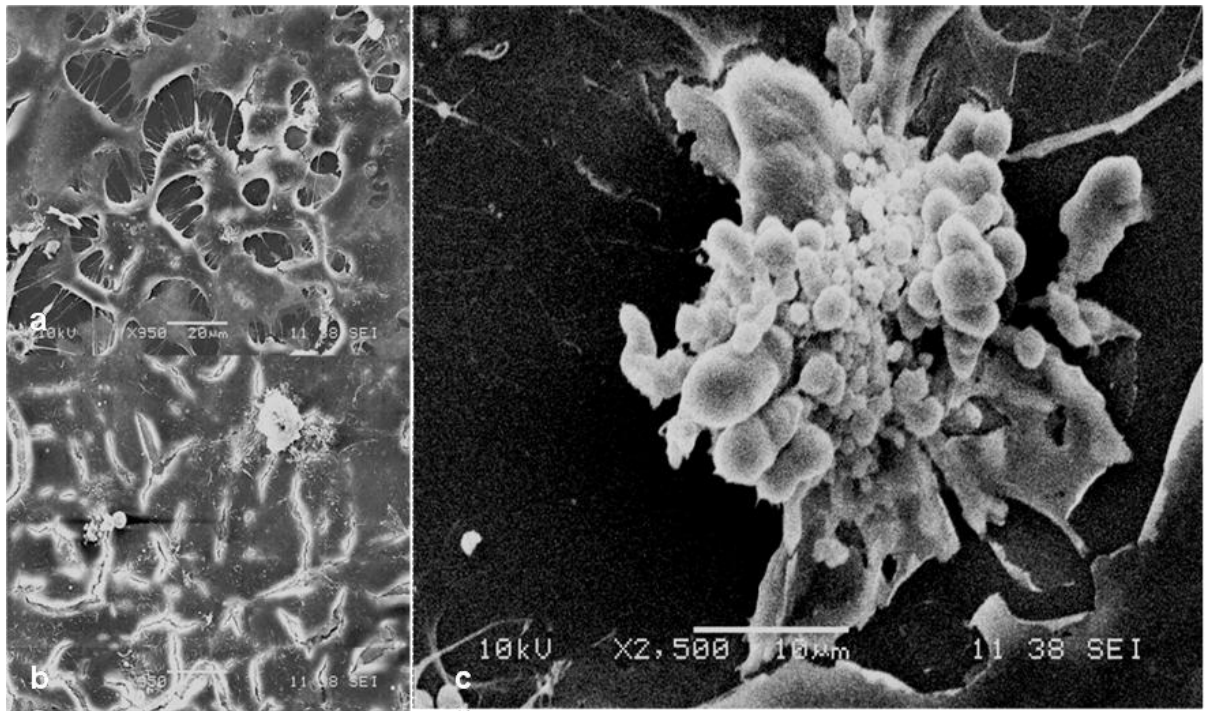
Figure 6. 4 Scanning electron micrographs of CHSE-214 cells at 48 h.p.in. (a) Mock infected cells, (b & c) SAV1 infected cells with (c) cellular blebbing suggesting apoptosis.

6. 3. 3 DNA laddering

Examination of genomic DNA run on agarose gels revealed a characteristic intra-nucleosomal fragmentation of DNA in virus-infected cells from 48 h.p.in. The laddering pattern of 180 bp oligomers observed on the agarose gel is characteristic of apoptosis. No signs of nuclear fragmentation were observed in the cells before 48 h.p.in (Figure 6.5).
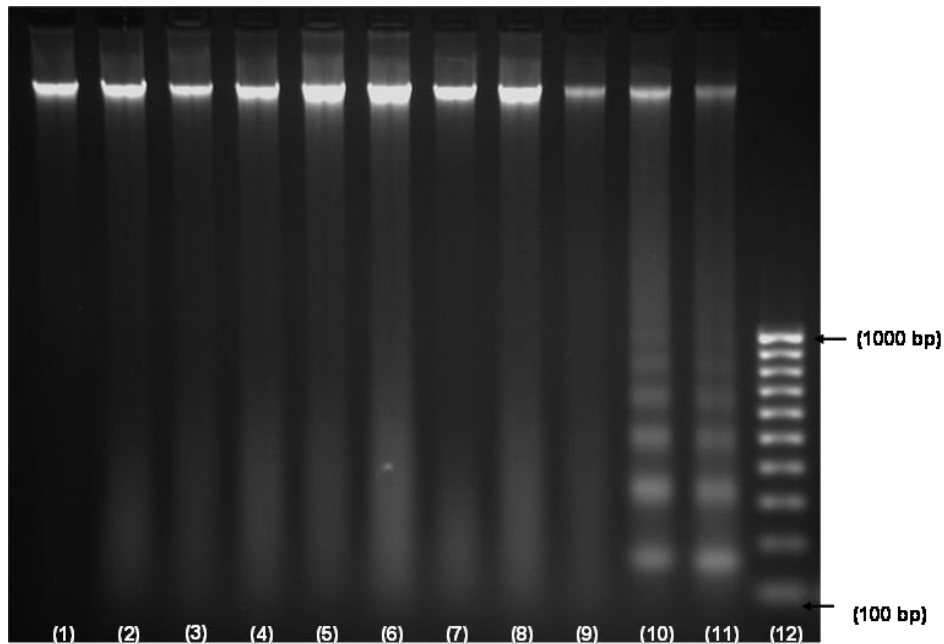
Figure 6. 5 Electrophoresis of DNA from CHH-1 cells and SAV1 infected CHH-1 cells on 1.2% agarose gel (1) uninfected control 0h, (2)-(6) mock infected and harvested at 4h, 8h, 24h, 48h, 96 h p.in and (7-11) SAV-1 infected and harvested at 4h, 8h, 24h, 48h, 96 h p.in. Lane 12 100 bp ladder.

6. 3. 4 **Apoptosis under confocal microscopy**

Under the grey channel of the confocal microscope, a few cells started to show signs of rounding and separation from the monolayer from 3 d.p.in onwards (Figure 6.6.c-e). There was a high level of red signal in these cells and their nuclei had different intensities of blue signal indicating a high level of caspase-3 and nuclear changes respectively. The caspase activated cells were overlaid with damaged nuclei as in Figure 6.6.d & f which was indicative of ongoing apoptosis. In comparison to control cells, infected cells were seen to undergo cell rounding and separation from the monolayer and their plasma membranes appeared irregular (Figure 6.7.e). The nuclei of these damaged cells were either misshapen or fragmented (Figure 6.7.e) and the cytoplasm was enriched with a high level of caspase signal compared to control cells (Figure 6.7.g). It was possible to demonstrate the relationship between caspase activation and

damaged nuclei in infected cells by overlaying images from the high-power magnification showing ongoing apoptosis in the SAV1 infected cells (Figure 6.8). The number of cells that underwent cell rounding increased in the virus-infected cells over time (Figure 6.9). The morphology and the degree of cell damage caused by virus isolates, F02-143 (Figure 6.9.d-f) and p42P (Figure 6.9 g-i) appeared similar.
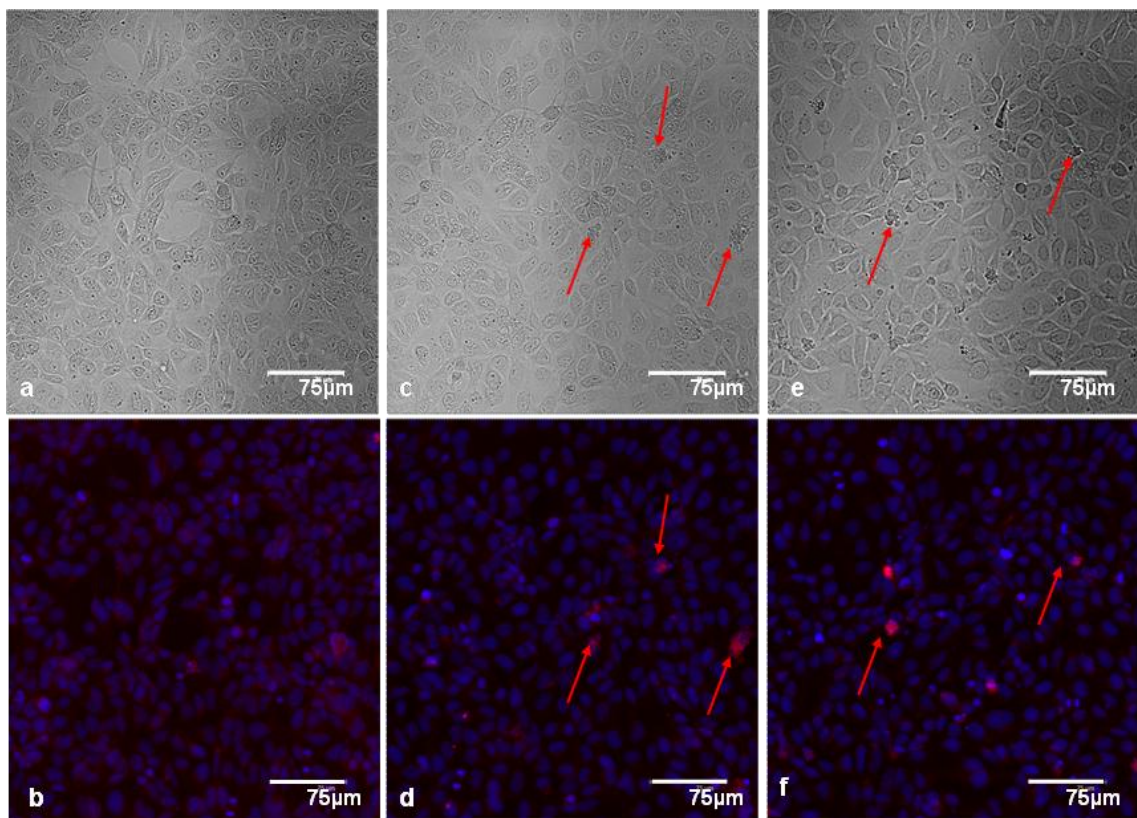
Figure 6. 6 Confocal micrograph of CHH-1 cells. (a-b) Mock infected cells, and the cells infected with SAV1 isolates F02-143 (c-d) and P42p (e-f) at 3 d.p.in. Cell rounding (red arrow) was seen in F02-143 (c) and P42p (e) infected cells in the gray channel and nuclear fragmentation and a high level of caspase-3 expression (red arrow) in (d) F02-143 and (e) P42p infected cells

The size of the nuclei of control and virus-infected (i.e. infected with isolate F02-143 and p42P) CHH-1 cells were examined using image analysis. The mean size of nuclei of virus-infected cells was smaller compared to control cells at all time points examined except 1 d.p.in at which, the mean nuclear size of p42P-infected cells was larger
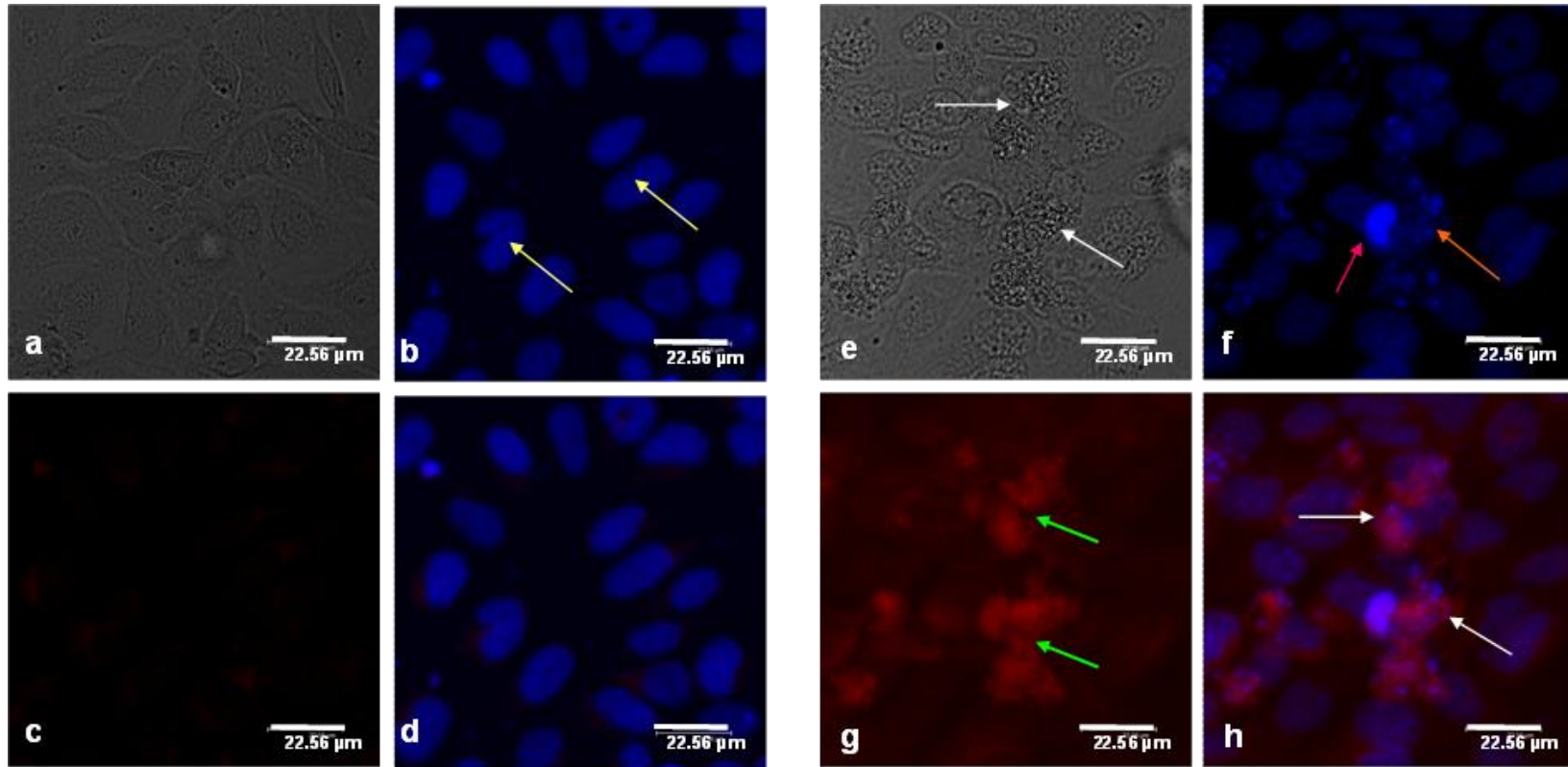
Figure 6. 7 SAV infection can induce cell death in CHH-1 cells. Confocal microscope images of (a-d) control cells and (e-h) SAV1 (F02-143 isolate) infected cells under different laser channels; (a) control (e) infected cells with irregular cellular margins and blebbing (white arrow) in the gray channel (b) normal nuclei (yellow arrow) of control and (f) damaged and fragmented nuclei (red arrow) of infected cells stained with Hoechst 33258 in the blue channel, (c) control and (g) infected cells stained with Texas red to visualise caspase-3 expression (green arrow) in the red channel and the overlay of double fluorescent staining (d) control and (h) infected cells undergoing apoptosis (white arrow) at 5 d.p.in. (Nuclear stain Hoechst 33258 and caspase 3 Texas red).
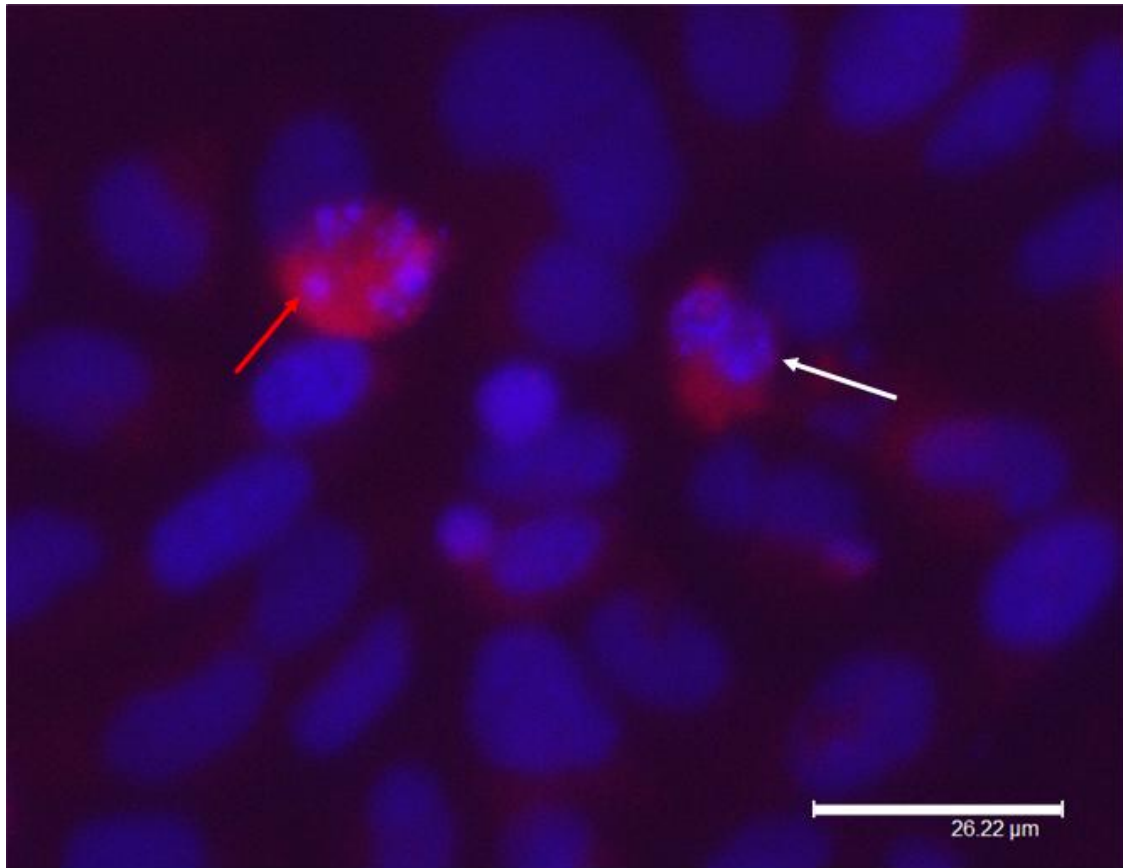
Figure 6. 8 Confocal microscope image of CHH-1 cells infected with F02-143 SAV1 isolate at 3 d.p.in. The damaged nuclei were either misshapen (white arrow) or fragmented (red arrow). Cells with damaged nuclei showed a high level of caspase-3 expression. (Nuclear stain Hoechst 33258 and caspase 3 Texas red).

compared to the control and F02-143 infected cells. The mean nuclear size of both the control and the virus-infected cells increased over time until 5 d.p.in and were then dramatically reduced at 7 d.p.in in the virus infected cells. However, the mean nuclear size of virus infected cells (both isolates) was significantly different from the mean size of the nuclei of control cells at all time points examined. The mean nuclear size of the cells that were infected with isolate F02-143 was smaller compared to p42P infected cells at all time points, and was significantly different from each other at 1 and 5 d.p.in (Figure 6.10).
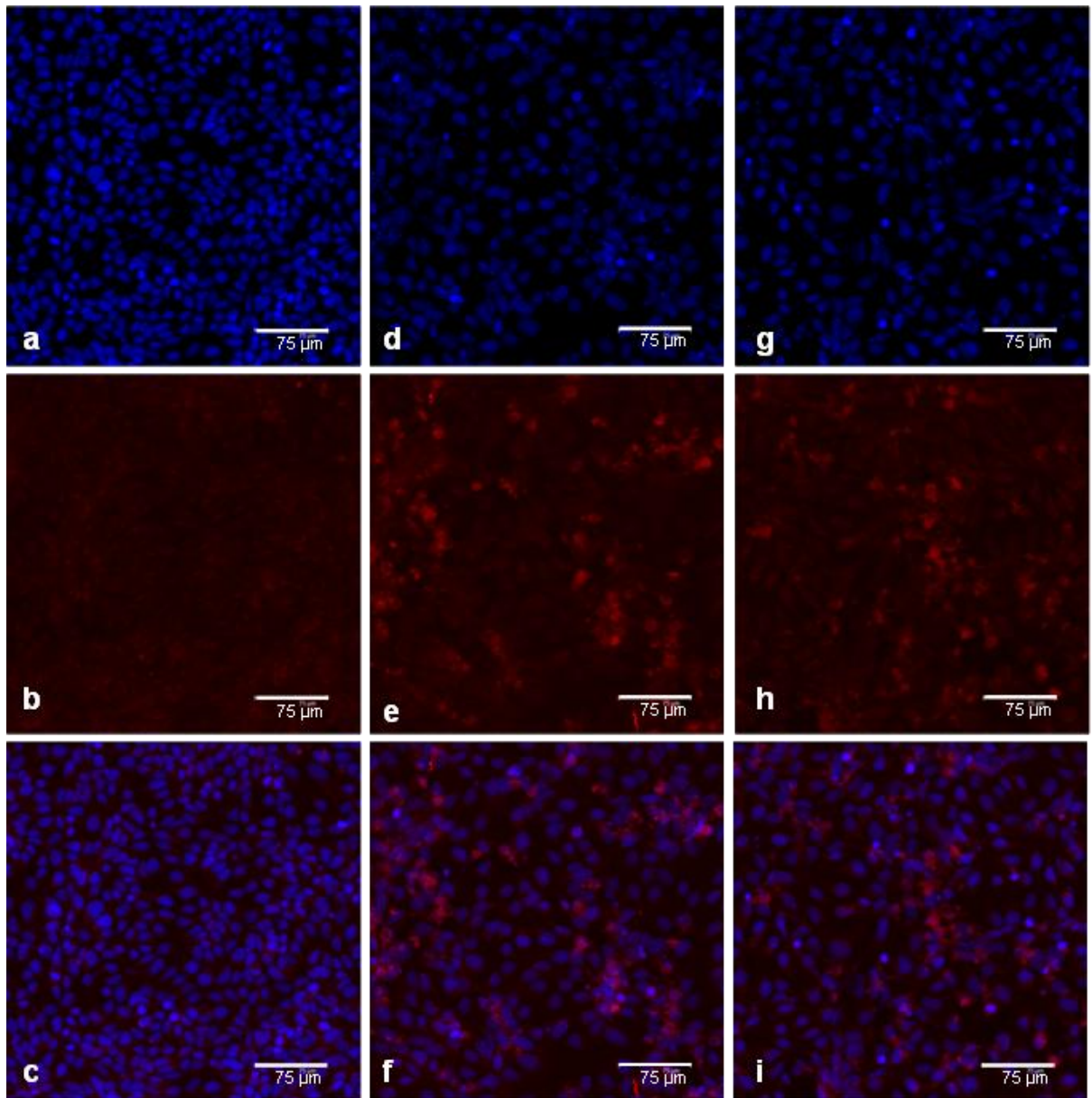
Figure 6. 9 Confocal micrographs of control and SAV1 infected CHH-1 cells at 7 d.p.in. Control cells (a-c), and SAV1 infected cells with isolate F02-143 (d-f) and isolate P42p (g-i) isolate at 7 d.p.in. Compared to control cells (a) nuclei of infected cells were severely damaged and fragmented (d & g) and a high level of caspase-3 expression was noted in the F02-143 (e) and P42p (h) infected cells. The cells with damaged nuclei were saturated with caspase-3 indicating ongoing apoptosis (f & i) compared to uninfected cells (c) in the overlay. (Nuclear stain Hoechst 33258 and caspase 3 Texas red)
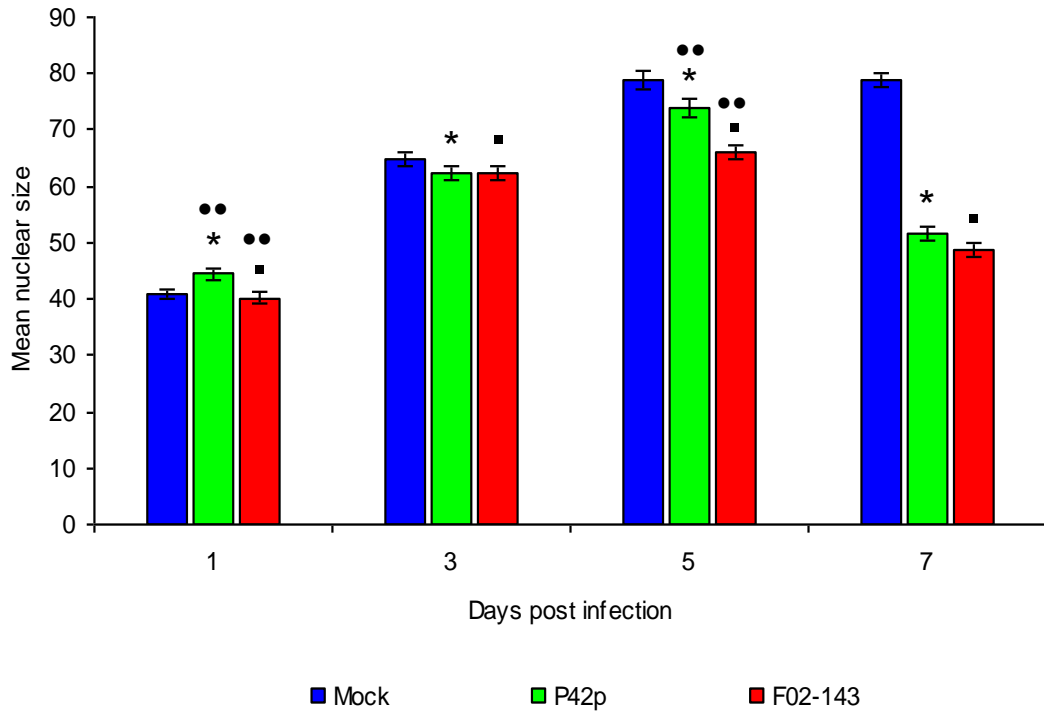
Figure 6. 10 The mean nuclear size obtained from image analysis of control (mock) and SAV1 infected (P42p and F02-143) CHH-1 cells at 1, 3, 5, and 7 days post infection. It was significantly different (p≤ 0.05) between control and infected P42p (*) and F02-143 (•) at all sampling points. The mean nuclear size of the virus infected cells infected with isolates P42p and the F02-143 were significantly different (p≤ 0.05) at 1 and 5 days post infection (••). (Error bars ± Standard error of mean)

The mean intensity of caspase-3 staning of mock infected cells compared to p42P and F03-143 at 1, 3, 5 and 7 d.p.in illustrated in Figure 6.11. The mean caspase-3 intensity was high in mock infected cells compared to virus infected cells at 3 and 5 d.p.in and was low compared to virus infected at day 3 and 5 d.p.in. The high mean expression of caspase in mock infected cells was unexpected and could possibly result from technical error in assay development and thereore data were not urther analysed.
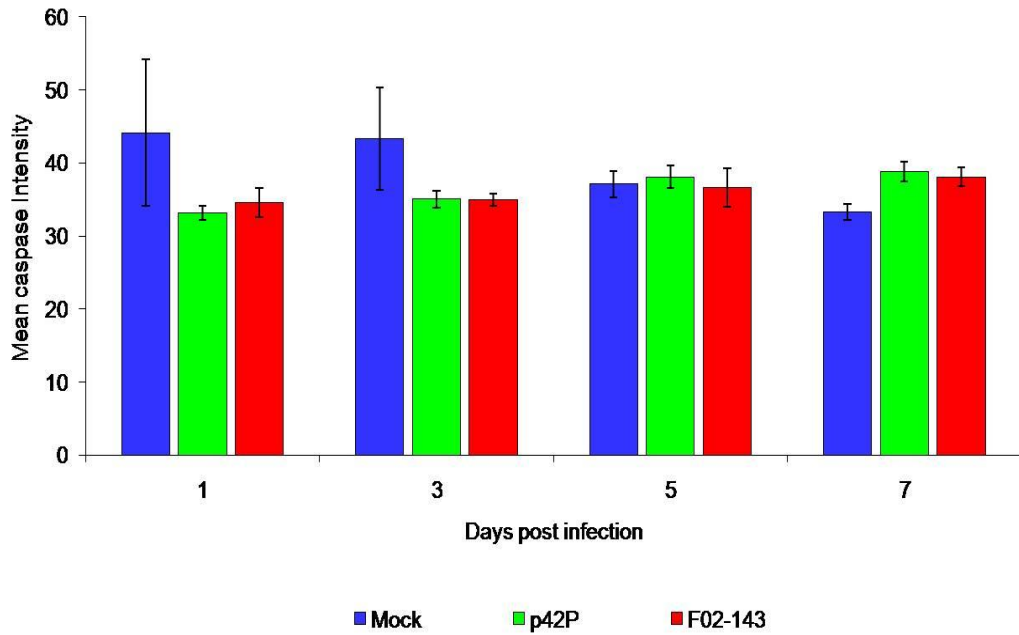
Figure 6. 11 The mean caspase intensity obtained from image analysis of control (mock) and SAV1 infected (P42p and F02-143) CHH-1 cells at 1, 3, 5, and 7 days post infection (Error bars ± Standard error of mean)

6.4 **Discussion**

Apoptosis is an energy dependent, genetically controlled cascade of events that occurs in response to a wide variety of stimuli including viral infections (White, 1996; O'Brien, 1998; Barber, 2001; Slauson & Cooper, 2002). The clearest way to demonstrate the evidence of cell death morphologically is still by electron microscopy (Pläsier *et al.*, 1999). However, light microscopy and fluorescent microscopy are also used for morphological evaluation of cell death in cellular systems.

Observing morphological changes and studying the altered biochemical and molecular pathways allows the cause of cell death due to disease to be determined. The morphological and biochemical changes associated with apoptosis occur both in the cytoplasm and the nucleus of the cell. Identification of morphological changes

associated with apoptosis is considered to be the most significant indicator of the apoptotic process (Frankfurt & Krishan, 2001), and is characterised by cell shrinkage, fragmentation and ultimate cell death. The main nuclear changes associated with apoptosis include chromatin condensation and margination during the initial stages of the process and preced fragmentation of the nuclei during the latter stages. In the present study, chromatin margination was seen at 8 and 24 h p.in together with the chromatin condensation at 24 h p.i. under TEM in both CHH-1 and CHSE-214 cells. Formation of electron dense multiple micronuclei, with loss of cytoplasmic characteristics were evident in cells from 48 h.p.in. Abnormal chromatin condensation and apoptotic body formation is indicative of programmed cell death.

The method of nuclear fragmentation varies depending on the apoptotic inducer, giving rise to a different appearance to the nuclei of the apoptotic cell before it becomes fragmented (Dini *et al*., 1996). Nuclear fragmentation of SAV1-infected cells, seen in the present study, appeared to be initiated by clumping of chromatin in the nucleus before splitting into fragments. Chromatin clumping may have resulted in multiple nuclear protrusions with in the cytoplasm giving rise to multiple cell blebbings seen on the cell surface by SEM in the present study. Cell blebbing is an unspecific sub-cellular change seen with ongoing apoptosis in cells. It is an actin-dependent process that is initiated by localised decoupling of the cytoskeleton from the plasma membrane of cells undergoing apoptosis (Fackler & Grosse, 2008). These protrusions eventually detach from the cell forming membrane-bound cellular fragments, referred to as apoptotic bodies (Dini *et al.*, 1996). Formation of multiple cellular protrusions was seen around 24 h- 48 h.p.in. during this study, further supporting the evidence for apoptosis as a cause of cell death during SAV in salmonid cells.

In apoptosis, the genomic DNA of the cell is cleaved into oligonucleosomal fragments forming a characteristic laddering appearance on agarose gels (Griffin & Hardwick, 1997; Pläsier *et al*., 1999). DNA extracted from cells after 48 h.p.in and 96 h.p.in gave laddering of 180 bp DNA fragments on agarose gels. DNA fragmentation during apoptosis occurs as a result of activation of Ca+ and Mg+-dependent endonucleases, which selectively cleave at linker DNA forming mono and/or oligonucleosomal DNA fragments. This endonuclease-mediated nuclear DNA fragmentation is the biochemical hall mark of nuclear damage in apoptosis. Necrosis also results in DNA damage, but the fragments are irregular in size and form DNA smearing on agarose gel in contrast to laddering induced by apoptosis (Dini *et al.*, 1996). Nuclear fragmentation was also observed under confocal microscopy using the fluorescent dye Hoechst 33258. Activation of cytoplasmic caspase-3 is also a characteristic of apoptosis, and was seen in infected cells from 3 d.p.in. The level of caspase-3 activation was high in cells that had damaged nuclei. Both nuclear fragmentation and caspase-3 activation occurred in CHH-1 cells infected with SAV.

Image analysis is a method employed for quantifying microscopic observations and has advanced greatly after starting to use computer-based automated systems, either using a computer connected to a microscope via a digital camera or using specified computer programs on captured images (Pläsier *et al.*, 1999). Image analysis is an operator-independent method with no scope for either inter or intra-observer variation. It prevents selection of subjective elements which is often the case in manual microscopy-associated quantifications (Pläsier *et al.*, 1999). Once a reliable method of image analysis is established it allows consistent results to be rapidly generated and interprets

the cellular changes to be quantified. Image analysis is widely used for quantifying and characterizing micro-organisms in biotechnical applications and cellular imaging in biomedical sciences. However this method seems very under-used in the field of aquaculture and aquatic disease diagnosis (DeWitte-Orr *et al.*, 2005; Chen *et al.*, 2010). In the present study the second method was adapted in which a computer program was used to analyse pre-captured confocal laser scanning microscopic images to quantify nuclear changes and caspase-3 activation in established cell culture systems during SAV1 infection and has demonstrated a significant difference in the size of the nuclei between infected and control cells over time. Sample preparation and protocol development are very important for a good image analysis. This can be clearly seen in the present study when attempting to analyse caspase staining. Activation of caspase appeared high in damaged cells undergoing apoptosis when viewed under the confocal microscope, but in image analysis the opposite was seen from the results (data not shown). This was probably a result of non-specific binding of the anti-caspase-3 polyclonal antibody to cells or background noise generated from improper washing and staining. As the primary antibody used was prepared against human caspase, non-specific binding was suspected, but it was shown recently that human anti-caspase-3 does recognize caspase-3 expressed in fish cells (Chen *et al.*, 2010). Therefore, from the strong staining seen by confocal microscopy we believe that further optimization of the assay is required to generate a reliable result for caspase-3 activation in these cell cultures.

Allthough the same stock virus have been used immunostained sample under confocal microscopy and EM, time line for detection of apoptosis appeared to be delayed in former. To initiate the infection in those experiments, the cells were grown on two

different vessels, in which, cells for immunostaing were grown on coverslips placed on 24 well plates, while cells for the EM were grown on 25 ml cell culture flasks. The difference in detecting apoptosis in these two cell culture systems is not very clear, however, differences in the development of CPE in cells grown on 24 well plate and flasks were noticed during the initial optimization studies of SAV-1 in cell cultures (personal observations). But, as these assays were carried out in different instances, the effect of infective virus titer present in the stock virus cannot be ignored and obtaining viral titer of stock viruses in parallel experiments is thefore recommended.

Apoptosis does not elicit an inflammatory response in tissues, unlike necrosis-induced cell death. In general, apoptotic cells are cleared by activated macrophages or by neighbouring cells. Clearance of apoptotic cells by neighbouring cells has been seen with IPNV infected CHSE-214 cells infect (Hong *et al.*, 1998; Chen *et al.*, 2010), but it was not possible to observe in the present study. Phagocytosis and clearing of cell debris is a rapid process in the cellular system and this could possibly explain the reason why it was not observed. In addition, the rapid clearance of apoptotic cells from the tissues by phagocytosis increases the difficulty in observing programmed cell death in tissues and characterising apoptosis *in-vivo.*

It is known that apoptosis induced by alphavirus in mammals provokes persistent infection in nervous tissues (Griffin, 2005; Griffin & Hardwick, 1997). Cells sloughed off from the cell monolayer were seen in the cell culture supernatant and appeared to be infectious even after 28 d.p.in, during virus optimisation studies for SAV1 in this thesis. The ultimate fate of these salmonid cells is not clear and it would be interesting to

evaluate this further to characterise whether it has any relationship to virus persistence as seen in mammalian alphaviruses (Griffin & Hardwick, 1997).

In summary, from the evidence obtained with the TEM and SEM, confocal microscopy and DNA fragmentation, there is a strong indication that cell death in SAV1 infection is associated with apoptosis. The occurrence of apoptosis in CHH-1 cells appears interesting, especially because of the cardiac origin of this cell line. The heart is one of the main target organs of the virus and apoptosis has already been observed in heart during SAV infections (Taksdal *et al.*, 2007). This therefore, increases the value of this cell line as a research tool for SAV studies. However, the actual cellular pathway involved in activating apoptosis during SAV infection is still unclear and the contribution it makes to the actual pathology observed *in- vivo* still remains to be established.

Chapter 7

General Discussion

Aquaculture continues to increase globally on an annual basis, and with it viral diseases have become a huge economic burden to the industry. Pancreas disease caused by SAV1 was first noted in Scottish farmed Atlantic salmon in the late 70s, and it has since become a severe problem to the Scottish, Irish and Norwegian salmon industries. Effective control strategies are needed to combat the disease, but limited knowledge on the spread of SAV and propagation of the virus in its host, and in the environment, has hindered the development of such control measures. The reason for the increase in the incidence of PD is still unclear. Sensitive diagnostic tools that are able to detect and measure the distribution of the virus in monitoring, screening and surveillance programmes of the host and the environment are urgently needed to combat the disease. Also, information on the host's response to SAV is limited, and increasing our understanding of how immune response and antiviral mechanisms help to combat the disease would assist in our understanding of disease pathogenesis, and in the design of effective management and control measures.

Virus isolation using cell cultures and observing the development of a CPE was one of the main methods used for virus characterization, especially before molecular tools become available. The viral aetiology of PD was confirmed by Nelson *et al.*, (1995) who isolated the virus on CHSE-214 cells nearly two decades after the disease was first described in Scotland (Munro *et al.*, 1984; Nelson *et al.*, 1995). This original virus isolate, F93-125, has been widely used as a reference isolate for many research and

phylogeny studies relating to SAV (Fringuelli *et al.*, 2008). During the preliminary work presented in this thesis, the F93-125 isolate appeared more virulent than isolate p42P, an isolate obtained from an experimental induction of SAV1 in rainbow trout in France, both *in-vitro* and *in-vivo*, and was therefore chosen for the subsequent experimental infections (data not shown).

Primary isolation of SAV from cell culture is based on observing a CPE, and this can be difficult to achieve. The initial development of a CPE from the primary isolation can take several days and several blind passages before obtaining a positive result. It also requires an experienced person to interpret the results of the CPE (Graham *et al.*, 2007a). Only CHSE-214 and RTG-2 cell lines have been widely used to isolate SAV, however Graham *et al.*, (2008) recently demonstrated that BF-2, TO, FHM, SHK-1, and EPC cells are also susceptible to infections by SAV. The appearance and severity of the CPE caused by SAV is widely dependent on the cell line used for the isolation of virus (Graham *et al.*, 2008). Virus isolation from head kidney tissue of experimentally infected Atlantic salmon was carried out in the present study using three established salmonid cell lines, CHH-1, CHSE-214 and SHK-1. Successful viral growth was obtained on the first attempt at inoculating the infected kidney homogenate on to all three cell lines, with the fastest CPE development occurring in CHH-1 cells. The appearance of the CPE in the CHH-1 and CHSE-214 was similar but different to the CPE in the SHK-1cells (Figure 2.2). The SHK-1 cells are derived from the head kidney of Atlantic salmon and are reported to have macrophage-like activities. These cell lines have been used for many different functional studies, such as examining antiviral activity against different viral diseases of salmonids and in functional genomics studies (Jensen & Robertsen, 2002; Martin *et al.*, 2007; Gahlawat *et al*., 2009). The delay in the

development of a CPE in SHK-1, as observed in the present study, means that they have limited use as a diagnostic tool for SAV virus isolation. They are however still useful for other investigations such as monitoring antiviral mechanisms and virus-host interactions (Graham *et al*., 2008; Gahlawat *et al.*, 2009). The ability of SAV to infect both SHK-1 and TO cells (Graham *et al.*, 2008) may indicate that the virus has tropism towards leukocytes, supporting the observations made by Houghton, (1995) and Graham *et al.*, (2003b). One of the experimental infections carried out in parallel to the present study, showed a progressive apoptosis in the blood and head kidney of Atlantic salmon around 5 d.p.i. (Costa *et al.*, 2007). Taksdal *et al.*, (2007) have described a cellular population with eosinophilic granules, present in the kidneys of Atlantic salmon and rainbow trout derived from field outbreaks caused by SAV3. Similar lesions have also been reported in SAV1-affected Atlantic salmon from the Shetland Islands, Scotland (McLoughlin and Graham, 2007). It was possible to isolate virus using SHK-1 again in the present study, supporting the idea of possible tropism of SAV towards the reticuloendothelial system and blood. This is of particular interest for describing the pathogenesis and the immune mechanisms of SAV infection.

It was shown in the present study that CHH-1 cells are susceptible to SAV infection (Herath *et al.*, 2009), and thus these cells are useful for diagnostics and as a research tool to examine host-virus interactions, as was used in the present study to examine the cell death mechanism of SAV (Chapter 6). The sensitivity of cell culture isolation of SAV has been improved by using a rapid immunoperoxidase-based staining method described by Graham *et al.*, (2003a). This method helps to overcome the problems of false negative results sometimes obtained in conventional cell cultures used in SAV diagnosis, because of the problems associated with delayed development of a CPE. It

would be interesting to determine the usefulness of CHH-1 cells in combination with the immunoperoxidase based immuno-staining method using monoclonal antibodies for virus isolation from different clinical samples derived from field outbreaks, to elucidate whether it can improve SAV diagnostics further.

The virus load is used as a reliable indicator to establish the extent of active virus present in a host during infection or in response to a treatment (e.g. vaccines or drugs) (Niesters, 2001; Mackay *et al.*, 2002). Determining the virus load present in a tissue during the course of an infection facilitates our understanding of virus replication over the course of infection, which is useful for interpreting the pathology associated with the disease. The level of virus present in different tissues and serum of fish infected with SAV during both experimental and natural infections has been assessed by virus isolation and end-point titration of the virus in cell cultures (McLoughlin *et al*., 1995, 1996, 2006). Although the development of the immunoperoxidase based virus neutralisation test has improved virus isolation and titration compared with conventional cell culture methods, it was not possible to estimate actual viral genomic RNA copy numbers present in these samples, therefore molecular tools have been employed for this purpose. Graham *et al.*, (2006b) were able to detect and quantify the level of SAV present in the heart of experimentally infected salmon and in the serum of naturally infected salmon using a qRT-PCR assay. In this particular assay, using a constant W/V ratio of tissue and SG chemistry it was possible to detect virus for a considerable period after the infection (90 d.p.i). Using Taqman$^{®}$ qRT-PCR, relative to an internal housekeeping gene, ELF1α, Andersen *et al.*, (2007) were able to characterise the pantropic tissue distribution of SAV in the heart, kidney, gill, gut, pseudobranch, and the somatic muscle of diseased fish. The experimental samples used for their work

were derived from two independent experimental infections, (1) from fish injected I.P with tissue homogenate derived from salmon clinically infected with SAV3 and (2) from fish injected with tissue culture grown SAV1 (reference isolate F93-125). They also demonstrated the presence of viral RNA as late as 190 d.p.i. In the present study, the same reference isolate F93-125 was used to infect fish I.P. and the peak level of viral RNA was detected as early as 5 d.p.i., which was 2 days earlier than the peak levels of SAV detected in the experiment carried out by Andersen *et al.*, (2007) in their study. The semi-quantitative assay developed by Andersen *et al.*, (2007) used a housekeeping gene to determine the fold change of viral gene expression. In the present study has quantified the copy number of the viral RNA present with the help of a standard curve prepared from RNA synthesized *in-vitro*. Use of a standard curve prepared from RNA transcribed *in-vitro,* using the same transcript as used for testing the samples in qRT-PCR assay, has minimised the effect of external factors toward to the final result of the assay (Workenhe *et al.*, 2008)). However, normalization of data comparative to a standared reference gene is still recommended for the accuracy of the final results. It is known that use of a host encoded housekeeping gene to quantify viral RNA expression could affect the final result of the test as the expression pattern of housekeeping gene could change across different tissues and during pathogen challenges (Mackay *et al.*, 2002). Spiking extracted RNA with *in-vitro* transcribed cRNA without homology to the total RNA is been used as a alternative approach for assay normalization in in realtime qRT-PCR to minimise the inherent variability of RNA extraction, storage, cDNA synthesis, data acquisition, analysis of qRT-PCR assays (Gilsbach *et al.,* 2006) and variation of house keeping gene. Therefore use of 'universal RNA reference' would be useful to improve the results of the present study.

From the infection kinetics examined using both cell culture and molecular techniques revealed that the highest level of SAV was present in the early stage of the experimental infection, before either clinical or pathological signs become evident. Furthermore, it was only possible to detect SAV-positive fish up to 42 d.p.i. Other studies reported in the literature, have detected SAV relatively late in the infection; in one study, SAV was present in the heart of the infected fish at 90 d.p.i (Graham *et al.*, 2006b) while Andersen *et al.*, (2007) detected SAV as late as 190 d.p.i. The viral RNA, detected late in these experimental infections, could be from complete intracellular virions, free/unpacked virus particles inside the cells, replication intermediates, defective virus particles, or free intracellular viral RNA from defective cells. Therefore, detection of SAV late in the infection may not directly reflective of active replicating virus but persistent or residual RNA in the tissue (McLoughlin & Graham, 2007). The absence of viral RNA detected later in the infection in the present study could be related to early clearance of the virus from the host mediated via potent interferon mediated immune defence and the broad range of antiviral mechanisms that have been observed during this experimental infection (see Chapter 3 and 4).

Similar to the present study, most published results on the experimental infections using SAV were carried out using cell culture-adapted viruses (Boucher *et al.*, 1995; McLoughlin *et al.*, 1995, 1996, 1997, 2006; Christie *et al*., 1998, 2007; Desvignes *et al.*, 2002; Graham *et al.*, 2006b). It is known that continuous passaging of alphavirus in cell culture tends to attenuate the infectivity of the virus to its natural host, while adapting to the cell line used to culture virus *in vitro* (Karlsen *et al.*, 2006). The level of SAV present and the time taken to induce the infection between fish experimentally infected I.P with cell culture adapted virus and fish injected with homogenised clinical material

I.P appeared to be different. In the experiment conducted by Andersen *et al.*, (2007) it was found that viral RNA expression in the kidney of fish injected with clinical samples was 20,000 fold higher than in the fish injected with the virus grown in cell cultures. In addition, the experimental infection induced by injecting F93-125 isolate I.P. gave a peak level of viral RNA around 1 week post-infection compared to the peak level of viral RNA detected at 3 weeks post-infection with kidney homogenates from SAV3 infected fish. This difference could possibly be attributed to changes in the virus, as a result of mutations that takes place during cell culture adaptation. On the other hand, the difference in viral kinetics could be related to a difference between subtypes SAV1 and SAV3 themselves (Karlsen *et al.*, 2006). To understand this better, the infection kinetics and the clinical outcomes of different SAV subtypes need to be studied further, also comparing clinical material and cell culture grown virus to infect fish.

Field outbreaks of SAV are generally associated with mortalities ranging from 5 to 50 % of the affected population (Rodger & Mitchell, 2007). However, mortalities are difficult to reproduce in SAV infections under experimental conditions (McLoughlin *et al.*, 1996; Desvignes *et al.*, 2002; Graham *et al.*, 2006a), or it may be that the mortalities seen in clinical diseases are associated with secondary complications rather than as an outcome of the infection itself (Christie *et al.*, 2007). Reports of gross pathological lesions tend to be mild or absent in experimental infections, similar to that was seen in the present study. Ascites and a yellow, enlarged liver have been observed in the experimental infections carried out using homogenised clinical materials from SAV3-infected fish indicating that clinical samples possibly give rise to more severe pathologies than cell culture-derived virus (Andersen *et al.*, 2007). In the present study, fish started to show mild clinical signs early in the infection but no mortalities were detected. Both the absence of mortalities and minimal or absence of gross pathological

changes could also have resulted from attenuation of the virus by repeated passaging *in vitro*.

Sequential pathology described for SAV, based on field and experimental infections have been used to help describe the pathogenesis of SAV (McLoughlin & Graham, 2007). A comprehensive description of the pathology in different target tissues indicating distribution of the lesions in tissues and the severity of the lesion at different stages of both natural and experimental infections is available for both PD and SD (McVicar, 1987; McLoughlin *et al.*, 1995, 1996; Graham *et a*l., 2007a). A comparative study between Atlantic salmon, rainbow trout and brown trout identified differences in the severity, the extent of tissue damage, and the distribution of the lesions (Boucher *et al.*, 1995). There were also reports of differences in the susceptibility to SAV1 by different strains of Atlantic salmon from experimental infection data, suggesting that there could be a variation in genetic susceptibility of fish to SAV1 infection (McLoughlin *et al.*, 2006).

Heart, pancreas and skeletal muscle are the main targets of virus infection. In the present study, severe pathology was observed in the pancreas and mild to moderate pathology in the heart of infected fish, but no pathology was seen in the skeletal muscle of any of the infected fish throughout the 90 day experimental period. Both red and white skeletal muscle necrosis occurs under natural conditions, and this occurs late in the infection after pancreatic and heart pathology can be seen. Most of the experimental infections of SAV have been unable to reproduce or cause only mild skeletal muscle lesions with degenerative changes occurring in the myofibrils compared to field outbreaks of SAV (McLoughlin *et al.*, 1996). The low incidence of muscular lesions was suspected to be result of lower virulence of the cell culture adapted virus used to

induce the infection, and also the less intense physical activity of the experimentally infected fish compared to conditions experienced by farmed fish. McLoughlin *et al*, (1996) reported a high number of deaths in populations with severe skeletal muscle lesions in natural outbreaks indicating the significance of the skeletal myopathy for causing death in SAV infected fish. In general, skeletal muscle pathology occurs 3-4 weeks post-infection. The absence of skeletal muscle lesions in the present study could also possibly be a result of viral clearance by an early immune response.

Infection of the virus has been transmitted to healthy individuals through co-habitation of the fish with SAV-infected fish. This is a characteristic feature of SAV, since other alphaviruses require an arthropod vector for transmission (Strauss & Strauss, 1994). The mucosal membranes may act as the portal of entry of SAV into the fish but there is no information on this as yet. The present study showed increased production of Mx protein in the mucous membranes of virus-infected fish, with the highest level detected in gills, compared to the skin and gut. Further, a high Mx protein expression was also detected in cardiac muscle of infected fish, early in the infection before pathological lesions become evident in heart. The high levels of Mx expression in the gill of SAV-infected fish are interesting. Previously Andersen *et al.*, (2007) also found that a higher level of viral RNA was present in the gill of fish compared to other tissues in a qRT-PCR study of experimentally induced SAV in salmon. Many fish viruses use gill as a portal of entry, and there could be a relationship to gill in SAV infection, thus, a detailed investigation would be useful for elucidating the role of the gill in SAV pathogenesis. However, the lack of sensitive tools to visualise the spread of the virus in the tissues is a major drawback for such studies, and sensitive methods such as *in situ* hybridization and immunohistochemistry need to be developed to be able to study this.

Availability of such tools will also facilitate the understanding of tissue tropism of the virus.

In general, sequential pathology helps in describing pathogenesis of diseases, however, this is not very useful for understanding the functional mechanisms of the disease. Understanding the relationship between the pathogen kinetics and the altered host physiological and structural mechanisms is useful for describing the pathogenic outcomes of the disease (Slauson & Cooper, 2002). Microarray analysis was performed to examine the co-opted molecular mechanisms in the initial stages of SAV1 infection in Atlantic salmon experimentally infected with the virus. A large number of cellular transcription and translation associated genes were shown to be differentially expressed and these were associated with the possible shutdown of cellular metabolic functions, as seen with mammalian alphavirus infections. Changes were seen in the genes associated with the establishment of infection and cell death using the microarray. In general, fish largely depend on their innate immune system to defend them from pathogens. The innate immune response of fish includes a large array of mechanisms for responding to viral diseases (Ellis, 2001; Magnadóttir, 2006; Whyte, 2007). In SAV infections, the role of the innate immune response is largely unknown, but the microarray used in the present study indicated that a large number of innate immune signatures responded at an early stage in the infection. For example, the INF-1 pathway was seen to be highly activated using the microarray, and this was confirmed using immunohistochemistry for the Mx protein, an INF-I induced antiviral protein, detected in a variety of different tissues. A higher degree of Mx expression was seen in the heart and the mucous membranes of SAV infected fish. Again with the microarray, an early induction of adaptive immune associated genes, such as MHC-I and Ig associated genes was observed, highlighting the involvement of the adaptive immune system in SAV

infection. Understanding the antiviral mechanisms of the host also helps to describe the pathogenesis of viral diseases. In the present study, expression of some of the unique antiviral associated genes such as zinc finger protein were observed in common with mammalian alphaviruses suggesting possibilities of similar antiviral mechanisms between fish and higher vertebrates.

Evaluation of the effects of different treatments (i.e. vaccines, feed, immunostimulants) and host response to different subtypes of SAV using microarray will hopefully give a better insight into the disease mechanisms of the virus and help in designing effective control measures against SAV infections. The presence of a poly-A tail at 3' of the viral genome allows a possible incorporation of the SAV genome into the microarray platform, and such a tool would be useful as an indicator of the host infectious status, along with global expression studies of the infection.

The life cycle of a virus is a complex interaction between virus and host cells. Understanding the viral biogenesis process helps to describe the ultra-structural damage and the cellular pathogenesis during the replication process. Electron microscopy based ultra-structural imaging is popular as a tool for characterising virus types in fish viral diseases and on a few occasions EM was also used to describe the ultra-structural morphogenesis and replication cycle in established cell lines (Granzow *et al*., 1995; Workenhe *et al*., 2008b; Miwa & Sanao, 2007). In the present study electron microscopy was used to describe ultra-structural morphology of SAV and it was seen to closely resemble that of mammalian alphaviruses (Nelson *et al*., 1995). In Chapter 5, virus particles 45-55 nm in size were clearly observed under negative-stained electron microscopy. It also possible to observe typical alphavirus replication in CHSE-214 cells

infected with SAV1, although a few unique characteristics were observed with the virus. Membrane budding, a unique feature of enveloped viruses (Groff *et al.*, 1998, Garoff *et al.,* 2004), has been clearly demonstrated for SAV (McLoughlin & Graham, 2007), and in the present study virus budding was observed through surface projections acquiring envelope from the CHSE-214 cells. Virus budding in SAV1 infection appears to be detrimental to host cells. From the TEM and virology studies it was shown that CPE developed subsequent to extensive virus budding from CHSE-214 cells. Pinching of cell membrane to form a virus envelope may induce cell death characterised by the rounding and detachment from the monolayers observed under the light microscope, and cellular and nuclear fragmentation detected under TEM. Virus endocytosis was difficult to demonstrate at the level of infection *in vitro,* but was frequently observed later in the infection process during this study and was mediated by the formation of coated pits. The vesicles with fuzzy-looking membrane derived from Golgi apparatus appeared to be responsible for generating the coated pits involved in virus uptake. Components of the secretory pathway of the cell, for example, endosomes, lysozomes, RER and Golgi apparatus, were extensively involved in the SAV replication process. Changes in the expression of genes involved in the cellular secretory pathway were seen in SAV infected fish *in vivo* using the microarray and this may be reflective of the morphological changes associated with secretory pathway seen under TEM.

The process of viral biogenesis described in the present study was based on the comparative morphology of mammalian alphavirus. Combinations of specific antibodies and electron dense markers, specific for different cell organelles, have been used to confirm the structures involved in virus assembly by mammalian alphavirus (Kujala *et al.*, 2001) ,and this would be useful too for SAV. Fluorescent tagged

infectious-RNA prepared by reverse-genetics, would be useful for imaging various events in the virus biogenesis process (Müller *et al.*, 2004). Studies on the structural assembly of virus are currently being pursued to identify the different events of the virus biogenesis process in order to develop different molecules that counteract particular events (Perera *et al.*, 2008). This is also helpful in the development of effective vaccines and antiviral drugs. Use of advanced cryo-electron microscopy and atomic resolution has provided an important insight in to the structures of enveloped viruses (Mukhopadhyay *et al.*, 2005). Use of these tools has allowed examination of different intermediates involved in the virus cellular entry that have helped to understand virus replication at molecular level. Following on from this, studies of structural conformational changes using pseudo-atomic structures of virion and atomic resolution structures of viral proteins have proved promising targets to develop structure-based antivirals for flaviviruses (family *Flaviviridae*). Although such applications would be useful in clinical infections, the practicality of developing such products is not probably economically feasible for aquaculture.

The alphavirus +ssRNA genome, itself, is infectious to the host cells (Strauss & Strauss, 1994; Kujala *et al.*, 2001). This feature has been exploited in the generation of alphavirus expression vectors and has been used in many different molecular applications, such as vectors for vaccine delivery for different viral and tumour conditions, and recombinant protein expression (Schelesinger & Dubenskey, 1999; Riezebos-Brilman *et al.*, 2005). In the 'Reverse Genetic' process, the alphavirus RNA genome is converted into an intermediate cDNA in which the desired genetic manipulation is performed by inserting or deleting genetic components and re-recovering RNA as recombinant RNA (rRNA) either *in-vitro* or *in–vivo*. For SAV2, an

infectious full length cDNA clone was generated by inserting the RNA genome into a plasmid and transfecting this into BF-2 cell cultures to produce a recombinant SAV2 virus (rSPDV2) (Moriette *et al.*, 2006). The rSDV2 has been used in trials *in-vivo* in which it has been found to be infectious, but non-pathogenic to rainbow trout at temperatures other than 14°C. This virus was able to elicit a protective response for 5 months to subsequent wild type virus challenges (Moriette *et al.*, 2006), suggesting a potential use of rSAV2 as a recombinant vaccine for SAV (McLoughlin & Graham, 2007). Some additional sequences have been transfected into the rSAV2 and successfully expressed, highlighting the possible use of SAV as an expression vector for other applications such as delivering other viral vaccines to salmonids. However this technology has yet not been exploited for this purpose.

Alphaviruses are known inducers of apoptosis in different tissues in mammals (Griffin *et al.*, 1994; Griffin & Hardwick, 1997, 1998). SAV induced apoptosis was seen in the pancreas and heart of diseased fish under H&E staining (Taksdal *et al.*, 2007). Progressive apoptosis in blood and head kidney leucocytes was recently seen in an *in-vivo* study performed in our laboratory. In addition, the present study was able to characterise apoptosis-mediated cell death in two established cell lines (CHH-1 and CHSE-214), supporting earlier results. The apoptosis observed in CHH-1 appeared particularly interesting because of the cardiac origin of these cells, and suggests that SAV infection is able to induce active killing in the cells of the heart mediated via apoptosis. However, pro-apoptotic, apoptotic and anti-apoptotic events were encountered in the microarray experiment performed using samples derived from experimental infection induced in Atlantic salmon. This highlights the complexity of cell death in the host itself compared to the cell culture system in which the anti-viral or

anti-apoptotic mechanisms are minimal. It would be interesting to investigate the apoptosis events further to clarify whether it is a consequence of virus replication in the cell or as a result of host immune response.

This thesis has examined the different aspects of host responses during SAV1 infection in Atlantic salmon and in cell cultures of salmonid origin, highlighting some key features of cellular and molecular pathogenesis of SAV infection. In summary, the induction of SAV infection by injecting cell culture adapted SAV I.P. established an infection rapidly, and also elicited a potent immune response at a very early stage during the infection in Atlantic salmon. Interferon appeared to be a key antiviral factor in response to the SAV infection, and signatures of INF-1 expression were seen in different tissues of the host during the infection using microarray. Characterisation of INF-1 mediated antiviral response associated with SAV in this study suggested that mild pathology observed in the heart and absence of any pathology in skeletal muscle is possibly a result of clearance of virus at the early stages of infection. The ultrastructural morphogenesis of SAV appeared to be similar to mammalian alphavirus replication in cells, and the death of cells in SAV infections appeared to be mediated via apoptosis during the infection. These results have given an interesting insight into SAV pathogenesis emphasising the importance of the innate immune response during the infection. Thus, it would be interesting to explore the innate immune mechanisms further for the development of effective vaccines and evaluating vaccination and immunostimulation regimes against SAV1 infections in order to maintain the health status of the susceptible stocks.

References

Abbas, A. K., Lichtman, A. H., & Pober, J. S., (2000). *Cellular and molecular immunology*. 4th edition , W. B. Saunders Company USA..

Acheson, N. & Tamm, I., (1967). Replication of Semliki forest virus: an electron microscopic study. *Virology* **32** (128-148).

Acosta, F., Petrie, A., Lockhart, K., Lorenzen, N., & Ellis, A. E., (2005). Kinetics of Mx expression in rainbow trout (*Oncorhynchus mykiss*) and Atlantic salmon (*Salmo salar* L.) parr in response to VHS-DNA vaccination. *Fish & Shellfish Immunology* **18** (81-89).

Adams, A. & Thompson, K. D., (2006). Biotechnology offers revolution to fish health management. *Trends in Biotechnology* **24** (201-205).

Adzhubei, A. A., Vlasova, A. V., Hagen-Larsen, H., Ruden, T. A., Laerdahl, J. K., & Hoyheim, B., (2007). Annotated Expressed Sequence Tags (ESTs) from pre-smolt Atlantic salmon (*Salmo salar*) in a searchable data resource. *BMC Genomics* **8** (209)

Aldrin, M., Storvik, B., Frigessi, A., Vilijugrein, H., & Jansen, P., (2010). A stochastic model for the assessment of the transmission pathways of heart and skeleton muscle inflammation, pancreas disease and infectious salmon anaemia in marine fish farms in Norway. *Preventive Veterinary Medicine* **93** (51-61).

Alne, H., Chen, Y., Mckillen, D. J., Wu, S., Jenny, M. J., Chapan, R., Gross, P. S., Warr, G. W., & Almeida, J. S., (2004). Optimal cDNA microarray design using expressed sequence tags for organisms with limited genomic information. *BMC Bioinformatics* **5** (191).

Alvarez-Pellitero, P., (2008). Fish immunity and parasite infections: from innate immunity to immunoprophylactic prospects. *Veterinary Immunology and Immunopathology* **126** (171-198).

Andersen, L., Bratland, A., Hodneland, K., & Nylund, A., (2007). Tissue tropism of salmonid alphaviruses (subtypes SAV1 and SAV3) in experimentally challenged Atlantic salmon (*Salmo salar* L.). *Archives of Virology* **152** (1871-1883).

Anonymous, (2003). *Manual of diagnostic tests for aquatic animals*. 4th edition, Office International des Epizooties, Paris, France.

Barber, G. N., (2001). Host defense, virus and apoptosis. *Cell Death and Differentiation* **8** (113-126).

Barry, G., Breakwell, L., Fragkoudis, R., Attarzadeh-Yazdi, G., Rodriguez-Andres, J., Kohl, A., & Fazakerley, J. K., (2009). PKR act early in infection to suppress Semliki forest virus production and strongly enhances the type I interferon response. *Journal of General Virology* **90** (1382-1391).

Bell, J. G., Mcvicar, A. H., & Cowey, C. B., (1987). Pyruvate-kinase isozymes in farmed Atlantic salmon (*Salmo salar*) - pyruvate-kinase and antioxidant parameters in pancreas disease. *Aquaculture* **66** (33-41).

Bergan, V., Jagus, R., Lauksund, S., Kileng, O., & Robertsen, B., (2008). The Atlantic salmon Z-DNA binding protein kinase phosphorylates translation initiation factor 2 alpha and constitutes a unique orthologue to the mammalian dsRNA-activated protein kinase R. *FEBS Journal* **275** (184-97).

Berger, A., Preiser, W., & Doerr, H. W., (2001). The role of viral load determination for the management of human immunodeficiency virus, hepatitis B virus and hepatitis C virus infection. *Journal of Clinical Virology* **20** (23-30).

Bergmann, S. M., Fichtner, D., Riebe, R., & Castric, J., (2008). First isolation and identification of sleeping disease virus (SDV) in Germany. *Bulletin of the European Association of Fish Pathologists* **28** (148-156).

Bick, M. J., Carroll, J. W. N., Gao, G. X., Goff, S. P., Rice, C. M., & MacDonald, M. R., (2003). Expression of the zinc-finger antiviral protein inhibits alphavirus replication. *Journal of Virology* **77** (11555-11562).

Boscher, S. K., McLoughlin, M., Le Ven, A., Cabon, J., Baud, M., & Castric, J., (2006). Experimental transmission of sleeping disease in one-year-old rainbow trout, *Oncorhynchus mykiss* (Walbaum), induced by sleeping disease virus. *Journal of Fish Diseases* **29** (263-273).

Boshra, H., Li, J., & Sunyer, J. O., (2006). Recent advances on the complement system of teleost fish. *Fish & Shellfish Immunology* **20** (239-262).

Boucher, P., (1995). Sleeping diseases (SD) of salmonids. *European Association of Fish Pathologists* **14** (180).

Boucher, P., Raynard, R. S., Houghton, G., & Laurencin, F. B., (1995). Comparative experimental transmission of pancreas disease in Atlantic salmon, rainbow trout and brown trout. *Diseases of Aquatic Organisms* **22** (19-24).

Boucher, P. & Laurencin, F. B., (1996). Sleeping disease and pancreas disease: Comparative histopathology and acquired cross-protection. *Journal of Fish Diseases* **19** (303-310).

Boudinot, P., Massin, P., Blanco, M., Riffault, S., & Benmansour, A., (1999). Vig-1, a new fish gene induced by the rhabdovirus glycoprotein, has a virus-induced homologue in humans and shares conserved motifs with the MoaA family. *Journal of Virology* **73** (1846-1852).

Boudinot, P., Salhi, S., Blanco, M., & Benmansour, A., (2001). Viral haemorrhagic septicaemia virus induces Vig-2, a new interferon responsive gene in rainbow trout. *Fish & Shellfish Immunology* **11** (383-397).

Branson, E. J., (2002). Sleeping disease in trout. *Veterinary Record* **150** (759-760).

Bruno, D. W. & Noguera, P. A., (2009). Comparative experimental transmission of cardiomyopathy syndrome (CMS) in Atlantic salmon *Salmo salar*. *Diseases of Aquatic Organisms* **87** (235-242).

Buckley, C. D., Pilling, D., Lord, J. M., Akbar, A. N., Scheel-Toellner, D., & Salmon.M., (2001). Fibroblasts regulate the switch from acute resolving to chronic persistent inflammation. *Trends in Immunology* **22** (199-204).

Burleson, F. G., Chamber, T. M., & Wiedbrauk, A. (1992). *Virology: A laboratory manual*. London: Acedemic Press

Bustin, S. A., (2000). Absolute quantification of mRNA using real-time reverse transcription polymerase chain reaction assays. *Journal of Molecular Endocrinology* **25** (169-193).

Bustin, S. A., (2002). Quantification of mRNA using real-time reverse transcription PCR (RT-PCR): trends and problems. *Journal of Molecular Endocrinology* **29** (586).

Bustin, S. A., (2005). Real-time, fluorescence-based quantitative PCR: a snapshot of current procedures and preferences. *Expert Review of Molecular Diagnostics* **5** (493-498).

Bustin, S. A. & Mueller, R., (2005). Real-time reverse transcription PCR (qRT-PCR) and its potential use in clinical diagnosis. *Clinical Science* **109** (365-379).

Bustin, S. A., Benes, V., Nolan, T., & Pfaffl, M. W., (2005). Quantitative real-time RT-PCR - a perspective. *Journal of Molecular Endocrinology* **34** (597-601).

Bustin, S. A., Benes, V., Garson, J. A., Hellemans, J., Huggett, J., Kubista, M., Mueller, R., Nolan, T., Pfaffl, M. W., Shipley, G. L., Vandesompele, J., & Wittwer, C. T., (2009). The MIQE Guidelines: *M*inimum *I*nformation for Publication of *Q*uantitative Real-Time PCR *E*xperiments. *Clinical Chemistry* **55** (611-622).

Byon, J. Y., Ohira, T., Hirono, I., & Aoki, T., (2005). Use of a cDNA microarray to study immunity against viral hemorrhagic septicemia (VHS) in Japanese flounder (*Paralichthys olivaceus*) following DNA vaccination. *Fish & Shellfish Immunology* **18** (135-147).

Cann, A. J., (2005). *Principles in molecular virology*. 4th edition , Elsevier London, UK.

Castric, J., Baudin Laurencin, F., Bermont, M., Jeffroy, J., Le Ven, A., & Bearzotti, M., (1997). Isolation of the virus reponsible for sleeping disease in experimentally infected rainbow trout *Oncorhynchus mykiss*. *Bulletin of the European Association of Fish Pathologists* **17** (27-30).

Castro, R., Martin, S. A. M., Bird, S., Lamas, J., & Secombes, C. J., (2008). Characterisation of gamma-interferon responsive promoters in fish. *Molecular Immunology* **45** (3454-3462).

Chen, P., Wu, J., Her, G. H., & Hong, J., (2010). Aquatic birnavirus induces necrotic cell death via the mitochondria-mediated caspase pathway. *Fish & Shellfish Immunology* **28** (344-353).

Christie, K. E., Fyrand, K., Holtet, L., & Rowley, H. M., (1998). Isolation of pancreas disease virus from farmed Atlantic salmon, *Salmo salar* L., in Norway. *Journal of Fish Diseases* **21** (391-394).

Christie, K. E., Graham, D. A., McLoughlin, M. F., Villoing, S., Todd, D., & Knappskog, D., (2007). Experimental infection of Atlantic salmon *Salmo salar* pre-smolts by i.p. injection with new Irish and Norwegian salmonid alphavirus (SAV) isolates: a comparative study. *Diseases of Aquatic Organisms* **75** (13-22).

Christoper, T., Dimitri, S., Victor, D., & Choong-Chin, L., (2002). Construction of a zebrafish cDNA microarray: gene expression profiling of the zebrafish during development. *Biochemical and Biophysical Research Communications* **296** (1134-1142).

Costa, J. Z., Bron, J. E., Thompson, J. Z., Adams, A., Bricknell, I. R., & Ferguson, H. (2007) Apoptosis detection during a salmon alphavirus (SAV) *in-vivo* study. 13th International Conference of European Association of Fish Pathologists, A book of abstracts, pp76.

Cummings, C. A. & Relman, D. A., (2000). Using DNA microarrays to study host-microbe interactions. *Emerging Infectious Diseases* **6** (513-525).

Cunningham, C. O., (2002). Molecular diagnosis of fish and shellfish diseases: present status and potential use in disease control. *Aquaculture* **206** (19-55).

Dalmo, R. A., Ingebrigtsen, K., & Bogwald, J., (1997). Non-specific defense mechanisms in fish, with particular reference to the reticuloendothelial system (RES). *Journal of Fish Diseases* **20** (241-273).

Dannevig, B. H., Brudeseth, B., Gjoen, T., Rode, M., Wergeland, H. I., Evensen, O., & Press, C. M., (1997). Characterization of a long-term cell line (SHK-1) developed from the head kidney of Atlantic salmon (*Salmo sala*r L.). *Fish and Shellfish Immunology* **7** (226).

Das, B. K., Nayak, K. K., Fourrier, M., Collet, B., Snow, M., & Ellis, A. E., (2007). Expression of Mx protein in tissues of Atlantic salmon post-smolts - An immunohistochemical study. *Fish & Shellfish Immunology* **23** (1209-1217).

Das, B. K., Urquhart, K., Ellis, A. E., & Collet, B., (2008). Induction of Mx protein in Atlantic cod with poly I:C : Immunocross reactive studies of antibodies to Atlantic salmon Mx with Atlantic cod. *Fish & Shellfish Immunology* **25** (321-324).

Das, B. K., Ellis, A. E., & Collet, B., (2009). Induction and persistence of Mx protein in tissues, blood and plasma of Atlantic salmon parr, *Salmo salar*, injected with poly I:C. *Fish & Shellfish Immunology* **26** (40-48).

de Lamballerie, X., Ninove, L., & Charrel, R. N., (2009). Antiviral Treatment of Chikungunya Virus Infection. *Infectious Disorders - Drug Targets* **9** (101-104).

Desvignes, L., Quentel, C., Lamour, F., & Le Ven, A., (2002). Pathogenesis and immune response in Atlantic salmon (*Salmo salar* L.) parr experimentally infected with salmon pancreas disease virus (SPDV). *Fish & Shellfish Immunology* **12** (77-95).

DeTulleo, L. & Kirchhausen, T., (1998). The clathrin endocytic pathway in viral infection. *The EMBO Journal* **17** (4585-4593).

DeWitte-Orr, S. J., Sutton, L. P., & Bols, N. C., (2005). Preferential induction of apoptosis in the rainbow trout macrophage cell line, RTS11, by actinomycin D, cyclohexamide and double stranded RNA. *Fish & Shellfish Immunology* **18** (279-295).

Dini, L., Coppola, S., Ruzittu, M. T., & Ghibelli, L., (1996). Multiple pathways for apoptotic nuclear fragmentation. *Experimental Cell Research* **233** (340-347).

Douglas, S. E., (2006). Microarray studies of gene expression in fish. *OMICS-A Journal of Integrative Biology* **10** (474-489).

Douglas, S. E., Knickle, L. C., Kimball, J., & Reith, M. E., (2007). Comprehensive EST analysis of Atlantic halibut (*Hippoglossus hippoglossus*), a commercially relevant aquaculture species. *BMC Genomics* **8** (144.).

Ellis, A. E., (2001). Innate host defense mechanisms of fish against viruses and bacteria. *Developmental and Comparative Immunology* **25** (827-839).

Everette, H. & McFadden, G., (1999). Apoptosis: an innate immune response to virus infection. *Trends in Microbiology* **7** (160-165).

Fackler, O. T. & Grosse, R., (2008). Cell motility through plasma membrane blebbing. *Journal of Cell Biology* **181** (879-884).

FAO. (2008). *The state of the world fisheries and aquaculture*. Fisheries and Aquaculture Department, Food and Agriculture Organization of the United Nations. Rome, Italy.

Faquet, C. M., Mayo, M. A., Maniloff, J., Desselberger, U., & Ball.L.A., (2005). *Virus Taxonomy: VIII*[th] *Report of the International committee on taxonomy of viruses*. Elsevier, London , UK.

Ferguson, H. W., Rice, D. A., & Lynas, J. K., (1986a). Clinical pathology of myodegeneration (pancreas disease) in Atlantic salmon (*Salmo salar*). *Veterinary Record* **119** (297-299).

Ferguson, H. W., Roberts, R. J., Richards, R. H., Collins, R. O., & Rice, D. A., (1986b). Severe degenerative cardiomyopathy associated with pancreas disease in Atlantic salmon, *Salmo salar* L. *Journal of Fish Diseases* **9** (95-98).

Ferguson, H. W., Poppe, T., & Speare, D. J., (1990). Cardiyomayopathy in farmed Norwegian salmon. *Diseases of Aquatic Organisms* **8** (225-231).

Ferguson, H. W., Kongtorp, R. T., Taksdal, T., Graham, D., & Falk, K., (2005). An outbreak of disease resembling heart and skeletal muscle inflammation in Scottish farmed salmon, *Salmo salar* L., with observations on myocardial regeneration. *Journal of Fish Diseases* **28** (119-123).

Ferguson, H. W. (2006). *Systemic pathology of fish; a text and atlas of normal tissue in teleosts and their response in disease*. 2nd edition, Scotian press, Windsor Avenue, London.

Firth, A. E., Chung, B. Y., Fleeton, M. N. & Atkins, J. F. (2008) Discovery of frameshifting in Alphavirus 6K resolves a 20-year enigma. *Virology Journal* **5** (108)

Fischer, U., Utke, K., Somamoto, T., Kollner, B., Ototake, M., & Nakanishi, T., (2006). Cytotoxic activities of fish leucocytes. *Fish & Shellfish Immunology* **20** (209-226).

Forsell, K., Xian, L., Kozlovaska, T., Cheng, H., & Garoff, H., (2000). Membrane proteins organize a symmetrical virus. *EMBO Journal* **19** (5071-5081).

Frankfurt, O. & Krishan, A., (2001). Identification of Apoptotic Cells by Formamide-induced DNA Denaturation in Condensed Chromatin. *Journal of Histochemistry and Cytochemistry* **49** (369-378).

Fringuelli, E., Rowley, H. M., Wilson, J. C., Hunter, R., Rodger, H., & Graham, D. A., (2008). Phylogenetic analyses and molecular epidemiology of European salmonid alphaviruses (SAV) based on partial E2 and nsP3 gene nucleotide sequences. *Journal of Fish Diseases* **31** (811-823).

Fritsvold, C., Alarcon, M., Johansen, R., Rode, M., Nilsen, P., Jørgensen, J. B., Kongtorp, R. T., Breck, O., Taksdal, T., Heum, M., & Poppe, T. T., (2009) Cardiomyopathy syndrome (CMS) in Atlantic salmon (*Salmo salar* L.) challenge models and pathogenesis studies. 14th International Conference of European Association of Fish Pathologists, A book of abstracts, pp329.

Frolov, I. & Schlesinger, S., (2009). Comparison of the effect of Sindibis virus and Sindibis virus replicons on host cell protein synthesis and cytopathogenicity in BHK cells. *Journal of Virology* **68** (1721-1727).

Fronhoffs, S., Totzke, G., Stier, S., Wernert, N., Rothe, M., Bruning, T., Koch, B., Sachinidis, A., Vetter, H., & Ko, Y., (2002). A method for the rapid construction of cRNA standard curves in quantitative real-time reverse transcription polymerase chain reaction. *Molecular and Cellular Probes* **16** (99-110).

Froshauer, S., Davidson, S., Hoover-Litty, H., & Helenius, A., (1988a). The cell biology of early cytoplasmic events of alphavirus RNA replication. *Journal of Cell Biology* **107** (134).

Froshauer, S., Kartenbeck, J., & Helenius, A., (1988b). Alphavirus RNA replicase is located on the cytoplasmic surface of endosomes and lysosomes. *Journal of Cell Biology* **107** (2075-2086).

Froshauer, S., Kartenbeck, J., Stukenbrok, H., Bolzau, E., & Helenius, A., (1988c). The lysosomal membrane is the site of alphavirus replication. *Journal of Cellular Biochemistry Supplement* pp33.

Fryer, R. J. & Lannan, C. N., (1994). Three decades of fish cell culture: A current listing of cell lines derived from fish. *Journal of Tissue Culture Methods* **16** (87-94).

Gahlawat, S. K., Ellis, A. E., & Collet, B., (2009). Expression of interferon and interferon - Induced genes in Atlantic salmon *Salmo salar* cell lines SHK-1 and TO following infection with salmon alphavirus SAV. *Fish & Shellfish Immunology* **26** (672-675).

Garoff, H., Simons, K., & Renkonen, O., (1978). Assembly of the Semliki forest virus membrane glycoprotein in the membrane of the endoplasmic reticulum. *Journal of Molecular Biology* **124** (587-600).

Garoff, H., Wilschut, J., Liljestrom, P., Wahlberg, J. M., Bron, R., Suomalainen, M., Smyth, J., Salminen, A., Barth, B. U., & Zhao, H., (1994). Assembly and entry mechanisms of Semliki Forest virus. *Archives of Virology Supplement* **9** (329-338).

Garoff, H., Sjoberg, M., & Cheng, R. H., (2004). Budding of alphaviruses. *Virus Research* **106** (103-116).

Gilsbach, R., Kouta, M., Bönisch, H., & Brüss, M., (2006). Comparison of *in vitro* and *in vivo* reence genes for internal standardization of real time PCR data. *BioTechniques* **40** (173-177).

Glasgow, G. M., Mcgee, M. M., Tarbatt, C. J., Mooney, D. A., Sheahan, B. J., & Atkins, G. J., (1998). The Semliki Forest virus vector induces p53-independent apoptosis. *Journal of General Virology* **79** (2405-2410).

Goetz, F. W. & MacKenzie, S., (2008). Functional genomics with microarrays in fish biology and fisheries. *Fish and Fisheries* **9** (378-395).

Govoroun, M., Le Gac, F., & Guiguen, Y., (2006). Generation of a large scale repertoire of Expressed Sequence Tags (ESTs) from normalised rainbow trout cDNA libraries. *BMC Genomics* **7** (196).

Gozlan, R. E., Peeler, E. J., Longshaw, M., St-Hilaire, S., & Feisr, S. W., (2006). Effect of microbial pathogens on the diversity of aquatic populations, notably in Europe. *Microbes and Infection* **8** (1358-1364).

Gracey, A. Y. & Cossins, A. R., (2003). Application of microarray technology in environmental and comparative physiology. *Annual Review of Physiology* **65** (231-259).

Graham, D. A., Jewhurst, V. A., Rowley, H. M., McLoughlin, M. F., & Todd, D., (2003a). A rapid immunoperoxidase-based virus neutralization assay for salmonid alphavirus used for a serological survey in Northern Ireland. *Journal of Fish Diseases* **26** (407-413).

Graham, D. A., Rowley, H. M., Walker, I. W., Weston, J. H., Branson, E. J., & Todd, D., (2003b). First isolation of sleeping disease virus from rainbow trout, *Oncorhynchus mykiss* (Walbaum), in the United Kingdom. *Journal of Fish Diseases* **26** (691-694).

Graham, D. A., Jewhurst, V. A., Rowley, H. M., McLoughlin, M. F., Rodger, H., & Todd, D., (2005). Longitudinal serological surveys of Atlantic salmon, *Salmo salar* L., using a rapid immunoperoxidase-based neutralization assay for salmonid alphavirus. *Journal of Fish Diseases* **28** (373-379).

Graham, D. A., Jewhurst, H., McLoughlin, M. F., Sourd, P., Rowley, H. M., Taylor, C., & Todd, D., (2006a). Sub-clinical infection of farmed Atlantic salmon *Salmo salar* with salmonid alphavirus - a prospective longitudinal study. *Diseases of Aquatic Organisms* **72** (193-199).

Graham, D. A., Taylor, C., Rodgers, D., Weston, J., Khalili, M., Ball, N., Christie, K. E., & Todd, D., (2006b). Development and evaluation of a one-step real-time reverse transcription polymerase chain reaction assay for the detection of salmonid alphaviruses in serum and tissues. *Diseases of Aquatic Organisms* **70** (47-54).

Graham, D. A., Jewhurst, H. L., McLoughlin, M. F., Branson, E. J., McKenzie, K., Rowley, H. M., & Todd, D., (2007a). Serological, virological and histopathological study of an outbreak of sleeping disease in farmed rainbow trout *Oncorhynchus mykiss*. *Diseases of Aquatic Organisms* **74** (191-197).

Graham, D. A., Rowley, H. M., Fringuelli, E., Bovo, G., Manfrin, A., McLoughlin, M. F., Zarza, C., Khalili, M., & Todd, D., (2007b). First laboratory confirmation of salmonid alphavirus infection in Italy and Spain. *Journal of Fish Diseases* **30** (569-572).

Graham, D. A., Wilson, C., Jewhurst, H., & Rowley, H., (2008). Cultural characteristics of salmonid alphaviruses - influence of cell line and temperature. *Journal of Fish Diseases* **31** (859-868).

Graham, D. A., Fringuelli, E., Rowley, H., Brown, A. G., & Cockerill, D., (2009). Sequence analysis of SAV strains in Scottish Atlantic salmon marine production. 14th International Conference of European Association of Fish Pathologists, A book of abstracts, pp198.

Graham, D., Fringuelli, E., Wilson, C., Rowley, H., Brown, A. G., Rodger, H., McLoughlin, M., McManus, C., Casey, E., McCathy, L. J., & Ruane, N. M., (2010). Prospective longitudinal studies of salmonid alphavirus infections on two Atlantic salmon farms in Ireland; evidence for viral persistence. *Journal of Fish Diseases* **33** (123-135).

Graham, S. & Secombes, C. J., (1988). The production of a macrophage-activating factor from rainbow trout *Salmo gairdneri* leukocytes. *Immunology* **65** (293-297).

Grant, A. N., Brown, A. G., & Laidler, L. A., (1994). Plasma lipase concentration as an aid to the early detection of pancreas disease in farmed Atlantic Salmon (*Salmo salar*). *Veterinary Record* **135** (107-108).

Granzow, H., Weiland, F., Fichtner, D., & Enzmann. P.J., (1995). Studies of the ultrastructure and morphogenesis of fish pathogenic viruses grown in cell culture. *Journal of Fish Diseases* **20** (1-10).

Griffin, D. E., (2005). Neuronal cell death in alphavirus encephalomyelitis. *Role of Apoptosis in Infection* **289** (57-77).

Griffin, D. E., Levine, B., Ubol, S., & Hardwick, J. M., (1994). The Effects of Alphavirus Infection on Neurons. *Annals of Neurology* **35** (S23-S27).

Griffin, D. E. & Hardwick, J. M., (1997). Regulators of apoptosis on the road to persistent alphavirus infection. *Annual Review of Microbiology* **51** (565-592).

Griffin, D. E. & Hardwick, J. M., (1998). Apoptosis in alphavirus encephalitis. *Seminars in Virology* **8** (481-489).

Grimholt, U., Drablos, F., Jorgensen, S. M., Hoyheim, B., & Stet, R. J. M., (2002). The major histocompatibility class I locus in Atlantic salmon *(Salmo salar* L.): polymorphism, linkage analysis and protein modelling. *Immunogenetics* **54** (570-581).

Grimley, P. M., Berezesky, I. K., & Friedman, R. M., (1968). Cytoplasmic structures associated with an arbovirus infection:Loci of viral ribonucleic acid synthesis. *Journal of Virology* **2** (326-338).

Groff, H., Hewson, R., & Opstelten, D., (1998). Virus maturation by budding. *Microbiology and Molecular Biology Reviews* **62** (1171-1190).

Haller, O., Stertz, S., & Kochs, G., (2007a). The Mx GTPase family of interferon-induced antiviral proteins. *Microbes and Infection* **9** (1636-1643).

Haller, O., Staeheli P., & Kochs, G., (2007b). Interferon-induced Mx proteins in antiviral host defense. *Biochimie* **89** (812-818).

Hardwick, J. M., (2001). Apoptosis in viral pathogenesis. *Cell Death and Differentiation* **8** (109-110).

Hay, S. & Kannourakis, G., (2002). A time to kill: viral manipulation of the cell death program. *Journal of General Virology* **83** (1547-1564).

Helenius, A., (1995). Alphavirus and flavivirus glycoproteins - structures and functions. *Cell* **81** (651-653).

Helenius, A., Kartenbeck, J., Simons, K., & Fries, E., (1980). On the entry of Simliki forest virus into BHK-1 cells. *Journal of Cell Biology* **84** (404-420).

Helenius, A., Kielian, M., Wellsteed, J., Mellman, I., & Rudnick, G., (1985). Effects of monovalent cations on Semiliki forest virus entry into BHK-21 cells. *The Journal of Biological Chemistry* **260** (5691-5697).

Helenius, A., Kielian, M., Mellman, I., & Schmid, S., (1988). *In* Entry of enveloped viruses into their host cells. in.*Helenius A. R. W. andOldstone M. B. A., ed. Symposia on Molecular and Cellular Biology New Series University of California-Los Angele, .Cell Biology of Virus Entry, Replication, and Pathogenesis;* Taos, New Mexico, USA (pp145-162).

Herath, T., Costa, J., Thompson, K., Adams, A., & Richards, R., (2009). Alternative cell lines for the isolation of salmonid alphavirus-1. *Icelandic Agricultural Sciences* **22** (19-27).

Hierholzer, J., Killngton, R. A., & Stockes, A., (1996). *Virus Isolation and quantification*. Academic Press Limited, London, UK.

Hodneland, K., Bratland, A., Christie, K. E., Endresen, C., & Nylund, A., (2005). New subtype of salmonid alphavirus (SAV), Togaviridae, from Atlantic salmon *Salmo salar* and rainbow trout *Oncorhynchus mykiss* in Norway. *Diseases of Aquatic Organisms* **66** (113-120).

Hodneland, K. & Endresen, C., (2006). Sensitive and specific detection of Salmonid alphavirus using real-time PCR (TaqMan®). *Journal of Virological Methods* **131** (184-192).

Hogstad, I. M., (1993). Diseases in Atlantic salmon during the first six months in sea water: field observations 1985-1992. *Norsk Veterinaertidsskrift* **105** (1199-1205).

Hong, J., Lin, T., Hus, Y., & Wu, J., (1998). Apoptosis precedes necrosis of fish cell lines with infectious pancreatic necrosis virus infection. *Virology* **250** (76-84).

Hong, E. M., Perera, R., & Kuhn, R., (2006). Alphavirus capsid protein helix I controls a checkpoint in nucleocapsid core assembly. *Journal of Virology* **80** (8848-8855).

Houghton, G., (1994). Acquired protection in Atlantic salmon *Salmo salar* parr and post-smolts against pancreas disease. *Diseases of Aquatic Organisms* **18** (109-118).

Houghton, G., (1995). Kinetics of infection of plasma, blood leukocytes and lymphoid-tissue from Atlantic salmon *Salmo salar* experimentally infected with pancreas disease 84. *Diseases of Aquatic Organisms* **22** (193-198).

Houghton, G. & Ellis, A. E., (1996). Pancreas disease in Atlantic salmon: serum neutralisation and passive immunisation. *Fish & Shellfish Immunology* **6** (465-472).

Huggett, J., Dheda, K., Bustin, S. A., & Zumala., (2005). Real-time RT-PCR normalization: statergies and consideration. *Genes and Immunity* 1-6).

Jensen, I. & Robertsen, B., (2000). The effect of interferon and Mx protein on infection of Atlantic salmon cells by infectious salmon anaemia virus (ISAV). *Developmental and Comparative Immunology* **24** (S3-S4).

Jensen, I., Albuqueque, A., Sommer, A. I., & Robertsen, B., (2002). Effect of poly I:C on the expression of Mx proteins and resistance against infection by infectious salmon anaemia virus in Atlantic salmon. *Fish & Shellfish Immunology* **13** (311-326).

Jensen, I. & Robertsen, B., (2002). Effect of double-stranded RNA and interferon on the antiviral activity of Atlantic salmon cells against infectious salmon anemia virus and infectious pancreatic necrosis virus. *Fish & Shellfish Immunology* **13** (221-241).

Jewhurst, V. A., Todd, D., Rowley, H. M., Walker, I. W., Weston, J. H., McLoughlin, M. F., & Graham, D. A., (2004). Detection and antigenic characterization of salmonid alphavirus isolates from sera obtained from farmed Atlantic salmon, *Salmo salar* L., and farmed rainbow trout, *Oncorhynchus mykiss* Walbaum. *Journal of Fish Diseases* **27** (143-149).

Johnston, C., Jiang, W. X., Chu, T., & Levine, B., (2001). Identification of genes involved in the host response to neurovirulent alphavirus infection. *Journal of Virology* **75** (10431-10445).

Jorgensen, S. M., Lyng-Syvertsen, B., Lukacs, M., Grimholt, U., & Gjoen, T., (2006). Expression of MHC class I pathway genes in response to infectious salmon anaemia virus in Atlantic salmon (*Salmo salar* L.) cells. *Fish & Shellfish Immunology* **21** (548-560).

Jorgensen, S. M., Hetland, D. L., Press, C. M., Grimholt, U., & Gjoen, T., (2007). Effect of early infectious salmon anaemia virus (ISAV) infection on expression of MHC pathway genes and type I and II interferon in Atlantic salmon (*Salmo salar* L.) tissues. *Fish & Shellfish Immunology* **23** (576-588).

Jorgensen, S. M., Afanasyev, S., & Krasnov, A., (2008). Gene expression analyses in Atlantic salmon challenged with infectious salmon anemia virus reveal differences between individuals with early, intermediate and late mortality. *BMC Genomics* **9** (179).

Joseph, T., Cepica, A., Brown, L., Ikede, B., & Kibenge, F. S. B., (2004). Mechanism of cell death during infectious salmon anemia virus infection is cell type-specific. *Journal of General Virology* **85** (3027-3036).

Jung, K. & Chae, C., (2006). Expression of Mx protein and interferon-alpha in pigs experimentally infected with swine influenza virus. *Veterinary Pathology* **43** (161-167).

Kaattari, S. L., (1994). Development of a piscine paradigm of immunological memory. *Fish & Shellfish Immunology* **4** (447-457).

Karlsen, M., Hodneland, K., Endresen, C., & Nylund, A., (2006). Genetic stability within the Norwegian subtype of salmonid alphavirus (family *Togaviridae*). *Archives of Virology* **151** (861-874).

Karlsen, M., Villoing, S., Rimstad, E., & Nylund, A., (2009). Characterization of untranslated region of the salmonid alphavirus 3 (SAV3) genome and construction of a SAV3 based replicon. *Virology Journal* **6** (173).

Kent, M. L. & Elston, R. A., (1987). Pancreas disease in pen-reared Atlantic salmon in North America. *Bulletin of the European Association of Fish Pathologists* **7** (29-31).

Kibenge, F. S. B., Whyte, S. K., Hammell, K. L., Rainnie, D., Kibenge, M. T., & Martin, C. K., (2000). A dual infection of infectious salmon anaemia (ISA) virus and a togavirus-like virus in ISA of Atlantic salmon *Salmo salar* in New Brunswick, Canada *Diseases of Aquatic Organisms* **42** (11-15).

Kileng, O., Brundtland, M. I., & Robertsen, B., (2007). Infectious salmon anemia virus is a powerful inducer of key genes of the type I interferon system of Atlantic salmon, but is not inhibited by interferon. *Fish & Shellfish Immunology* **23** (378-389).

Kim, K. H., Rumenapf, T., Strauss, E. G., & Strauss, J. H., (2004). Regulation of Semliki Forest virus RNA replication: a model for the control of alphavirus pathogenesis in invertebrate hosts. *Virology* **323** (153-163).

Kjoglum, S., Larsen, S., Bakke, H. G., & Grimholt, U., (2006). How specific MHC class I and class II combinations affect disease resistance against infectious salmon anaemia in Atlantic salmon (*Salmo salar*). *Fish & Shellfish Immunology* **21** (431-441).

Klimstra, W. B. & Ryman, K. D., (2009).Togaviruses, in Brasier, A. R., García-Sastre, A., and Lemon, S. M. (ed) Cellular signaling and innate immune responses to RNA virus infection. A.M.S press, Washington D.C. USA (353-372).

Kongtorp, R. T., Kjerstad, A., Taksdal, T., Guttvik, A., & Falk, K., (2004a). Heart and skeletal muscle inflammation in Atlantic salmon, *Salmo salar* L.: A new infectious disease. *Journal of Fish Diseases* **27** (351-358).

Kongtorp, R. T., Taksdal, T., & Lyngoy, A., (2004b). Pathology of heart and skeletal muscle inflammation (HSMI) in farmed Atlantic salmon *Salmo salar*. *Diseases of Aquatic Organisms* **59** (217-224).

Kongtorp, R. T. & Taksdal, T., (2009). Studies with experimental transmission of heart and skeletal muscle inflammation in Atlantic salmon, *Salmo salar* L. *Journal of Fish Diseases* **32** (253-262).

Korth, M. J. & Katze, M. G., (2002). Unlocking the mysteries of virus-host interactions - Does functional genomics hold the key? *Immune Responses and Vaccines* **975** (160-168).

Krasnov, A., Koskinen, H., Afanasyev, S., & Molsa, H., (2005). Transcribed Tcl-like transposons in salmonid fish. *BMC Genomics* **6** (107).

Kujala, P., Ikaheimonen, A., Ehsani, N., Vihinen, H., Auvinen, P., & Kaariainen, L., (2001). Biogenesis of the Semliki Forest virus RNA replication complex. *Journal of Virology* **75** (3873-3884).

Landis, H., Simon-Jodicke, A., Kloti, A., Di Paolo, C., Schnorr, J., Schneider-Schaulies, S., Hefti, P., & Pavlovic, J., (1998). Human MxA protein confers resistance to Simliki forest virus and inhibits the amplification of a Simliki forest virus-based replication in the absence of viral structural protein. *Journal of Virology* **72** (1516-1522).

Lannan, C. N., Winton, J. R., & Fryer, R. J., (1984). Fish cell lines: establishment and characterization of nine cell lines from salmonids. *In Vitro* **20** (671).

Lee J. & Burckart, G. J., (1998). Nuclear factor kappa B: important transcription factor and theraputic target. *Theraputic Review* **38** (993).

Lee, S. & Vidal, S. M., (2002). Funtional diversity of Mx proteins: variations on a theme of host resistance to infection. *Genome Research* (527-530).

Leong, J. C., Torbridge, G. D., Kim, C. H., Johnson, M., & Simon, B., (1998). Interferon-inducible Mx proteins in fish. *Immunological Reviews* **166** (346-363).

Levin, B., Hardwick, JM., Trapp, B. D., Crawford, T., Bollinger, R. C., & Griffin, D. E., (1991). Antibody-mediated clearance of alphavirus infection from neurons. *Science* **254** (856-860).

Linn, M. L., Gardner, J., Warrilow, D., Darnell, G. A., McMahon, C. R., Field, I., Hyatt, A. D., Slade, R. W., & Suhrbier, A., (2001). Arbovirus of marine mammals: a new alphavirus isolated from the elephant seal louse, *Lepidophthirus macrorhini*. *Journal of Virology* **75** (4103-4109).

Linn, M. L., Eble, J. A., Lubken, C., Slade, R. W., Heino, J., Davies, J., & Suhrbier, A., (2005). An arthritogenic alphavirus uses the α1β1 integrin collagen receptor. *Virology* **336** (229-239).

Liu, Y. & Sumalia, U. R., (2007). Can farmed salmon production keep growing? *Marine Policy* **32** (497-501).

Liu, Z., Li, R. W., & Waldbieser, G. C., (2008). Utilization of microarray technology for functional genomics in ictalurid catfish. *Journal of Fish Biology* **72** (2377-2390).

Lundstrom, K., (2009). Alpha virus gene therapy. *Viruses* **1** (25).

Mackay, I. M., Arden, K. E., & Nitsche, A., (2002). Real-time PCR in virology. *Nucleic Acids Research* **30** (1292-1305).

MacKenzie, S., Bardolet, T. L., & Balasch, J. C. (2004). Fish health challenge after stress. Indicators of immunocompetence. *Contributions to Science* **2** (443-454).

MacKenzie, S., Stertz, S., Reichelt, M., Krijnse-Locker, J., MacKenzie, J. C., Simpson, O., Haller, O., & Kochs, G., (2006). Interferon-induced, antiviral human MxA protein localizes to a distinct sub-compartment of the smooth endoplasmic reticulum. *Journal of Interferon and Cytokine Research* **25** (650-660).

Magliano, D., Marshall, J. A., Bowden, D. S., Vardaxis, N., Meanger, J., & Lee, J. Y., (1998). Rubella virus replication complexes are virus-modified lysosomes. *Virology* **240** (57-63).

Magnadóttir, B., (2006). Innate immunity of fish. *Fish & Shellfish Immunology* **20** (137-151).

Marsh, M., Griffiths, G., Dean, G., Mellman, I., & Helenius, A., (1986). Three-dimensional structure of endosomes in BHK-21 cells. *Cell Biology* **83** (2899-2903).

Martin, S. A. M., Blaney, S. C., Houlihan, D. F., & Secombes, C. J., (2006). Transcriptome response following administration of a live bacterial vaccine in Atlantic salmon (*Salmo salar*). *Molecular Immunology* **43** (1900-1911).

Martin, S. A. M., Taggart, J. B., Seear, P., Bron, J. E., Talbot, R., Teale, A. J., Sweeney, G. E., Hoyheim, B., Houlihan, D. F., Tocher, D. R., Zou, J., & Secombes, C. J., (2007). Interferon type I and type II responses in an Atlantic salmon (*Salmo salar*) SHK-1 cell line by the salmon TRAITS/SGP microarray. *Physiological Genomics* **32** (33-44).

Martin, S. A. M., Collet, B., MacKenzie, S., Evensen, O., & Secombes, C. J., (2008). Genomic tools for examining immune gene function in salmonid fish. *Reviews in Fisheries Science* **16** (112-118).

McBeath A. J. A., Snow, M., Secombes, C. J., Ellis, A. T., & Collet, B., (2007). Expression kinetics of interferon and interferon-induced genes in Atlantic salmon (*Salmo salar*) following infection with infectious pancreatic necrosis virus and infectious salmon anaemia virus. *Fish & Shellfish Immunology* **22** (241-247).

McLauchlan, P. E., Collet, B., Ingerslev, E., Secombes, C., Lorenzen, N., & Ellis, A. E., (2003). DNA vaccination against viral haemorrhagic septicaemia (VHS) in rainbow trout: size, dose, route of injection and duration of protection-early protection correlates with Mx expression. *Fish & Shellfish Immunology* **15** (39-50).

McLoughlin, M., Nelson, R., McCormick, J., I, & Rowley, H., (1995). Pathology of experimental pancreas disease in freshwater Atlantic salmon parr. *Journal of Aquatic Animal Health* **7** (104-110).

McLoughlin, M. F., Nelson, R. T., Rowley, H. M., Cox, D. I., & Grant, A. N., (1996). Experimental pancreas disease in Atlantic salmon *Salmo sala*r post-smolts induced by salmon pancreas disease virus (SPDV). *Diseases of Aquatic Organisms* **26** (117-124).

McLoughlin, M. F., Nelson, R. T., Rowley, H. M., Cox, D. I., & Grant, A. N., (1997). The development of an experimental model of pancreas disease in Atlantic salmon (*Salmo salar*) post-smolts. *Fish Vaccinology* **90** (467).

McLoughlin, M. F., Rowley, H. M., & Doherty, C. E., (1998). A serological survey of salmon pancreas disease virus (SPDV) antibodies in farmed Atlantic salmon, *Salmo salar* L. *Journal of Fish Diseases* **21** (305-307).

McLoughlin, M., Nelson, R., McCormick, J., I, Rowley, H., & Bryson, D. G., (2002). Clinical and histopathological features of naturally occurring pancreas diseases in farmed Atlantic salmon (*Salmo salar* L). *Journal of Fish Diseases* **25** (33-43).

McLoughlin, M., Graham, D. A., Norris, A., Matthews, D., Foyle, L., Rowley, H., Jewhurst, H., MacPhee, J., & Todd, D., (2006). Virological, serological and histopathological evaluation of fish strain susceptibility to experimental infection with salmonid alphavirus. *Diseases of Aquatic Organisms* **72** (125-133).

McLoughlin, M. F. & Graham, D. A., (2007). Alphavirus infections in salmonids - a review. *Journal of Fish Diseases* **30** (511-531).

McVicar, A. H., (1987). Pancreas disease of farmed Atlantic salmon, *Salmo salar*, in Scotland - epidemiology and early pathology. *Aquaculture* **67** (71-78).

McVicar, A. H., (1990). Infection as a primary cause of pancrease disease in farmed Atlantic salmon. *European Association of Fish Pathologists* **10** (84-87).

Medigeshi, G. R., Hirsch, A. J., Streblow, D. N., Nikolich-Zugich, J., & Nelson, J. A., (2008). West nile virus entry requires cholesterol-rich membrane microdomains and is independent of alpha v beta 3 integrin. *Journal of Virology* **82** (5212-5219).

Miller K.M. & Maclean., (2008). Teleost microarrays: development in a broad phylogenetic range reflecting diverse application. *Journal of Fish Biology* **72** (2039-2050).

Miller, K., Traxler, G., Kaukinen, K., Li, S., Richard, J., & Ginther, N., (2007). Salmonid host response to infectious hematopoietic necrosis (IHN) virus: cellular receptors, viral control, and novel pathways of defense. *Aquaculture* **272** (S217-S237).

Miwa, S. & Sanao, M., (2007). Morphogensis of koi herpesvirus observed by electron microscopy. *Journal of Fish Diseases* **30** (715-722).

Moody, C. E., Serreze, D. V., & Reno, P. W., (1985). Non-specific cytotoxic activity of teleost leukocytes. *Developmental and Comparative Immunology* **9** (51-64).

Morgan, V. W., Howe, C., & Rose, H., (1960). Structure and development of viruses as observed in the electron microscope. *The journal of experimental medicine* **113** (234).

Moriette, C., LeBerre, M., Lamoureux, A., Lai, T. L., & Bremont, M., (2006). Recovery of a recombinant Salmonid alphavirus fully attenuated and protective for rainbow trout. *Journal of Virology* **80** (4088-4098).

Mukhopadhyay, S., Kuhn, R. J., & Rossmann, M. G., (2005). A structural perspective of the Flavivirus life cycle. *Nature Reviews Microbiology* **3** (13-22).

Mukhopadhyay, S., Chipman, P. R., Eunmee, M., Kuhn, R., & Rossmann, G., (2010). In vitro assembled alphavirus core-like particles maintain a structure similar to that of nucleocapsid cores in mature virus. *Journal of Virology* **76** (11128-11132).

Munir, K. & Kibenge, F. S. B., (2004). Detection of infectious salmon anaemia virus by real-time RT-PCR. *Journal of Virological Methods* **117** (37-47).

Munro, A. L. S., Ellis, A. E., Mcvicar, A. H., Mclay, H. A., & Needham, E. A., (1984). An exocrine pancreas disease of farmed Atlantic salmon in Scotland. *Helgolander Meeresuntersuchungen* **37** (571-586).

Murphy, T. M., Rodger, H. D., Drinan, E. M., Gannon, F., Kruse, P., & Korting, W., (1992). The sequential pathology of pancreas disease in Atlantic salmon farms in Ireland. *Journal of Fish Diseases* **15** (401-408).

Murphy, T., Drinan, E., & Gannon, F., (1995). Studies with an experimental model for pancreas disease of Atlantic salmon *Salmo salar* L. *Aquaculture Research* **26** (861-864).

Murray, A. & Peeler, E. J., (2004). A framework for understanding the potential for emerging diseases in aquaculture. *Preventive Veterinary Medicine* **67** (223-235).

Murray, A. & Kilburn, R., (2009). Update on pancreas disease in Scotland. *Presented at 9th Tri-Nation Pancreas Disease Seminar, University of Stirling, UK*.

Müller, B. D. J., Fackler, O. T., Dittmat, M. T., Zenrgraf, H., & Kräusslich, H., (2004). Construction and characterization of a fluorescently labeled infectious human immunodeficiency virus type 1 derivative. *Journal of Virology* **78** (10803-10813).

Nelson, R. T., McLoughlin, M. F., Rowley, H. M., Platten, M. A., & Mccormick, J. I., (1995). Isolation of a Toga-like virus from farmed Atlantic salmon *Salmo salar* with pancreas disease. *Diseases of Aquatic Organisms* **22** (25-32).

Ng, S. H. S., Artieri, C. G., Bosdet, I. E., Chiu, R., Danzmann, R. G., Davidson, W. S., Ferguson, M. M., Fjell, C. D., Hoyheim, B., Jones, S. J. M., de Jong, P. J., Koop, B. F., Krzywinski, M. I., Lubieniecki, K., Marra, M. A., Mitchell, L. A., Mathewson, C., Osoegawa, K., Parisotto, S. E., Phillips, R. B., Rise, M. L., von Schalburg, K. R.,

Schein, J. E., Shin, H. S., Siddiqui, A., Thorsen, J., Wye, N., Yang, G., & Zhu, B. L., (2005). A physical map of the genome of Atlantic salmon, *Salmo salar*. *Genomics* **86** (396-404)

Ng, C. G., Coppens, I., Govindarajan, D., Pisciotta, J., Shulaev, V., & Griffin, D. E., (2008). Effect of host cell lipid metabolism on alphavirus replication, virion morphogenesis, and infectivity. *Proceedings of the National Academy of Sciences of the USA* **105** (16326-16331).

.

Nicola, A. V., Chen, W., & Helenius, A., (1999). Co-translational folding of an alphavirus capsid protein in the cytosol of living cells. *Nature Cell Biology* **1** (341-345).

Niesters, H. G. M., (2001). Quantification of viral load using real-time amplification techniques. *Methods* **25** (419-429).

Novoa, R. R., Calderita, G., Arranz, R., Fontana, J., Granzow, H., & Risco, C., (2005). Virus factories: association of cell organelles for viral replication and morphogenesis. *Biology of Cell* **97** (147-172).

O'Brien., (1998). Viruses and apoptosis. *Journal of General Virology* **79** (1833-1845).

Pavlidis, P., (2003). Using ANOVA for gene selection from microarray studies of the nervous system. *Methods* **31** (282-289).

Peranen, J. & Kaariainen, L., (1991). Biogenesis of type I cytopathic vacuoles in Semliki forest virus-infected BHK cells. *Journal of Virology* **65** (1623-1627).

Perera, R., Khaliq, M., & Kuhn, R. J., (2008). Closing the door on flaviviruses: entry as a target for antiviral drug design. *Antiviral Research* **80** (11-22).

Petterson, E., Sandberg, M., & Santi, N., (2009). Salmonid alphavirus associated with *Lepeophtheirus salmonis* (Copepoda: Caligidae) from Atlantic salmon, *Salmo salar* L. *Journal of Fish Diseases* **32** (477-479).

Pfaffl, M. W., (2001). A new mathematical model for relative quantification in real-time RT-PCR. *Nucleic Acids Research* **29** (e45).

Pfaffl, M. W., (2006). Relative quantification, in Dorak, T. (ed) Real Time PCR, *BIOS Advanced Methods*. pp63-82.

Pfaffl, M. W. & Hageleit, M., (2001). Validities of mRNA quantification using recombinant RNA and recombinant DNA external calibration curves in real-time RT-PCR. *Biotechnology Letters* **23** (275-282).

Pfaffl, M. W., Horgan, G. W., & Dempfle, L., (2002). Relative expression software tool (REST[©]) for group-wise comparison and statistical analysis of relative expression results in real-time PCR. *Nucleic Acids Research* **30** (e36).

Pfaffl, M. W., Tichopad, A., Prgomet, C., & Neuvians, T. P., (2004). Determination of stable housekeeping genes, differentially regulated target genes and sample integrity:

BestKeeper - Excel-based tool using pair-wise correlations. *Biotechnology Letters* **26** (509-515).

Philstrom, L. & Bengten, E., (1996). Immunoglobulin in fish-genes, expression and structure. *Fish & Shellfish Immunology* **6** (243-262).

Pläsier, B., Lloyd, D. R., Paul, G. C., THomas, C. R., & Al-Rubeai, M., (1999). Automatic image analysis for quantification of apoptosis in animal cell culture by annexine-V affinity assay. *Journal of Immunological Methods* **229** (81-95).

Plouffe, D. A., Hanington, P. C., Walsh, J. G., Wilson, E. C., & Belosevic, M., (2005). Comparison of select innate immune mechanisms of fish and mammals. *Xenotransplantation* **12** (266-277).

Pohjala, L., Barni, V., Azhayev, A., Lapinjoki, S., & Ahola, T., (2008). A luciferase-based screening method for inhibitors of alphavirus replication applied to nucleoside analog. *Antiviral Research* **78** (215-222).

Poppe, T., Rimstad, E., & Hyllseth, B., (1989). Pancreas disease of Atlantic salmon (*salmo salar* L.) post-smolt infected with infectious pancreatic necrosis virus (IPNV). *Bulletin of the European Association of Fish Pathologists* **9** (83).

Powers, A. M., Brault, A. C., Shirako, Y., Strauss, E. G., Kang, W. L., Strauss, J. H., & Weaver, S. C., (2001). Evolutionary relationships and systematics of the alphaviruses. *Journal of Virology* **75** (10118-10131).

Preiser, W., Elzinger, B., & Brink, N. C., (2000). Quantitative molecular virology in patient management. *Journal of Clinical Pathology* **53** (83).

Press, C. M. & Evensen, Ø., (1999). The morphology of immune system in teleost fish. *Fish & Shellfish Immunology* **9** (309-318).

Pringle, G. M., Houlihan, D. F., Callanan, K. R., Mitchell, A. I., Raynard, R. S., & Houghton, G. H., (1992). Digestive enzyme levels and histopathology of pancreas disease in farmed Atlantic salmon (*Salmo salar*). *Comparative Biochemistry and Physiology A-Physiology* **102** (759-768).

Purcell, M. K., Smith, K. D., Hood, L., Winton, J., & Roach, J. C., (2006). Conservation of Toll-like receptor signaling pathways in teleost fish. *Comparative Biochemistry and Physiology part D Genomics proteomics* **1** (77-88).

Purcell, M. K., Laing, K. J., Woodson, J. C., Thorgassrd, G. H., & Hansen, J. D., (2009). Characterization of the interferon genes in homozygous rainbow trout reveals two novel genes, alternate splicing and differential regulation of duplicated genes. *Fish & Shellfish Immunology* **26** (293-304).

Qi, R., Zang, L., & Chi, C., (2008). Biological characteristics of dengue virus and potential targets for drug design. *Acta Biochimica Biophysica Sinica* **40** (91-101).

Randelli, E., Buonocore, F., & Scapigliati, G., (2008). Cell markers and determinants in fish immunology. *Fish & Shellfish Immunology* **25** (326-340).

Raymen, K. D. & Klimstra, W. B., (2008). Host response to alphavirus infection. *Immunological Reviews* **225** (27-45).

Raynard, R. S., Mcvicar, A. H., Bell, J. G., Youngson, A., Knox, D., & Fraser, C. O., (1991). Nutritional aspects of pancreas disease of Atlantic salmon - the effects of dietary Vitamin-E and polyunsaturated fatty-Acids. *Comparative Biochemistry and Physiology A-Physiology* **98** (125-131).

Raynard, R. S. & Houghton, G., (1993). Development towards an experimental protocol for the transmission of pancreas disease of Atlantic salmon *Salmo salar*. *Diseases of Aquatic Organisms* **15** (123-128).

Reite, O. B. & Evensen, Ø., (2006). Inflammatory cells of teleostean fish: A review focusing on mast cells/eosinophilic granule cells and rodlet cells. *Fish & Shellfish Immunology* **20** (192-208).

Riezebos-Brilman, A., Mare, A., Bungener, L., Huckriede, A., Wilschut, J., & Daemen, T., (2005). Recombinant alphaviruses as vectors for anti-tumour and anti-microbial immunotherapy. *Journal of Clinical Virology* **35** (233-243).

Rise, M. L., Jones, S. R. M., Brown, G. D., von Schalburg, K. R., Davidson, W. S., & Koop, B. F., (2004). Microarray analyses identify molecular biomarkers of Atlantic salmon macrophage and hematopoietic kidney response to *Piscirickettsia salmonis* infection. *Physiological Genomics* **20** (21-35).

Rise, M. L., von Schalburg, K. R., Brown, G. D., Mawer, M. A., Devlin, R. H., Kuipers, N., Busby, M., Beetz-Sargent, M., Alberto, R., Gibbs, A. R., Hunt, P., Shukin, R., Zeznik, J. A., Nelson, C., Jones, S. R. M., Smailus, D. E., Jones, S. J. M., Schein, J. E., Marra, M. A., Butterfield, Y. S. N., Stott, J. M., Ng, S. H. S., Davidson, W. S., & Koop, B. F., (2006). Development and application of a salmonid EST database and cDNA microarray: Data mining and interspecific hybridization characteristics. *Genome research* **14** (478-490).

Roberts, R. J., (2003). *Fish Pathology*. 3rd edition , WB. Saunders, USA.

Roberts, R. J. & Pearson, M. D., (2005). Infectious pancreatic necrosis in Atlantic salmon, *Salmo salar* L. *Journal of Fish Diseases* **28** (383-390).

Robertsen, B., (2006). The interferon system of teleost fish. *Fish & Shellfish Immunology* **20** (172-191).

Robertsen, B., (2008). Expression of interferon and interferon-induced genes in salmonids in response to virus infection, interferon-inducing compounds and vaccination. *Fish & Shellfish Immunology* **25** (351-357).

Robertsen, B., Bergan, V., Rokenes, T., Larsen, R., & Albuquerque, A., (2003). Atlantic salmon interferon genes: Cloning, sequence analysis, expression, and biological activity 161. *Journal of Interferon and Cytokine Research* **23** (601-612).

Rodger, H. D., (1991). Summer lesion syndrome in salmon - A retrospective study. *Veterinary Record* **129** (237-239).

Rodger, H. D., Murphy, T. M., Drinan, E. M., & Rice, D. A., (1991). Acute skeletal myopathy in farmed Atlantic salmon *Salmo Salar*. *Diseases of Aquatic Organisms* **12** (17-23).

Rodger, H. D., Turnbull, T., & Richards, R. H., (1994). Myopathy and pancreas disease in salmon - A retrospective study in Scotland. *Veterinary Record* **135** (234-235).

Rodger, H. D., Murphy, K., Drinan, E. M., & Kennedy, G., (1995). Apparent lack of response of salmon affected by pancreas disease to pancreatic-enzyme replacement therapy. *Veterinary Record* **136** (489-491).

Rodger, H. & Turnbull, T., (2000). Cardiomyopathy syndrome in farmed Scottish salmon. *Veterinary Record* **146** (500-501).

Rodger, H. & Mitchell, S., (2007). Epidemiological observations of pancreas disease of farmed Atlantic salmon, *Salmo salar* L., in Ireland. *Journal of Fish Diseases* **30** (157-167).

Rokenes, T. P., Larsen, R., & Robertsen, B., (2007). Atlantic salmon ISG15: Expression and conjugation to cellular proteins in response to interferon, double-stranded RNA and virus infections. *Molecular Immunology* **44** (950-959).

Ryman, K. D. & Klimstra, W. B., (2008). Host responses to alphavirus infection. *Immunological Reviews* **225** (27-45).

Schelesinger, A. & Dubenskey, T. W., (1999). Alphavirus vector for gene expression and vaccine. *Current Opinion in Biotechnology* **10** (434-439).

Schena, M., Shalon, D., Davis, R. W., & Brown, P. O., (1995). Quantitative monitoring of gene expression pattern with complementary DNA microarray. *Science* **270** (467-470).

Schroder, K., Hertzog, P. J., Ravasi, T., & Hume, D., (2004). Interferon -gamma: an overview of signals, mechanisms, and functions. *Journal of Leukocyte Biology* **75** (163-189).

Schulze, A. & Downward, J., (2001). Navigating gene expression using microarray- a technology review. *Nature Cell Biology* **3** (E190-E195).

Schwartz, M., Chen, J., Lee, W., Janda, M., & Ahiquist, P., (2004). Alternate, virus-induced membrane re-arrangements support positive-strand RNA virus genome replication. *PNAS* **101** (11263-11268).

Secombes, C. J. & Fletcher, T. C., (1992). The role of phagocytes in the protective mechanisms of fish. *Annual Review of Fih Diseases* **2** (53-71).

Secombes, C. & Zou, J., (2005). Adaptive immunity in teleosts: cellular immunity. *Developmental Biologicals* **121** (25-32).

Segura-Totten, M. & Wilson, K. L., (2004). BAF: roles in chromatin, nuclear structure and retrovirus integration. *Trends in Cell Biology* **14** (261-266).

Sen, G. C., (2001). Viruses and interferons. *Annual Review of Microbiology* **55** (255-281).

Singh, I. & Helenius, A., (1992). Role of ribosomes in similiki forest virus nucleocapsid uncoating. *Journal of Virology* **66** (7049-7058).

Slauson, D. O. & Cooper, B. J. (2002). *Mechanisms of diseases, a text book of comparative general pathology.* 3rd edition , Mosby Inc, Missouri, USA..

Solem, S. T. & Stenvik, J., (2006). Antibody repertoire development in teleosts-a review with emphasis on salmonids and *Gadus moruha* L. *Developmental and Comparative Immunology* **30** (57-76).

Söderlund, H., (1973). Kinetics of formation of the Semliki forest virus nucleocapsid. *Intervirology* **1** (354-361).

Starkey, W. G., Smail, D. A., Bleie, H., Muir, K. F., Ireland, J. H., & Richards, R. H., (2006). Detection of infectious salmon anaemia virus by real-time nucleic acid sequence based amplification. *Diseases of Aquatic Organisms* **72** (107-113).

Strauss, J. H. & Strauss, E. G., (1994). The alphaviruses - gene-expression, replication, and evolution. *Microbiological Reviews* **58** (491-562).

Sunyer, J. O., Boshra, H., Lorenzo, G., Parra, D., Freedman, B., & Bosch, N., (2003). Evolution of complement as an effector system in innate and adaptive immunity. *Immunologic Research* **27** (549-564).

Sunyer, O., Zang, Y., Parr, D., & LaPatra, S., (2009). Is IgT the evolutionary equivalent of IgA? Insights into its structure and function. *The Journal of Immunology* **181** (81.21).

Suomalainen, M., Liljestrom, P., & Garoff, H., (1992). Spike protein-nucleocapsid interaction drive the budding of alpahavirus. *Journal of Virology* **66** (4737-4747).

Susuki, T. & Susuki, Y., (2006). Virus infection and lipid raft. *Biological & Pharmaceutical Bulletin* **29** (1538-1541).

Taggart, J. B., Bron, J. E., Martin, S. A. M., Seear, P. J., Hoyheim, B., Talbot, R., Carmichael, S. N., Villeneuve, L. A. N., Sweeney, G. E., Houlihan, D. F., Secombes, C. J., Tocher, D. R., & Teale, A. J., (2008). A description of the origins, design and performance of the TRAITS-SGP Atlantic salmon *Salmo salar* L. cDNA microarray. *Journal of Fish Biology* **72** (2071-2094).

Takle, H., McLeod, A., & Andersen, Ø., (2006). Cloning and characterization of of the executioner caspase 3, 6, 7 and Hsp70 in hyperthermic Atlantic salmon (Salmo salar) embryos. *Comparative Biochemical Physiology* **B144** (188-198).

Takle, H. & Andersen, Ø., (2007). Caspase and apoptosis in fish: Review paper. *Journal of Fish Biology* **71** (326-349).

Taksdal, T., Olsen, A. B., Bjerkas, I., Hjortaas, M. J., Dannevig, B. H., Graham, D. A., & McLoughlin, M. F., (2007). Pancreas disease in farmed Atlantic salmon, *Salmo salar*

L., and rainbow trout, *Oncorhynchus mykiss* (Walbaum), in Norway. *Journal of Fish Diseases* **30** (545-558).

Taylor, L. A., Carthy, C. M., Yang, D. C., Saad, K., Wong, D., Schreiner, G., Stanton, L. W., & McManus, B. M., (2008). Host gene regulation during coxsackievirus B3 infection in mice - Assessment by microarrays. *Circulation Research* **87** (328-334).

Todd, D., Jewhurst, V. A., Welsh, M. D., Borghmans, B. J., Weston, J. H., Rowley, H. M., Mackie, D. P., & McLoughlin, M. F., (2001). Production and characterisation of monoclonal antibodies to salmon pancreas disease virus. *Diseases of Aquatic Organisms* **46** (101-108).

Tort, L., Padros, F., Rotllant, J., & Crespo, S., (1998). Winter syndrome in the gilthead sea bream Sparus aurata. Immunological and histopathological features. *Fish & Shellfish Immunology* **8** (37-47).

Trot, L., Balasch, S., & MacKenzie, S., (2003). Fish immune system. A crossroads between innate and adaptive responses. *Revisión* **22** (277-286).

Valasek, M. & Repa, J., (2005). The power of real-time PCR. *Advances in Physiological Eduation* **29** (151-159).

Viljugrein, H., Staalstrøm, A., Molvær, J., Urke, H. A., & Jansen, P. A., (2009). Integration of hydrodynamics into a statistical model on the spread of pancreas disease (PD) in salmon farming. *Diseases of Aquatic Organisms* **88** (35-44).

Villoing, S., Bearzotti, M., Chilmonczyk, S., Castric, J., & Bremont, M., (2000a). Rainbow trout sleeping disease virus is an atypical alphavirus. *Journal of Virology* **74** (173-183).

Villoing, S., Castric, J., Jeffroy, J., Le Ven, A., Thiery, R., & Bremont, M., (2000b). An RT-PCR-based method for the diagnosis of the sleeping disease virus in experimentally and naturally infected salmonids. *Diseases of Aquatic Organisms* **40** (19-27).

von Schalburg, K. R., Rise, M. L., Cooper, G. A., Brown, G. D., Gibbs, A. R., Nelson, C. C., Davidson, W. S., & Koop, B. F., (2005). Fish and chips: Various methodologies demonstrate utility of a 16,006-gene salmonid microarray. *BMC Genomics* **6** (126).

Vonderheit, A. & Helenius, A., (2005). Rab7 associates with early endosomes to mediate sorting and transport of Semiliki forst virus to late endosome. *PLoS Biology* **3** (1225-1233).

Waarts, B., Bittman, R., & Wilschut, J., (2002). Sphingolipid and cholesterol dependence of alphavirus membrane fusion; lack of correlation with lipid raft formation in target liposomes. *The Journal of Biological Chemistry* **277** (38141-38147).

Waheed, A. D. & Freed, E. O., (2007). Influenza virus not cRAFTy enough to dodge viperin. *Cell Host and Microbe* **2** (71-72).

Walker, J. A. & Quirke, P., (2001). Viewing apoptosis through 'TUNEL'. *Journal of Pathology* **195** (275-276).

Watts, M., Munday, B. L., & Burke, C. M., (2001). Immune responses of teleost fish. *Australian Veterinary Journal* **79** (570-574).

Weaver, S. C., Brault, A. C., Kang, W., & Holland, J. J., (1999). Genetic and fitness changes accompanying adaptation of an arbovirus to vertebrate and invertebrate cells. *Journal of Virology* **73** (4316-4326).

Welsh, M., Weston, J., Borghmans, B. J., Mackie, D., Rowley, H., Nelson, R., McLoughlin, M., & Todd, D., (2000). Biochemical characterization of salmon pancreas disease virus. *Journal of General Virology* **81** (813-820).

Wengler, G., Koschinski, A., Wengler, G., & Dreyer, F., (2003). Entry of alphaviruses at the plasma membrane converts the viral surface proteins into an ion-permeable pore that can be detected by electrophysiological analyses of whole-cell membrane currents. *Journal of General Virology* **84** (173-181).

Weston, J. H., Welsh, M. D., McLoughlin, M. F., & Todd, D., (1999). Salmon pancreas disease virus, an alphavirus infecting farmed Atlantic salmon, *Salmo salar* L. *Virology* **256** (188-195).

Weston, J., Villoing, S., Bremont, M., Castric, J., Pfeffer, M., Jewhurst, V., McLoughlin, M., Rodseth, O., Christie, K. E., Koumans, J., & Todd, D., (2002). Comparison of two aquatic alphaviruses, salmon pancreas disease virus and sleeping disease virus, by using genome sequence analysis, monoclonal reactivity, and cross-infection. *Journal of Virology* **76** (6155-6163).

Wheatley, S. B., Goodall, E. A., Menzies, F. D., & McLoughlin, M. F., (1994). An epidemiologic investigation of diseases of farmed Atlantic salmon - preliminary findings. *Society for Veterinary Epidemiology and Preventive Medicine: Proceedings* pp85.

White, E., (1996). Life, death, and pursuit of apoptosis. *Gene and development* **10** (1-15).

Whyte, S. K., (2007). The innate immune response of finfish – a review of current knowledge. *Fish & Shellfish Immunology* **23** (1127-1151).

Wolf, K. (1988). *Fish Viruses and fish viral diseases*. Cornell University Press Cornell, USA.

Workenhe, S. T., Wadowska, D. W., Wright, G. M., Kibenge, M. J. T., & Kibenge, F. S. B., (2007). Demonstration of infectious salmon anaemia virus (ISAV) endocytosis in erythrocytes of Atlantic salmon. *Virology Journal* **4** (13).

Workenhe, S. T., Kibenge, M. J. T., Iwamoto, T., & Kibenge, F. S. B., (2008a). Absolute quantitation of infectious salmon anaemia virus using different real-time reverse transcription PCR chemistries. *Journal of Virological Methods* **154** (128-134).

Workenhe, S. T., Kibenge, M. J. T., Wright, G. M., Wadowska, D. W., Groman, D. B., & Kibenge, F. S. B., (2008b). Infectious salmon anaemia virus replication and induction of alpha interferon in Atlantic salmon erythrocytes. *Virology Journal* **5** (36).

Workenhe, S. T., Hori, T. S., Rise, M. L., Kibenge, M. J. T., & Kibenge, F. S. B., (2009). Infectious salmon anaemia virus (ISAV) isolates induce distinct gene expression responses in the Atlantic salmon (*Salmo salar*) macrophage/dendritic-like cell line TO, assessed using genomic techniques. *Moecular immunology Immunol* **46** (2955-2974).

Yano, T. The non-specific immune system:humoral defense (1996), in Iwama, G and Nakanishi, T., (The fish immune system, organism, pathogen and environment, Academic press, London.

Young, N. D., Cooper, G. A., Nowak, B. F., Koop, B. F., & Morrison, R. N., (2008). Coordinated down-regulation of the antigen processing machinery in the gills of amoebic gill disease-affected Atlantic salmon (*Salmo salar* L.). *Molecular Immunology* **45** (2581-2597).

Zhang, Y. G., Burke, C. W., Rayman, K. D., & Klimstra, W. B., (2007). Identification and characterization of interferon-induced proteins that inhibit alphavirus replication. *Journal of Virology* **81** (11246-11255).

Zou, J., Carrington, A., Collet, B., Dijkstra, J. M., Yoshiura, Y., Bols, N., & Secombes, C., (2005). Identification and bioactivities of IFN-gamma in rainbow trout *Oncorhynchus mykiss*: The first Th1-type cytokine characterized functionally in fish. *Journal of Immunology* **175** (2484-2494).

Appendix

General Buffers

Phosphate buffered saline, pH 7.4 (PBS)
NaH_2PO_4 (VWR)	0.438g
Na_2HPO_4 (VWR)	1.28g
Sodium chloride	4.385g

Dissolve in 400ml distilled water, pH to 7.4 make up to 500ml and autoclave.

Tris buffered saline (TBS), pH 7.6
Trisma base	1.21g
Sodium chloride	14.62g

Dissolve in 400ml distilled water, pH to 7.2-7.6 and make up to 500ml.

Stains

Mayer's Haematoxylin
Haematoxylin	2g
Sodium iodate	0.4g
Potassium alum	100g
Citric acid	2g
Chloral hydrate	100g
Distilled water	2L

Allow haematoxylin, potassium alum and sodium iodate to dissolve in distilled water overnight. Add chloral hydrate and citric acid and boil for 5 min.

Eosin
1% Eosin	40ml
Putt's Eosin	80ml
Eosin yellowish	20g

Pre-dissolve in 600ml distilled water and then make up to 2L.

Putt's Eosin
Eosin yellowish	4g
Potassium dichromate	2g
Saturated aqueous picric acid	40ml
Absolute alcohol	40ml
Distilled water	320ml

Dissolve eosin and potassium dichromate in the ethanol, add the water and then the picric acid.

Scott's tap water substitute
Sodium bicarbonate	3.5g
Magnesium sulphate	20g
Tap water	1L

Dissolve by heating if necessary and add a few thymol crystals to preserve.

Hoechst 33342 dye and staining

Hochest 33342(Fluka, Biochemia cat 14933) 100mg
Stock 1: Dilute 100 mg of Hoechst 33342 (Sigma B2261) in 2 ml of distilled water. The concentration of this solution is 50 mg/ml. Store at 4 C.
Stock 2: On the day of use, dilute 2 µl of Stock 1 solution in 10 ml of PBS containing 1 mg/ml polyvinylpyrrolidone. The concentration is 10 µg/ml.
Working Solution: Dilute 100 µl of the Stock 2 solution in 900 µl of PBS-PVP for a final concentration of 1 µg/ml. (all solutions are made in light-proof tubes - wrapping in aluminium foil is sufficient)

Fixatives

10% Neutral buffered saline (10% NBF)
Sodium dihydrogen phosphate (monohydrate; VWR)	4g
Disodium hydrogen phosphate (anhydrous; VWR)	6.5g
Formaldehyde (Sigma)	100ml

distilled water make up to 1 litre

Carnoy's fixative for cells
Methanol	30 ml
Glacial acetic acid	90 ml

Add fixative direct onto the existing media of the cells (0.5 ml/ 1.5ml tissue culture media)and remove caerefully with the media after 2 min and follow another 2 x 5 min fixations with fresh Carnoy media (0.5 ml).

Molecular Biology

TAE buffer (x50)
Tris base	242g
Glacial acetic acid	57.1 ml
$Na_2EDTA.H_2O$	81.61 g

Adjust the final volume to 1000 ml and pH 8.5

Agarose gel

Agarose	1g
TAE	100ml

Dissolve in the microwave. Add 50 µl ethidium bromide (1 mg/l) when the gel temperature < 60°C.